HIGH STRENGTH STEEL REINFORCEMENT

IN

ORDINARY REINFORCED AND FIBRE REINFORCED CEMENT COMPOSITE

LIGHTWEIGHT CONCRETE BEAMS

A thesis presented

for the degree of Dcctor of Philosophy

by

Kosai Abdul Aziz Al-Sanjary B.Sc.

Department of Civil Engineering

The University of Salford

May 1975

TO

MY FATHER AND MOTHER

ACKNOWLEDGEMENTS

The author is grateful to Professor T. Constantine, B.Sc., Ph.D, C.Eng., F.I.C.E., F.I.M un.E., M. Inst. H.E., Professor of Civil Engineering and Chairman of the Civil Engineering Department for providing the facilities for the research work.

The author wishes to express his gratitude to Professor E.R. Bryan, M.Sc. (Eng) Ph.D, D.Sc., C. Eng., F.I.C.E., FI Struct. E., Professor of Structural Engineering for recommending and providing the opportunity to the author to study for a higher degree, and also for the encouragement to the progress of the author since his early enrol ment at the University.

The author is deeply indebted to his supervisor Dr. N.J. Dave, M. Eng, Ph.D, C. Eng, M.I.C.E., D.C.T., A.M.I.E. M.A.S.C.E., who first introduced him to the subject for his constant encouragement, guidance and above all patience throughout the work.

The author would like to thank Mr. D.C. O'Leary, M.Sc., C. Eng., M.I.C.E, for his help during the testing programme.

The author is most thankful to the technical staff, for their practical help in the concrete and Fitton structures laboratories. In this respect thanks are due to Messrs. T. Clark, W. Deakin, C. Eng., MI Strut. E, K. Naylor, T. Ward, R. Smith, H. Whewell and C. Lomax.

The author is especially thankful to Mr. N. Beaver, A.R.T.C.S., for reading through the thesis and for his most valued remarks.

Thanks are also due to the Building Research Establishment for providing the rig for the sustained loading tests.

Thanks are also due to TAC Construction Materials Limited for manufacturing and supplying the fibre reinforced cement channels used in this research.

The author is grateful to the British Council for paying the University fees for the first two years of the enrol ment.

The author acknowledges with gratitude the financial support provided by the Iraqi Ministry of Oil and Minerals.

Finally my special thanks to my wife Neda for typing the draft of the thesis and for her encouragement and patience throughout the work.

SYNOPSIS

When high strength steel is used as reinforcement in lightweight concrete members, great economies can be achieved. However, because lightweight concrete has low tensile strength and modulus of elasticity, the working steel stresses hoped for may not be fully utilised due to the limit states of serviceability (cracking and deflection) not being satisfied. To control the amount of cracking and deflection in flexural concrete members, a new type of construction has been employed, whereby precast fibre reinforced cement (f.r.c) units in the form of thin channels are used as a surface reinforcement at the flexural tensile zone of the concrete members. The concrete in the tensile zone, confined by the f.r.c. channel, will have a greater resistance to formation and extension of crack; consequently the rate of reduction in the flexural rigidity of the member will be decreased.

A total of 27 ordinary reinforced and fibre reinforced cement composite lightweight concrete beams, 150mm wide, 300mm deep and 5m long were tested, 18 under static load test, 5 under fatigue load test and 4 under sustained load test. The composite beams were similar to the ordinary beams in every respect, except that f.r.c.channels (150mm width, 60mm length of upstands and 6mm thickness) were incorporated as integral parts on their flexural tensile sides. The main parameters employed for both beams were the type and amount of steel provided for the tension reinforcement. The various types of reinforcement with the corresponding nominal yield, or 0.2% proof stress employed were mild steel (275 N/mm^2), Unisteel 410 (410 N/mm^2), Unisteel 550 (550 N/mm^2), "Kam 60" (590 N/mm^2) and "Kam 90" (875 N/mm^2).

The flexural behaviour of both types of beams under static, fatigue and sustained types of loading has been studied, great emphasis being placed upon the limit states of ultimate strength, cracking and deflection with particular reference to the contribution of the f.r.c.channels in the composite beams.

From the results, it is concluded that a considerable reduction in the amount of deflection and cracking can be achieved by using f.r.c.channels at the flexural tensile zone of concrete members, thus allowing a more efficient use of the high-strength steel.

OUTLINE OF THESIS

In chapter one the structural and economic aspects of high strength steel and lightweight concrete when employed in concrete construction are discussed. Emphasis is placed on the structural aspects and application of fibre reinforced concrete and the techniques employed for mixing the fibres. The limitations of three-dimensional random distribution of fibres on controlling deflection and cracking are also presented.

In chapter two the work carried out in the past using high strength steel in lightweight concrete is reviewed, and a general conclusion is drawn. The other part of the chapter is concerned with the origin, development and use of the proposed measures to reduce cracking and deflection in flexural concrete members. Tests carried out at the University of Salford and other places are also discussed.

Chapter three covers the design of test beams and materials used in this research. Information given for the test beams includes their dimensions, parameters employed, condition of loading and analysis of the working and ultimate moments. Also included is the design of the f.r.c.units with regard to their properties and geometry. The mix proportions for the concrete and the properties of the steel used are also given.

Chapter four deals with the proposed theoretical analysis developed in this research for the stresses in the concrete, f.r.c.channel and steel. The various relationships established together with the idealised curves are also presented.

In chapter five the theoretical considerations regarding the proposed methods for the limit states of ultimate strength, cracking and deflection are also discussed.

Chapter six covers the manufacture and methods of testing employed for the test beams and the control specimens for the concrete properties.

The observations made and the behaviour of the beams tested under static loading are discussed in chapter seven. A comparison of the observed values with those predicted in accordance with chapters four and five is also presented. This chapter also includes a direct comparison of behaviour between ordinary and composite beams.

In chapter eight the behaviour and the observations made for the beams tested under fatigue and sustained loading are discussed. A direct comparison of behaviour between ordinary and composite beams is also presented.

Finally, in chapter nine, the conclusions of the research are drawn up, and suggestions are made for future work to be carried out in this field.

HIGH STRENGTH STEEL REINFORCEMENT

IN

ORDINARY REINFORCED AND FIBRE REINFORCED CEMENT COMPOSITE

LIGHTWEIGHT CONCRETE BEAMS

ERRATA

For units of moments substitute "kN . m" for "KN. m" throughout .

For neutral axis depth substitute "X" for "x" throughout .

CONTENTS

	Page No.
ACKNOWLEDGEMENT	i
SYNOPSIS	ii
OUTLINE OF THESIS	iii
CONTENTS	v
LIST OF SYMBOLS	xi
ABBREVIATIONS	xv
CODING REFERENCE FOR TEST BEAMS	xvi
CHAPTER ONE : INTRODUCTION	1
1.1 Summary	1
1.2 High-Strength Steel	2
1.2.1 General	2
1.2.2 Economic Aspects	3
1.3 Structural Lightweight Concrete	4
1.3.1 General	4
1.3.2 Economic Aspects	5
1.4 Weakness of Concrete in Tension	6
1.5 Fibre-Reinforced Concrete	8
1.6 The Need for this Investigation	11
CHAPTER TWO : PREVIOUS INVESTIGATIONS	
2.1 Use of High-Strength Steel in Structural Lightweight Concrete	12
2.1.1 General	12
2.1.2 Summary of Past Research	12
2.1.3 Conclusions From Past Research	19
2.2 Approaches Employed to Control Cracking and Deflection in Flexural Members Reinforced with High-Strength Steel.	20
2.2.1 General	20
2.2.2 Closely Spaced Continuous Reinforcement	20
2.2.3 Fibre Reinforced Concrete	22
2.2.4 Composite Concrete Construction Using Steel Channels	26
2.2.5 Work at Salford	27

Page No

CHAPTER THREE : MATERIALS USED AND DESIGN OF TEST BEAMS

3.1 General 30

3.2 Design Considerations 30

3.2.1 Ordinary Reinforced Lightweight Concrete Beams 30

3.2.2 Composite Reinforced Lightweight Concrete Beams 32

3.2.3 Fibre Reinforced Cement Units (f.r.c. Units) 33

3.2.3.1 Properties 33

3.2.3.2 Geometry 34

3.3 Materials 35

3.3.1 Lightweight Aggregate Concrete 35

3.3.2 Reinforcement 36

CHAPTER FOUR : THEORETICAL BASIS OF ANALYSIS FOR STRESSES IN CONCRETE, STEEL AND f.r.c. CHANNELS

4.1 Introduction 37

4.2 Variations of the Neutral Axis Level 37

4.3 Analysis of Compressive Stresses in Concrete 41

4.3.1 Stress-Strain Relationship of Lightweight Concrete in Compression 41

4.3.2 Variations of the Flexural Compressive Strain in Concrete 41

4.3.3 Variations of the Area and Centroid of the Compressive Stress Distribution in Concrete 42

4.4 Analysis of Stresses in f.r.c. Channels 44

4.5 Calculation of Steel Stresses 46

4.5.1 Assumptions 46

4.5.2 Ordinary Lightweight Concrete Beams 47

4.5.3 Composite Lightweight Concrete Beams 47

4.5.4 Summary for the Theoretical Calculation of Steel Stresses 48

4.6 Suggested Method for Calculation of Steel Stresses Based on Experimental Results 48

Page No

CHAPTER FIVE : THEORETICAL CONSIDERATIONS FOR LIMIT STATES OF DESIGN FOR ORDINARY AND COMPOSITE BEAMS

5.1 Introduction 50

5.2 Limit State of Ultimate Strength 51

5.2.1 General Considerations and Assumptions 51

5.2.2. Comments on the Basic Assumptions 52

5.2.3 Composite Beams 53

5.3 Limit State of Deflection 54

5.3.1 Introduction 54

5.3.2. Considerations for Ordinary and Composite Lightweight Concrete Beams 56

5.3.3 Behaviour of Ordinary Lightweight Concrete Beams 58

5.3.4 Behaviour of Composite Lightweight Concrete Beams 58

5.3.5 Methods of Calculation 62

Approach One - Existing Theories for Ordinary Beams 62

Approach Two - Empirical Method for Ordinary and Composite Beams 63

Approach Three - Proposed Methods

(a) Ordinary Beams 63

(b) Composite Beams 65

5.4 Limit State of Cracking 67

5.4.1 Introduction 67

5.4.2 Cracking Mechanism in Composite Lightweight Concrete Beams 68

5.4.3 Methods of Calculation 71

CHAPTER SIX : MANUFACTURE AND METHODS OF TESTING

6.1 General 73

6.2 Manufacture 73

6.2.1 Ordinary Reinforced Lightweight Concrete Beams 73

6.2.2 Composite Reinforced Lightweight Concrete Beams 74

6.2.3 Control Specimens for Concrete 74

6.2.4 Fibre Reinforced Cement Channels (f.r.c. Channels) 75

Page No.

6.3 Static Loading Tests 75

6.3.1 Arrangements and Conditions of Loading 75

6.3.2 Testing Procedure 76

6.4 Fatigue Loading Tests 77

6.4.1. Arrangements and Conditions of Loading 77

6.4.2 Testing Procedure 78

6.5 Sustained Loading Tests 78

6.5.1 Arrangements and Conditions of Loading 78

6.5.2 Testing Procedure 80

6.6 Instrumentation 80

6.7 Other Tests 81

6.7.1 Control Tests on Concrete 81

6.7.2 Tensile Tests on Steel 82

6.7.3 Tests on f.r.c. Units 83

CHAPTER SEVEN : DISCUSSION OF TEST RESULTS AND COMPARISON OF TEST BEHAVIOUR WITH THEORETICAL PREDICTION FOR ORDINARY AND COMPOSITE BEAMS

7.1 Introduction 84

7.2 Variations of the Neutral Axis Level 84

7.3 Flexural Strain Distribution 87

7.4 Varations of the Flexural Compressive Strain in Concrete 88

7.5 Stresses in the f.r.c. Channels 91

7.6 Stresses in the Steel Reinforcement 93

7.7 Limit States of Design 95

7.7.1 Limit State of Ultimate Strength 95

7.7.2 Limit State of Deflection 97

7.7.2.1 Behaviour of Ordinary Beams 97

7.7.2.2. Behaviour of Composite Beams 101

7.7.2.3 Comparison Between the Behaviour of Ordinary and Composite Beams 103

7.7.2.4 Comparison with Theory 105

Page No.

7.7.3 Limit State of Cracking 108

7.7.3.1 Behaviour of Ordinary Beams 108

7.7.3.2 Behaviour of Composite Beams 111

7.7.3.3 Comparison Between the Behaviour of Ordinary and Composite Beams 113

7.7.3.4 Comparison with Theory 114

CHAPTER EIGHT : EFFECTS OF LONG TERM LOADING ON TEST BEHAVIOUR FOR ORDINARY AND COMPOSITE BEAMS

8.1 Introduction 116

8.2 Fatigue Loading Tests 116

8.2.1 Variations of the Neutral Axis Depth 116

8.2.2 Variations of the Maximum Flexural Compressive Strain in Concrete 118

8.2.3 Stresses in the f.r.c. Channels 120

8.2.4 Variations of the Steel Stresses 121

8.2.5 Principal Limit States 123

8.2.5.1 Limit State of Ultimate Strength 123

8.2.5.2 Limit State of Deflection 124

8.2.5.3 Limit State of Cracking 128

8.3 Sustained Loading Tests 131

8.3.1 Time-Dependent Flexural Strain Distribution 131

8.3.2 Variations of the Tensile Strains in the f.r.c. Channels 134

8.3.3 Variations of the Steel Stresses 135

8.3.4 Limit States of Serviceability 136

8.3.4.1 Limit State of Deflection 136

8.3.4.2 Limit State of Cracking 139

CHAPTER NINE : CONCLUSIONS AND SUGGESTIONS FOR FUTURE WORKS

9.1 Conclusions 142

9.2 Advantages of Using f.r.c. Channels at the Tensile Sides of Flexural Members 143

9.3 Suggestions for Future Work 143

Page No.

REFERENCES 145 - 156

TABLES

FIGURES

PLATES

APPENDICIES

LIST OF SYMBOLS

A_{ch}	cross section area of f.r.c.channel
A_e	effective concrete area in tension
A_s	area of tension reinforcement
A_{sv}	cross-sectional area of the two legs of a link
a	deflection
a'	distance from compression face to the point at which the crack width is being calculated
a_{cr}	distance from the point (crack) considered to the surface of the nearest logitudinal bar
b	width of section and also width of f.r.c.channel
C	compression force in concrete
C_o, C_1, C_2	ratios of applied moment to ultimate moment, for the prediction of the neutral axis level
C_p	ratio of applied moment to ultimate moment for the prediction of the maximum compressive strain in concrete
c	concrete cover to tension steel
D_c	density of concrete at time of test
d	total depth of beam
d'	height of upstand of f.r.c. channel
d_a	centroid of stress distribution from soffit of f.r.c.channel
d_1	effective depth of reinforcement
d_2	effective depth of the tensile force (T_a) in f.r.c.channel
E	modulus of elasticity
E_a	initial modulus of elasticity of f.r.c. units
E_c	initial modulus of elasticity of concrete
E_s	modulus of elasticity of steel
e_c	compressive strain in concrete
e_j	strain at which maximum compressive stress of concrete is first attained

e_{max}	maximum compressive strain of concrete
e_p	compressive strain in concrete at $M/M_u = C_p$, for the variation of the flexural strain in concrete with applied moment
e_t	strain in main tension reinforcement
f_{ab}	tensile stress at soffit of f.r.c.channel
f_{at}	tensile stress at top of the upstands of the f.r.c.channel
f_{bs}	bond stress
f_c	compressive stress in the extreme element of concrete in the compression zone
f_{cu}	characteristic strength of concrete in compression-cube tests
f_r	flexural tensile stress of plain concrete (modulus of rupture)
f_{rc}	flexural tensile stress in concrete at interface for composite section
f_s	stress in main tension reinforcement
f_s'	tensile stress resisted by concrete between cracks
f_{save}	average stress in main tension reinforcement
f_{smin}	minimum stress in main tension reinforcement
f_t	average tensile stress in concrete
f_y	characteristic strength of reinforcement. (Nominal yield or 0.2% proof stress)
f_{yv}	characteristic strength of link reinforcement
I	second moment of area-general
I_{cc}	second moment of area for cracked composite section
I_{co}	second moment of area for cracked ordinary section
I_o	second moment of area for uncracked concrete section - general
I_p	second moment of area for partially cracked section. (composite beams)
I_{uc}	second moment of area for uncracked composite section
I_{uo}	second moment of area for uncracked ordinary section
K, K'	constants for deflection calculations for composite beams
K_o, K_1, K_2, K_3	constants used for deriving formula for the deflection calculations for ordinary beams. ($K_3 = K_o K_1 K_2$)

L	span of beam
l_c	lever arm of tensile force in concrete
M	applied bending moment
M_a	cracking moment of f.r.c.channel
M_c	cracking moment of concrete
M_{dw}	design working moment
M_u	ultimate resistance moment
m	modular ratio = E_s/E_c
m_1	modular ratio = E_a/E_c
n	ratio of neutral axis depth to effective depth
p	geometrical ratio of main tension reinforcement = A_s/bd_1
p_1	geometrical ratio of f.r.c.channel = A_{ch}/bd_2
r_b	radius of curvature
$\frac{1}{r_b}$	curvature of beam at midspan
S_v	spacing of links along the member
T_c	tensile force of concrete in tension
T_s	tensile force in main reinforcement
T_a	tensile force in f.r.c.channel
t	thickness of f.r.c.channel
u	perimeter
V	shear force due to ultimate load
v	shear stress
V_c	ultimate shear stress in concrete
W	total applied load on beam
w	crack width
X	neutral axis depth-general
X_c	neutral axis depth of cracked section-general
X_{cc}	neutral axis depth of cracked composite section
X_{co}	neutral axis depth of cracked ordinary section
X_p	neutral axis depth of partially cracked composite section
X_u	neutral axis depth of uncracked section-general

X_{uc} neutral axis depth of uncracked composite section

X_{uo} neutral axis depth of uncracked ordinary section

Z moment lever arm for steel reinforcement

α coefficient for calculating area of concrete compressive stress distribution diagram

β coefficient for calculating centroid of concrete compressive stress distribution diagram

β_1 constant depending upon effective cracked second moment of area, and modulus of elasticity of f.r.c. channel and concrete, for composite beams (for calculation of stresses in f.r.c. channels)

γ coefficient = $1 - \beta$

γ_m partial safety factor for strength ($\gamma_m = 1.5$ for concrete and 1.15 for steel)

σ_c compressive stress in concrete

σ_o maximum compressive stress in stress-strain relationship for concrete = $\frac{0.67 f_{cu}}{\gamma_m}$

η ratio of effective depth of tensile force in f.r.c. channel to that of steel = d_2/d_1

η' ratio of length of upstand for f.r.c. channel to effective depth of steel = d'/d_1

λ ratio of total depth to effective depth of steel = d/d_1

ϕ curvature

ϕ_{ave} average curvature

ABREVIATIONS

A.C.I.	American Concrete Institute
A.S.C.E.	American Society of Civil Engineers
B.R.E.	Building Research Establishment
B.S.I.	British Standards Institution
C. & C.A.	Cement and Concrete Association
C.E.B.	"Comite Europeen du Beton" (European Concrete Committee)
C.P.	Code of Practice
F.I.P.	"Federation International de la Precontrainte" (International Prestressing Federation)
f.r.c.	Fibre Reinforced Cement
I.A.B.S.E.	International Association for Bridge and Structural Engineering
I.C.E.	Institution of Civil Engineers
I.C.L.C.	International Congress on Lighweight Concrete
P.C.A.	Portland Cement Association
R.C.R.	Reinforced Concrete Review

CODING REFERENCE FOR TEST BEAMS

The coding reference below refers to ordinary and composite lightweight concrete beams. For each beam the coding reference was given in the following manner; two letters, number and a letter, e.g. ST4-0

The first two letters refer to the type of loading employed.

These are:-

ST : Beams tested under static loading

FA : Beams tested under fatigue loading

SU : Beams tested under sustained loading

The number refers to the amount and type of reinforcements employed in the beams, e.g.

1 : 2-16mm, mild steel

2 : 2-16mm, Uni-steel 410

3 : 2-16mm, Uni-steel 550

The last letter refers to the type of the beam tested.

These are:-

O : Ordinary reinforced lightweight concrete beams

C : Composite reinforced lightweight concrete beams

CHAPTER ONE

INTRODUCTION

1.1 Summary

When high strength steel is used as reinforcement in concrete members, great economies can be achieved. There are, however, certain limitations on its use; these are imposed mainly to satisfy the limit states of serviceability (cracking and deflection) at the working load conditions. When lightweight concrete is used cracking and deflection becomes even more critical, due to its low modulus of elasticity and tensile strength.

Since the introduction of the conventional elastic theory, attempts have been made to rectify the limitations of concrete in tension, and also to reduce the amount of cracking and deflection taking place under load. This has been partly achieved by:-

1) Fully or partially prestressing the concrete, basic techniques being employed to improve the structural performance of the members.

2) Using fibre-reinforced concrete whereby certain improvements may be obtained in the flexural behaviour of the concrete by the addition of high modulus fibres.

A new concept of fibre-reinforced cement composite concrete construction as a means of controlling cracking and deflection has been evolved at and patented by the University of Salford.

The present investigation was initiated to study the possibility of using high strength steel in flexural lightweight concrete members. The programme of investigation then was extended to employ a new concept of fibre composite construction as a means of controlling cracking and deflection for lightweight concrete members. In the present investigation the asbestos cement units were employed as surface reinforcement.

In the following paragraphs the structural properties and economical aspects of lightweight aggregate concrete, high-strength steel and fibre-reinforced composite concrete are discussed.

1.2 High Strength Steel

1.2.1 General

In this investigation the general term high-strength steel denotes reinforcing bars having a yield or 0.2% proof stress of 410 N/mm^2 or higher.

High-strength steel bars have been produced and used in various parts of the world as a means of economy in reinforced concrete design. These reinforcing bars differ significantly in their ultimate strength, extent of surface deformation and method of manufacture.

To control the distribution and width of cracks the steel bars should have surface characteristics enabling high stresses to be developed without any bond failure occurring.

The effect of the manufacturing process on the tensile properties of the bars can be seen in fig. 1, where hot rolled bars have a definite yield point while cold worked bars yield gradually.

The advantages claimed by many investigators (1) (2) (3) (4) on the use of high-strength steel in reinforced concrete may be summarized in the following

1. When the full strength of the reinforcing bars is considered in the design, a significant reduction can be obtained in the amount of steel. The percentage saving in steel area compared with mild steel would be equal to $(1 - f_y/f_y') 100$,

   where f_y = yield stress of mild steel

   f_y' = yield or 0.2% proof stress of high-strength steel used

2. Ease and speed of construction due to a reduction of end hooks and also a possible reduction in the size of the structural member.
3. Economy. This is discussed in detail in 1.2.2.

There are certain limitations, however, on the use of high-strength steel in reinforced concrete members. These are mainly imposed to satisfy the safety requirements (cracking and deflection) at the working loading conditions. These limitations arise from the fact that high-strength steel bars have nearly the same modulus of elasticity as mild steel, so that when high working steel stresses are employed, greater strains result which lead to wider cracks and greater deflection.

The Code of Practice CP110 (5) permits the use of reinforcing bars with 0.2% proof or yield stress between (410 - 460 N/mm^2), depending on the type and the nominal size of the reinforcement. On the continent (2), however, permissible stresses of up to 380 N/mm^2 are being allowed under working load conditions. Considering a load factor of 1.8, this will permit 0.2% proof or yield stress of 685 N/mm^2 to be used.

In the past a considerable amount of research has been carried out in Britain and other parts of the world, investigating the behaviour of normal weight concrete beams reinforced with high-strength steel. There has been, however, only a limited amount of work carried out into the use of high strength steel in lightweight concrete members. Further investigation in this respect is, therefore, deemed to be necessary as the limit states of serviceability (cracking and deflection) at the working load conditions may be critical when lightweight concrete is used. This is discussed in 1.3.1.

1.2.2. Economic Aspects

Many researchers have established that by using high-strength steel in place of mild steel, a direct reduction can be made in the amount of reinforcement used (1) (2) (6).

The American Iron and Steel Institute (7) has presented design analyses based on the A.C.I. code recommendations for beams and columns reinforced with high-strength steel. These analyses showed that when high-strength steel was used instead of mild steel a considerable saving in the amount of steel could be made.

For beams with balanced section it was suggested that by using Unisteel 550 instead of Unisteel 410 savings of 25% could be obtained in the steel area with an overall saving of 4% in the total cost of the member (4).

An analysis of a six-storeyed office building (3) indicated that a saving of 28.5% in the amount of steel could be obtained when high-strength steel with a yield stress of 417 N/mm^2 replaced mild steel of 255 N/mm^2 yield stress.

1.3 Structural Lightweight Concrete

1.3.1 General

Because of the advantages lightweight concrete possesses, it has in the last two decades become an important structural material used in various types of construction. Among these advantages are its lower unit weight, greater fire resistance, improved thermal insulation and ease of construction (8) (9) (10).

Lightweight concrete, however, has certain shortcomings, which include a low tensile strength and modulus of elasticity, with high values for shrinkage and creep. These considerations together with a lack of available data on its behaviour have limited its use to a minor role in concrete structures.

When high-strength steel is used as a reinforcement in lightweight concrete beams and the various limit states are satisfied great economies can be achieved. These beams, however, tend to exhibit a considerable amount of cracking and deflection at working loads. It is for this reason that the use of this type of steel is limited.

The maximum characteristic strength for steel bars which can be used in accordance with CP110 for both normal weight and lightweight concrete ranges between 410 - 460 N/mm^2.

The code also specifies that the design should be based on lower values of steel stresses where necessary to satisfy the limit states of deflection and crack width. In addition the recommended span-depth ratio for normal weight concrete should be multiplied by a factor of 0.85 when lightweight concrete is used. It is believed that this takes into account the reduced flexural rigidity of the lightweight concrete members compared with normal-weight concrete.

In the past there has been a considerable amount of research into the structural properties of lightweight concrete as a material (11) (12) (13). A limited amount of research, however, has been carried out into the flexural behaviour of full scale reinforced lightweight concrete members. Considering the shortcomings of lightweight concrete (low tensile strength and modulus of elasticity, and high values for shrinkage and creep) it was thought that the limit states of serviceability would not be fully satisfied; especially when fatigue or sustained types of loading

were considered. It was for this reason thought necessary to study the flexural behaviour of reinforced lightweight concrete members under static, fatigue and sustained types of loading

1.3.2 Economic Aspects

It is rather difficult to assess the actual saving in cost brought about by using lightweight concrete instead of normal weight concrete. It may be true that freshly mixed lightweight concrete is more expensive than normal-weight concrete, but this should not form the only basis of comparison. To make a complete estimation of the savings all the relevant factors for the use of lightweight concrete should be considered; these include the lower total dead weight and the consequent use of lighter transportation and lifting equipment.

An analysis of cost made on a typical multi-storey office building showed results slightly in favour of the use of lightweight concrete. Although it was concluded that no set rule could be drawn, the use of lightweight concrete was competitive when the circumstances were right. (14)

Recently a working party of the Concrete Society was formed to study the economics of lightweight concrete construction. In this study suspended floor units were considered, and it was concluded that lightweight concrete was comparable in cost to normal-weight concrete, and would even be cheaper if other factors, e.g., possible higher output and suitable plant, were taken into consideration (15)

In the C.E.B. recommendations (10) the economies of lightweight concrete in relation to normal-weight concrete were divided into the following categories:-

(i) Economies due to lower dead weight

(ii) Economies due to other properties of lightweight concrete

Considering the lower unit weight of lightweight concrete, the reduction of the total load will depend upon the density of the lightweight concrete and the ratio of the live load to dead load. The amount of reduction compared with normal weight concrete may be calculated as follows:-

Considering:-

p = live load KN/m^2

g = dead load (normal weight concrete) (KN/m^2)

γ_2 = density of lightweight concrete (Kg/m^3)

γ_1 = density of normal weight concrete (Kg/m^3)

a_1 = p/g

$\beta_o = \gamma_2 / \gamma_1$

The weight saving in relation to normal weight concrete being

$$\frac{\gamma_1 - \gamma_2}{\gamma_1} \quad 100\% = (1 - \beta_o) \quad 100\%$$

The ratio of total load to dead load is $\frac{p + g}{g} = 1 + a_1$

Then the reduction of the total load, when lightweight concrete is to be used is $\frac{1 - \beta_o}{1 + a_1}$ 100%

A graph has been established correlating the reduction in total load and the different values of β_o and a_1 as shown in fig. 2. In this figure, it can be seen that the reduction in total load increases as the ratios of live load to the dead load (a_1), and the density of the lightweight to normal weight concrete (β_o) decreases. This was concluded to be the most important factor in the economic considerations.

Other factors also considered to have a great influence on the economies are the cost reduction of formwork and scaffolding, savings in the cost of foundations, reduced column sizes, cheaper transport per unit volume and faster building.

The other advantages, e.g., additional resistance to heat, frost and fire, were considered to cause an indirect reduction in building costs.

1.4 Weakness of Concrete in Tension

Concrete widely used as a building material has certain shortcomings, among these are its low tensile strength and limited extensibility. When the tensile strength of the concrete is reached, either due to applied tensile stress or shrinkage, the concrete will crack. This will lead to a greater rate of increase in the deflection of a flexural member with applied load. Wide cracks can also lead to corrosion of the steel, consequently the limit state of ultimate strength may

not be fully satisfied.

Much has been done to improve the strength of concrete in compression. Concrete of more than 100 N/mm^2 can now be produced (16). There has, however, been no significant improvement in the tensile strength of the concrete, which is only about 1/10 to 1/20 the value of its compressive strength. It is for this reason that the tensile strength of the concrete is ignored in most design considerations.

In 1906 (17) the basic assumptions were formulated for the elastic theory of reinforced concrete, in which the tensile resistance of the concrete was to be ignored. This formed the basis of various codes of practices used by many different countries.

In the load factor method introduced in CP114 (18) and the recent limit state theory of design in CP110, the structure being considered is analysed at its ultimate load condition. At this stage the concrete in tension is ignored in calculating the bending resistance of the beam, and only the steel is considered to carry the tensile stresses.

In CP110 hypothetical values are given to include the stiffening effect of the concrete in tension for calculating the deflection and cracking. For calculating the deflection at the working load, a triangular stress distribution for the concrete in tension is assumed as 1 N/mm^2 at the steel level and zero at the level of the neutral axis. This assumed tensile stress has in fact taken into consideration the average contribution of the concrete between the cracks in the tension zone to the stiffness of the concrete member. For the calculation of the crack width the stiffening effect of the concrete has also been considered.

For concrete members reinforced with high-strength steel high stresses and strains are expected at the working load condition which will cause wider cracks and greater deflection. Hence there is an essential need to improve the structural performance of the concrete members. This may be achieved by improving the tensile strength of the concrete.

Prestressing was introduced as a means to improve the structural performance of flexural members at working load conditions. In prestressed concrete class 1 the concrete is assumed not to carry any tensile stress; this results in an absence

of cracking. As there is no loss of rigidity due to cracking the deflection would be considerably reduced.

Partially prestressed concrete was then introduced as an economical improvement on fully prestressed concrete. This permitted tensile stresses and in some cases limited cracking to occur in the concrete at working load.

In general prestressing could well be regarded as a forward step towards the improvement of performance of concrete members.

Recently attempts have been made to improve the tensile strength of concrete by the introduction of fibres in the concrete mix. This is discussed in the following paragraph.

1.5 Fibre-Reinforced Concrete

The problem of the low tensile strength of concrete has occupied the attention of many engineers in the past. In 1910 (19) it was suggested that the characteristics of the concrete could be greatly improved by the addition of short pieces of steel mixed in the concrete matrix. Recent attempts in this field have incorporated different types of fibres in a cement or a concrete matrix. Indeed, fibre-reinforced cement and concrete has opened up a whole new field of concrete technology which could result in new concepts of design for concrete structures.

Generally, when fibres are incorporated in a cementatious matrix, certain improvements in the structural properties of the matrix can be achieved. These improvements however mainly depend upon:-

1) The properties of the fibres with regard to their modulus of elasticity, tensile strength, extensibility and bond efficiency.
2) The volume content and uniformity of distribution of the fibres in the matrix.
3) The degree of effectiveness of the fibres in the matrix; this depends upon the technique of mixing employed. These are:-
   a. Three-dimensional random distribution.
   b. Two-dimensional random distribution.
   c. Unidirectional distribution.

In the following these are discussed at further length.

Three-dimensional random distribution techniques have been employed for some time incorporating various types of fibres in a cement or concrete matrix. When steel wires are used in a concrete matrix, a considerable improvement can be obtained in the impact, ductility and flexural strength (20) (21) (22) (23).

There are certain points, however, which need to be considered when fibres are to be dispersed in three-dimensional random distribution in plain or reinforced concrete members.

These are:-

1) Difficulty of mixing and handling the fibres. In some instances a special technique may have to be adopted in their use (24)
2) A good workability needs to be ensured for a better distribution of fibres and compaction of the matrix. This may be achieved by:-
   (a) Using a low fibre content and aspect ratio which may tend to reduce the strength of the matrix (21) (23)
   (b) By controlling the size and quantity of the coarse aggregate used in the concrete mix (23)
   (c) By the addition of liquid additives and a partial replacement of cement by pulverised fuel ash content (23)
3) Flexural strength and crack control depends on the bond characteristics between the fibres and the concrete. In the case of steel fibres this may be relatively inefficient due to the smooth surface of their finish.
4) The possible corrosion of the steel wires in the long term (22) (25). This may apply especially to those wires bridging crack widths in the concrete.
5) The fibres will be dispersed in areas where they are not mostly needed, e.g., in the compression zone of the flexural member, i.e., full utilization of all the fibres would not be achieved.
6) The cost of fibre-reinforced concrete, when incorporating 2% of steel wires is about five times that of plain concrete (22) (25)
7) In three-dimensional random distribution of fibres in a matrix the fibres which effectively carry the stress in any given direction are between 0-20% of the total volume included in the mix (25).

In reinforced concrete, where only the flexural strength of the concrete needs to be improved, three-dimensional random distribution of fibres may not be very efficient, and an economical design may not be achieved. This conclusion is based on the present state of knowledge. The material is still in the development stage, and a more efficient use of the material will result when there is a better understanding of the techniques in dealing with fibres. Recently the Delft Conference (26) (27) has shown how much Engineers were enthusiastic about developing and processing this material. The future seems promising in this field of research, as work is being carried out in the United Kingdom and other parts of the world.

In two-dimensional random distribution of fibres in one plane the efficiency of the fibres carrying stress in a given direction is between 30 - 37% of the total volume of the fibres compared with 0 - 20% for the three-dimensional (25). When high-modulus fibres are dispersed in two-dimensional random distribution in a cement matrix, the composite has a better resistance to impact, fire and tensile stresses (28) (29). Two-dimensional distribution of fibres can not be employed in a concrete matrix, but has been used successfully for some time to produce high quality fibrous cement composite units. Glass or asbestos fibrous cement composite units are good examples of this.

Unidirectional distribution of fibres in a matrix would appear to give the most effective use of the material, but it is not possible to employ this method with the existing techniques of mixing the fibres. It is possible that in the future this type of distribution may dominate the construction of fibre-reinforced concrete when a better technique of mixing is known.

At the University of Salford a new technique in construction employing precast units of fibre-reinforced cement as surface reinforcements to concrete members has been evolved by Dr. Dave. This type of fibre-reinforced cement composite concrete and its structural behaviour forms a major part of the work presented in this thesis.

1.6 The Need for this Investigation

In carrying out this investigation the following points were considered:-

1) It was realised that in the past only a limited amount of research had been conducted into the flexural behaviour of full-scale reinforced lightweight concrete members. A study in this respect, considering static, fatigue and sustained types of loading was deemed to be necessary.

2) The maximum specified characteristic steel stress for reinforcing bars allowed in CP110 is 425 to 460 N/mm^2, depending on the size and type of the bars used. However, it is believed that this limit can be increased without the limit states of ultimate strength and serviceability of the structure being reached.

3) Since lightweight concrete has a low tensile strength and modulus of elasticity, a considerable amount of cracking and deflection when employing high working steel stresses in flexural members is expected. Means for controlling this deflection and cracking therefore seems necessary. In this respect a new form of construction is to be employed, in which precast fibre-reinforced cement units in the form of thin channels are used as a surface reinforcement at the tensile zone of the concrete members.

4) Experimental data is necessary to ascertain values for constants that are to be used in proposed empirical relationships for various aspects of behaviour.

CHAPTER TWO

PREVIOUS INVESTIGATIONS

2.1 Use of High-Strength Steel in Structural Lightweight Concrete

2.1.1 General

In the past mild steel has been usually employed as reinforcement in lightweight concrete members. Very limited tests have been carried out into the flexural behaviour of such members when reinforced with high strength steel especially under fatigue and sustained types of loading.

In general most of the investigators have considered the behaviour of reinforced normal weight concrete as a basis of comparison for reinforced lightweight concrete.

In the following paragraph a brief review of the available data from previous investigations is presented. This, however, covers only lightweight concrete made with various types of synthetic lightweight aggregate.

2.1.2 Summary of Past Research

Many researchers have been involved for some time investigating the physical and structural aspects of various types of lightweight aggregate concrete, which can be used in construction. It would be difficult to draw conclusions regarding the physical and structural properties of lightweight concrete due to the great variation in the choice of produced lightweight aggregate. This is generally beyond the scope of the present investigation. However, the properties relevant to the present investigation are the modulus of elasticity, flexural strength, extensibility, shrinkage and creep.

As regards the modulus of elasticity of lightweight concrete, many investigators have compared this value with that of normal weight concrete of similar strength. The following table is prepared to illustrate this difference.

Reported by	$\frac{E\ (lightweight)}{E\ (normal\ weight)} \times 100$	Types of lightweight aggregate
J.J. Shideler, 1957 (11)	53 - 82	Various types produced in U.S.A.
J.A. Hanson, 1958 (30) and 1961 (31)	50 - 67	Ditto
A. Short, 1958 (8)	33.3 - 67	Various types produced in U.K.
D.C. Teychenne, 1967 (9)	50 - 60	Sintered expanded and sintered pulverised fuel ash.
G.B. Welch & B.J.F. Patten 1964 (32)	No specific value given	Sand - expanded shale.
R.H. Evans & T.R. Hardwick 1960 (33)	about 60	Sintered expanded clay

One of the very early investigations on the structural behaviour of reinforced lightweight concrete members was carried out by Richart and Jensen in 1931 (34). They reported test results at the University of Illinois, for 32 lightweight and normal weight concrete beams reinforced with mild steel. These beams (152.4mm wide, x 304.8mm deep, with 2438.4mm span) were tested under short - term static loading. The main variables in the investigation were the concrete compressive strength and the effect of replacing fine lightweight aggregate by natural sand.

The experimental results showed that the compressive strength had little effect on the ultimate load of the beams. This was possibly due to the beams being under reinforced, where the ultimate strength depended mainly on the moment of resistance of the steel.

In general the deflections of lightweight concrete members are greater than those of the corresponding normal weight concrete. However, when the fine lightweight aggregate was replaced by natural sand, the difference between the deflection of the lightweight and normal weight concrete beams was reduced. The concrete cylinder compressive strength of the beams considered ranged between (12 - 32.6) N/mm^2. It was also concluded that, due to the lower modulus of

elasticity of lightweight concrete, the neutral axis of such beams was lower than those of normal weight concrete.

Hanson carried out a series of tests at the Portland Cement Association laboratories on the structural aspects of lightweight concrete. In 1958 (30) and 1961 (31) he conducted shear investigations on a total of 57 reinforced lightweight and normal weight concrete beams in short-term static loading tests. The beams were tested using span lengths of 1981.2mm and 3048mm with a cross section of 152.4mm wide and 304.8mm deep. The yield stress of the steel reinforcement used was 334 N/mm^2 for the lightweight concrete beams.

The main variables in the investigation were the concrete compressive strength which ranged between (20.7 - 62 N/mm^2), the steel area and the shearing span.

The calculated deflection based on the "Cracked transformed cross section" method showed that the method could predict the actual deflection with reasonable accuracy.

The deflections of lightweight concrete beams at loads where initial diagonal cracking occurred were found to be 15% to 35% greater than those of normal weight concrete beams. The modulus of elasticity of the lightweight concrete, however, was between 50% to 66% of that for normal weight concrete.

Short carried out an extensive research investigation at the Building Research Establishment on the physical and structural properties of lightweight aggregate concrete. In 1959 (8) he reported results of tests carried out to study the flexural behaviour of reinforced lightweight concrete beams. A wide range of lightweight aggregates produced in the U.K. were covered, with different percentages of mild steel employed for the main reinforcement. Similar beams made of normal weight concrete were also tested so as to form a basis of comparison.

In short-term static tests the deflections of lightweight concrete beams at the working load were found to be 10% to 50% greater than the deflections of normal weight concrete beams. The cracking for lightweight concrete beams was also found to be more severe than for similar normal weight concrete beams.

In sustained loading tests the total permanent deflections due to shrinkage and creep, of some lightweight concrete beams were 15% to 45% greater than those

of normal weight concrete beams when measured under the same conditions of temperature and humidity.

As regards the use of high strength steel, Short suggested that, this should be limited by the values of deflection and cracking, other wise, the values of span/depth ratios given in CP114 / 1957 for normal weight concrete should be multiplied by a factor of 0.75.

Evans, also conducted an extensive amount of research at Leeds University on the behaviour of reinforced and prestressed lightweight concrete.

In 1960 Evans and Hardwick (33) reported tests on 34 lightweight and normal weight concrete beams reinforced with mild steel. High strength steel was also used for normal weight concrete beams. It was mainly intended to study the ultimate strength, deflection and cracking characteristics of concrete beams made from sintered expanded clay aggregates.

In short - term static loading tests the immediate deflections of reinforced lightweight concrete beams were 10% to 25% greater than those for corresponding normal weight concrete beams. It was also observed that the cracks in lightweight concrete beams were about 50% wider than those in normal weight concrete beams, and also that they were spaced about 60% closer. At a working steel stress of 138 N/mm^2 the average crack width and spacing in lightweight concrete beams was 0.07mm and 90mm respectively.

They also concluded that the ultimate strength of lightweight concrete beams could be obtained with reasonable accuracy by using Whitney's theory.

In 1964 Evans and Orangun (35). reported the results of short - term static loading tests on 28 sintered pulverised - fuel ash "(Lytag)" concrete beams. The beams were 229mm wide and 381mm deep with 2438mm span.

Two types of steel were used,mild steel with a yield stress of about 275 N/mm^2 and high strength square twisted bars of about 410 N/mm^2 yield stress, various percentages of steel and a wide range of concrete compressive strengths were adopted.

They concluded that the immediate deflection at working load could be calculated by the conventional transformed cracked section method employing a modular ratio of 17, a modular ratio of 30 was suggested for the calculations of

deflection under sustained load.

At a steel stress of about 205 N/mm^2 the maximum crack widths in the beams reinforced with the largest size of the square twisted bars (31.75mm) did not exceed 0.254mm. To control deflection and cracking, a working steel stress of 186 N/mm^2 was suggested.

It was also concluded that the ultimate loads of "Lytag" concrete beams could be satisfactorily calculated by using Whitney's theory. The design by either the load factor method or the elastic method would ensure the required safety factor.

In 1967 Evans and Paterson (36) presented a paper describing tests carried out to investigate the long term deformation characteristics of sintered pulverised fuel ash "(Lytag)" concrete members in both axial compression and bending.

The creep in bending was investigated in two types of beams, the first being 190.5mm wide and 416mm deep with 2438mm span reinforced with different percentages of high strength steel, the second had a cross sectional dimension of (101.6mm x 101.6mm) with 660.4mm span reinforced with a similar percentage of steel. The high strength steel used had a yield stress of about 410 N/mm^2. Normal weight concrete beams were also tested so as to form a basis of comparison.

For the first type of beams it was observed that after 750 days, the ratio of final to initial deflection of lightweight concrete beams ranged between (2-2.33), this however was (2.34 - 3.09) for normal weight concrete.

The maximum crack width at working load in lightweight concrete was found to be greater, but it did not exceed a value of 0.2mm recommended for normal weight concrete in an exposed condition (37).

For the second type of beams a direct comparison for long term behaviour was made with normal weight concrete. The initial deformation of the lightweight concrete was 1.5 to 2.0 times that of normal weight concrete. This ratio dropped rapidly within 100 to 200 days, and then levelled off to a reasonable constant value after a period of 300 days, leaving the total deflection of lightweight concrete beams marginally higher than that of normal weight concrete.

Generally the improvement in the long term deformation of lightweight concrete beams was mainly due to the following:-

1) Greater improvement in the concrete compressive strength for light-weight concrete with time.
2) The low value of the modulus of elasticity of lightweight concrete resulting in a lower neutral axis, consequently a lower average concrete stress for a given applied load.
3) A slow rate of shrinkage which will enable the concrete to gain its full tensile strength, hence it will be more resistant to crack formations.

Roberts, in 1962 (38), presented work carried out at Northampton College, investigating the bond and crack characteristics of reinforced sintered expanded clay aggregate concrete beams tested under short - term static loading tests.

The beams were 190.5mm wide and 304.8mm deep; two types of reinforcement were used, mild steel with a yield stress of 275 N/mm^2 and high strength steel with 0.2% proof stress of 410 N/mm^2.

It was concluded that steel embedded in lightweight concrete had adequate bond strength and therefore there was no need to provide end hooks with deformed bars.

At the level of the working moment spacing of cracks in both lightweight and normal weight concrete beams was about 127mm when deformed bars were used, and 165mm when mild steel was used. The average crack width if deformed bars were used was about 0.1mm at a steel stress of 206.8 N/mm^2. The same crack width was observed at a steel stress of 138 N/mm^2 when mild steel was used.

It was concluded, however, that deformed bars with a working stress of 206.8 N/mm^2 could be used in lightweight concrete beams.

In 1968 Kanoh (39) presented results for a series of tests on long - term deflection of reinforced concrete beams employing artificial lightweight aggregate made in Japan.

Thirty-one reinforced concrete beams were tested, incorporating various percentages and types of tension reinforcement. The concrete used had an average cylinder compressive strength of about 30 N/mm^2 and a modulus of elasticity of about 13.8 KN/mm^2. It was concluded that the general behaviour of the long - term deflection of lightweight aggregate concrete beams was similar to that of normal weight concrete beams. However, it was observed that the ratio of final to initial

deflection for lightweight concrete beams was some what less than that for normal weight concrete beams. This conclusion agrees well with that stated previously by Evans (36).

Swamy and Ibrahim, in 1974 (40), presented results of an investigation carried out to study the short and long - term deflection characteristics of reinforced and prestressed concrete beams made from expanded slate ("Solite", U.K.) lightweight aggregate.

The ordinary reinforced beams were 127mm wide with an effective depth equal to 156mm and 2286mm span.

Of the ordinary reinforced beams, three were made with all lightweight aggregate and one was made with partial replacement of lightweight fines with natural sand. A beam made from normal weight concrete was also tested so as to form a basis of comparison. In these beams various percentages of steel reinforcement were employed; the steel bars used had a minimum yield stress of 410 N/mm^2. The design concrete cube strength at 28 days was 51 N/mm^2.

When a steel ratio of 3.16% was employed, the beams made from all lightweight concrete, concrete with partial replacement of lightweight fines with natural sand and normal weight concrete gave a span to deflection ratios of 434, 317 and 378 respectively at the design load. This showed that lightweight concrete beams had adequate flexural rigidity compared with normal weight concrete.

The maximum crack width at the design load in lightweight concrete beams was nearly equal to that in the corresponding normal weight concrete. At a working steel stress of 207 N/mm^2, the maximum crack width did not exceed a value of 0.15mm.

In long - term loading, after a period of 193 days, the ratio of final to initial deflection was 1.94 for a beam made from all lightweight concrete, and 1.72 for a beam made with partial replacement of lightweight fines with natural sand.

The investigators have shown that the short and long - term deflection of lightweight concrete beams could be calculated by employing CP110 and ACI 318-71 standards.

2.1.3. Conclusions From Past Research

As stated before, due to the wide variation of the lightweight aggregate used, and also due to the limited amount of tests carried out using high strength steel as reinforcement in lightweight concrete members, it would be difficult to draw a definite conclusion regarding the flexural behaviour for these members. It has also been noticed that most of the previous investigators have presented their data in a form of comparison with normal weight concrete beams.

However, the following points on the general behaviour of reinforced lightweight concrete members may be drawn:-

1) The ultimate load of lightweight concrete members could well be predicted by the existing ultimate load theories. The design by either the elastic theory or the load factor method would ensure the required safety factor.
2) The instantaneous deflection of lightweight concrete beam is greater than that of normal weight concrete; this however depends mainly on the modulus of elasticity for both normal and lightweight concrete. The deflection of lightweight concrete members can be calculated by the conventional transformed cross section method using a suitable modular ratio.
3) The crack widths in lightweight concrete beams, in general, are wider than those in normal weight concrete. This, however, is possibly due to the low tensile strength and the additional tensile stresses caused by shrinkage in lightweight concrete beams.
4) In sustained load tests the total deformation of lightweight concrete members may not be significantly greater than that of normal weight concrete. This, however, again depends on the shrinkage and creep characteristics as well as on the modulus of elasticity of the particular type of lightweight concrete under consideration.
5) At this point of time there is not enough data available regarding the behaviour of reinforced lightweight concrete members under fatigue type of loading.

The maximum steel strength used in the past was 410 N/mm^2. This may follow that the above conclusions apply only to lightweight concrete members

reinforced with steel bars of strength not greater than 410 N/mm^2.

2.2. Approaches Employed to Control Cracking and Deflection in Flexural Members Reinforced with High-Strength Steel

2.2.1 General

The problem of concrete weakness in tension is commonly overcome by the traditional use of reinforcing bars, or by prestressing the reinforcement in concrete; the latter method is rather costly.

In flexural members the problem of concrete weakness in tension leads to a considerable amount of cracking and deflection, especially when high working steel stresses are employed.

Recently various methods to try and overcome this deficiency of the concrete have been proposed by various investigators. In a direct approach to this problem methods of employing a closely spaced continuous wire reinforcement (41) and fibre reinforced concrete have been suggested (42) (20). Another method employing a steel channel placed at the soffit of a concrete member fixed and held in position by means of shear connectors has also been adopted (43). These methods are discussed in the following paragraphs:

2.2.2. Closely Spaced Continuous Reinforcement

In conventional reinforced concrete members cracks would form in the tensile zone at relatively low tensile stresses, for this reason the area of concrete in tension, which forms more than half of the total area is usually ignored for design purposes. Past research (44) (45) indicated that good control on the width and spacing of the cracks can be obtained by using smaller diameter reinforcing bars well distributed over the effective concrete area. This concept, however, has not led to a substantial improvement in the cracking mechanism for conventional types of reinforced concrete members. This is mainly due to the traditional limitations of size and spacing of reinforcing bars.

An early suggestion for the use of a more fine and closely spaced reinforcement was first made by Nervi (46). This was reported by Romualdi and Batson (41). This suggestion came out as a result of an experimental investigation carried out on the behaviour of a concrete slab reinforced with a closely

spaced steel wire mesh. The spacing of the wires was about (10.16mm), and the cracks were not observed until the steel was stressed nearly to its yield point. Following this research, in the field of fracture mechanics, a study was made on the effect of riveted stiffeners placed perpendicular to the line of the projected crack extension; these acted as crack arresters in stressed plate structures. In this study Romualdi (47) indicated that: "for certain stiffener spacing and rivet sizes, a condition could be obtained whereby a crack is arrested, or prevented from enlarging at stresses larger than those required to extend the crack in the absence of stiffeners".

It was thought, however, that this mechanism could be applied to reinforced concrete construction where the role of the riveted stiffeners in plate structures is similar to that of reinforcing bars in a concrete matrix. From this concept Romualdi and Batson (41) concluded that "at a reinforcement spacing less than a certain critical value, all potential cracks could be contained between adjacent groups of bars".

Romualdi and Batson presented an experimental investigation on the flexural behaviour of reinforced concrete beams with a closely spaced continuous reinforcement (41).

A total of 19 small scale beams were tested under short - term static loading tests. The reinforcements employed were steel wires of 1.59 and 0.89mm diameter with a yield stress of 634.5 N/mm^2 and 758.6 N/mm^2 respectively. The wire reinforcement was woven into a mesh to facilitate placing in the mould. The horizontal spacings employed between these wires were 12.7mm, 8.45mm and 4.242mm. The vertical distance between the wires was varied according to the diameter of the wires used, for keeping the same percentage of steel. The concrete mix used was relatively wet, and the only aggregate used was sand. This was mainly to facilitate pouring the concrete. Two of the beams were reinforced with ordinary deformed bars of 9.5mm diameter and 275 N/mm^2 yield stress employing a 1.47% of steel area; this percentage of steel was also employed for most of the wire reinforced beams.

It was claimed that for a wire spacing of about 5.08 to 7.62mm, the ultimate strength of the beams was substantially increased; this increase in ultimate strength was about 50%.

The beams did not exhibit any noticeable cracks until the very final stages of loading. The neutral axis was also observed to be lower than that for conventional reinforced concrete beams.

It was concluded that for the failure mechanism obtained this technique could be used for a wide variety of structural applications.

An important feature claimed for this type of construction was that the ultimate strength was much greater than that predicted by the ultimate strength theories. This increase in strength was dependent on the spacing of the reinforcement; the lower the spacing the higher was the ultimate load.

On this point Broms and Shah (48) pointed out that to maintain the same percentage of reinforcement Romualdi and Batson used a small diameter reinforcement with high ultimate strength values. These values, however, were not used in their calculations. Broms and Shah recalculated the ultimate strength of the beams based on these higher values, and found that the effect caused by the spacing of the reinforcement wires on the ultimate strength was negligible.

Abeles (49) on the same line, discussing the paper by Romualdi and Batson (41), suggested that besides the spacing effect on the ultimate strength, the bond between the wires and the concrete should also be taken into consideration. The high efficiency of beams with closely spaced reinforcement may not be obtained, because the space between the wires hardly allows satisfactory insertion and compaction of the mortar around the wires.

Furthermore the method has a restricted usefulness due to practical difficulties in casting and also has very little to offer in economical savings due to the high cost of material and labour involved (50).

However, the concept of using this technique for reducing crack widths may well converge on an idea to employ a new type of construction (fibre reinforced concrete) which is discussed in the following paragraph.

2.2.3 Fibre Reinforced Concrete

The suggestion to use short pieces of steel to improve the properties of concrete was first made in 1910 by Porter (19) as reported by Hannant (22). This was then followed by Biryukovitch et al (42) and Romualdi and Mandel (20)

when they initiated a more practical investigation in this field.

In an early study (41) (51) it was suggested that by the use of closely spaced continuous wire reinforcement a substantial increase in the tensile cracking strength of concrete could be obtained. This was accomplished by arresting the growth of cracks which originate from internal flaws in the concrete. A theoretical study revealed that the tensile strength of concrete was proportional to the inverse square root of the wire spacing.

To provide a more practical technique. Romualdi and Mandel (20) considered that the same concept of crack arrest mechanism could be achieved by adding short pieces of fine wires directly into the concrete mix. It was considered important that the percentage of wires added to the mix should be sufficient, so as to obtain an adequate average spacing of the wires. In their theoretical study they derived an approximate expression for the effective wire spacing for a given percentage and size of fibres. The experimental part of their study included short - term static tests on sand-cement mortar beams.

Most of the beams tested in bending were 44.45mm wide, 76.2 mm deep with 965.2mm span length reinforced with various sizes and percentages of steel wires. Plain beams without any reinforcements were also tested so as to form a basis of comparison.

The ratio for the flexural tensile strength for beams reinforced with fibres to plain beams varied between 1.2 to 2.52 depending on the aspect ratio and percentage of fibres used.

A good agreement was obtained between the earlier theoretical prediction for the tensile cracking stresses and the observed values. It was concluded that the material had unique features which could be used in a wide variety of structural applications where fatigue, thermal shock and cracking are important considerations.

Untraur and Works (52), in their discussion on Romualdi and Mandel's paper, doubted the validity of the claim regarding the effectiveness of the addition of fibre reinforcement to the tensile cracking strength. The tensile cracking strength as defined by Romualdi and Mandel is the stress which corresponds to the first deviation from linearity of the load-deformation characteristic of the material.

If this definition is to be applied, their results show little increase in the tensile cracking strength resulting from the addition of fibre reinforcement. They did, however, confirm Romualdi and Mandel's results that the addition of fibres substantially improved the tensile strength of the concrete.

Abolitz (53), discussing the same paper, placed more emphasis on the stress carrying efficiency of fibres within the matrix. He suggested that the low effectiveness of randomly distributed wires would not be a favourable factor in economic considerations with regards to their use in reinforced concrete construction.

Agbim (54), in discussion of the same paper, drew attention to the difficulty which he experienced in mixing the fibres. He also pointed out that improvements in the strength over plain concrete were mainly obtained in short - term tests. The time effect on these improvements should also be taken into consideration, as in some cases it was found that the improvements obtained may be reduced with time.

Due to the conflicting conclusions drawn on fibre reinforced cement and concrete, many attempts have been made to study the mechanism of fibre reinforcement, and also to investigate the various properties of fibre reinforced cement and concrete.

Shah and Rangan, in 1971 (55), reported an investigation on the mechanical properties of fibre reinforced concrete and mortar. The intention was to study the reinforcing action of randomly distributed steel wires.

In this investigation various small fibrous reinforced concrete and mortar beams were tested to study the tensile, flexural and compressive strengths in relation to conventional reinforced concrete beams.

The steel wires used for the majority of the specimens tested had a cross-sectional dimension of (0.254mm x 0.254mm) with a tensile strength of 828 N/mm^2. The length of the wires varied between 6.4mm and 25.4mm.

From the results obtained Shah and Rangan (55) concluded that the addition of wire reinforcement to concrete and mortar beams had a negligible effect on the load at which cracks initiate in the matrix. This effect was observed for specimens tested with a steel content up to 1.5%. Considering other investigator's results, Shah and Rangan also suggested that this could apply to specimens reinforced with up to 4% of steel wires. They also concluded that the spacing had

little effect on the ultimate tensile strength.

The conclusions suggested by Shah and Rangan differ from that suggested earlier by Romualdi et al (20) (41) with regard to the effect of addition of fibres and the effect of the spacing of the fibres on the tensile strength of the concrete.

In a comparison between fibre reinforced concrete (incorporating three dimensional random distribution of fibres) and conventional reinforced concrete, Shah and Rangan observed that for a 1% reinforcement content beams with a conventional reinforcement gave a maximum flexural load of more than three times that of fibre reinforced concrete.

Swamy and Lankard (56) recently presented a paper describing several practical applications of steel fibre reinforced concrete both in Britain and the U.S.A.

Among the practical applications discussed were the use of steel fibrereinforced concrete in a slab deck of a car park, concrete pipes, pavements, overlays, marine structures and mining and tunnelling constructions.

It was concluded that the ability of steel fibre reinforced concrete to resist cracks propogation and its resistance to thermal shock, fire and dynamic loads make fibrous concrete a unique new construction material.

It is not in the scope of this research to cover investigations carried out in the field of fibre reinforced concrete; however, there are very few examples on the use of fibres in reinforced concrete flexural members.

In 1972 Hannant (57) presented an investigation on the use of steel wires in reinforced lightweight concrete beams. A total of four beams (127mm wide and 230mm deep with 1.83m span) reinforced with 2-13mm diameter bars of 375 N/mm^2 yield stress were tested. The steel wires used were of 0.38mm diameter x 25mm length, two percentages of fibres being employed; these were 1.2% and 1.6% by volume.

Conventionally reinforced normal and lightweight concrete beams with no fibre reinforcement were also tested to form a basis of comparison.

The deflection of the lightweight concrete beams without fibres were between 40% and 50% greater than those for normal weight concrete. With the addition of fibres to lightweight concrete beams, the deflection was similar to that of normal weight concrete.

The cracking tensile stresses for the fibrous lightweight concrete beams were approximately twice that for the plain lightweight concrete beams; the crack widths observed were lower in the fibrous lightweight concrete beams.

Hannant suggested that the saving in deflection and cracking may well lead to the use of high strength steel as a reinforcement in concrete beams.

At the University of London. Samarrai and Elvery (58) have carried out investigation into the use of steel fibres in reinforced concrete members. It was mainly intended to study the effect of steel fibres on controlling crack widths in reinforced concrete members tested in uniaxial tension. The possibility of using high strength steel has also been studied. Variables that were also studied included type (plain or Duoform) size and quantity of fibre and type of main tension reinforcement.

The experimental results showed that the addition of steel wires to reinforced concrete had substantially increased the stress in the main tension reinforcement before a particular crack width occurs. The improvements were also found to be greater when deformed high strength steel bars were used for the main tension reinforcement.

2.2.4 Composite Concrete Construction Using Steel Channels

The idea of employing this method of construction emerged from combining the material of the following types of construction

(i) The use of high strength steel in flexural concrete members

(ii) The composite construction with deep haunches, where a mild steel beam section is incorporated by shear connectors to the soffit of the concrete haunches.

It was thought (43), for a deep haunch section, that by using a channel section instead of a beam section, the bursting or spalling of the concrete due to the low effective side cover to the shear connectors in the haunch could be prevented. The channel could also provide an adequate rigidity to the section so that high strength steel could be used.

On the application of this type of construction (59) a total of 9 beams were tested in short - term static loading tests. These beams were of 4572mm length incorporating different dimension and size of the concrete cross section and the steel

channel. Various amounts of steel were used, the ultimate steel stresses employed ranging between 283 N/mm^2 and 966 N/mm^2.

The beams were designed so that at the working load condition, the maximum stress in the channel did not exceed about 90% of its yield stress.

From the results obtained cracking and deflection at the working load were well below the limits specified in CP110. However, beams reinforced with mild steel and the shallow section beams showed a considerable amount of cracking and deflection respectively.

It was concluded, however, that steel of 828 N/mm^2 ultimate stress could be used while satisfying the limit states of serviceability at the working load conditions.

This type of construction, indeed,has new merits of potential importance in the field of concrete technology; however, there are certain shortcomings and doubts which should be carefully considered, these are:-

(1) The construction has little resistance to fatigue; tests have showed that after about 500,000 cycles failure would occur.

(2) The steel channel being exposed would offer little resistance to fire

2.2.5 Work at Salford

At the University of Salford an extensive amount of research has been conducted into the structural aspects of fibre reinforced cement and concrete.

In 1971 (60). research was conducted on the use of chopped steel wires in a concrete matrix. The major part of the work was carried out using two sizes of fibres 0.5mm diameter x 38mm length and 0.38mm x 25mm length, the wires were plain and Duoform. The percentages of steel used varied between 1% and 3% by volume.

Properties investigated were the cube crushing strength, flexural strength, direct and indirect tensile strengths. In carrying out the experimental investigation difficulty of mixing and compacting the wires was experienced. It was also observed that the greater the aspect ratio of the wires the greater is the tendency for the wires to knit into balls.

The results showed that certain improvements were obtained in the compressive and the flexural properties of the fibrous concrete. The peak of the improvement was

at a spacing of about 4mm, below which the results obtained became erratic.

Comparing the performance of fibrous concrete containing plain steel fibres at 4mm spacing with that of plain concrete, the improvements expressed as a percentage for the compressive, flexural, indirect and direct tensile strength were 11, 83, 57 and 20 respectively.

In 1972 (24) a research was carried out investigating the structural properties of normal and lightweight concrete and cement mortar reinforced with three dimensional random distribution of asbestos fibres.

Various types and percentages of asbestos fibres by weight of cement were incorporated in the matrix . The workability of the mixes was observed to decrease as the amount of fibres increased.

Certain improvements in the compressive, tensile and impact strengths of the cement mortar and concrete were also obtained. These improvements were fairly small and largely influenced by the volume content of fibres, the type of aggregate and the water cement ratio of the mix.

Other reasons why the improvements in the properties of the fibrous matrices were low are as follows:

(i) The low directional efficiency of three dimensional random distribution of fibres.

(ii) The short length of the asbestos fibres used (less than 6mm) allowed little stress transfer from the matrix to the fibre.

It was suggested in this investigation that ways of preferentially aligning the fibres should be found.

Investigation has also been carried out into the flexural behaviour of full scale partially prestressed composite T-beams with three dimensional random distribution of steel fibres in their tensile zone (61). This investigation showed that steel fibre reinforcement can result in some improvement in cracking and deflection of partially prestressed composite T-beams.

Conclusions drawn from previous investigations show that substantial improvements were obtained in the properties of the concrete when high modulus fibres were used. However, it is still doubtful to what extent these improvements could be utilized in reducing the cracking and deflection in reinforced concrete members.

The material is still in the development stage, and there are not enough data available regarding the effect of the fibres on the control of deflection and cracking, especially under long term loading conditions.

The initial work at Salford and other places has revealed that the addition of fibre reinforcement in three dimensional random distribution is not a practical or an economical proposition in reinforced concrete construction. A new concept has been developed at Salford which involves the use of precast units of fibre reinforced cement as surface reinforcement for concrete members with a view to controlling cracking and deflection (62) (63).

This type of fibre reinforced cement composite concrete construction in which precast asbestos cement units are used as surface reinforcement forms the basis of work presented in this thesis.

CHAPTER THREE

MATERIALS USED AND DESIGN OF TEST BEAMS

3.1 General

The main aim of this investigation was to study the structural behaviour of ordinary and composite lightweight concrete members reinforced with high - strength steel.

It was deemed necessary to provide experimental evidence regarding the cracking and deflection behaviour of these members for a comparison to be made with the predicted values. Furthermore the experimental results would also help to ascertain values of constants in empirical relationships.

The programme of investigation consisted of testing full-scale reinforced lightweight concrete beams, containing different types and percentages of steel bars for the main tension reinforcement.

The size of beams was chosen to represent members commonly used in building construction and to enable the performance of such members to be critically examined.

The beams adopted were 150mm wide, 300mm deep and 5m long. These were simply supported over a span of 4.5m. The loading arrangement of the beams is shown in Fig. 3.

The composite beams were similar to the ordinary beams in every respect, except that the f.r.c. units were incorporated as integral parts at their tensile zones.

Control specimens, e.g. cubes and prisms, were also cast to ascertain the compressive and tensile strengths of the concrete. The design, manufacture and test procedures employed in this research were in accordance with the specifications given in CP110 and the various British Standards.

In the following paragraphs the materials used and the design considerations for the f.r.c. units and the test beams are discussed.

3.2 Design Considerations

3.2.1 Ordinary Reinforced Lightweight Concrete Beams

As mentioned in 3.1, the beams adopted were 150mm wide, 300mm deep with 4.5m span and were designed as under reinforced beams. The nominal yield or 0.2%

proof stresses of the reinforcing bars used were 275 N/mm^2, 410 N/mm^2, 550 N/mm^2, 590 N/mm^2 and 875 N/mm^2; the steel ratios employed were 0.582%, 1.044%, 1.483% and 1.643%. Details of the beams reinforcements are given in tables 1, 2 and 3; these are also shown in Figs.4 and 5.

The designed characteristic cube strength of concrete was 50 N/mm^2. The nominal concrete cover to the main reinforcements was 35mm, this being the minimum allowed for lightweight concrete members in severe conditions of exposure as per CP110.

For calculating the design working moment of the various beams, the limit state of ultimate strength, as per CP110, was considered to be the main criterion for design. In this calculation a rectangular - parabolic stress distribution incorporating the partial safety factor for the concrete at the ultimate condition was used. The adopted stress-strain relationship for the lightweight concrete in compression is shown in Fig. 6. Fig. 7, shows the stress-strain curves as per CP110.

The beams being under reinforced, their ultimate resistance moments would be those based on the yielding of the steel.

The values of the ultimate moments can be calculated as follows:

$$M_u = \frac{f_y}{\gamma_m} A_s Z \qquad (3.1)$$

γ_m = partial safety factor for steel (1.15)

$$\text{where} \quad Z = d_1 - \frac{\beta f_y A_s}{\alpha \gamma_m b f_{cu}} \qquad (3.2)$$

The values of β and α can be derived by considering a rectangular - parabolic stress distribution for the concrete in compression; this is shown in appendix B. The working moment was obtained by subtracting 1.4 times the moment due to dead load of the beam from the ultimate resistance moment, then dividing by (1.6), the values 1.4 and 1.6 being the partial safety factors for dead and live load respectively. The air dry density used in the calculation for the lightweight concrete was 1800 kg/m^3.

The details of the reinforcement and the calculated values of the ultimate and working moments for the various beams tested under static, fatigue and sustained types of loading are given in tables 1, 2 and 3 respectively. A typical analysis of a beam is given in appendix C.

For the shear reinforcements rectangular mild steel stirrups of 6mm diameter were provided for all the beams at a uniform spacing of 100mm. None, however, was provided in the constant moment zone, mainly to avoid any effect which the stirrups might have on the initiation and distribution of the cracks. This practice has also been adopted by previous investigators (35) (64) (65). The design of the stirrups was carried out in accordance with the ultimate shear stress requirements for lightweight concrete as given in CP110. It was necessary to ensure that the beams would not fail in shear, as the flexural behaviour of the beams up to failure was to be studied.

The local and anchorage bond stresses for the various beams were calculated in accordance with CP110. When mild steel was used for the main tension reinforcement, U-type hooks were provided; however, no hooks or any type of anchorage devices were provided for the deformed bars as it was not necessary. It was also intended to prevent bond failure at the ultimate load, since the ultimate flexural resistance moment based on yielding of the steel was to be observed.

3.2.2 Composite Reinforced Lightweight Concrete Beams

The parameters employed for the composite beams were the same as those for the ordinary beams. To allow a direct comparison to be made between the flexural behaviour of both types of beams, the composite beams were similar to the ordinary beams in every respect, except that the f.r.c.units were incorporated as integral parts at their tensile sides.

For the various composite beams, the nominal yield or 0.2% proof stresses used for the reinforcements were 275 N/mm^2, 410 N/mm^2, 550 N/mm^2 and 590 N/mm^2. The steel ratios employed were 0.582%, 0.874%, 1.044% and 1.643%. The details of the reinforcements are given in tables 1, 2 and 3 and also are shown in Figs 4 and 5.

In deriving the working moment, the limit state of ultimate strength was considered to be the main criterion for design, no account being taken of the contribution made by the f.r.c.units. The contribution made by the f.r.c.units, if any, was considered to be an additional factor of safety.

The calculated values of the ultimate and working moments for the various beams tested under static, fatigue and sustained types of loading are given in

tables 1, 2 and 3 respectively.

The properties and design considerations for the f.r.c units are discussed in detail in 3.2.3.

3.2.3 Fibre Reinforced Cement Units (f.r.c.Units)

3.2.3.1 Properties

It was most important that the f.r.c.units to be used should have much higher tensile strength and greater extensibility compared with those of concrete. Properties also considered desirable for these units were the impact strength, thermal insulation, fire resistance, durability and resistance to the attack by alkalanity from the atmosphere.

The choice of fibres was limited to those having a high modulus of elasticity and which could be easily incorporated into a cement matrix and be fabricated into sheet or channel forms.

The types of fibres which in general fitted most of these requirements were glass and asbestos.

Steel wires also have a high modulus, but they cannot be easily incorporated into a cement matrix and be fabricated into sheets or channel forms.

As regard the E-glass fibres, there is a problem of long-term durability in the presence of an alkali environment. E-glass fibre when incorporated in ordinary portland cement would loose most of its strength due to the alkalanity of ordinary portland cement. This problem can be overcome to some extent by the use of alkali resistant glass fibre which can be incorporated in a cement matrix by a spray and suction technique, allowing f.r.c.sheets or channel forms to be fabricated. The durability of these f.r.c.units in long term application, however, is not known.

Asbestos fibres being the cheapest form of high modulus fibres, and having a greater durability under moist conditions were considered to be the most favourable type that could be used in a cement matrix. The asbestos cement sheets are manufactured in layers. This process results in the asbestos fibres being distributed in predominantly two dimensional random fashion.

For normal asbestos cement products the length of fibre used is 6mm and less, the fibre content normally being 10-12% by weight of cement, giving a product density

of 1700 - 1900 Kg/m^3 (66) (67).

To satisfy the requirements of this investigation for ease of construction and economy in cost per unit, the channels were manufactured as normal asbestos cement products.

The mechanical properties of the fibre reinforced cement units used are given in table 4 with the tensile properties shown in Fig. 8.

For the various composite beams, initial calculations were carried out, using the simple bending theory to obtain the amount of tensile stresses which could be developed in the f.r.c. units when placed at the soffits of the beams. These stresses were then checked against the tensile stress of the f.r.c. units. The important consideration in the use of the f.r.c. units was that they would not crack at the working load conditions.

3.2.3.2 Geometry

Throughout the investigation one type of fibre reinforced cement unit with similar properties and geometry was used. A channel section was chosen to provide a surface reinforcement on the area which was subjected to maximum flexural tensile stresses and strains. The length and width of a channel depended on the dimensions of the concrete beam.

In choosing the thickness and height of the upstands, the following points were considered:-

1) The thickness and height of the upstand should be such, that an adequate tensile strength is provided so as to avoid surface cracking at the working load conditions.
2) Consideration was also given to eliminate cracking under design working load, at the soffit of the beams as well as at the level of the reinforcement to prevent the corrosion of the steel. The concrete cover to the main reinforcement was 35mm and the maximum size of bar used was 20mm; this gave an overall dimension of 55mm. For the purpose of this research the average height of upstand chosen was 60mm.

Considering these points, the cross section chosen for the f.r.c. channels was 150mm wide, 6mm thickness with 60mm height of upstands, the length of the channel being 4900mm.

The cross section of the f.r.c. channels is shown in Fig. 5.

3.3. Materials

3.3.1 Lightweight Aggregate Concrete

The lightweight aggregate chosen was the sintered pulverised fuel ash commercially known as "Lytag". The choice of this type of aggregate was made mainly because previous investigations showed, that it had good prospects in structural applications (35).

The constituents of the lightweight aggregate concrete used in the investigation were rapid-hardening cement, natural sand zone 3 as a fine aggregate and medium "lytag" 13 - 10mm as coarse aggregate.

The use of natural sand as a fine aggregate was mainly intended to improve the structural properties of the concrete (12) (3).

The intended 28 days cube strength was 50 N/mm^2 with a concrete air dry density of 1700 - 1800 Kg/m^3. When choosing the size and mix proportions of the aggregate, the recommendations of the manufacturers (68) and a previous research (69) were considered. The mix proportions finally adopted were 1:0.83:1.64 by weight for rapid-hardening cement, natural sand and medium "Lytag" respectively.

The grading of the aggregate used was checked according to the B.S. 3797:1964 (70) for the lightweight aggregate and B.S. 882 and 1201:1965 (71) for the natural aggregate; this is shown in Fig. 9. The sieve analysis tests were carried out according to B.S. 812 (72).

Trial mixes for the concrete were carried out to fix the water cement ratio for the required workability and strength. The water cement ratio was found to be 0.59, which gave a medium workability for the mix. The air-dry density for the concrete varied between 1675 Kg/m^3 and 1860 Kg/m^3.

To improve the workability of the mix without increasing the water cement ratio and to maintain the required cube strength the admixture "Febflow" standard grade was added to the mix. The amount of "Febflow" added was 140cm^3 per 50 Kg cement; this was according to the manufacturers' recommendations.

3.3.2 Reinforcement

The sizes and types of the various bars used in this research as main tension reinforcements were as follows:-

1) mild steel; plain round bars with a nominal yield stress of 275 N/mm^2. The sizes used were 12mm, 16mm and 20mm.
2) Unisteel 410; hot rolled deformed bars with a nominal yield stress of 410 N/mm^2. The sizes used were 12mm, 16mm and 20mm.
3) Unisteel 550; cold worked deformed bars, produced by cold stretching Unisteel 410, with a nominal 0.2% proof stress of 550 N/mm^2. The sizes used were 16mm and 19.05mm.
4) Kam 60; natural hard ribbed steel, manufactured in Sweden. The figure 60 refers to the yield stress in Kg/mm^2. The nominal yield stress adopted in this research was 590 N/mm^2. The sizes used were 12mm and 16mm.
5) Kam 90; cold worked steel, produced by cold stretching Kam 60 steel by 5%. The number 90 refers to the 0.2% proof stress in Kg/mm^2. The nominal 0.2% proof stress adopted in the research was 875 N/mm^2. The size of the bars used was 16mm.
6) Lancasteel 60; hot rolled heavily deformed steel bars, the number 60 refers to the yield stress in Ksi. The nominal yield stress adopted in this research was 410 N/mm^2. The size of the bars used was 16mm.

Typical stress-strain curves for the various types of reinforcement are shown in Fig. 1 their tensile properties are given in table 5.

CHAPTER FOUR

THEORETICAL BASIS OF ANALYSIS FOR STRESSES IN CONCRETE, STEEL AND f.r.c.CHANNELS

4.1 Introduction

In reinforced concrete flexural members the steel stress is an important factor when determining the width of the cracks and the curvature of the beam. When determining the steel stresses in composite beams the stresses in the f.r.c. channels are also an important consideration.

The steel stresses for ordinary and composite beams are calculated by employing the general equation of compatibility of moments. In using this equation it is important that the level of the neutral axis and the geometric shape, centroid and area of the compressive stress distribution in the concrete are determined. For composite beams it is necessary to determine the stress distribution in the f.r.c. channels in order to calculate the position and magnitude of the tensile force.

Relationships based on theoretical considerations and analysis of test results have been established with the applied moment for the neutral axis level, flexural compressive strain in concrete, area and centroid of the compressive stress distribution in concrete and stress in the f.r.c.channels. These relationships have been established to enable the stress in the tension reinforcement for both ordinary and composite beams to be calculated at any level of applied moment.

4.2 Variations of the Neutral Axis Level

The level of the neutral axis is an important factor when determining the steel stress and the curvature of reinforced concrete flexural members. In general, the position of the neutral axis depth at any level of applied moment depends upon the geometry of the section (this includes the percentage of steel), the properties of the materials and whether the member is cracked or not. Conditions of equilibrium for the member should also be satisfied.

The depth of the neutral axis for a fully cracked or an uncracked concrete section can be determined by employing the elastic theory approach. A fully cracked concrete section is that when most of flexural cracks have been developed and that the contribution of the concrete in the tensile zone has become negligible. At the stage between the uncracked and fully cracked conditions the level of the neutral axis can be calculated by relationships based on experimental results. The variation of the neutral axis level in relation to the applied moment at this stage is primarily caused by the propagation of flexural cracks towards the compression face of the member.

For the stage between the uncracked and fully cracked conditions of a concrete member a simplified straight line relationship has been suggested (73). However, analysis of the experimental results of previous investigations suggests that a curvilinear relationship could be used. (4) (74) (75).

In this research a study is made regarding the variation of the neutral axis depth in relation to the applied moment up to failure. An idealised relationship is suggested between the level of the neutral axis and the ratio of the applied to ultimate moment as shown in Fig.10 .

The relationship can be divided into the following stages:- (The values of C_o, C_1 and C_2 are discussed in 7.2)

Uncracked stage From $M/M_u = 0$ to $M/M_u = C_o$

At this stage it is assumed that the concrete is uncracked and the neutral axis level can be determined by considering an uncracked transformed section employing the elastic theory approach. The equations are:

For ordinary beams:

$$n = \frac{X_{uo}}{d_1} = \frac{\lambda^2 + 2\,(m-1)p}{2\,[\lambda + (m-1)]\,p} \qquad (4.1)$$

For composite beams:

$$n = \frac{X_{uc}}{d_1} = \frac{0.5\,\lambda^2 + (m-1)p + (m_1-1)p_1\,\eta^2}{\lambda + (m-1)p + (m_1-1)p_1\,\eta} \qquad (4.2)$$

Where $\lambda = d/d_1$, $\eta = d_2/d_1$

The derivation of equation 4.2 is shown in appendix D1, a similar approach can be employed for deriving equation 4.1

For ordinary lightweight concrete beams the range of the uncracked behaviour is very limited mainly because of the early formation of cracks in these members. This suggests that the value of C_o in Fig.10 can be taken as zero and that the neutral axis level would rise above the level of the calculated value for the uncracked transformed section once loading has commenced. Experimental evidence, however, in this respect is necessary.

Transition Stage From $M/M_u = C_o$ to $M/M_u = C_1$

At this stage the movement of the neutral axis as mentioned earlier is greatly influenced by the formation and extension of the flexural cracks. When cracking occurs the steel will be strained considerably, mainly because of the sudden transfer of the tensile stresses from the concrete to the steel. This immediate increase in the steel strains can further raise the levelof the neutral axis towards the compression face of the member.

Considering a gradual propagation of flexural cracks, the variation of the neutral axis with the applied moment can follow a curvilinear relationship. This behaviour as mentioned before can also be seen in results of previous investigations. It is therefore suggested that a parabolic curve may be used for the relationship at this stage between the neutral axis depth and the ratio of applied to ultimate moment. The assumptions used and the derivation of the equations can be seen in appendix D3. The equations are:-

For ordinary beams:

$$X = \frac{X_{uc} - X_{cc}}{C_1^2} (R^2 - 2 C_1 R) + X_{uc} \qquad (4.3)$$

For composite beams:

$$X = \frac{X_{uc} - X_{cc}}{C_o^2 - 2 C_o C_1 + C_1^2} (R^2 - 2 C_1 R + C_1^2) + X_{cc} \qquad (4.4)$$

For both equations $R = M/M_u$

Fully Cracked Stage From $M/M_u = C_1$ to $M/M_u = C_2$

At this stage the concrete is assumed to be fully cracked, and the neutral axis depth can be determined by considering a cracked transformed section employing the elastic theory approach. The variation of the neutral axis at this stage is very small and can almost be neglected.

The equations are:

For ordinary beams:

$$n = \frac{X_{co}}{d_1} = mp \left(\sqrt{1 + \frac{2}{mp}} - 1 \right) \qquad (4.5)$$

For composite beams:

$$n = \frac{X_{cc}}{d_1} = (mp + m_1 p_1 \eta) \left(\sqrt{1 + \frac{2 (mp + m_1 p_1 \eta^2)}{(mp + m_1 p_1 \eta)^2}} - 1 \right) \qquad (4.6)$$

The derivation of equation (4.6) is given in appendix (D2), a similar approach can also be employed for deriving equation (4.5)

Non-elastic stage From $M/M_u = C_2$ to $M/M_u = 1$

At this stage it is assumed that steel and/or concrete are in their non-elastic range of behaviour, and that. therefore the rate of strain due to the applied moment is considerably increased. This increase in the rate of strain, especially in the steel, can have a considerable effect on raising the neutral axis level towards the compression face of the member. Another factor which also may be considered is that the rate of increase in the steel stress at this stage is much lower than that at the elastic range of behaviour. The level of the neutral axis will therefore rise to provide a greater lever arm to the forces in the steel, thus satisfying the conditions of equilibrium.

An attempt is made to correlate the neutral axis depth calculated by the strain compatibility method at the ultimate moment with the value of $M/M_u = 1$. The behaviour described above is generally applicable to under reinforced beams.

4.3 Analysis of Compressive Stresses in Concrete

4.3.1 Stress-Strain Relationship of lightweight Concrete in Compression

The rectangular - parabolic design stress-strain curve for concrete in compression given in CP110, and as shown in Fig.7 incorporates the properties of normal weight concrete. This is shown by the initial tangent modulus drawn to the curve at zero strain given in terms of the modulus of elasticity for normal weight concrete, and also by the value of strain at the junction (e_j).

For lightweight concrete having a similar strength to that of normal weight concrete the modulus of elasticity would be lower. Assuming a similar stress-strain relationship in compression, the initial tangent modulus at zero strain for lightweight concrete will be lower. This will affect the value of strain at the junction (e_j), which will be greater than that for normal weight concrete. Considering both concretes have the same maximum value of strain (0.0035), the area under the curve for lightweight concrete, at the same level of stress, would be smaller than that of normal weight concrete.

In this research the stress-strain curve for the lightweight concrete was derived, employing the initial modulus of elasticity for lightweight concrete as recommended by CP110. This is shown in appendix (A). The stress-strain relationship without incorporating the partial safety factor for the material is shown in Fig. 6 a. The design relationship can be obtained by dividing the values of Fig.6a by the partial safety factor ($\gamma_m = 1.5$).

4.3.2 Variations of the Flexural Compressive Strain in Concrete

For determining the shape, centroid and area of the stress distribution across the depth of the compression zone it is important that the strain profile is known. The compressive strain profile is also important in the determination of the curvature of a flexural member.

In this research it is intended to study the variation of the flexural compressive strain in the concrete in relation to the applied moment up to failure. As shown in Fig.11 a a simplified bilinear relationship is suggested between the ratio of the applied moment to ultimate moment and the maximum compressive strain in the concrete. This concept agrees well with experimental results of a previous

investigation on normal weight concrete flexural members (4). The variation of the compressive strain in the concrete is assumed to have a straight line relationship with the applied moment up to a value of $M/M_u = C_p$ (The value of C_p is discussed in 7.4). The values of the concrete strain at this stage can be predicted by employing the equation of compatibility of moments together with the assumption of a straight line strain distribution. For the composite beams the moment of the tension side also includesthe resisting moment of the f.r.c.channels.

However, at the value $M/M_u = C_p$, the f.r.c. channels in the composite beams might have been cracked. If this was the case, the analysis of the composite beams should be carried out without considering the effect of the f.r.c. channels.

In the non-elastic phase (From $M/M_u = C_p$ to $M/M_u = 1$) it is assumed that the [illegible] concrete and/or steel are in their non-elastic range of behaviour and that, therefore, the rate of strain in the concrete is considerably increased due to applied moment. What also may affect the values of the concrete strain is the considerable rise of the neutral axis and the consequent reduction in the area of the compression zone. In order to satisfy the conditions of equilibrium, higher stress values will be developed in the concrete, which will lead to a greater rate of strain up to failure.

At the moment of failure ($M/M_u = 1$) the maximum strain in the concrete (e_{max}) will be reached. The factors which may affect the maximum compressive strain in the concrete are discussed in 5.2.1 , As per CP110 the value of e_{max} is equal to 0.0035. The relationship at the non-elastic phase as shown in Fig.11 a is represented by a straight line between $M/M_u = C_p$ at $e_c = e_p$ and $M/M_u = 1$ at $e_{max} = 0.0035$.

4.3.3. Variations of the Area and Centroid of the Compressive Stress Distribution in Concrete

The area and centroid of the compressive stress distribution in the concrete are important considerations when determining the steel stresses in flexural members. In CP110 the stress-strain relationship for concrete in compression is assumed to have a parabolic-rectangular distribution. The derived relationship for lightweight concrete is shown in Fig. 6 a ,

Values of coefficients for the centroid and area of the stress distribution diagram depend upon the magnitude of the compressive strain in the concrete. In flexural members this would depend upon the flexural compressive strain in the concrete at the extreme element of the compression zone. It is therefore deemed necessary to derive relationships between the concrete compressive strain and the centroid and area of the compressive stress distribution diagram in the concrete. From theseit would then be possible to predict the values of β for the centroid of the stress distribution diagram and a for the area of the stress distribution diagram at any level of moment once the maximum flexural strain in the concrete at that moment is known. Fig 12b shows the variation of the values of β and a in relation to the compressive strain in the concrete. The geometrical shape of the stress-strain relationship of the concrete as shown in Fig. 12a was considered in the derivation of the equations. This is shown in appendix E.

The equations are: (Reference can be made to Fig 12)

For (i) when the compressive strain in concrete e_c is less or equal than e_j ($0 < e_c \leq e_j$)

$$\beta = \frac{4\ e_j - e_c}{12\ e_j - 4\ e_c} \tag{4.7}$$

$$a = \frac{3\ e_j - e_c}{6\ e_j - 3e_c} \tag{4.8}$$

For (ii) $(e_j \leq e_c \leq e_{max})$

$$\beta = \frac{6\ e_c^{\,2} - 4\ e_c\ e_j + e_j^{\,2}}{12\ e_c^{\,2} - 4\ e_c\ e_j} \tag{4.9}$$

$$a = \frac{3\ e_c - e_j}{3\ e_c} \tag{4.10}$$

$e_j = 0.00282$ see appendix (A) Fig. 6

$e_{max} = 0.0035$ (assumed compressive strain in concrete at failure)

Values of e_c which represent the maximum concrete compressive strain at the extreme element of the compression zone of flexural members can be determined at any level of applied moment either from experimental data or calculated as shown in 4.3.2.

4.4 Analysis of Stresses in f.r.c.Channels

Magnitude, distribution and centroid of tensile stresses in the f.r.c channels are important in determining the steel stresses for composite beams. The assumed distribution of tensile stress in the f.r.c.channels for the composite beams is shown in Fig. 13.

Considering the basic assumptions as stated in 4.5.1 to calculate the steel stresses in composite beams (plane sections remain plane after bending and perfect bond between the f.r.c.channel and concrete), the composite section can be analysed by the simple bending theory. As shown in Fig.11b, a bilinear concept is used for the relationship between the maximum stress in the f.r.c.channels and the applied moment, taking into consideration whether the concrete section is cracked or not.

For the first stage the composite section is analysed assuming an uncracked concrete section. Once the concrete has cracked (at M_c) the composite section should then be treated as a cracked concrete section taking into consideration the initial uncracked behaviour and an effective values for the second moment of area of a cracked section and modulus of elasticity for the f.r.c.channels and concrete.

The mathematical expressions for the calculation of the maximum stresses in the f.r.c.channel at the two stages are given in the following:

(i) For ($M \leq M_c$)

$$f_{ab} = \frac{M\ (d - X_{uc})}{I_{uc}}\ m_1 \qquad (4.11)$$

Where M_c : is the cracking moment for the concrete at the interface.

$$M_c = \frac{f_{rc}\ I_{uc}}{d - \frac{d - X_{uc}}{}} \qquad (4.12)$$

(ii) For $(M_c \leq M \leq M_a)$

At an applied moment M (greater than the cracking moment of the concrete M_c) as shown in Fig. 11b the stress at the soffit (f_{ab}) is equal to:

$$f_{ab} = f'_{ab} + f''_{ab}$$

Where f'_{ab} and f''_{ab} are the stresses corresponding to the bending moment (M_c) and $(M - M_c)$ respectively.

Therefore:

$$f_{ab} = \frac{M_c \ (d - Xuc)}{I_{uc}} m_1 + \frac{(M - M_c) \ (d - X_{cc})}{\beta_1 \ I_{cc}} m_1 \qquad (4.13)$$

Where β_1 is a factor depending on an effective second moment of area for a cracked section (I_{cc}) and the modular ratio (m_1).

The assumed cracking moment of the concrete in the composite beams is that when cracks are observed at the interface. This is mainly because cracks which may form in the confined concrete will have no significant effect on the flexural behaviour of the member due to the restraint action of the f.r.c units.

Average values of the modulus of rupture for lightweight concrete are between 2 and 2.5 N/mm^2. This, however, can be increased to 3 N/mm^2 for the composite section at the interface due to the restraint action of the f.r.c.channels.

Considering the straight line stress distribution for f.r.c.channel as shown in Fig.13 the tensile stress at the top element of the upstand (f_{at}) can be obtained as follows:-

$$f_{at} = \frac{d - \acute{d} - x}{d - x} \ f_{ab} \qquad (4.14)$$

The tensile force in the f.r.c channel (T_a) can be determined from the following:-

$$T_a = (f_{at} + f_{ab}) \ (\acute{d} - t)t + f_{ab} \cdot \ b \cdot t \qquad (4.15)$$

To determine the effective depth d_2 for the tensile force T_a, the centroid of the stress distribution should be determined. The distance (d_a) for the centroid of the stress distribution from the soffit can be obtained from the following expression:

$$d_a = \frac{f_{at} \ (\acute{d}^2 - t^2) + (f_{ab} - f_{at}) \ (\acute{d}^2 + t\acute{d} - 2t^2) \ /_3 + f_{ab} \cdot b \cdot t/_2}{(f_{at} + f_{ab}) \ (\acute{d} - t) + f_{ab} \cdot b} \qquad (4.16)$$

This was obtained by taking moments of area of the stress distribution in the f.r.c. channel shown in Fig. 13, about the soffit of the channel.

Therefore $d_2 = d - d_a$

4.5 Calculation of Steel Stresses

4.5.1 Assumptions

The assumptions made for the calculation of the steel stresses for ordinary and composite beams are as follows:

(1) Average strain distributions for concrete in compression, reinforcement and the f.r.c.channels are derived from the assumption that plane sections remain plane after bending, irrespective of whether the concrete section is cracked or not.

(2) The stress-strain relationship for concrete in the compression zone of a beam follows a parabolic-rectangular distribution as shown in Fig. 6a

(3) The contribution of the concrete in tension is ignored.

(4) The variation of the neutral axis depth in relation to the ratio of applied to ultimate moment follows a parabolic straight line relationship as shown in Fig. 10.

(5) The relationship between the flexural compressive strain and the applied moment is based on a bilinear concept as shown in Fig. 11

Additional assumptions made for the composite beams are as follows:-

(1) Stresses in the f.r.c.channels can be obtained either from the bilinear relationship between the stress and the applied moment suggested earlier or from the experimental stress-strain curve of the f.r.c.units as shown in Fig. 8

(2) The stress gradient for the f.r.c. channels is a straight line which passes through the neutral axis Fig. 13.

(3) The contribution of the f.r.c. channels on the tensile side is ignored once cracking occurs in them.

(4) There is a perfect bond between the f.r.c.channels and the concrete enabling the units to be fully co-operative in the composite action.

The mathematical procedure adopted for the calculation of the steel stress for the ordinary and composite beams is discussed in the following paragraphs.

4.5.2 Ordinary Lightweight Concrete Beams

The steel stress at any level of moment is calculated by employing the general equation of equilibrium for the applied moment and the internal moment of resistance based on steel. The equation is:

$$M = A_s f_s (d_1 - \beta x) \qquad (4.18)$$

The values of the neutral axis depth (X) and the coefficient for the centroid of the compressive stress distribution (β) can be determined at any level of moment as shown in the previous paragraphs.

For X paragraph (4.2)

For β paragraph (4.3.3)

The steel stress may also be checked by the equation of equilibrium for the tensile and compressive forces

$$A_s f_s = a f_c b X \qquad (4.19)$$

This, however, requires an accurate prediction of the value (f_c) at any calculated or experimental value used for the strain in the concrete (e_c)

The stress-strain relationship assumed for the concrete in the compression zone of flexural members is shown in Fig. 6a. It should be noted that this relationship is based on direct compressive tests on concrete cylinders.

The stress-strain relationship in flexure, as discussed in 5.2.2, may be different from that assumed above. Therefore, the results obtained by using the idealised stress-strain relationship, Fig. 6a, may not be very accurate.

4.5.3. Composite Lightweight Concrete Beams

The steel stress in the composite beams is calculated by the following stages:

(1) For applied moment up to the cracking moment of the f.r.c. channels ($M \leq M_a$). At this stage the contribution of the f.r.c. channels in tension is considered in the calculation. The equation employed is:

$$M = f_s A_s (d_1 - \beta X) + Ta (d_2 - \beta X) \qquad (4.20)$$

The values of X and β can be determined in a similar manner as that for the ordinary beams (explained in 4.2, and 4.3.3). The values of the tensile force

in the f.r.c. units (T_a) is dependent upon the state of the composite section whether the concrete is cracked or not. This is discussed in 4.4. The effective depth d_2 can also be determined as shown in the same paragraph.

(2) For an applied moment greater than the cracking moment of the f.r.c. channel ($M \geq M_a$).

At this stage the contribution of the f.r.c. channels in tension is ignored and the section is analysed as that for ordinary beams. This is mainly because the maximum steel stress will occur in the vicinity of cracks where the restraint action of the f.r.c. channel is not effective. The equation employed is the same as that for the ordinary beams (e.g. equation 4.18 in 4.5.2)

The values of β and X can be determined in similar manner as explained previously.

4.5.4 Summary for the Theoretical Calculation of Steel Stresses

(1) Calculate the ultimate moment of the member by a suitable plastic method.

(2) For any level of moment calculate the neutral axis depth as shown in 4.2 and Fig. 10.

(3) For any level of moment calculate the maximum flexural compressive strain in the concrete as shown in 4.3.2 and Fig. 11a.

(4) Calculate the values of β and α for the centroid and the area of the compressive stress distribution in the concrete, as shown in 4.3.3. and Fig. 12.

(5) For ordinary beams the stresses are calculated by equation (4.18) in 4.5.2.

(6) For composite beams the magnitude and the centroid of the tensile force in the f.r.c. channels are calculated in accordance with 4.4.

(7) Steel stresses for the composite beams are calculated in accordance with 4.5.3.

4.6. Suggested Method for Calculation of Steel Stresses Based on Experimental Results

In order to demonstrate the validity of the theoretical predictions for the

steel stresses, calculations using the experimental results (Neutral axis depth, compressive strain in concrete and tensile strain in the f.r.c. channels) should be carried out. In these calculations the general equations for equilibrium (4.18)and (4.20) for the ordinary and composite beams respectively can be used.

CHAPTER FIVE

THEORETICAL CONSIDERATIONS FOR LIMIT STATES OF DESIGN FOR ORDINARY AND COMPOSITE BEAMS

5.1 Introduction

Until recently the design of an individual reinforced concrete member was based on either the elastic theory or the load factor method as recommended by CP114.

The limit state theory recently adopted in CP110 has the concept for considering various limit states in design. In the assessment of these limit states partial safety factors are employed for the strength of the materials and magnitude of loads. The values of these partial safety factors are predicted from statistical data; they take into consideration the probable variation in the strength of the constructional materials and magnitude of the loads on the structure throughout its specified design life.

The concept of limit state design, however, has been well explained by many investigators (64) (76) (77) (78); hence it is considered not necessary to discuss this in more detail.

The principal limit states considered in design as per CP110, which are relevant to this research are the following:-

(1) Limit State of Ultimate Strength.

(2) Limit states of serviceability

  (i) Deflection.

  (ii) Cracking.

For the limit state of ultimate strength an adequate safety factor is provided for the working load condition by employing partial safety factors for the materials and loads. This will also ensure that the stress in the steel does not exceed its limit of proportionality.

Apart from limiting the span - depth ratios and the spacings of the reinforcements, the code does not recommend any suitable method for the control of cracking and deflection.

In general, methods of calculating the various limit states proposed in the past should be reviewed, and if possible modified to fit the requirements of fibre reinforced cement composite concrete construction.

In appendix (F) methods for calculating the limit state of deflection proposed in the past are reviewed.

In the following paragraphs proposed methods, behaviour and points associated with the prediction of ultimate strength, cracking and deflection for ordinary and composite lightweight concrete beams are discussed.

5.2 Limit State of Ultimate Strength

5.2.1 General Considerations and Assumptions

The flexural failure of reinforced concrete members occurs when either the concrete or steel reaches its maximum strain capacity. Since steel usually has a higher strain capacity compared to that of concrete, failure often occurs by the concrete being crushed in the compression zone.

In case of under reinforced beams failure starts by yielding of the steel which will be followed by the crushing of the concrete. The maximum compressive strain in concrete may vary between 0.19 to 0.52% depending on the shape of the compression zone for the beam, the position of the neutral axis, the quality of concrete and the rate of loading (37). The shape of the compressive stress distribution diagram for a flexural concrete member mainly depends upon the quality of the concrete and also on the rate of loading (37).

For under reinforced beams, where the load-carrying capacity is determined almost entirely by the tensile force that the steel is capable of resisting, the shape of the compressive stress distribution would not significantly affect the ultimate resistance of the beams; at the most, it may slightly alter the lever arm of the internal forces.

The basic assumptions for calculating the ultimate strength as per CP110 are as follows:

(1) The strain distribution for concrete in compression and the strains in the reinforcement are derived from the assumption that plane sections remain plane after bending.

(2) For the concrete in compression a rectangular-parabolic stress distribution is assumed. An alternative to this is a simplified version using a rectangular stress block. The rectangular-parabolic design curve incorporating the partial safety factor for the concrete ($\gamma_m = 1.5$) as per CP110 is shown in Fig. 7a, the assumed maximum compressive strain in the concrete being 0.0035.

(3) The concrete does not resist any tension.

(4) A specified design stress-strain relationship for the steel is given incorporating a partial safety factor $\gamma_m = 1.15$. This is shown in Fig. 7b.

From the above considerations at the ultimate load condition the depth of the neutral axis is adjusted by a trial and error procedure so that the compression forces balance the tensile forces across the section. With the attainment of equilibrium the ultimate design moment can be determined by taking moments for the tensile forces about the centroid of the compressive stress block. The working moment can then be obtained by dividing the design ultimate moment by the appropriate partial safety factors for the live and dead loads.

5.2.2. Comments on the Basic Assumptions

Considering the previous basic assumptions for predicting the ultimate strength of flexural members, the method as used in CP110 would give only a fairly accurate value for flexural members when the following points are considered:-

(1) The assumption of a straight line strain distribution may not be valid at the ultimate condition according to the theory proposed by Baker (79), where he assumes that there is a slip between the steel and the concrete.

(2) Partial safety factors for the materials and loads should not be used.

(3) The maximum compressive strain in the concrete should be carefully assessed, taking into consideration the factors previously discussed in 5.2.1.

(4) The stress-strain relationship for the reinforcement should be that obtained from a direct tensile test. It should also be emphasised here that the

design stress-strain curve for the reinforcement suggested by CP110 Fig. 7b, does not allow for any strain hardening properties which some of the steel reinforcements are capable of exhibiting. It can also be seen that there is no proper distinction made between hot-rolled and cold-worked steels. The differences in their stress-strain characteristics are that the cold-worked steel bars, in general, have no yield plateau, and are capable of exhibiting high stresses with rather low strains when compared with hot-rolled bars. The code, however, does allow a 12.2% increase in stress for a limited range of diameters when cold-worked steel bars are used.

(5) The distribution of the concrete stress in the compression zone in flexure can be different from that obtained from compressive tests on cylinders. This is mainly due to the fact that in a flexural member the different levels of the compression zone undergo strain at different rates, which are proportional to their distance from the neutral axis. It would therefore be rather difficult to assess the true stress distribution for the compression zone. In this respect most of the previous theories depended on experimental data. However, since the shape of the stress distribution diagram would not significantly affect the ultimate strength of an under-reinforced beam, the rectangular-parabolic stress distribution diagram suggested by the code may be used. Additionally, CP110 does not give in particular the compressive stress-strain relationship for lightweight concrete which can be used in design. This relationship, however, can be derived from the assumptions stated by CP110 and the CEB (10) recommendations for the shape of curve and the value of initial tangent modulus of elasticity. This is discussed in 4.3.1., and the derivation is given in appendix (A).

5.2.3 Composite Beams

An assessment of the ultimate strength for composite beams can be obtained by following a similar approach to that employed for the ordinary beams. By assuming a full interaction between the concrete and the f.r.c. channels,

assumption (1) in 5.2.1. is still valid. This follows that the strain in the f.r.c. channels can be obtained from the assumption of a straight line strain distribution. However, at the ultimate load condition the tensile strain induced at the soffit of the composite beams will be greater than the tensile strain capacity of the f.r.c. units. Therefore, at this stage, and when only the ultimate strength of the beam is to be calculated, the contribution of the f.r.c. units can be ignored. The contribution of the f.r.c. channels, if any, can be considered as an additional factor of safety.

5.3 Limit State of Deflection

5.3.1. Introduction

The limitations on the amount of deflection by various codes of practice are mainly based on the smallest deformation which neither impaires the appearance of the structure nor causes any damage to finishes or partitions. In research carried out in Germany (80). it was found that the deflection for the majority of structures which had given rise to complaint had a deflection more than span/250. It was suggested that this limit might vary according to the capacity of the partitions or finishes to absorb or resist strain, since the damage to these had often been the criterion for limiting the deflection (81).

The design of concrete members using the limit state theory, while employing high strength materials,has made it possible for the size of such members to be reduced when only the strength of the material is taken into consideration. Since the increase in strength of the material is not associated with a corresponding increase in the elastic modulus, the flexural rigidity of such members is considerably reduced, and this will result in a greater deflection for the members under the same applied load. In addition, by employing high working steel stresses, higher strains are expected leading to a greater curvature and possibly a greater width of cracks. Therefore, it would seem necessary in certain cases to carry out deflection calculations in order to assess the correct amount of deflection that would result under load.

Various methods have been proposed for the calculation of deflection; these can predict the deflection for laboratory specimens within an accuracy of $\bar{+}$ 20% (81) (82). These methods are reviewed in appendix (F).

In general, the deflection of a beam can be calculated if the magnitude and distribution of the curvature are known along the span of the beam. By employing the straight line theory the curvature of a homogeneous flexural member can be obtained from the following expression:-

$$\phi = \frac{1}{r_b} = \frac{e_c + e_t}{d_1} \qquad (5.1)$$

where e_c and e_t are the maximum compressive and tensile strains in the concrete and steel respectively.

The curvature of an uncracked concrete section can also be expressed in the following form:-

$$\phi = \frac{M}{E_c I_u} \qquad (5.2)$$

I_u : second moment of area for an uncracked section.

For a cracked section the assessment of the curvature becomes rather difficult. Once the concrete is cracked, a condition will be created where the distribution of the curvature along the span of the beam does not have a linear relationship with the moment. This is mainly due to the fact that the values of the steel strains which directly affect the curvature vary between a maximum value in the vicinity of the cracks and a minimum value at a point between two adjacent cracks. This variation for the steel strain is mainly caused by the restrained and non-restrained action of concrete at and between the cracks. Since the deflection depends more upon the curvature along the span of a beam than at a particular point, the assessment of the curvature should be based on the average strain values for the steel where the restrained action of the concrete in the tension zone is considered.

The restraint action of the concrete in the tensile zone has been considered in the calculation of the curvature by various existing theories in different ways; these are discussed in detail in appendix (F).

In the following paragraphs the considerations, behaviour and proposed methods of calculation for the deflection of ordinary and composite lightweight concrete beams are discussed.

5.3.2. Considerations for Ordinary and Composite Lightweight Concrete Beams

Lightweight concrete, in general, is characterised by having a lower modulus of elasticity compared with normal weight concrete. This will to a certain extent affect the deflection behaviour of the structural member. However, the deflection depends upon the flexural rigidity of the member, i.e, the modulus of elasticity (E_c) as well as the second moment of area (I).

For the same geometrical concrete section analysed by the elastic theory, concrete of lower modulus of elasticity will lead to a greater neutral axis depth; consequently a greater moment of inertia is results.

This indicates that the reduction in the flexural rigidity of the member due to the lower modulus of elasticity is partially compensated by an increase in the moment of inertia. To illustrate this point, a graph is established as shown in Fig. 14, for both ordinary and composite beams relating the ratio of the neutral axis depth to the effective depth ($n = \frac{X}{d_1}$) to the modular ratio ($m = E_s/E_c$)

The equations used are based on the elastic theory approach for a cracked transformed section incorporating the properties of the test beams. The equations are discussed in 4.2 :-

For the ordinary beams

$$n = \frac{X_{co}}{d_1} = mp \left(\sqrt{1 + \frac{2}{mp}} - 1\right) \qquad \S\ (4.5)$$

For the composite beams

$$n = \frac{X_{cc}}{d_1} = (mp + m_1 p_1 \eta) \left(\sqrt{1 + \frac{2\,(mp + m_1 p_1 \eta^2)}{(mp + m_1 p_1 \eta)^2}} - 1\right) \qquad \S\ (4.6)$$

The values of the parameters incorporated in these equations are:-

p : As shown in the graph

m_1 : $\frac{E_a}{E_c} = 0.7$, $p_1 = \frac{A_{ch}}{bd_2} = 0.03623$, $\eta = \frac{d_2}{d_1} = 1.1$

From the graph it can be seen that the greater the value of the modular ratio (i.e. lower concrete modulus of elasticity) the lower is the level of the neutral axis depth.

In Fig. 14 a direct comparison can also be made between the level of the neutral axis depth of ordinary and composite beams. For a concrete section with a modular ratio of 12 and a steel percentage area of 0.582, the neutral axis depth of a composite beam is 16% greater than that of an ordinary beam. The difference between the level of the neutral axis depth of ordinary and composite beams decreases when higher percentages of steel are employed; for a modular ratio of 12 and a steel percentage of 1.643 the difference is 6%.

It can also be seen from the same graph that when lower values of the modular ratio (m) are used (i.e., high modulus of elasticity of concrete), the difference between the neutral axis level of the composite and ordinary beams becomes greater; this, however, may be considered as an advantage for normal weight concrete composite construction.

In general, a lower position of the neutral axis in concrete beams may result in the following advantages:-

(1) Greater flexural rigidity for a cracked section.

(2) A more efficient use of the material, that is by subjecting a larger area of concrete in compression.

(3) A smaller concrete area in the tensile zone and reduction in cracking.

Fig. 15 illustrates the effect of the ratio of the modulus of elasticity of the f.r.c. units to that of concrete on the level of the neutral axis depth. For this graph, equation 4.6 discussed earlier was used.

From the graph it can be seen that the rate of change in the neutral axis ($n = \frac{X_{cc}}{d_1}$) with respect to the modular ratio ($m_1 = E_a/E_c$) is very small. It can also be seen that the rate of change becomes smaller when high percentages of steel are employed.

It must be emphasised here that the above considerations are limited to the type and shape of the f.r.c. channels employed in this research.

5.3.3. Behaviour of Ordinary Lightweight Concrete Beams

The load-deflection behaviour of the ordinary lightweight concrete beams is similar to that of normal weight concrete beams. However, with the existence of shrinkage cracks in the lightweight concrete, the load-deflection range within which the beam behave as an uncracked member may be very limited. Furthermore, the contribution of the concrete in the tensile zone to the stiffness of the member may differ from that of normal weight concrete.

To justify these arguments experimental results are necessary.

5.3.4. Behaviour of Composite Lightweight Concrete Beams

The load deflection curve of a composite beam in relation to that of an ordinary beam can be schematically represented as shown in Fig 16a. The load deflection behaviour of the composite beam can be divided into three main stages, these are:-

(i) Uncracked stage (0 to 1)

(ii) Partially cracked stage (1 to 3)

(Concrete cracked but not the channel)

(iii) Fully cracked stage (3 to 4)

(both concrete and channel are cracked)

The corresponding cross sections for each of these stages are shown in Fig. 17. These stages are discussed in the following:-

(i) Uncracked stage, (section No. 1 in Fig. 17)

The behaviour at this stage is based on the assumption that the section is uncracked and that the materials are in their elastic range of behaviour. The relationship, therefore, is assumed to follow a straight line for the loading and unloading process.

When a comparison is to be made between the flexural rigidities for ordinary and composite beams of similar properties and cross sections it must be realised that part of the concrete in the tensile zone of a composite beam is replaced by a material (f.r.c. units) with a relatively lower modulus of elasticity. This will result in an overall reduction in the flexural rigidity (EI) for an uncracked composite section. This may give the impression that the composite beams give a greater

deflection at the uncracked stage than the ordinary beams. However, this is not so because of the following:-

(1) The second moment of area based on an uncracked transformed section for the composite beams (I_{uc}) is only 1.67% and 2.1% less than that for the ordinary beams (I_{uo}) for steel percentages of 1.643 and 0.852 respectively. Therefore, the overall difference in the flexural rigidity (EI) between ordinary and composite beams is minimal and will have little influence on the deflection. For the above values the area and modulus of elasticity of the f.r.c. units were taken into account for calculating the second moment of area for the composite beams. The neutral axis depths were calculated by employing equations 4.1 and 4.2 for the ordinary and composite beams respectively.

(2) In the ordinary type of construction it is quite possible that cracks may initiate in flexural members once loading commences. Furthermore, the tensile strength of the concrete in the ordinary beams may not be fully utilized due to the existence of micro cracks in the concrete. In the composite beams a large area of the concrete in the tensile zone is confined by the f.r.c. channels. This will delay the formation of cracks and consequently the loading range within which the beam behave as an uncracked member is increased. The cracking mechanism of composite beams is discussed in more detail in 5.4.2.

(3) The formation of shrinkage cracks in flexural lightweight concrete members can significantly affect the deflection behaviour. The effect of these cracks, however, is normally ignored in ordinary reinforced beams. In composite beams the formation of shrinkage cracks will be delayed and their width reduced. This is probably due to a slow rate of shrinkage in the composite beams, thus allowing the concrete to have a greater strength and be more resistant to the induced tensile stresses. This is discussed in 5.4.2.

Considering the above points, it is therefore reasonable to assume that the properties of concrete in tension will be fully utilized in composite beams and modified values for the tensile properties over those employed for ordinary beams can be considered in design. The above points may

also suggest that for ordinary types of construction a fully uncracked behaviour may not exist in reality especially for ordinary lightweight concrete construction.

(ii) Partially cracked stage (sections Nos. 2 and 3 in Fig. 17)

After the cracking load for the concrete is reached at point (1) in Fig. 16a, the slope of the curve will gradually change. The rate of this change will depend entirely on the rate of formation and propagation of the cracks in the tensile zone. The saving in deflection, therefore, will depend on the properties of the f.r.c. channels and on the amount of restraint action that these channels will exert on the width and extension of the cracks. It appears therefore that the contribution of the f.r.c. channels to the stiffness of the member is more pronounced at this stage.

With the composite beams having a large area of concrete confined by the f.r.c. channels, the growth and propagation of the cracks will be more gradual and better controlled than with the ordinary beams. Therefore, the transition zone between the uncracked and fully cracked behaviour of the composite beams will be considerably longer than that for the ordinary reinforced beams. Comparison can be made between the transition zone for the ordinary beams (a - $\bar{a}$) and that for the composite beams (1 - 3), where the behaviour of the composite beams at this stage can be characterised by a curvilinear relationship.

Considering the curvilinear load-deflection relationship for composite beams, this stage can be divided for analytical purposes into two parts:

(a) Partially cracked concrete (1 to 2)

Where only part of the concrete in the tensile zone is assumed to be cracked. The corresponding cross section for this stage is No. 2 in Fig. 17. The uncracked concrete area in the tensile zone is equivalent to the confined concrete by the presence of the f.r.c. channel. The logic behind this assumption is that the f.r.c. channel is controlling the width and height of travel of the cracks. Therefore, the extension of the flexural cracks towards the neutral axis level is limited and will mainly be affected by the height of the upstands of the f.r.c. channel.

(b) Fully cracked concrete (2 to 3).

Where concrete in the tensile zone is assumed to be completely cracked and only the contribution of the f.r.c. channel is considered in the calculation of the flexural rigidity, the corresponding cross section for this stage is No. 3 in Fig. 17. The distribution of the curvature along the span of the composite beam can be lower and more uniform when compared with ordinary beams.

(iii) Fully cracked stage (section No. 4 in Fig. 17)

The behaviour at this stage is represented from points 3 to 4 on the curve shown in Fig. 16a. At point 3 it is assumed that the maximum tensile strength of the f.r.c. units is reached and cracks will form in the channels.

At this stage the tensile stresses which are carried by the f.r.c. channels will be transferred to the steel at cracked concrete sections. This increase in the steel strain could affect the average curvature of the beam and a greater deflection is expected.

However, the deflection behaviour at this stage can be affected by each, or a combination of the following factors:-

(1) The degree of contribution of the f.r.c. channels to the flexural rigidity of the member.

(2) The magnitude of the cracking load of the f.r.c. units in relation to the ultimate strength of the beam.

(3) The effect of the fracture mechanism of the f.r.c. units, and the amount of flexibility that these channels exhibit before cracking.

(4) The bond efficiency between the f.r.c. units and the concrete.

At point 4 in Fig. 16a the deflection for both ordinary and composite beams is expected to be equal. This is especially so when the f.r.c. channels are severely cracked, and they are not making any more contribution to the flexural rigidity of the member.

5.3.5. Methods of Calculation

Approaches employed for predicting the short-term deflection for ordinary and composite lightweight concrete beams are discussed in the following:-

Approach one - Existing Theories for Ordinary Beams

To illustrate the extent of the existing theories in predicting the deflections for lightweight concrete beams, a comparison is to be made between the predicted values of deflections using these methods and those observed. The methods used are discussed in appendix (F). These are:-

Based on a cracked section.

CEB formula (37).

Branson method (82).

Yu and Winter method (83).

Beeby and the Unified draft code method (81) (84).

CP110 method (5).

The calculated values obtained by employing the above methods are discussed in 7.7.2.4.

Approach two - Empirical Method for Ordinary and Composite Beams

In this approach the flexural strain distribution of the beam is to be used in the calculation of the average curvature. From the strain distribution the maximum compressive strain in the concrete at the top element of the compression zone, the strain at the level of the steel and the level of the neutral axis depth can be determined. From these values the experimental curvature (ϕexp) can be obtained from the following expression:-

$$\phi \text{exp} = \frac{e_{cexp}}{X_{exp}} \qquad (5.4)$$

or

$$\phi_{exp} = \frac{e_{cexp} + e_{texp}}{d_1} \qquad (5.5)$$

Where

e_{cexp} : experimental compressive strain in concrete at the extreme element of the compression zone.

e_{texp} : experimental steel strain

X_{exp} : average experimental neutral axis depth

The accuracy of this method in predicting the amount of deflection depends on the following points:-

(1) The measured strain distribution across the depth of the beam represents the average values.

(2) The general accuracy of the readings taken regarding strain measurements, deflection and the determination of the position of the neutral axis level.

This method also proves that a logical approach can be made to calculate the average curvature of the beam from the observed values of the flexural strains and the neutral axis depth.

Approach three - Proposed Method

(a) - Ordinary Beams

In this approach the average curvature of flexural members is calcualted by considering an average value for the steel stress. This average steel stress, is calculated by considering the restraint action of the concrete between the cracks in the tensile zone. As stated earlier in 5.3.1., the steel stress is maximum in the vicinity of a crack and minimum at a point mid-way between two adjacent cracks. This is represented in a diagram shown in Fig. 18.

To simplify the derivation of the average steel stress, the average contribution of the concrete in the tensile zone is represented in section 2-2 of Fig. 18. It is assumed that the average steel stress can be obtained by deducting the average stresses resisted by the concrete between the cracks from the maximum steel stress

i.e. $f_{save} = f_s - f_s'$

Hence the average curvature can be calculated from the following expression:-

$$\phi \text{ ave} = \frac{f_s - f_s'}{E_s (d_1 - X)} \qquad (5.6)$$

it can also be expressed by

$$\phi \text{ ave} = \frac{(f_s - f_s')/E_s + f_c'/E_c}{d_1} \qquad (5.7)$$

Where f_s : maximum steel stress

f_s' : average tensile stress resisted by concrete between cracks

X : neutral axis depth for a cracked section

f_c' : compressive stress in concrete at top element of the compression zone calculated by considering the contribution of concrete in tension

E_c : modulus of elasticity of concrete

To obtain the value of f_s', the following procedure is adopted: considering Fig. 18, the tensile force T_c for the concrete in tension is equal to $Tc = k_o A_e f_t$

Where k_o : constant depends on the distribution of the stress and bond efficiency of the steel

A_e : effective concrete area in tension

f_t : average tensile strength of concrete

By expressing

$$A_e = K_1 bd_1$$

$$f_t = k_2 f_r \quad (f_r : \text{modulus of rupture})$$

The equation of the tensile force in the concrete becomes

$$T_c = K_o K_1 K_2 bd_1 f_r = K_3 bd_1 f_r \qquad (5.8)$$

The moment of resistance due to the force T_c is $T_c l_c$, l_c being the lever arm of the force T_c.

The stress due to the contribution of concrete in tension (f_s') is equal to:

$$f_s' = \frac{T_c l_c}{A_s (d_1 - \beta x)} \qquad (5.9)$$

By assuming $l_c = d_1 - \beta x$

$$f_s' = K_3 bd_1 f_r/A_s$$

$$= K_3 f_r/p \qquad (5.10)$$

Where $p = A_s/bd_1$

The average curvature as given in equation (5.6) is $\phi ave = \frac{(f_s - f_s')}{E_s (d_1 - x)}$

By substituting the value of f_s' in equation (5.6)

$$\phi ave = \frac{f_s - k_3 f_r/p}{E_s (d_1 - x)} \qquad (5.11)$$

$$\phi \text{ ave } E_s (d_1 - x) = f_s - K_3 f_r/p \qquad (5.12)$$

$$K_3 = p/f_r \left\{ f_s - \phi \text{ ave } E_s (d_1 - x) \right\} \qquad (5.13)$$

From this equation with the experimental values of ϕ ave, X, f_r and f_s the value of K_3 can be determined.

It must be emphasised here that the assumption given in the CEB recommendations with regard to the calculation for the average steel stresses is similarly adopted in this method. The average curvature (as the CEB recommended (79), can be calculated from the following expression:-

$$\phi = \frac{e_c + e_t}{d_1} \qquad (5.14)$$

$$e_t = e_t' - e_t'' \qquad (5.15)$$

Where e_c : compressive strain in concrete

e_t' : strain in steel at a cracked section

e_t'' : reduction of that strain including the contribution of the tension zone of the concrete.

The sequence employed in the derivation of equation (5.11) (i.e., some of the minor assumptions) is also influenced by a method suggested in the journal of the A.C.I. (85) for calculating the average curvature of flexural members.

(b) Composite Beams

The load deflection behaviour of the composite beams has been fully discussed in 5.3.4. According to that, an idealised trilinear moment deflection relationship up to the level of the cracking moment of the f.r.c. channels (M_a) is assumed. This is shown in Fig. 16b. The corresponding cross sections for analysis are shown in Fig. 17. For a given moment (M) the curvature of a beam can be calculated as in the following: For reference see 5.3.4.

(i) Uncracked stage

For $M \leq M_c$; from 0 to 1 in Fig. 16b, and cross section No. 1 in Fig. 17.

$$\phi = \frac{M}{E_c I_o} \qquad (5.16)$$

Where M_c : cracking moment of concrete which can be calculated as shown in 4.4.

I_o : second moment of area based on an uncracked concrete section

E_c : initial modulus of elasticity of concrete

(ii) Partially Cracked Stage

(a) Partially cracked concrete

For $M_c \geq M \leq M_p$, from 1 to 2 in Fig. 16b and cross section No. 2 in Fig. 17.

$$\phi = \frac{M_c}{E_c I_o} + \frac{M - M_c}{K E_c I_p} \qquad (5.17)$$

$$M_p = \frac{M_a + M_c}{2} \qquad (5.18)$$

I_p : is the second moment of area based on a partially cracked section, cross section No. 2 in Fig. 17.

The neutral axis depth (X_p) and the second moment of area (I_p) can be calculated by considering an uncracked area of concrete equal to that confined by the presence of the f.r.c. channel in the tensile zone as shown in section No. 2 Fig. 17. This is discussed in 5.3.4 for the partially cracked stage of the load-deflection behaviour. The assumptions and derivations of the equations are given in appendix II.

(b) Fully Cracked Concrete

For $M_p \leq M \leq M_a$: from 2 to 3 in Fig. 16b, and cross section No. 3 in Fig. 17.

$$\phi = \frac{M_c}{E_c I_o} + \frac{M_p - M_c}{K E_c I_p} + \frac{M - M_p}{K' E_c I_{cc}} \qquad (5.19)$$

Where

$$(M_p - M_c = \frac{M_a - M_c}{2}) \qquad (5.20)$$

M_a : cracking moment of the f.r.c. channel

K, Ḱ: constants depending on an effective flexural rigidity for the section at the stage in consideration

Values for constants K, Ḱ can be determined by applying the equation to experimental results. Using the foregoing relationship, it will be possible to calculate the curvature at any section along the member, consequently the deflection can be found by normal integration procedure.

5.4 Limit State of Cracking

5.4.1 Introduction

The limitations on the width of cracks in reinforced concrete members are mainly intended to prevent corrosion of the reinforcement, and also to preserve the aesthetic appearance of the structure. A reduction in the width and length of travel of the cracks will also improve the flexural rigidity of the member.

CP110 recommends that the surface crack width in general should not exceed 0.3mm. For members exposed to certain categories of environments, the allowable crack widths should not exceed 0.004 times the nominal concrete cover as given in the code for that particular category.

In general, the width of flexural cracks in ordinary reinforced concrete members depend upon the magnitude of the tensile strain in the steel and concrete. Thus the use of high working steel stresses, while not associated with a corresponding increase in the modulus of elasticity would result in greater steel strains and consequently greater width of cracks. The limited tensile strain of the concrete presented further difficulties regarding the control of crack widths. The limit state of cracking, therefore, became more critical especially for members reinforced with high strength steel. In flexural concrete members cracks can be formed by shrinkage and/or applied flexural tensile stresses.

(i) Shrinkage cracks

These cracks form due to the stresses that are set up by the varying rates of contraction of the cement matrix during the hydration and curing period. This

is mainly caused by the drying shrinkage that takes place in the concrete matrix.

In order to control the drying shrinkage the most effective way found was to reduce the water content of the concrete. This, however, may present certain difficulties in the mixing and compaction of the concrete. Other methods that could also be utilized are the use of a larger size of aggregate or the application of a special surface coating to the concrete (86).

(ii) Flexural cracks

Flexural cracks form initially at the soffit of the member once the tensile strength of the concrete is reached. When the applied stresses are increased, these cracks become wider and propagate towards the compression zone of the flexural member.

The incompatibility of tensile strain between the steel and concrete is a major factor which affects the formation and width of these cracks. It has been suggested that the state of incompatibility can be reached at a steel stress lower than 62 N/mm^2, at which microcracking can develop (86) (87).

The analysis and mechanism of flexural cracking in ordinary reinforced beams has been well studied in the past. In this research it is thought only necessary to discuss the cracking mechanism in the composite beams with special reference to the contribution of the f.r.c. channels. This is discussed in the following paragraph.

5.4.2 Cracking Mechanism in Composite Lightweight Concrete Beams

(a) Shrinkage Cracks

The formation of shrinkage cracks in flexural members depends mainly on the amount and rate of drying shrinkage that takes place in the concrete.

In composite beams a large volume of the concrete in the tensile zone is confined by the f.r.c. channels. This permits a reduction in the rate and amount of shrinkage that takes place, thus allowing the concrete to reach its full tensile properties and be more resistant to cracks formation.

Furthermore, the surface shrinkage strains may be distributed through bond stresses along the length and area of the f.r.c. channels which enable more fine cracks to occur instead of a few wide cracks.

(b) Flexural Cracks

To improve the flexural tensile strength of concrete, flexural cracks should be prevented from forming and extending. To illustrate the theoretical improvements in the tensile resistance of the concrete due to the restraint action of the f.r.c. units a simple example is considered where a concrete prism is confined by f.r.c. units and subjects to a direct tension, as shown in Fig. 19. The example is mainly intended to simulate the restraint action of the f.r.c. channels in the flexural composite beams.

The direct tensile stresses acting on the concrete will be transferred by means of bond to the f.r.c. units. By assuming a perfect bond relationship between the concrete and the f.r.c. units the strain in the concrete and the units are expected to be equal at any level of applied stress. The corresponding stress in the f.r.c. units, therefore, depends upon the modular ratio $m_1 = E_a/E_c$ (the ratio of the modulus of elasticity for the f.r.c. units to that of the concrete).

The formation of cracks due to applied tensile stresses and the corresponding action of the f.r.c. units is discussed in the following:

(1) At rather low applied stresses (lower than the tensile strength of the concrete), microcracks can form at the weak sections in the concrete, an increase in width and extension of these cracks may lead to a complete concrete failure. Microcracks which originate either from the outer surface or the inside mass of the concrete can be controlled to a great extent by the restraint action of the f.r.c. units. For cracks originating from the outer surface of the concrete (cracks (a) in Fig. 19), the f.r.c. units will arrest them from further width increase, hence their extension will be controlled. For the cracks that originate from the inside concrete mass (cracks (b) in Fig. 19), their extension towards the outer surface of the concrete will be limited, mainly because the elements near the outer surface of the concrete, due to the restraint action of the f.r.c. units, will have a greater resistance to crack propagation. The restraint action of the f.r.c. units, therefore, allows greater tensile stresses in concrete, thus allowing values nearer the full tensile strength to be achieved.

(2) When the theoretical tensile strength of the concrete is reached tensile cracks form in the concrete and local bond failure between the concrete and the f.r.c. units may occur in the vicinity of these cracks. This, however, will not lead to a complete failure of the concrete prism since the restraint action exerted by the f.r.c. units help in arresting the growth and the width of these cracks.

The restraint action of the f.r.c. units at this stage mainly depends on the bond efficiency of the f.r.c. units and the capacity of absorbing the strain produced by the formation of the cracks.

For effective crack control the f.r.c. units compared with the concrete should have:-

(a) A higher tensile strength.

(b) A greater extensibility.

An increase in the modulus of elasticity of the f.r.c. units will further help in arresting the phenomenon of cracking. When the concrete cracks, the tensile stresses in concrete will be transferred to the f.r.c. units. Fibre reinforced cement units of a low modulus of elasticity will have a greater local strain compared with those of a high modulus. This may result in a reduction of the restraint action and the effectiveness of f.r.c. units in controlling the cracks.

(3) At the point where the concrete is heavily cracked, as shown in (4) of Fig. 19, the applied tensile stresses will be completely resisted by the f.r.c. units, When the units reach their maximum tensile strength or extensibility cracks will occur. This can be at the vicinity of a crack that has already occurred in the concrete. At this stage a complete failure of the prism would be expected.

It can be seen from this example, that the possible advantages that can be obtained from incorporating f.r.c. units are:-

(a) The full utilisation of the tensile strength of the concrete.

(b) Additional tensile strength.

In flexural members, the flexural rigidity will be reduced mainly by cracks which originate from the outer tension face of the beam. The rate of reduction in

the flexural rigidity depends mainly on the rate of formation and propagation of the flexural cracks. In general, the flexural cracks have their maximum width at the outer tension surface of the concrete (soffit of the beam in flexural members) and gradually diminish in size as the crack extends throughout its length. It would then follow that the f.r.c. units should be placed at the tensile zone of the member. The restraint action exerted by the f.r.c. units in arresting the cracks will be effectively utilised at this position.

The flexural rigidity of a member can also be affected by the cracks which originate from internal flaws. These cracks can be controlled in similar manner as previously explained.

The restraint action of the f.r.c. units, therefore, can increase the loading range within which the beam would behave as an uncracked member. This range could be adjusted by the design of the f.r.c. units so that no surface cracking would occur up to the design working load.

Although the modulus of elasticity of these units is slightly lower than that of the concrete, the stiffness of the member at the uncracked stage is not severely affected. This is discussed in 5.3.4.

When the concrete reaches its full tensile strength cracks will occur. The action of the f.r.c. units as explained earlier will be to prevent these cracks from opening excessively; hence their extension towards the compression zone will be in a gradual manner. The role of the f.r.c. units at this stage is important for diminishing the rate of reduction in the flexural rigidity of the member. Furthermore, the reduction in crack widths will also diminish the risk of corrosion to the steel and preserve the aesthetic appearance of the concrete member.

The final stage is when the f.r.c. units reach their maximum tensile strength or extensibility and cracking occurs.. However, the composite action may not be completely lost at the formation of the first crack. Provided that there is a good bond between the f.r.c. units and the concrete the f.r.c. units will still be effective for the rest of the beam in arresting flexural cracks.

5.4.3 Methods of Calculation (Ordinary Beams)

Crack widths for ordinary lightweight concrete beams can be calculated

employing the methods suggested in C and CA (88) and CP110

The CP110 formula is:

$$\overset{\omega}{w} = \frac{3\, a_{cr}\, e_m}{1 + 2\,\dfrac{(a_{cr} - c)}{d - x}} \qquad (5.21)$$

Where

$$e_m = e_1 - \frac{1.2\, bd\, (a' - x)}{A_s\, (d-x)\, f_y} \times 10^{-3} \qquad (5.22)$$

e_1 : is the strain at the level considered, calculated ignoring the stiffening effect of the concrete in the tension zone.

The C and CA formula for the maximum crack width is:-

$$w = 3.3c\, \frac{f_s}{E_s}\, \frac{(d - x)}{(d_1 - x)} \qquad (5.23)$$

The term $\frac{d - x}{d_1 - x}$ reduces the 1.0 when crack width at the steel level is sought

The calculated values obtained by employing the above methods are discussed in 7.7.3.3

CHAPTER SIX

MANUFACTURE AND METHODS OF TESTING

6.1 General

A total of 27 ordinary and composite beams were tested. The loading configuration and types of tests employed were mainly adopted to simulate conditions met in practice.

All the beams tested were simply supported, and the loading was applied through two symmetrical points acting at one-third the span length of the beam. This provided a constant moment zone for the middle third region of the beam.

With this system of loading the central deflection is 2.04% greater than that produced by a uniformly distributed load for the same applied moment. Static, fatigue and sustained loading tests were carried out under the same configuration of loading. In the following paragraphs the manufacture of beams and specimens and the tests employed are discussed.

6.2 Manufacture

6.2.1 Ordinary Reinforced Lightweight Concrete Beams

The beams were cast in the concrete laboratory where a horizontal pan type mixer with a capacity of 0.25 m^3 was used. The cement and air dried aggregate were first mixed dry for two minutes, then the water was added and the total time for mixing was about five minutes.

The concrete mix was carried out for each beam in two batches. For each batch the workability was measured by the compacting factor apparatus and the slump test. These tests were carried out in accordance with B.S. 1881 Values obtained for the compacting factor and slump tests for all the beams varied between 0.8 - 0.95, and between 20 - 40mm respectively.

The mould used for the test beams consisted of two steel channels, which formed the sides of the beam. These channels were 150mm apart fixed to a steel table.

Cover to the main reinforcement at the soffit of the beam was obtained by

temporarily lifting the reinforcement cage to the desired height by wires fixed to the top of the mould. Pieces of timber 35mm thickness were then placed between the steel channels and the reinforcement to fix the appropriate side cover. The wires and timbers were then withdrawn during the process of casting. This method was adopted to avoid the use of reinforcement spacers, as it was thought that their use might affect the initiation and distribution of the cracks.

Compaction of the concrete was achieved by the use of three vibrators clamped to the bed of the mould and also by the use of a 25mm diameter poker vibrator. When the concrete had been fully compacted the top face of the beam was carefully levelled off. The beams were then left to cure after casting, covered with wet hessian and polythene sheeting.

After 24 hours. the sides of the mould were stripped and the beam was kept on the steel table for a further three to four days, after which it was then marked for positions of support and load. At the middle of the span "Demec" discs were placed in position over the depth of the beam. This is shown in Fig. 20. These Demec discs were affixed by an 'Araldite" glue over a gauge length of 200mm. Demec locating discs were also fixed on the sides of one small prism and three cylinders so that shrinkage measurements and the modulus of elasticity for the concrete could be obtained.

6.2.2 Composite Reinforced Lightweight Concrete Beams

The manufacturing process of the composite beams was nearly the same as that for the ordinary beams, the difference being that fibre reinforced channels were placed at the soffit of the mould before the reinforcement cage was fixed.

Before casting of the beams commenced the channels were wetted with plenty of water. This prevented water being absorbed from the freshly mixed concrete.

6.2.3 Control Specimens for Concrete

From the first batch of concrete which formed the lower half of the beam the following control specimens were cast:-

(i) Six beams of 100 m x 100mm x 500mm for flexural and direct tensile tests

(ii) Three 100mm cubes for the concrete compressive tests. These were only for a comparison with the strength of the concrete in the upper half.

From the second batch of concrete which formed the upper half of the beam the following control specimens were cast:-

(i) Six 100mm cubes for the concrete compressive strength tests

(ii) Three cylinders of 150mm diameter and 300mm long for the static modulus of elasticity and the concrete compressive strength tests.

6.2.4 Fibre Reinforced Cement Channels (f.r.c.channels)

The process employed for manufacturing the f.r.c.channels was basically the same as that applied for normal asbestos cement products.

The f.r.c channels were first manufactured in the form of thin sheets to the required length, total width and thickness. While still wet, the sheets were placed on a wooden mould and formed into shape. In the bending process employed to form the upstands of the channel longitudinal cracks occasionally occurred at the corners.

6.3 Static Loading Tests

6.3.1 Arrangements and Conditions of Loading

The static tests for most of the beams were carried out in the concrete laboratory with the loading arrangement as shown in Fig. 3, and plate (1). The rig used for testing the beams consisted of a steel portal frame whose columns were made of steel channel section, bolted to the sides and floor of a 1.27 m width trench. The end supports were Universal steel section beams (165mm wide x 310mm deep x 2 m long). These were placed, fixed and supported across the trench, their centres being symmetrically placed 4.5 m apart from the centre line of the portal frame.

At each support the beam was rested on a 25mm diameter steel roller sandwiched by two steel plates of 25mm thickness. The lower steel plate was glued with "Evostick" to the support, while the upper one was fixed likewise to the soffit of the beam.

At one of the supports the roller was welded to the lower plate, and at the other support the roller was allowed free rotation to accommodate the longitudinal movement when the beam deflected under load.

Load was applied by a hydraulic jack which reacted against the beam of the portal frame. The hydraulic jack was operated by a "Denison" model T 60 J Console machine. The jack load was transferred to the beam by means of a steel spreader beam, which was stiffened by steel plates welded at the load point positions.

The spreader beam was placed on two 75mm diameter steel rollers resting on steel plates. One of the rollers was fixed to the plate while the other rested freely. The plates were bedded on to the beam with plaster, which allowed a fair level face to be achieved so that the plates were in correct alignment.

The static tests carried out in the Fitton Structures Laboratory had a similar arrangement to those previously described, except that stools were used as supports instead of Universal steel beams.

6.3.2 Testing Procedure

A total of 18 beams were tested under a static type of loading. Before testing commenced the sides of the beams in the region of the constant moment zone were marked in a grid pattern of 100mm squares to facilitate tracing of the cracks as and when they occurred.. The beams were also examined for shrinkage cracks if any, and their width was measured.

All static tests were carried out in three cycles of loading as follows:

(1) Up to the working load. As defined in 3.2 and then to zero.

(2) Up to 1.5 times the working load and then to zero.

(3) Up to the calculated ultimate loads of the beams and then on to failure.

In the first cycle the load was applied by increment of 2KN for all the beams, except for beams ST 5-0 and ST 9-0, for which the increments were 4KN. At every increment deflection readings were taken, while strains and cracks were generally measured at every alternate increment.

The deflection readings were taken at the centre line of the beam and at the third point along the span length. Flexural strains were measured over the depth of the beam on both sides at mid span. The formation and extension of cracks on

both sides of the beam in the constant moment zone were carefully observed. The width of cracks for the ordinary beams were measured at the level of the steel and at the bottom edge of the beams. For composite beams the cracks in the concrete were measured at the interface (top of the upstands of the channels) and at the soffit of the channel as and when they formed. Cracks that formed in the shearing zone were also observed, and their widths checked to see whether they exceeded crack widths that had formed in the constant moment zone.

In the unloading process the decrements were twice the order of the increments, with readings for deflections and strains being taken in a similar manner as employed in the loading process, measurements for width of cracks, however, were only taken at zero load.

In the second cycle a similar approach to that employed in the first cycle for loading and unloading the beam was followed.

In the third cycle the beams were loaded by increments of 4KN up to 1.5 times the working load, after which the increments were then reduced to 2KN up to failure load. For beams ST 5-0 and ST 9-0 the first increments were 8KN and thereafter reduced to 4KN. All the measurements for strains, crack widths and deflections were taken in a similar manner as employed in cycles one and two.

At the very final stages of loading, when warning of approaching failure was clearly imminent by the increased rate of deflection and crack widths, the dial gauges were removed and replaced by a vertical scale rule fixed and placed at the mid span of the beam. so as to enable the final amount of deflection to be observed.

For some beams an attempt was made to measure the compressive strains in the concrete as near as possible to failure. Final readings were taken at 0.95 and 0.97 of the failure load for beams ST 10-0 and ST 2-C respectively.

6.4 Fatigue Loading Tests

6.4.1 Arrangements and Conditions of Loading

The arrangements and conditions of loading used for static tests were similarly adopted for fatigue tests. The difference was that the load was applied through a hydraulic jack, connected to either an S.B.E. 120, or an S.B.E. 80 Losenhausen fatigue tests machine.

The range of loading cycles consisted of an upper limit equal to the applied working load and a lower limit equal to half the applied working load. The rate of cycling employed was dependent on the maximum deflection of the beams at the upper and lower limits. For the beams tested the rate of load employed varied between 60 and 100 cycles per minute.

6.4.2 Testing Procedure

A total of five beams were tested under fatigue loading conditions. These beams initially were subjected to a static test similar to the first cycle as previously explained in 6.3.2.

After the completion of the first static test the beams were subjected to a cyclic loading. A total of three million repetitions was applied to the beams tested under fatigue loading. The sequence of cycling was stopped at intervals of about every half million, so that a static loading test could be carried out with all the relevant data being obtained as was the procedure previously mentioned.

On completion of the total number of cycles the beams were subjected to a static loading test up to failure. The test was carried out in three cycles similar to that explained in 6.3.2.

Occasional stoppages due to mechanical failure of the machine occurred during the test, but apart from the time being lengthened for the test the testing procedure was satisfactory. Table (6) shows the number of cycles and age of the various beams tested.

6.5 Sustained Loading Tests

6.5.1 Arrangements and Conditions of Loading

The sustained loading tests were carried out by setting two beams (ordinary and composite) back to back; the load was applied by means of tension springs acting at the end supports of the beams, as shown in Plate (5). The two beams (ordinary and composite) had the same working moment, and were separated by spacing units which were positioned 1.5 m apart.

The two beams were supported on two steel trestles; the distance between each support and the mid span point was calculated so as to produce a similar

moment at the mid point of the beams. In calculating this distance the dead weight of the beams and the weights of the spring assembly acting at the end supports of the top beam was taken into consideration. See appendix (G).

Since the deflection of the beams at the mid point was measured relative to the spacing units, it can be shown that for the loading configuration adopted the total deflection of the beam is equal to 7.7 times the deflection at the mid point relative to the spacing units. See appendix (G).

After the supporting trestles had been positioned and levelled the lower beam was placed on these supports. At each support the beam was rested on a roller which was sandwiched between two steel plates. For one of these rollers movement was restricted by V shaped grooves machined in the plates; at the other support the roller was free to rotate, thus compensating for any longitudinal movement of the beam.

The spacing units separating the two concrete beams consisted of a square steel bar sandwiched between two pieces of square steel block with a V shaped incision. These blocks allowed free rotation and were fixed to the concrete beam with a plaster mix. The upper beam was placed in position with its compressive face resting on the spacing units.

At each end of the beams two tension springs each of 35KN capacity were connected to steel plates by means of riveted shackles. The applied load was transmitted to the beams through a steel ball and plate assembly.

When load was applied to the beam, demountable loading plates as shown in plate (5) were attached by steel rods to the springs. The load was then applied by the use of a calibrated "EPCO" hydraulic jack which was placed between the plate at the spring connection and the demountable plate. When the required load was reached by the jack it was held in position by means of screws that were part of the spring assembly.

Each time measurements were taken the load was brought up to its initial value (applied working load). This was necessary as the load could be reduced due to creep despite the compensating effect of the springs.

6.5.2 Testing Procedure

For each pair of beams a static test was carried out, in which the load was applied by increments of 2KN up to their working load. At each increment deflection readings were taken by means of dial gauges positioned at the level of the spacing units, deflection measurements were also taken at the supports and one-third the span length of the lower beam. Strains and cracks measurements were also taken.

The applied working load was then sustained on the beams, with further readings for strains, deflections and crack width being taken at periodic intervals. These were more frequent in the early stages of the sustained loading period.

6.6 Instrumentation

(a) Deflection Measurements

The deflections of the test beams were measured by setting three dial gauges, one at the mid span and one at each of the one-third span loading points. The dial gauges of 50mm travel with 0.01mm scale divisions were fixed by means of a stand with a magnetic base. The spindles of the gauges came into contact with thin steel plates glued to the soffit of the beams. For the sustained loading system the dial gauges used were of 25mm travel with 0.01mm scale divisions, the gauges at the mid span being fastened to light steel channels fixed to the spacing units.

(b) Strain Measurements

The flexural strains across the depth of the beam were measured by means of demountable mechanical "Demec" strain gauge of 200mm length with scale divisions indicating a strain of (0.82×10^{-5}). The same "Demec" gauge was used to measure strains due to shrinkage, creep and also for tests to find the modulus of elasticity.

(c) Crack Measurements

For measuring the width of the cracks a small illuminated hand microscope with scale divisions of 0.1mm was used.

6.7 Other Tests

6.7.1 Control Tests on Concrete

All the control specimens for the concrete properties were tested according to the B.S 1881:1970 (89).These control tests were carried out to investigate the structural properties of the concrete used, and also to ensure the uniformity of the concrete for all the beams tested. The average values of these properties are presented in table (6). The tests employed are:-

(a) Cube Compressive Strength

From the second batch of concrete which formed the upper half of the beam six 100mm cubes were cast as control specimens. Of these, three were tested at an age of 7 days and three were tested at the time of testing the beams. The cubes were tested in an Avery hydraulic testing machine with a maximum loading range of 1800KN.

(b) Modulus of Elasticity and Cylinder Compressive Strength

Three cylinders of concrete size 150mm diameter x 300mm length were tested from the batch of concrete placed in the upper half of the beam.

The cylinders were marked out at 90^{o} intervals, at which positions strain measurements were taken. Before testing, the cylinders were capped with high alumina cement mortar and then were tested in a Denison Universal testing machine of 3000KN capacity. At each 5KN increment, strain measurements were taken at the four positions on the cylinder, after an adequate number of readings had been taken the cylinders were then tested to failure and their maximum load recorded, the total testing time was about (15 minutes).

A typical experimental stress-strain curve of the lightweight concrete is shown in Fig. 6b. Values obtained for the initial modulus of elasticity from the experimental curves for the various beams are given in table (6).

(c) Direct Tensile Strength

To obtain values for the tensile strength of the concrete three prisms 100mm x 100mm x 500mm were tested in a "Denison T.42. B4 machine" of 500KN

capacity. To avoid eccentricity of loading during the testing of the prisms special jaws were used. The values obtained for the various beams are given in table (6)

(d) Modulus of Rupture

To obtain values for the modulus of rupture at the time of testing the beams three 100mm x 100mm x 500mm prisms were tested in flexure in a "Denison Universal testing machine" of 500KN capacity by which the load was applied at one-third the span length.

(e) Shrinkage

Values for shrinkage were obtained by means of a "Demec" strain gauge 200mm length with readings being taken on four sides of a prism (100mm x 100mm x 500mm). These prisms were kept in the concrete laboratory under similar conditions of exposure as the full scale beams. The maximum values of the free shrinkage strain measured on these prisms were 0.0005 and 0.00066 after a period of about 30 days and 60 days respectively.

For beams tested under sustained loading. the shrinkage strains were also measured on the sides of the beams near their end supports. The total length of a beam was 5m and the span length adopted was 4.5mm. This left a 250mm length unloaded at each end, at which the measurements of shrinkage were made. The values obtained are discussed in 8.3.1.

6.7.2 Tensile Tests on Steel

To obtain the tensile properties of the various steel reinforcement used in this investigation. samples 500mm long were tested in direct tension using a "Denison T42. C2 testing machine" with a capacity of 200KN. The strain measurements were made by using a "Lindley" extensometer of 50.8mm gauge length and maximum extension of 2.54mm, with scale divisions indicating a strain of 2.5×10^{-5}.

The mechanical properties of the steel bars used are given in table (5) Typical stress-strain curves for the various types of bars used are shown in Fig. 1 The yield or 0.2% proof stress of the various bars tested, in general, differed by $\pm$ 5%.

6.7.3 Tests on f.r.c.Units

In order to investigate the tensile and bending properties of the f.r.c.units used in this investigation, various samples were tested in direct tension and bending. These samples were obtained either by cutting from the channels used or from sheets supplied especially for this purpose. The mechanical properties of the various samples tested are given in table (4); the load deformation characteristics in direct tension and bending are shown in Fig. 8

The testscarried out are:-

(i) Direct Tensile Test

Samples of 50mm width, 5mm thickness and 250mm long were tested in a "Denison T.42 machine" of (65KN) capacity. The samples were fixed by an epoxy resin mortar to special clamps, so as to avoid any eccentricity during the process of loading.

Strains in the direction of the applied stress were measured at increments of 0.5KN by means of a "Demec" gauge of 50.8mm length with scale division of 2.48×10^{-5}.

The tensile properties of the various samples tested are shown in Fig. 8a

(ii) Bending Test

Samples of 30mm width, 6mm thickness and 240mm span were tested in bending. The samples were supported on steel trestles where the load was applied manually in kgs. The load was transferred to two points at one-third the span length. At each increment, which was 1 Kg, the central deflection was measured with a dial gauge of 50.8mm travel and a scale division of 0.01mm. The deflection near failure and the failure load were recorded. A typical load deflection curve is shown in Fig. 8b.

Values of the initial modulus of elasticity obtained from these tests are given in table (4).

CHAPTER SEVEN

DISCUSSION OF TEST RESULTS AND COMPARISON OF TEST BEHAVIOUR WITH THEORETICAL PREDICTION FOR ORDINARY AND COMPOSITE BEAMS

7.1 Introduction

This chapter discusses the actual behaviour of the test beams, and compares the various aspects of behaviour with the theoretical predictions in accordance with chapters four and five. This includes the variation with the applied moment for the neutral axis depth, flexural compressive strains in the concrete, stresses in the f.r.c. channels and the stresses in the steel. Emphasis is placed upon the limit states of ultimate strength, cracking and deflection.

A direct comparison is also made between the flexural behaviour of ordinary and composite beams.

7.2 Variations of the Neutral Axis Level

The level of the neutral axis depth for ordinary and composite beams at any level of applied moment was obtained from average values of strains measured on both sides of a beam. The "Demec" points used for measuring the values of strains for ordinary and composite beams are shown in Fig. 20.

The theoretical prediction for the level of the neutral axis depth in relation to the applied moment has been explained in 4.2 and the idealised relationships for ordinary and composite beams are shown in Fig. 10. To facilitate the determination of values C_o, C_1 and C_2 shown in Fig. 10, the results of beams with a similar percentage of steel are plotted on one graph, irrespective of the type of steel used. These are shown in Figs 21 to 25.

From an examination of the experimental results it was found suitable to assume values of 0.1, 0.6 and 0.8 for C_o, C_1 and C_2 respectively. For ordinary beams, however, the value of C_o was assumed to be zero.

(a) Ordinary Beams

In Figs. 21 and 22 are plotted the theoretical and experimental values of the neutral axis depth versus the ratio of applied moment to the observed ultimate moment.

The values of the observed ultimate moments used in the graphs are given in col. 9 of table (7). The theoretical values of the neutral axis depths were obtained in accordance with 4.2 by employing equations 4.1, 4.3 and 4.5. These equations are:

For the uncracked stage

$$n = \frac{X_{uo}}{d_1} = \frac{\lambda^2 + 2\,(m-1)\,p}{2\,[\,\lambda + (m-1)p]} \qquad (4.1)$$

For the transition stage

$$x = \frac{X_{uc} - X_{cc}}{C_1^{\,2}}\,(R^2 - 2\,C_1\,R) + X_{uc} \qquad (4.3)$$

where $R = M/M_u$

For the fully cracked stage

$$n = \frac{X_{co}}{d_1} = mp\,\left(\sqrt{1 + \frac{2}{mp}} - 1\right) \qquad (4.5)$$

The values of the parameters incorporated in these equations were as follows: p and d_1 are as given in table (1), $\lambda = d/d_1 = 300/d_1$ and $m = 12$.

From Figs. 21 and 22 it can be seen that the level of the neutral axis rises at an early stage of loading to a level higher than that calculated for an uncracked section. This clearly shows that the neutral axis depth does not have a stable position at the initial stage of loading. This behaviour as suggested in 4.2 is possibly due to an early formation of cracks in the ordinary reinforced lightweight concrete beams.

The theoretical graphs at the transition and cracked stages (i.e. up to $M/M_u = 0.8$) agree well with the experimental values.

For values between $M/M_u = 0.8$ and $M/M_u = 1$, some scatter in the results was observed. This could be mainly due to an error involved in the determination of the neutral axis level at the ultimate load conditions (at $M/M_u = 1$), where the neutral axis depth was calculated by the strain compatibility method using the actual values of strength for concrete and steel. However, a definite conclusion on the behaviour of the neutral axis level at values of M/M_u greater than 0.8 cannot be drawn because of the limited number of observations made at this stage and also because of the variation of the non-elastic strain of the materials accompanied by creep under high stresses.

(b) Composite Beams

In Figs. 23, 24 and 25 are plotted the theoretical and experimental values of the neutral axis depth versus the ratio of applied moment to the observed ultimate moment. The values of the observed ultimate moment used in these graphs are given in col. 9 of table (7). The theoretical values of the neutral axis depth were obtained in accordance with 4.2 by employing equations (4.2) (4.4) and (4.6). These equations are:-

For the uncracked stage

$$n = \frac{X_{cu}}{d_1} = \frac{0.5\ \lambda^2 + (m-1)\,p + (m_1 - 1)p_1\ \eta}{\lambda + (m-1)p + (m_1 - 1)p_1\ \eta}^2 \qquad \S \quad (4.2)$$

For the transition stage

$$X = \frac{X_{uc} - X_{cc}}{C_o^2 - 2\,C_o\,C_1 + C_1^2} \left(R^2 - 2\,C_1\,R + C_1^2 \right) + X_{cc} \qquad \S \quad (4.4)$$

For the fully cracked stage

$$n = \frac{X_{cc}}{d_1} = (mp = m_1 p_1 \eta\ ) \left(\sqrt{1 + \frac{2(mp + m_1 p_1\ \eta^2)}{(mp + m_1 p_1 \eta\ )^2}} - 1 \right) \qquad \S \quad (4.6)$$

The values of parameters incorporated in these equations for the beams were as follows: p and d_1 as given in table (1), $m = 12$, $\lambda = d/d_1 = 300/d_1$

$p_1 = A_{ch}/bd_1$ where $A_{ch} = 1548mm^2$, $m_1 = E_a/E_c = 0.7$ and $\eta = d_2/d_1 = 284/d_1$.

It can be seen that the level of the neutral axis depth does not rise higher than that calculated for an uncracked section at the early stage of loading. This clearly shows the distinct behaviour for an uncracked composite beam.

From the graphs it can be seen that good agreement is obtained between the theoretical and experimental values for the uncracked, transition and cracked stages (i.e. up to $M/M_u = 0.8$). In the non-elastic stage (when $M/M_u > 0.8$) some scatter in the results was observed, the behaviour being similar to that for ordinary beams. The arguments suggested earlier for the ordinary beams can be similarly applied to the composite beams.

(c) Comparison Between Ordinary and Composite Beams

For both ordinary and composite beams a good correlation was obtained between the theoretical and experimental values of the neutral axis depth. In most cases the experimental values of the neutral axis depth were greater than the theoretical ones.

In general, the neutral axis depths for the composite beams were greater than those of the corresponding ordinary beams as long as the f.r.c. channels did not crack. The ratios of the experimental neutral axis depths for composite beams to those of corresponding ordinary beams, at applied working load, varied between 1.09 and 1.213 depending on the percentage of steel employed. The exception to this was beam ST 4-C which had a neutral axis depth at the working moment slightly less than that of the corresponding ordinary beam ST 4-0. This was mainly due to the f.r.c. channel of beam ST 4 -C cracking at a level lower than the working moment. The behaviour therefore agrees well with the theoretical predictions as suggested in 5.3.2.

7.3 Flexural Strain Distribution

The values of the flexural strains across the depth of the members were obtained from the "Demec" readings at the mid span of the member as shown in Fig. 20.

(a) Ordinary Beams

A typical flexural strain distribution for an ordinary beam is shown in Fig. 26. For this it can be seen that the distribution of strains agrees with the assumption of a straight line distribution. Erratic results, however, were observed for strains in the flexural tensile zone when cracks started to form. The distribution of these strains then depended on the disposition and propagation of cracks within and outside the "Demec gauge length". The linearity of the compressive strains in the concrete was maintained up to the failure load.

Values for strain at the level of the working moment were not significantly affected by the second and third cycles of loading. Similarly the values of strain at 1.5 times the working moment (the highest level at the second cycle) were nearly the same in the second and third cycles of loading.

(b) Composite Beams

In Fig. 27 a typical strain distribution for a composite beam is shown. The linearity of the compressive strains in the concrete and the tensile strains in the f.r.c. channels was well maintained up to the cracking moment of the f.r.c. channel, irrespective of whether the concrete was cracked or not. This is important in justifying the assumption of a straight line strain distribution used in the calculation of stresses for the f.r.c. channels as discussed in 4.4.

The disposition of cracks in the flexural tensile zone of the concrete in the portion between the top of upstands of the f.r.c. channels and the neutral axis level caused some erratic results for strains measured in this region. When the cracking moment of the f.r.c. channel was reached, as can be seen in Fig. 27, erratic results for the tensile strains in the f.r.c. channel were observed (e.g. at 43 KN). Provided that the f.r.c. channel did not show any signs of cracking, the second cycle of loading had a negligible effect on the strain values.

(c) Comparison Between Ordinary and Composite Beams

The strain distribution for composite beams in general was more uniform than for ordinary beams. The composite beams also showed lower values of strain and greater values for the neutral axis depth up to the cracking moment of the f.r.c. channels.

For the same cycle of loading the remaining strains in the composite beams were lower compared with those of the corresponding ordinary beams. The remaining strains after the first cycle of loading in beams ST 3-0 and ST 3 - C are shown in Figs 26 and 27 respectively. At the outer element of the compression zone beam ST 3 - C had a remaining strain equal to 0.0083% compared with 0.0133% for beam ST 3 - 0.

This shows that the remaining strains in the ordinary beams are usually much greater than those in the composite beams. The cracking moment of the f.r.c. channels in some beams had a considerable effect on the values of the compressive strain in the concrete. This is discussed in 7.4

7.4 Variations of the Flexural Compressive Strain in Concrete

The variation of the maximum compressive strain in the concrete with applied

moment is explained in 4.3.2; the idealised relationships of the ordinary and composite beams are shown in Fig. 11a. From an examination of the experimental results it was found suitable to assume a value of 0.8 for C_p (shown in Fig. 11a). This agreed well with experimental results obtained in a previous investigation carried out on normal weight concrete beams (4).

(a) Ordinary Beams

The calculated and experimental values of the maximum flexural compressive strain in concrete are plotted against the ratio of applied moment to the observed ultimate moment as shown in Figs. 28 and 29.

The theoretical values were obtained in accordance with 4.3.2. by employing the equation of compatibility of moments and the assumption of a straight line strain distribution.

The equation employed is:

$$M = f_s \; A_s \; (d_1 - \beta \, x) \qquad \S = \quad (4.18)$$

The values of e_c (compressive strain in the concrete) can be obtained from:

$$e_c = \frac{f_s}{E_s} \quad \frac{x}{(d_1 - x)}$$

Values of the parameters employed in the equation (up to the level of $M/M_u = 0.8$) were as follows : x = the calculated value of neutral axis depth for cracked transformed section given in Figs. 21 and 22, $E_s = 200 \text{ N/mm}^2$, $\beta = 0.345$. The value of β used was an average value where the measured maximum compressive strains in the concrete up to $M/M_u = 0.8$ were considered. The relation between the value of β and the compressive strain in the concrete is explained in 4.3.3.

From the graphs it can be seen that a good agreement is obtained between the predicted and the experimental values. However, above the value of $M/M_u = 0.8$ some scatter in the results was observed. This could be due to the difference between the assumed and actual values for the maximum compressive strain in the concrete at failure. The values of the measured maximum compressive strain for the test beams are discussed in section C below.

(b) Composite Beams

In Figs. 30 and 31 are shown the experimental and the theoretical values for the maximum compressive strain in the concrete versus the ratio of applied moment to the observed ultimate moment.

The theoretical values were calculated in accordance with 4.3.2, the equations employed being the same as for the ordinary beams. This was mainly due to the formation of cracks in the f.r.c. channels at values lower than $M/M_u = 0.8$, and the behaviour of the members was regarded as similar to that of the ordinary beams. It can be seen in Figs. 30 and 31 that the theoretical values are slightly greater than the experimental ones obtained at the initial stages of loading. This was mainly because the contribution of the f.r.c. channels was not included in the calculation. Thereafter a good agreement is obtained between the theoretical and the experimental values.

Similar to the behaviour of ordinary beams, some scatter in the results was observed at the stage between $M/M_u = 0.8$ and $M/M_u = 1$. The compressive strains in the concrete for the composite beams can be greatly affected by the formation of cracks in the f.r.c. channels. Typical examples are beams ST 7 - C, ST 10 - C, ST 11 - C and ST 12 - C as shown in Fig. 31, where they show a considerable amount of strain at the stage between $M/M_u = 0.8$ and $M/M_u = 1$.

(c) Comparison Between Ordinary and Composite Beams

As mentioned earlier in section (a), the scatter of the results in the non-elastic phase of behaviour (i.e. at values between $M/M_u = 0.8$ and $M/M_u = 1$) could be caused by the difference between the assumed and the actual values of the maximum compressive strain in the concrete at failure. For both types of beams strain values greater than 0.0035 (assumed in CP110) were obtained.

The last readings taken for the maximum compressive strain in the concrete with the corresponding levels of moments are given in cols. 11 and 12 of table (7). At levels between 0.9 and 0.97 of the observed ultimate moment the values of strains ranged between 0.00217 and 0.00395.

A previous investigation (90), reported values for the maximum compressive strains ranging between 0.003 and 0.0055 at 90% to 100% of the observed ultimate

moment. The values of the maximum compressive strain in the concrete at failure as suggested in 5.2.1 depends upon various factors such as the shape of the compressive zone, the type and strength of the concrete, the rate of loading and the percentage of steel employed. Therefore, the values obtained in this work are only applicable to beams of similar conditions to those tested in this investigation. A definite conclusion therefore on this point can not be made.

The experimental results of the present investigation showed that the values of compressive strain in the concrete for the composite beams at the initial stages of loading were lower than those for the ordinary beams. However, when the cracking moment of the f.r.c. channel was reached the strain values of the composite beams became greater than those for the corresponding ordinary beams. This could be mainly due to the following reasons:

(a) When cracks form in the f.r.c. channel the tensile stresses resisted by the channel will be transferred to the steel; this will cause an increase in the tensile strain of the steel. Considering the assumption of a straight line strain distribution, the increase in the tensile strain in the steel can lead to a corresponding increase in the maximum flexural compressive strain in the concrete.

(b) When cracks form in the f.r.c. channel more cracks will propagate in the concrete. Consequently the neutral axis level will rise and this will confine the compressive zone to a smaller area. Due to a higher concentration of compressive stresses, greater compressive strains can be expected.

7.5 Stresses in the f.r.c. Channels

In Figs. 32 and 33 are plotted the theoretical and experimental values of the tensile stresses in the f.r.c. channels against the applied moment. The experimental values were obtained by correlating the measuredstrains in the f.r.c. channels with the experimental stress strain relationship of the f.r.c. units shown in Fig. 8. The theoretical values of the stresses in the f.r.c. channels were obtained in accordance with 4.4. The equations employed are:

For $M \leq M_c$

$$f_{ab} = \frac{M\ (d - X_{uc})}{I_{uc}}\ m_1 \qquad \S \quad (4.11)$$

$$M_c = \frac{f_{rc}\ I_{uc}}{d - \acute{d} - X_{uc}} \qquad \S \quad (4.12)$$

For $M_c \leq M \leq M_a$

$$f_{ab} = \frac{M_c\ (d - X_{uc})}{I_{uc}}\ m_1 + \frac{(M - M_c)\ (d - X_{cc})}{\beta_1\ I_{cc}}\ m_1 \qquad \S \quad (4.13)$$

The parameters employed in these equations are as follows: $f_{rc} = 3\ N/mm^2$, $\beta_1 = 0.9$ $m = 12$, $m_1 = 0.7$. The values of X_{cc} are given in Figs. 23, 24 and 25.

In Figs. 32 and 33 it can be seen that a good agreement is obtained between the theoretical and experimental values up to the cracking moment of the f.r.c. channel (M_a). The stresses due to the self weight of the beams are shown in the same figures and also given in col. 6 of table (8).

The observed values of strains at the soffits of the f.r.c. channels with the corresponding values of stresses, at levels just before the channels cracked, are given in cols. 4 and 5 of table (8). The values of strains varied from 800 to 1700 x 10^{-6} the corresponding tensile stresses varied between 8 and 14.5 N/mm^2. The maximum tensile strains obtained from testing the f.r.c. units in direct tension varied between 1250 and 1800 x 10^{-6}; the corresponding tensile stresses varied between 14.5 and 18.4 N/mm^2. These are already given in table (4). A comparison between these values and those measured at the soffits of the f.r.c. channels would seem to indicate that the tensile properties of the f.r.c. units had not been fully utilized. This, however, could not be the case for the following reasons:

(1) The strain measurements for the f.r.c. channels were obtained over a "Demec" gauge length of 200mm Fig. 20, the values, therefore, represent average surface strains over this region. The maximum local strain in the f.r.c. channel just before cracking could only be measured if the initial crack in the f.r.c. channel had formed within the "Demec" gauge length.

What also made it difficult to measure the actual and local strain in the f.r.c. channel was that the maximum strain might occur on the inside face of the channel and transference to the outer surface might not have occurred due to a possible slip or shear within the layers of the f.r.c. channels.

(2) The existence of some weak sections along the length of the f.r.c. channels. This could be due to the presence of longitudinal cracks along the corner of the f.r.c. channels which might have formed at the time of manufacture during the process of forming the upstands.

Another factor which may be considered is the probable variation of strength through the length of the f.r.c. channel due to a non-uniform distribution of fibres.

The f.r.c. channels for all the beams cracked in the second cycle of loading at values greater than the working moment, the exception being beam ST 4 - C reinforced with Kam 60 steel, where the channel cracked during the first cycle of loading (below the working moment level). The ratios of the cracking moments of the f.r.c. channels to the corresponding working moments for the test beams are given in col. 8 of table (8). The ratios for the beams excluding beam ST 4 - C ranged between 1.14 and 1.81.

It may be pointed out here that the f.r.c. channels for the beams tested under fatigue and sustained loading also did not crack during the first cycle of loading.

7.6 Stresses in the Steel Reinforcement

(a) Ordinary Beams

In Figs. 34 and 35 the theoretical graphs of the steel stresses calculated in accordance with 4.5 are superimposed on the experimental values obtained in accordance with 4.6. The equation employed is:

$$M = A_s f_s (d_1 - \beta x) \qquad (4.18)$$

It can be seen that full agreement is obtained between the theoretical and experimental values. The variation of the steel stress in relation to the applied moment can almost be represented by a straight line. The values of the working steel stresses based on experimental results are given in col. 3 of table (7). These values are compared with the stresses in the composite beams in section c.

(b) Composite Beams

In Figs. 36 and 37 the theoretical graphs for the stresses calculated in accordance with 4.5 are superimposed on the experimental values obtained in accordance with 4.6.

The equations employed in calculating the steel stresses are:

$$M = A_s f_s (d_1 - \beta x) + T_a (d_2 - \beta x) \qquad \S \quad (4.20)$$

$$M = A_s f_s (d_1 - \beta x) \qquad \S \quad (4.18)$$

The various stages at which the stresses were calculated in each beam are as follows (Reference can be made to Figs. 36 and 37.):

(1) At the cracking moment of the concrete where the contribution of the f.r.c. channel is considered (equation 4.20)

(2) At a level of moment just before the cracking moment of the f.r.c. channel, where the contribution of the f.r.c. channel is considered (equation 4.20).

(3) At a level of moment just after the cracking moment of the f.r.c. channel, where the contribution of the f.r.c. channel is not considered (equation 4.18)

(4) At a level greater than the cracking moment of the f.r.c. channel (at about 0.8 times the ultimate moment), where the contribution of the f.r.c. channel is not considered (equation 4.18).

From Figs. 36 and 37 it can be seen that good agreement is obtained between the theoretical and experimental values of the steel stresses.

(c) Comparison Between Ordinary and Composite Beams

The values of the steel stresses at the level of the working moments for both ordinary and composite beams are given in col. 3 of table (7). Col. 4 of table (7) shows the reduction in the steel stress due to the contribution of the f.r.c. channels in the composite beams ranging between 9% and 16.7% of the stresses in the corresponding ordinary beams. The amount of reduction depends mainly on the type and percentage of the steel employed. Beam ST 10 - C reinforced with 0.582% of Kam 60 steel showed the highest level of reduction in the steel stress. No reduction was obtained in the working steel stress of beam ST 4 -C. This was due to the f.r.c. channel being cracked at a stage earlier than the level of the working moment.

The moments at which the composite beams attained the same working steel stress for the ordinary beams varied between 1.12 and 1.2 times the working moment of the beams.

The reduction in the steel stress in the composite beams became even more at levels greater than the working moment. At the levels just before the cracking moments of the f.r.c. channels the steel stresses in the composite beams were between 10.7% and 18.4% lower than those in the corresponding ordinary beams. The values of the steel stresses and the amounts of reduction are given in cols. 5 and 6 of table (7). This reduction in the steel stress was a major factor in reducing the width of the cracks and deflection of the composite beams.

7.7 Limit States of Design

7.7.1 Limit State of Ultimate Strength

The mechanism of failure for the test beams was initially started by yielding of the steel, which was followed by the crushing of the concrete in the compression zone. This was mainly due to the beams being under-reinforced. Beams near to the failurestage can be seen in plate 2. In plate 3 a typical failure for the beams tested is shown.

The yielding of the steel for the various beams was observed by a greater rate of increase in crack widths and deflections.

At loads near to the failure stage crack widths of 2mm with deflections of 100mm (giving span to deflection ratio of 45) were observed, thus a good warning of impending failure was obtained (see plate 2).

In the following sections the observed and calculated values of the ultimate moment for the test beams are discussed.

(a) Ordinary Beams

The ultimate strength of the members was calculated by employing two approaches, the first one was in accordance with the recommendations of CP110 employing partial safety factors for materials and using nominal design strengths for concrete and steel. This is discussed is 3.2.1. Values of the ultimate strengths for the test beams employing this approach are given in col. 7 of table (7).

The second approach was based on the strain compatibility method, using the actual values of strength for the materials without the partial safety factors as described in 5.2.1. The stress strain relationship for the reinforcement shown in

Fig. 1 and for the concrete shown in Fig. 6a were used. The concrete cube strengths used were those obtained at the time of testing the beams as given in table (6). The values of the ultimate strength of the various beams employing this approach are given in col. 8 of table (7).

A comparison between the observed and calculated values of the ultimate moments cols. 7, 8 and 9 in table (7), shows that the approach based on the actual values of strengths described in 5.2.1. gives a better agreement than that based on CP110 recommendations. It can also be seen that the approach based on the actual strengths described in 5.2.1. underestimates the observed values of ultimate strength for all the beams except ST 3 - 0, where the values are nearly equal.

The ratios of the observed values of ultimate moments to those calculated using the actual values of strength for the ordinary beams (given in col. 10, table (7)) varied between 0.98 and 1.39. Values ranging between 1.05 and 1.25 for the ratio of the observed to calculated ultimate moments have been reported earlier (90). It has been suggested (90) that this variation in the ultimate strength could be due to the difference between the values of the actual steel stresses at failure and those used in the calculation.

It is of interest to mention here that steel bars embedded in concrete can exhibit an ultimate strength or yield stress greater than that obtained from a conventional tensile test (91).

However, the increase in the ultimate strength is difficult to predict and therefore can not be used in design but should be considered as an additional safety factor.

(b) Composite Beams

The analysis employed for the composite beams was similar to that for the ordinary beams explained in section (a), that is, by neglecting the contribution of the f.r.c. channels at the ultimate load conditions.

Calculated values of ultimate strength employing the CP110 method (nominal values of strength with the partial safety factors) are given in col. 7 of table (7). This shows that the CP110 method considerably underestimates the observed values of the ultimate strength.

The strain compatibility method described in 5.2.1. (based on the actual values of strengths without partial safety factors) gave a better agreement with the observed values. The observed and calculated values are given in cols. 8 and 9 of table (7).

It can be seen that the observed values are greater than the calculated ones for six out of the eight beams tested. The ratios of the observed to calculated values of the ultimate moments for the composite beams ranged between 0.95 and 1.38.

The arguments discussed earlier in section (a) with regard to the increase in the ultimate strengths of the ordinary beams are also applicable to the composite beams.

Considering the observed values of ultimate moments, a factor of safety of more than 2 was ensured for the working moment against collapse. This may suggest that an increase in the working moment may be utilised provided that the limit states of cracking and deflection are satisfied.

(c) Comparison Between Ordinary and Composite Beams

The observed values of the ultimate strengths of the composite beams did not differ significantly from those of the corresponding ordinary beams. This can be seen in cols. 9 of table (7).

However, an increase in the ultimate strength was obtained for beams reinforced with a low percentage of steel, e.g. beam ST 10 - C reinforced with 0.582% of Kam 60 had an ultimate strength equal to 17% greater than that of the corresponding beam ST 10 - 0. This may suggest that the f.r.c. channels makes a greater contribution to beams reinforced with a low percentage of steel. A definite conclusion, however, in this respect can not be drawn due to the limited amount of test results.

7.7.2 Limit State of Deflection

7.7.2.1. Behaviour of Ordinary Beams

(a) General

In theory the load deflection curve of an ordinary beam, when first loaded, has two initial phases of behaviour. These represent an uncracked and a cracked

section. The idealised relationship for ordinary beams is represented by the dotted line shown in Fig. 16.

The observed load deflection curves for the test beams are shown in Figs. 38, 39 and 40. In these the flexural rigidity of an uncracked section (E_cI_o) is indicated by the tangent θ_1 shown on the same figures.

When the tensile strenth of the concrete is reached and the first crack appears, the load deflection curve will deviate from linearity. With increasing load, further cracks form until a stable crack pattern is achieved. When this point is reached very little change occurs in the gradient of the load deflection curve until the yield point of the steel is reached. At this stage the flexural rigidity of a cracked section (kE_cI_c; k is a constant for an effective flexural rigidity) is indicated by the tangent θ_2. To be consistent these tangents are drawn at levels corresponding to the working moments as shown in the figures. It may be noted, however, that all the beams cracked long before the level of the working moment.

Examination of Figs. 38, 39 and 40 shows that the difference between the flexural rigidity of an uncracked section (θ_1) and that of a cracked section (θ_2) is more pronounced for beams reinforced with a low percentage of steel; e.g., for Beams ST 7 - 0 and ST 8 - 0 reinforced with a steel ratio of 1.643% and beam ST 9 - 0 reinforced with a steel ratio of 1.483% the ratios θ_1/θ_2 were 1.17, 1.25 and 1.08 respectively, whereas for beams containing 1.044% of steel the ratio varied between 1.48 and 2.02.

In general, this behaviour is mainly due to the difference between the flexural rigidities of cracked (kE_cI_c) and uncracked (E_cI_u) sections being lower for members reinforced with high percentages of steel. To illustrate this point the relative ratios $\frac{E_cI_u}{kE_cI_c}$ for beams ST 10 - 0

(0.584%), ST 1 - 0 (1.044%), ST 9 - 0 (1.483%) and ST 7 - 0 (1.643%) are 3.28, 2.27, 1.9 and 1.8 respectively. A modular ratio of 12 was employed in these calculations.

Other factors which might have also affected this behaviour was the amount of shrinkage that took place in the beams. Cracks which form due to shrinkage tend to reduce the flexural rigidities of concrete members.

It can also be seen that the range of an uncracked section in the load deflection curves is small. This indicated an early formation of cracks which could be due to the effect of greater shrinkage and the lower tensile strength of lightweight concrete.

As mentioned in 7.7.1 the beams showed a significant amount of deflection at the final stages of loading, giving a good warning of approaching failure. In plate 2a an ordinary beam near the failure stage is shown.

(b) Working Moment Condition

The observed deflections at the working moments for the test beams (given in col. 2 of table (9)) varied between 7.6mm and 27.2mm, which gave a corresponding span to deflection ratios of 592 and 165 respectively. The beams which gave a span to deflection ratio lower than 250 were ST 5 - 0, ST9 - 0 and ST 3 - 0. The values are given in col. 7 of table (9). Beam ST 5 - 0 was reinforced with Kam 90 steel, the highest grade of steel employed in the present investigation, gave a span to deflection ratio of 165, which was the lowest value. Beams ST 9 - 0 and ST 5 - 0 reinforced with 1.483% and 1.044% of Unisteel 550 gave a span to deflection ratios of 212 and 245 respectively. It can therefore be assumed that if a lower percentage of Unisteel 550 is employed, a span to deflection ratio greater than 250 can be expected.

For the sake of comparison, a reference is made to beam ST 10 - 0 reinforced with 0.582% of Kam 60 steel, which gave a span to deflection ratio of 317 under working load. Similarly beam ST 4 - 0 containing Kam 60 steel gave a span to deflection ratio greater than that of beam ST 3 - 0 reinforced with a similar amount of Unisteel 550 . The span to deflection ratio for beams ST 4 - 0 and ST 3 - 0 were 256 and 245 respectively. The improved flexural rigidity for beam ST 4 - 0 could mainly be due to the surface deformation of Kam 60 steel having a better control on the crack widths.

In a previous investigation (35) beams with a span to depth ratio of 7.6. reinforced with steel of 410 N/mm^2 nominal yield strength and percentages of steel varying between 1 and 4.2 gave a span to deflection ratio ranging between 1010 and 461. Another investigation (40) employing a greater span to depth ratio of 14.6 with percentages of steel varying between 1.14 and 3.16 of Unisteel 410 gave a span to deflection ratio between 291 and 434. The concrete cube strength for both investigations varied between 44 N/mm^2 and 59.6 N/mm^2.

A direct comparison between the values obtained in previous investigations and those obtained in this research can not be made mainly due to the difference in the span to depth ratio employed. Other factors, e.g., the type and amount of steel employed, concrete strength and the level of the steel stress at which the deflection was measured could also affect the values of the span to deflection ratios.

For each beam tested in the present investigation the deflection at the working moment was nearly the same at the first and second cycles of loading. Similarly the deflection at 1.5 times the working moment was nearly equal at the second and third cycles of loading.

(c) Relationship With Steel Stress

For various percentages of steel a relationship between the experimental steel stresses and the observed deflection can be established as shown in Fig. 41 in which three percentages of steel were considered. From this figure it can be seen that the deflection of a span/250 was reached at steel stresses of 400 N/mm^2, 312 N/mm^2 and 280 N/mm^2 corresponding to steel percentages at 0.582 (Kam 60), 1.044 (Unisteel 550), and 1.643 (Unisteel 410) respectively.

(d) Remaining Deflection

The remaining deflections for the test beams after the first cycle are given in col. 3 of table (9). The recovery in the amount of deflection ranged between 74% and 87% of the respective deflection at the working moment.

Previous investigations indicated that recoveries of about 80% for lightweight concrete (40) and between 62% and 83% for normal weight concrete (92) of the respective working deflection at the first cycle were obtained.

7.7.2.2. Behaviour of Composite Beams

(a) General

The load deflection behaviour for the composite beams based on theoretical considerations is discussed in 5.3.4., consequently an idealised relationship is established, as shown in Fig. 16b.

The observed load deflection curves for test beams are shown in Figs. 42 and 43. In these figures the beams show a steeper gradient for the load-deflection behaviour at the initial stages of loading. When the concrete cracks the gradient of the load deflection behaviour changes in a gradual manner; this indicates a reduction in the flexural rigidity of the members.

The curvilinear behaviour between the levels of the cracking moments of the concrete (M_c) and the cracking moments of the f.r.c. channels (M_a) is mainly due to the control of the f.r.c. channels on the width and extension of the cracks. This is discussed in 5.3.4.

When the f.r.c. channels cracked some scatter in the load-deflection behaviour

was observed, e.g., beams ST 1 - C, ST 7 - C, ST 10 - C and ST 12 - C showed a noticeable reduction in their flexural rigidity. The factors which might have affected the load deflection behaviour at levels greater than the cracking moment of the f.r.c. channels are discussed in 5.3.4.

For beams with a similar percentage of steel the load deflection behaviour was nearly the same up to the level of the cracking moment of the f.r.c. channels. Thereafter the behaviour of the beams slightly differed depending upon the effect that the formation of cracks in the f.r.c. channels had on the behaviour of the individual beams.

An example of this is that due to the cracking of the f.r.c. channel, the deflection of beam ST 1 - C containing mild steel increased at a greater rate than those of beams ST 2 - C and ST 3 - C which were reinforced with Unisteel 410 and Unisteel 550 respectively. This behaviour can be seen by comparing the load - deflection curves of the beams at levels greater than the cracking moments of the f.r.c. channel (M_a) as shown in Fig. 42, where the deflection of beam ST 1 - C increased at a greater rate than those of beam ST 2 - C and ST 3 - C. This could be due to the greater effect that the formation of cracks in the f.r.c. channels had on the cracks in the concrete of beam ST 1 - C. Reference can be made to Figs. 51 and 52, where the maximum crack width in the concrete of beam ST 1 - C was increased considerably greater than those in beams ST 2 - C and ST 3 - C due to the formation of a crack in the f.r.c. channel.

Similar to the behaviour of ordinary beams, the composite beams showed a significant amount of deflection at the final stages of loading, which gave a good warning of impending failure. A composite beam near the failure stage can be seen in plate 2b.

(b) Working Moment Condition

The observed deflections at the working moments for the test beams varied between 4.2mm and 18.4mm, which gave a corresponding span to deflection ratios ranging between 1071 and 245. The values for the various beams are given in cols. 2 and 7 of table (9). The lowest value for the span to deflection ratio obtained was for beam ST 4 - C reinforced with Kam 60 steel, where the f.r.c. channel cracked

at a stage before the working moment of the beam.

Considering the recommended span to deflection ratio of 250 the composite beams except beam ST 4 - C showed an adequate degree of stiffness at the level of the working moment.

For each beam tested the deflection at working moment in the second loading cycle was nearly the same as that obtained in the first loading cycle. Similarly the deflections at 1.5 times the working moment in the second and third cycle were the same. For both cases, when the cracking moment of the f.r.c. channel was reached some scatter in the results was observed.

(c) Remaining Deflection

The remaining deflections for test beams after the first cycle are given in col. 3 of table (9). The deflection recovery after the first cycle ranged between 77.4% and 86% of the respective deflection at the working moment.

7.7.2.3 Comparison Between the Behaviour of Ordinary and Composite Beams

The load deflection behaviour of a composite beam in relation to that of an ordinary beam is explained in 5.3.4. Typical and idealised relationships for both types of beam are shown in Fig. 16.

In Figs. 44, 45 and 46, are plotted the observed values of deflections for the ordinary and composite beams, so that a direct comparison of behaviour can be made. In these the composite beams show a greater degree of stiffness than the ordinary beams up to and well above the working moment.

The greatest saving in deflection was obtained at the level of the working moment of the beams. This could be due to the ordinary beams being completely cracked, whereas the cracks in the composite beams are effectively controlled by the restraint action of the f.r.c. channels.

The ratios of the deflections for the composite beams to those of the ordinary beams at the level of the working moment, varied between 0.96 and 1.54. The lowest value was obtained for beam ST 4 - C containing Kam 60 steel, where the f.r.c. channel cracked at a value lower than the working moment of the beam. It can also be seen that when a higher percentage of steel was employed the saving in

the amount of deflection was reduced, e.g., beam ST 7 - C reinforced with 1.643% gave the least amount of saving.

The moments at which the composite beams attained the same working deflection for the corresponding ordinary beams were at 1.2, 1.17, 1.15, 1.22 and 1.03 times the working moment for beams ST 1 - C, ST 2 - C, ST 3 - C, ST 10 - C and ST 7 - C respectively. These values are important when an increase in the working moment of a composite beam is to be considered.

The saving in deflections for the composite beams was maintained up to the level of the cracking moment of the f.r.c. channels. Thereafter the flexural rigidity of the composite beams gradually decreased. When more cracks were formed in the f.r.c. channel the rate of reduction in the flexural rigidity increased and finally a stage was reached where the ordinary and composite beam had the same flexural rigidity. This stage was reached at steel stresses of 230 N/mm^2 and 220 N/mm^2 for beams containing mild steel with steel ratios of 1.044% and 1.643%. respectively. For the beams that were reinforced with deformed bars (except beam ST 4 - C) this stage was reached at steel stresses with the corresponding ratio and type of steel of 405 N/mm^2 (1.044% Unisteel 410), 460 N/mm^2 (1.044% Unisteel 550) and 560 N/mm^2 (0.582% Kam 60).

At the levels well above the cracking moments of the f.r.c. channels some of the composite beams showed a slightly lower flexural rigidity than the corresponding ordinary beams, e.g., beams ST 1 - C, ST 4 - C, ST 7 - C and ST 10 - C shown in Figs. 44, 45 and 46. This was mainly due to the formation of cracks in the f.r.c. channels and the sudden transfer of tensile stresses from the f.r.c. channels to the steel, which consequently increased the curvature of the members.

In general, the saving in deflection when employing the same type of f.r.c. channel depends upon the following factors:-

(1) condition of the flexural member; whether the concrete of the member is cracked or not.
(2) the percentage of steel employed.
(3) the level of the cracking moment of the f.r.c. channels,
(4) the level of steel stress.

7.7.2.4. Comparison With Theory

The central deflection for the test beams was calculated by employing the approaches suggested in 5.3.5. In these calculations the values of the various parameters employed were as follows; $f_r = 2\ N/mm^2$, $E_c = 17\ kN/mm^2$, $E_s = 200\ kN/mm^2$, $E_a = 12\ kN/mm^2$, $m_2 = 0.7$, $f_{rc} = 3\ N/mm^2$ and M_a = as given in col. 3 of table (8).

The approaches employed are as follows:

Approach One : Existing Theories (Ordinary Beams)

The calculated deflections at the working moments of the ordinary beams obtained by employing the various existing theories reviewed in appendix (F) are plotted against the observed values as shown in Fig. 47. It can be seen that the existing theories can predict the actual amount of deflection to within an accuracy of $\mp$ 20%.

Approach Two : Empirical Method (Ordinary and Composite Beams)

In this approach the deflection was calculated by employing the empirical method discussed in 5.3.5. In this calculation the curvature was obtained from the experimental values of flexural strains and the neutral axis as in the following:

$$\phi_{exp} = \frac{e_{cexp}}{X_{exp}} \qquad \S \quad (5.4)$$

Where e_{cexp} : experimental maximum flexural compressive strain in concrete

X_{exp} : experimental neutral axis depth

The values for e_{cexp} and X_{exp} used were those obtained from the experimental results.

The calculated and observed load deflection curves for the ordinary beams are shown in Figs. 38, 39 and 40.

Good agreement is obtained between the calculated and the observed values.

Similar calculations were carried out for the composite beams and a good agreement has also been obtained with the observed values. In col. 4 of table (9) the predicted values at the level of the working moment are shown. The ratios

of the calculated to the observed values of deflections for the test beams varied between 0.96 and 1.15 with an average value equal to 1.06. The good agreement obtained between the calculated and the observed deflections as discussed in 5.3.5 indicates the following points:

(1) The measured strain distribution across the depth of the beam represents the average values.

(2) The readings taken with regard to strain measurements, deflection and the determination of the neutral axis depth at the central point of the beams were sufficiently accurate.

(3) The average curvature of a flexural member can be calculated from the observed values of the flexural strains across the depth of the beam and the neutral axis depth. The occasional scatter in the results could be due to the formation of cracks within the "Demec" gauge length.

Approach Three : Proposed Methods

(a) Ordinary Beams

The deflection at the working moments of the beams was calculated in accordance with 5.3.5, where the average curvature was obtained from the following:-

$$\phi_{ave} = \frac{f_s - k_3 f_r/p}{E_s(d_1 - x)} \qquad \S \quad (5.11)$$

From the experimental values obtained, it was found that a suitable value for k_3 was 0.3. The steel stresses (f_s) employed for the beams were calculated in accordance with 4.5.2 and are shown in Figs. 34 and 35. The value of the neutral axis depth used was that calculated for a cracked transformed section by employing equation 4.5.

The theoretical and observed values for the deflections at the level of working moments are given in cols. 2 and 5 of table (9). The ratios of the calculated to the observed values of deflections are given in col. 6 of table (9). These varied between 0.94 and 1.06 with an average value of 1.01. This clearly indicates the reliability of the proposed method in predicting the actual amount of deflection for lightweight concrete beams.

(b) Composite Beams

The central deflections for the composite beams were calculated throughout the loading stages and up to the level of the cracking moment of the f. r. c. channels by employing the proposed method suggested in 5.3.5. The idealised relationship is shown in Fig. 16b. In this method the curvature of a beam can be calculated by three stages as in the following:

(1) For $M \leq M_c$, cross section No. 1 in Fig. 17.

$$\phi = \frac{M}{E_c I_o} \qquad \S \quad (5.16)$$

(2) For $M_c \geq M \leq M_p$, cross section No. 2 in Fig. 17.

$$\phi = \frac{M}{E_c I_o} + \frac{M - M_c}{k\ E_c I_p} \qquad \S \quad (5.17)$$

where $$M_p = \frac{M_a + M_c}{2}$$

(3) For $M_p \leq M \leq M_a$, cross section No. 3 in Fig. 17.

$$\phi = \frac{M_c}{E_c I_o} + \frac{M_p - M_c}{k\ E_c\ I_p} + \frac{M - M_p}{k'\ E_c\ I_{cc}} \qquad \S \quad (5.19)$$

I_p : can be calculated as shown in appendix H

From an examination of the experimental results obtained it was found suitable to use values of 0.75 and 0.7 for k and k' respectively.

In Figs. 42 and 43 are plotted the theoretical values for the deflections obtained by employing this method together with the observed values. A good agreement has been obtained between the experimental and the theoretical values. It can also be seen that the experimental load deflection behaviour of the composite beams is well represented by the trilinear concept suggested for this method.

The calculated deflections at the level of the working moments are given in col. 5 of table (9). The ratios of the calculated to observed values of the deflections, as given in col. 6 of table (9), varied between 0.98 and 1.05 with an average value of 1.02.

It can be observed that the proposed method is quite reliable in predicting the actual amount of deflection for composite beams.

7.7.3 Limit State of Cracking

7.7.3.1 Behaviour of Ordinary Beams

(a) General

The mechanism of cracks formation in reinforced concrete members and the limitations put on their width are discussed in 5.4.1. In general the surface crack width under normal conditions of exposure should not exceed 0.3mm.

In this research the width of the cracks at the level of the steel reinforcement as well as at the bottom edge of the beams was measured.

Some of the beams showed surface cracking after a period of three to four weeks after casting. This could mainly be due to the shrinkage strain which occurred in the concrete members. The maximum values of shrinkage strain obtained after four weeks from casting were 0.0005 in the small concrete prisms (100mm x 100mm x 500mm). The maximum crack width observed was 0.08mm with an average value of 0.04mm. In a previous investigation a maximum crack width of 0.05mm was observed due to shrinkage for lightweight concrete members (90).

The early formation of cracks in some of the test beams made it difficult to observe the load at which flexural cracking occurs.

The values of the direct tensile strength given in table (6) ranged between 0.94 N/mm^2 and 3.5 N/mm^2 with an average value of 2.02 N/mm^2. The values of the modulus of rupture varied from 1.6 N/mm^2 to 4.2 N/mm^2 with an average value of 2.8 N/mm^2. The average ratio of the direct tensile strength to the modulus of rupture obtained was equal to 0.7.

The low values obtained for the tensile strength and the modulus of rupture for the concrete could mainly be due to the formation of shrinkage cracks in the concrete prisms.

In the calculation of the cracking moment of the concrete the average value of the direct tensile strength (2 N/mm^2) was used. This gave a good agreement between the calculated and the observed values of cracking moments. These are given in cols. 2 and 3 of table (10).

(b) Working Moment Condition

The observed crack widths at the steel level as well as at the bottom edge of the beams at the working moment level are given in table (10). The maximum crack widths varied between 0.13mm and 0.2mm at the level of the steel, and between 0.15mm and 0.3mm at the bottom edge of the beams. The average crack widths ranged between 0.05mm and 0.14mm at the steel level and between 0.09mm and 0.22mm at the bottom edge of the beams. This indicated that the crack widths at the level of the working moment did not exceed a value of 0.3mm. It can therefore be assumed that the limit state of cracking under static loading was satisfied for the beams tested.

The ratios of maximum to average crack widths at the level of the steel for the test beams varied between 1.1 and 2.4 with an average value of 1.68; the ratios for the crack widths at the bottom edge of the beams varied between 1.22 and 1.67 with an average value of 1.52.

The cracks observed in the region of the constant moment zone gave average spacings of 129mm and 145mm at the bottom edge of the beams and at the level of the steel respectively.

With regard to the effect of surface deformation of the bars, beam ST 4 - 0 reinforced with Kam 60 steel showed smaller crack widths compared with beam ST 3 - 0 reinforced with Unisteel 550. This could be due to the surface deformation of Kam 60 steel having a better control on the crack widths. The values of the crack widths are given in table (10).

The crack widths at the level of the working moment at the first cycle did not differ from that at the second cycle by more than 0.02mm. Similarly the crack widths at 1.5 times the working moment were nearly equal at the second and third cycles of loading.

(c) Steel Stress

The variation of the maximum crack width at the steel level in relation to the steel stress can be seen in Figs. 48, 49, and 50. These figures clearly show the effect that the steel stress has on the width of the cracks. The values of the steel stresses were calculated in accordance with 4.6, and shown in Figs. 34 and 35.

The observed maximum crack widths at the bottom edge of the beams with the corresponding steel stresses in the test beams were as follows:

Beam mark	p%	Type of steel	Steel stress (N/mm^2) at a crack width of	
			0.2mm	0.3mm
ST1-0	1.044	M.S.	235	305
ST2-0, ST3-0, ST4-0, ST5-0	1.044	Deformed bars	240 - 325	360 - 440
ST6-0	1.643	M.S.	160	296
ST7-0	1.643	Deformed bars	230	-
ST8-0	1.583	Deformed bars	220	384
ST9-0	0.582	Deformed bars	240	472
ST10-0				

From the results it can be seen that the deformed bars showed better control on the width of the cracks than did the mild steel bars.

In a previous investigation (35) an average maximum crack widths of 0.2mm with mild steel and 0.18mm with square twisted bars were observed at a steel stress of 207 N/mm^2. The percentages of steel employed ranged between 0.99% and 4.62%. A direct comparison, however, with the values obtained in this research can not be made mainly owing to the variation in type and percentage of steel and the type of concrete used. The amount of concrete cover to the main tension reinforcement is another factor which should be considered.

(c) Remaining Crack Width

The maximum remaining crack widths in the test beams after the first cycle of loading varied between 0.05mm and 0.09mm at the level of the steel, and between 0.06mm and 0.1mm at the bottom edge of the beams.

Values ranging between 0.02mm and 0.05mm for the remaining crack widths were reported in a previous investigation (35).

7.7.3.2 Behaviour of Composite Beams

(a) General

The mechanism of cracks formation in the composite beams and the role of the f.r.c. channels in arresting these cracks are discussed in 5.4.2.

The cracks in the composite beams were initially observed at the interface (top of the upstands of the f.r.c. channels). Cracks at the soffits of the beams were only observed after the f.r.c. channels cracked.

As mentioned in 7.7.3.1., the average values of the tensile strength and the modulus of rupture were 2.02 N/mm^2 and 2.84 N/mm^2 respectively. For the calculation of the cracking moment of the concrete by employing equation 4.2, a value of 3 N/mm^2 for the tensile strength of the concrete at the level of the interface was used. This gave a good agreement between the calculated and the observed values of the cracking moment of the concrete as can be seen in cols. 2 and 3 of table (10).

With increasing load (greater than the cracking load of the concrete) further cracks were formed in the concrete, and an increase in width and length of the cracks were also observed. A stage, then, was reached where the f.r.c. channel cracked. The cracking of the f.r.c. channel normally occurred by the formation of one crack at a position where there was a crack already formed in the concrete. This could be due to the tensile stress in the f.r.c. channel being maximum in the vicinity of an existing crack in the concrete (at a cracked concrete section) and minimum at a point between two adjacent crack (at an uncracked concrete section).

Furthermore the cracks which might have formed in the confined concrete by the presence of the f.r.c. channels could have induced additional local tensile strains in the f.r.c. channels. This might have contributed to the development of cracks in the f.r.c. channels at positions of existing cracks in the confined concrete.

Another factor is that the neutral axis depth at a cracked concrete section is less than that at an uncracked concrete section. Considering a straight line strain distribution, a greater tensile strain in the f.r.c. channels would be expected at the cracked section.

The maximum surface crack width measured on the f.r.c. channels when first cracked ranged between 0.1mm and 0.4mm depending on the level of the cracking moment of the f.r.c. channels. The corresponding cracks in the confined

concrete, however, might be smaller. This is discussed in section (d).

At higher levels of loads more cracks were formed in the f.r.c. channel. This indicated that the composite action was not completely lost by the formation of the first crack in the f.r.c. channel and also that the f.r.c. channel was still carrying tensile stresses at the uncracked sections. It also indicated that there was still a good bond between the f.r.c. channels and the concrete which enabled the f.r.c. channels to carry the tensile stresses.

The cracking behaviour of the beams can be seen in Figs 51, 52, 53 and 54, where the observed maximum crack widths at the interface (level of the steel) are plotted against the applied moment. The figures show that the width of the cracks up to and well beyond the level of the working moments are well within the recommended limits. However, when the cracking moments of the f.r.c. channels were reached the width of the cracks suddenly increased. This increase in the crack widths could mainly be due to the sudden transfer of the tensile stresses from the f.r.c. channels to the steel, which increased the tensile strain in the steel, resulting in a greater crack width.

(b) Working Moment Conditions

The observed crack widths at the level of the working moment for the test beams are given in table (10). The beams did not show any visible cracks at their soffits, the exception being beam ST 4 - C. This was mainly because the f.r.c. channels did not crack up to levels greater than their respective values of working moments, the exception being beam ST 4 - C containing Kam 60 steel, where the f.r.c. channel cracked at a level lower than the working moment.

The maximum crack width at the level of the steel (measured at the interface) ranged from 0 to 0.1mm, whilst the average crack widths varied between 0 and 0.08mm. The average ratio of the maximum to the average crack widths for the various beams was 1.5.

It may be concluded, therefore, that the composite beams showed a considerable reduction in the amount of cracking in concrete at the levels of the working moments.

(c) Remaining Crack Width

The remaining maximum crack width at the steel level for the test beams

after the first cycle of loading are given in col. 10 of table (10). These values varied between 0 and 0.04mm. Only beam ST 4 - C had a maximum residual crack width of 0.1mm at the bottom edge of the beam.

(d) Cracks in the Confined Concrete

To study the formation of the cracks in the confined concrete parts of the f.r.c. channel of a composite beam which had been subjected to the first and second cycles of loading were cut and removed while the beam was unloaded. The removed parts were 50mm to 100mm on either side of existing cracks in the concrete (observed at the interface) and also in the f.r.c. channel.

One of the interesting points observed at zero load was that at positions where cracks had formed in the channel the crack widths in the confined concrete were smaller than those measured on the surface of the channel. After reloading the beam similar behaviour was observed at the level of the working moment. A crack in the confined concrete observed at a position where the f.r.c. channel had been cracked can be seen in plate 4b. This was observed at the level of the working moment of the beam.

Another interesting point was that in the areas where there were no cracks in the f.r.c. channel the confined concrete did not show visible cracks. This was observed at zero load as well as at the level of the working moment. This behaviour at the level of the working moment can be seen in plate 4a.

7.7.3.3 Comparison Between Ordinary and Composite Beams

For a comparison between the cracking behaviour of the ordinary and composite beams, the following points were observed.

(1) Shrinkage cracks did not appear on the composite beams, whereas a maximum crack width of 0.08mm was observed due to shrinkage in the ordinary beams.

(2) An increase in the apparent cracking moment of concrete at which cracks were observed at the interface was obtained. The ratios of the cracking moments of concrete for the composite beams to those for corresponding ordinary beams varied between 2.2 and 4. This clearly indicated the contribution of the f.r.c. channel in controlling flexural cracks in the composite beams.

(3) At the working moment conditions the widths of the cracks in the composite beams were much smaller than those in the corresponding ordinary beams Figs. 51, 52, 53 and 54. The ratios of the maximum crack widths at the level of the steel in the ordinary beams to those in the composite beams, except beam ST 4 - C, varied between 2 and 6. At the soffits of the beams no cracks were observed in the composite beams, whereas the maximum crack widths in the corresponding ordinary beams ranged between 0.15mm and 0.26mm.

(4) When the f.r.c. channel cracked, some of the composite beams showed slightly greater crack widths at the interface than those in the corresponding ordinary beams, e.g. beams ST 1 - C, ST 4 - C and ST 7 - C (Figs. 51, 52 and 53). The maximum surface crack widths measured on the surface of the f.r.c. channels at the soffits of the composite beams were greater than those in the corresponding ordinary beams.

(5) The number of visible cracks in the composite beams was less than that in the ordinary beams. This can be seen in col. 6 of table (10), where in some beams the number of visible cracks in the composite beams at the level of the working moment was nearly half of that in the ordinary beams. The average spacings of cracks were 250mm and 145mm for the composite and the ordinary beams respectively.

(6) The length of the cracks in the composite beams was limited due to the restraint action of the f.r.c. channels. A direct comparison between the length of the cracks in ordinary and composite beams can be seen in Fig. 55.

7.7.3.4 Comparison With Theory

Ordinary Beams

As mentioned in 5.4.3., the crack widths for the ordinary beams were calculated by employing the proposed method in CP110 and also by employing the C. and C.A. formula.

The CP110 formula is:

$$w = \frac{3\, a_{cr}\, e_m}{1 + 2\,\frac{(a_{cr} - c)}{d - x}} \qquad \S \quad (5.21)$$

Where

$$e_m = e_1 - \frac{1.2\, bd\, (a' - x)\ \times 10^{-3}}{A_s\, (d - x)\, f_y} \qquad \S \quad (5.22)$$

In this formula the neutral axis depth and the steel stresses obtained from the experimental results were used.

The method underestimated the maximum crack widths at the steel level and at the bottom edge of the beams for seven out of the ten beams tested. The calculated values of the crack widths are given in cols. 12 and 13 and the observed values are given in cols. 4 and 7 of table (10).

Calculations were also carried out using the C and C.A. formula (88). The equation for the maximum crack width at the bottom edge of the beam is

$$w = 3.3c \frac{f_s}{E_s} \frac{(d - x)}{d_1 - x} \qquad (5.23)$$

c: cover the main reinforcement

The term $d - x/d_1 - x$ reduces to 1.0 when crack width at the steel is sought.

The calculated values obtained by employing this method for the maximum crack width at the steel level together with the observed values for the test beams are plotted against the applied moment as shown in Figs. 48, 49 and 50. These figures show that a good agreement is obtained between the calculated and the observed values. The calculated values of the crack widths at the steel level and at the bottom edge of the beams at the level of the working moment are given in cols. 14 and 15 of table (10).

The ratios of the calculated to observed values of the maximum crack widths at the steel level ranged between 0.7 and 1.1 with an average value of 0.98, the ratios at the bottom edge of the beams ranged between 0.9 and 1.8 with an average value of 1.3.

CHAPTER EIGHT

EFFECTS OF LONG TERM LOADING ON TEST BEHAVIOUR FOR ORDINARY AND COMPOSITE BEAMS

8.1 Introduction

This chapter discusses the effect that long-term loading had on the behaviour of the ordinary and the composite beams.

A total of nine beams were tested; five beams under fatigue and four beams under sustained loading tests. The properties of the various beams tested are given in tables (2) and (3). The methods of testing employed are explained in Chapter Six. Beams tested under fatigue loading were initially tested under static loading test. Thereafter they were subjected to a cyclic loading with an upper limit equal to the working moment of the beam and a lower limit equal to half the working moment. The number of repetitions applied to each of the test beams was about three million cycles.

Beams tested under sustained loading were initially tested under static loading up to the working moment. The beams then were kept under sustained loading for a minimum period of 500 days. The discussion of the test behaviour includes the effect of long term loading on the neutral axis depth, flexural compressive strain in the concrete and the stresses in the steel and the f.r.c. channels. More emphasis is placed on the limit states of ultimate strength, cracking and deflection.

A direct comparison between the flexural behaviour of the ordinary and the composite beams is also presented.

8.2 Fatigue Loading Tests

8.2.1 Variations of the Neutral Axis Depth

(a) Ordinary Beams

There are two major factors which can affect the position of the neutral axis depth of flexural members subjected to fatigue loading. These are:-

(1) An increase in width and height of travel of the cracks due to repeated loading can result in raising the neutral axis level towards the compression face.

(2) The increase in the flexural compressive strain in concrete due to repeated loading can lower the position of the neutral axis depth.

However, by referring to Fig. 56, it can be seen that cyclic loading had no appreciable effect on the level of the neutral axis depth for the beams tested in this investigation. At the levels of the working moments the ratios of the neutral axis depths measured after three million cycles to those obtained at the first cycle were 0.98, 1.05 and 1.17 for beams FA 1 - 0 (1.044% mild steel), FA 2 - 0 (1.044 Unisteel 410) and FA 4 - 0 (1.044% Kam 60) respectively.

It can be seen that the higher the level of the working moment the greater is the ratio of the final to initial neutral axis depth. This was mainly due to the fact that the initial values of the neutral axis depth were greater at low levels of working moments. Additionally, with higher levels of repeated working load a greater increase was observed in the flexural compressive strain in the concrete. This consequently increased the neutral axis depth. The effect of repeated loading on the flexural compressive strain in the concrete is explained in 8.2.2.

(b) Composite Beams

In Fig. 56 are plotted the experimental values of the neutral axis depth at the level of the working moment against the number of load repetitions.

In the early stages of the repeated loading process, beam FA 1 - C reinforced with mild steel showed a noticeable reduction in the neutral axis depth. Thereafter no practical change in the neutral axis depth was observed. Beam FA 2 - C, however, showed a slight increase in the neutral axis depth.

At the levels of the working moments the ratios of the neutral axis depths measured after three million cycles to those obtained at the first cycle were 0.84 and 1.1 for beams FA 1 - C and FA 2 - C respectively.

The factors which might have affected the position of the neutral axis in the ordinary beams, as discussed in section (a), also have a similar effect on the composite beams. Additionally, the formation of cracks in the f.r.c. channels due to repeated loading could result in reducing the neutral axis depth. This is mainly due to the reduction in the tension stiffening effect of the f.r.c. channels and also due to the propagation of the cracks towards the compression face once cracking occurs in these channels.

For beam FA 1 - C, the cracking of the f.r.c. channel had considerably reduced the neutral axis depth. This can be seen in Fig. 56, where most of the reduction in the neutral axis depth occurred in the early stages of the repeated loading, the f.r.c. channel being cracked after 450,000 cycles of loading. This resulted in a lower ratio for the final to initial neutral axis depth for beam FA 1 - 0.

The neutral axis depth of beam FA 2 - C, however, was not greatly affected by the cracking of the f.r.c. channels which occurred after 300,000 repetitions. The relatively higher level of moment of beam FA 2 - C had led to a greater rate of increase in the flexural compression strain in the concrete, consequently the neutral axis depth was increased. This resulted in a greater ratio for the final to initial neutral axis depth for beam FA 2 -C.

(c) Comparison Between Ordinary and Composite Beams

At the first static test the composite beams showed a greater neutral axis depth than the corresponding ordinary beams. After three million cycles the ratios of the neutral axis depths of the ordinary beams to those of the corresponding composite beams were 1.04 for beams FA 1 - 0 and FA 1 - C and 0.83 for beams FA 2 - 0 and FA 2 - C. This indicated that only in one case did a composite beam show a greater neutral axis depth than that of a corresponding ordinary beam.

8.2.2 Variations of the Maximum Flexural Compressive Strain in Concrete

(a) Ordinary Beams

In Fig. 57 are plotted the observed values of the maximum flexural compressive strain at the level of the working moment versus the number of load repetitions.

In general, repeated loading caused an increase in the compressive strain in the concrete; most of the increase, however, occurred during the first 600,000 cycles for beams FA 1 - 0 and FA 2 - 0 and 1.5 million cycles for beam FA 4 - 0. Thereafter no practical change was observed.

The ratios of the maximum flexural compressive strain in the concrete at the working moment measured after three million cycles to that measured at the first cycle were 1.18 for beam FA 1 - 0 (1.044% mild steel), 1.25 for beam FA 2 - 0 (1.044% Unisteel 410) and 1.4 for beam FA 4 - 0 (1.044% Kam 60). The initial values of stresses in the concrete at the upper limit of the cyclic loading were

23% (beam FA 1 - 0), 30% (beam FA 2 - 0) and 34% (beam FA 4 - 0) of the respective cylinder compressive strength. The stresses at the lower limit were equal to nearly half those at the upper limit.

These stresses were obtained by correlating the measured maximum compressive strains in concrete with the corresponding experimental stress-strain relationship of concrete in compression. This indicated that the greater the level of stress at the upper limit of the loading cycles, the greater is the rate of increase in the flexural compressive strains in the concrete. Similar behaviour was also observed in a previous investigation on normal weight concrete members (93).

(b) Composite Beams

The experimental values of the maximum flexural compressive strain in the concrete at the level of the working moment are plotted against number of load repetitions in Fig. 57.

This shows that repeated design load increased the compressive strain in the concrete. However, after about 1.5 million repetitions no practical change was observed.

The ratios of the maximum flexural compressive strain in the concrete at the working moment measured after three million cycles to that obtained at the first cycle were 1.78 and 1.8 for beams FA 1 - C and FA 2 - C respectively. These ratios are considerably greater than those obtained for the corresponding ordinary beams discussed in section (a). This is mainly because the f.r.c. channel did not crack at the first cycle which resulted in lower initial values for the flexural compressive strain in the concrete. In addition, cracks were formed in the f.r.c. channels during the process of repeated loading. This considerably increased the values of the flexural compressive strains in the concrete. This behaviour is explained in 7.4 (c).

(c) Comparison Between Ordinary and Composite Beams

The composite beams, at the first static test, showed lower values for the flexural compressive strains in the concrete than those in the corresponding ordinary beams. This was mainly due to the contribution of the f.r.c. channels which did not crack at the first cycle of loading. After three million cycles the

ratios of the maximum flexural compressive strains in concrete in the ordinary beams to those in the corresponding composite beams were 0.7 and for beams FA 1 - 0 and FA 1 - C (1.044%mild steel) and 0.87 for beams FA 2 - 0 and FA 2 - C (1.044% Unisteel 410). This indicated that the composite beams had greater flexural compressive strains in the concrete than the corresponding ordinary beams. This was mainly due to the formation of cracks in the f.r.c. channel during the process of repeated loading which consequently led to an increase in the flexural compressive strains.

8.2.3. Stresses in the f.r.c. Channels

The stresses in the f.r.c. channels were obtained by correlating the values of strains measured on these channels with their experimental stress-strain relationship shown in Fig. 8.

At the first cycle of loading the stresses in the f.r.c. channels for beams FA 1 - C and FA 2 - C which were subjected to fatigue loading were nearly the same as those for the corresponding beams ST 1 - C and ST 2 - C. At the level of the working moments (upper limit of the loading cycles) the maximum stresses in the f.r.c. channels for beams FA 1 - C and FA 2 - C were 5.83 N/mm^2 and 8.93 N/mm^2 respectively. The stresses in the f.r.c. channels of the corresponding beams ST 1 - C and ST 2 - C were 5.33 N/mm^2 and 9.13 N/mm^2 respectively.

The initial maximum stresses in the f.r.c. channels in the composite beams subjected to fatigue loading ranged between (2.3 - 5.83 N/mm^2) for beam FA 1 -C and between (3.2 - 8.93 N/mm^2) for beam FA 2 - C. These values expressed as percentages of a nominal tensile strength equal to 15 N/mm^2 for the f.r.c. units (see Fig. 8) are between 15.3 - 38.9% for beam FA 1 - C and between 21.3 - 59.5% for beam FA 2 - C.

The behaviour of the f.r.c. channels in the composite beams tested under fatigue loading could be mainly affected by the level of stresses at the lower and upper limits of the loading cycles.

It is worth pointing out that the increase in the strain of the f.r.c. channels under the stresses at the lower limit was mainly due to creep, as the channels were subjected to these stresses continuously for the period of repeated loading. Referring to Fig. 8, it can be seen that the stresses at the lower limit (2.3 N/mm^2

and 3.2 N/mm^2) are low and may be considered to be within the elastic range of the behaviour of the f.r.c. units. Thus the effect of these stresses on the behaviour of the f.r.c. channels may not be considerable.

It is most likely, therefore, that the increase in strain and the consequent formation of cracks in the f.r.c. channels was mainly due to the effect of repeated loading.

The formation of cracks in the f.r.c. channels was observed after 450,000 cycles and 300,000 cycles for beams FA 1 - C and FA 2 - C respectively. This indicated that the range of stresses in the f.r.c. channels between the lower and upper limit of the loading cycles which were 2.3 - 5.83 N/mm^2 for beam FA 1 - C and 3.2 - 8.93 N/mm^2 for beam FA 2 - C directly affected the number of cycles at which cracks were formed (i.e., the higher the range of applied stresses the lower is the number of repetitions at which the channel crack).

One of the important features in the behaviour of the f.r.c. channels under the effects of repeated loading was the good bond maintained between these channels and the concrete throughout the process of the fatigue test. No separation occurred between the concrete and the f.r.c. channel even when the beams were finally tested to destruction after the application of three million cycles.

8.2.4. Variations of the Steel Stresses

(a) Ordinary Beams

The main factor which might have affected the values of the steel stresses in beams subjected to fatigue loading was the variation of the neutral axis depth, which alter the lever arm of the steel.

The working steel stresses calculated in accordance with 4.6 for the beams at the first cycle (initial values) and after three million cycles (final values) are given in cols. 3 and 4 of table (11).

In this calculation equation (4.18) was used, where the only variable was the neutral axis depth. The value of β corresponded to the stress distribution of the concrete in compression at the first cycle of loading.

The ratios of the final to initial values of the steel stresses, as given in col. 5 of table (11), were 0.99, 1.02 and 1.03 for beams FA 1 - 0, FA 2 - 0 and

FA 4 - 0 respectively. This, however, indicated that repeated loading did not affect significantly the values of the steel stresses.

(b) Composite Beams

The initial and final values of the steel stresses calculated in accordance with 4.6 are given in cols. 3 and 4 of table (11). In this calculation equation 4.20 was used, the contribution of the f.r.c. units, however, was only considered in the calculation of the initial values, since the channels for both beams cracked during the process of repeated loading. The ratios of final to initial values of the steel stresses, as given in col. 5 of table (11), were 1.17 and 1.22 for beams FA 1 - C and FA 2 - C respectively. It can be seen that these ratios are greater than those for corresponding ordinary beams as discussed in section (a).

This is mainly due to the following:

i) The initial values of the steel stresses in the composite beams were lower than those in the corresponding ordinary beams. This was due to the contribution of the f.r.c. channels which did not crack at the first cycle of loading.

ii) The formation of cracks in the f.r.c. channels during the process of repeated loading. When the channels cracked the tensile stresses which were carried by the f.r.c. channels were transferred to the tension reinforcement of the member at cracked sections.

Another factor which might have affected the values of the steel stresses was the variation of the neutral axis depth due to repeated loading and the consequent change in the lever arm of the tension reinforcement in the member.

(c) Comparison Between Ordinary and Composite Beams

Col. 3 of table (11) shows that, at the first cycle of loading, the steel stresses in the composite beams are lower than those in the corresponding ordinary beams. This, as explained in section (a) earlier, was due to the contribution of the f.r.c. channel which did not crack at the first cycle. After three million cycles the values of the ratio of steel stress in the ordinary beams to that in the corresponding composite beams, as given in col. 4 of table (11), were 1.022 for beams (FA 1 - 0 and FA 1 - C) and 0.96 for beams (FA 2 - 0 and FA 2 - C). This indicated that the steel stresses in the composite beams did not

differ significantly from those in the corresponding ordinary beams even after three million cycles and in spite of the formation of cracks in the f.r.c. channels.

8.2.5. Principal Limit States

8.2.5.1. Limit State of Ultimate Strength

(a) Ordinary Beams

At the end of the fatigue loading test all the beams were tested up to failure under static loading, as none of the beams tested failed under fatigue loading. Beam FA 1 - 0 failed at an ultimate moment equal to 36.125 kN.m; the ultimate moment of the corresponding beam ST 1 - 0 was 39 kN.m. Beams FA 2 - 0 and FA 4 - 0 exhibited nearly the same ultimate strength as for the corresponding beams ST 2 - 0 and ST 4 - 0 respectively. Previous investigations on prestressed and reinforced normal weight concrete beams showed that repeated design working load did not have an appreciable effect on the ultimate strength of the members (64), (94), (95). In some cases, however, it was found that repeated design working load caused an increase in the ultimate strength of the members (73), (96).

The behaviour of the beams with regard to the failure mechanism was similar to that observed for the beams which were tested under static loading as explained in 7.6.1.

Col. 6 of table (11) gives the calculated ultimate moments of the beams using the strain compatibility method explained in 5.2.1. In this method the actual strength values of concrete and steel, without the partial safety factors of the material, were used.

The ratios of observed to calculated values of the ultimate moment, as given in col. 8 of table (11), were 1.13, 1.15 and 1.12 for beams FA 1 - 0, FA 2 - 0 and FA 4 - 0 respectively. This shows that the observed values of the ultimate moments were greater than the calculated ones. The factors which might have affected this behaviour are discussed in 7.7.1.

(b) Composite Beams

The composite beams tested did not fail under fatigue loading. An excellent bond between the f.r.c. channels and the concrete was maintained throughout the

process of repeated loading.

When the beams were finally tested to destruction, beam FA 1 - C failed at an ultimate moment of 38.375 kN.m; the corresponding beam ST 1 - C failed at 40.5 kN.m. Beam FA 2 - C had an ultimate strength equal to 50.5 kN.m compared with 46.5 kN.m for the corresponding beam ST 2 - C. It may be concluded, therefore, that fatigue loading did not have an appreciable effect on the ultimate strength of the composite beams.

The failure mechanism was similar to that for the beams tested under static loading only as explained in 7.6.1.

The calculated ultimate moments of the beams, using the strain compatibility method and incorporating the actual values of strengths for concrete and steel without the partial safety factors of materials are given in col. 6 of table (11). The ratios of observed to calculated ultimate moments as given in col. 8 of table (11) were 1.18 for beams FA 1 - C and 1.28 for beam FA 2 - C. The factors which could have influenced the observed values of the ultimate moments are the same as those for the ordinary beams as explained in 7.6.1.

(c) Comparison Between Ordinary and Composite Beams

The observed values of the ultimate moments for the ordinary and composite beams are given in col. 7 of table (11). This shows that the observed ultimate moments of the composite beams were slightly greater than those of the corresponding ordinary beams. This may indicate that the f.r.c. channels contributed to the ultimate strength of the composite beams. However, it must be emphasised that at the end of fatigue loading the channels were cracked at many sections and that the contribution of the f.r.c. channels if any would be negligible.

8.2.5.2. Limit State of Deflection

(a) Ordinary Beams

The remaining and working load deflections for beams FA 1 - 0, FA 2 - 0 and FA 4 - 0 at the first cycle (given in cols. 2 and 3 of table (12)) agree well with those observed for the corresponding beams ST 1 - 0, ST 2 - 0 and ST 3 - 0 (given in cols. 2 and 3 of table (9)). However, the maximum difference was that beam FA 2 - 0 had a working deflection 10% greater than that observed for the

corresponding beam ST 2 - 0. Typical load deflection curves for static loading tests carried out at frequent intervals during the repeated loading test are shown in Fig. 58.

This shows that the difference between the values of deflection at the loading and unloading stages diminishes with an increase in number of repetitions.

Typical load-deflection behaviour for the loading and unloading stages when the beams were finally tested to failure is shown in Fig. 59. The behaviour in general was similar to that observed for the beams tested under static loading only.

For each beam the deflection at the level of the working moment was nearly the same at the first and second cycles of loading. Similarly the deflection at 1.5 times the working moment was nearly equal at the second and third cycles of loading. The variations in the remaining deflection and the deflection at the working moment with number of repetitions for beams FA 1 - 0, FA 2 - 0 and FA 4 - 0 are shown in Fig. 60. It can be seen that most of the increase in the remaining deflection and the deflection at the working moment occurred during the first six hundred thousand repetitions. It is important to emphasise here that the first static test carried out during the process of fatigue loading was after about 500,000 cycles of loading. Hence the greater rate of increase in deflection might well have occurred during the first few thousand repetitions. Thereafter no practical increase in the amount of deflections was observed.

The ratios of the deflection at the working moment after three million cycles to that at the first cycle, as given in col. 6 of table (12), were 1.55 for beam FA 1 - 0 (mild steel), 1.31 for beam FA 2 - 0 (Unisteel 410) and 1.22 for beam FA 4 - 0 (Kam 60 steel). This indicates that when high working steel stresses were employed with the same percentage of steel a lower rate of increase in the amount of diflection with number of repetitions resulted. This was mainly because when high working steel stresses were employed with the same percentage of steel a greater deflection resulted at the first cycle of loading. Additionally, flexural members with high working steel stresses had greater width and height of travel of cracks at the first cycle of loading. In a previous investigation on normal weight concrete members. an increase between 20 and 25% in the amount of deflection was observed in the early stage of repeated loading (97). Col. 4 of table (12) shows that

the deflection at the working moment after three million cycles did not exceed the recommended limit of span/250 (i.e. 18mm) in beams reinforced with either mild steel or unisteel 410. This indicates that beams FA 1 - 0 and FA 2 - 0 satisfied the limit state of deflection even after three million cycles of loading.

(b) Composite Beams

The working and remaining deflection at the first static test for beams FA 1 - C and FA 2 - C (given in cols. 2 and 3 of table (12)) agree well with those observed for the corresponding beams ST 1 - C and ST 2 - C (given in cols. 2 and 3 of table (9)). However, the maximum difference was that beam FA 2 - C had a working deflection 8% lower than that observed for the corresponding beam ST2 - C.

Fig. 58 shows a typical load deflection curve obtained from static tests carried out at frequent intervals during the repeated loading test. The behaviour was similar to that of the ordinary beams, where the difference between the values of deflection at the loading and unloading ranges diminishes with an increase in number of repetitions. A typical load-deflection behaviour for the beams when finally tested to failure is shown in Fig. 59. For each beam tested the deflection at the level of the working moment was nearly the same in the first and second cycles of loading. Similarly the deflection at 1.5 times the working moment was the same in the second and the third cycle of loading.

The variations in the remaining deflections and deflections at the working moments with the number of repetitions for beams FA 1 - C and FA 2 - C are shown in Figs. 60. It can be seen that the rate of increase in both deflections was more pronounced during the first 1.5 million cycles. Thereafter no practical change in the deflection was observed.

A major factor which could have influenced the rate of increase in the deflection was the formation of cracks in the f.r.c. channels during the process of repeated loading. However, examination of Figs. 60 shows that the formation of cracks in the f.r.c. channels did not cause a sudden increase in the deflection of the members. This could be due to the fact that the channels cracked at the level of the working moment where the stresses in the f.r.c. channel were relatively low. It may follow from this that the transference of the stresses from

the f.r.c. channels to the steel did not affect significantly the curvature of the member.

The values of the remaining deflections and deflections at the working moment at the first and after three million cycles are given in table (12).

The values of the ratios of final to initial deflection at the working moment were 1.97 for beam FA 1 - C and 1.87 for beam FA 2 - C. These ratios were greater than those observed for the ordinary beams. This was mainly due to the f.r.c. channels did not crack at the first cycle which resulted in lower initial values for deflection. In addition, the cracking of the f.r.c. channels during the process of repeated loading caused in increase in the amount of deflection.

For both beams the recommended limit span/250 (i.e. 18mm) was not exceeded even after the application of three million cycles. Therefore, the composite beams FA 1 - C and FA 2 - C were considered to be serviceable with regard to the limit state of deflection under fatigue loading.

(c) Comparison between Ordinary and Composite Beams

The deflection behaviour in relation to the number of repetitions for the ordinary and composite beams is shown in Fig. 60.

In the first static tests the composite beams showed considerable saving in the deflections at the working moment and also in the remaining deflections. The ratios of the deflection at the working moment for the ordinary beams to that of the corresponding composite beams were 1.3 for beams FA 1 - 0 and FA 1 - C (mild steel), and 1.53 for beams FA 2 - 0 and FA 2 - C (Unisteel 410). The ratios of the remaining deflection for the ordinary beams to that of the corresponding composite beams were 1.29 for beam FA 1 - 0 and FA 1 - C, and 1.53 for beams FA 2 - 0 and FA 2 - C.

From the examination of Fig. 60 it can be seen that at the levels of the working moment the composite beams showed a greater stiffness than the corresponding ordinary beams within a range of 1.5 million repetitions. Thereafter beam FA 1 - C exhibited nearly the same stiffness as for beam FA 1 -0, whereas beam FA 2 - C maintained a greater stiffness than beam FA 2 - 0 up to three million cycles.

The values of deflection observed after three million cycles for ordinary and composite beams are given in col. 4 of table (12). The ratios of the deflection

at the working moment of the ordinary beams to that of the composite beams were 1.02 for beams FA 1 - 0 and FA 1 - C, and 1.07 for beams FA 2 - 0 and FA 2 - C.

From the same figures it can also be seen that the remaining deflections of the composite beams were lower than those of the corresponding ordinary beams up to 1.4 million cycles. Thereafter the remaining deflections of the composite beams did not differ significantly from those of the corresponding ordinary beams. After three million cycles the ratios of the remaining deflection of the ordinary beams to that of the corresponding composite beams were 1.15 for beams FA 1 - 0 and FA 1 - C, and 0.93 for beams FA 2 - 0 and FA 2 - C.

8.2.5.3. Limit State of Cracking

(a) Ordinary Beams

The maximum and average crack widths at the working moment for beams FA 1 - 0, FA 2 - 0 and FA 4 - 0 at the first cycle are given in table (13). These values fairly agree with those observed for the corresponding beams ST 1 -0, ST 2 - 0 and ST 4 - 0, the values of which are given in table (10).

The effect of repeated loading on the maximum and average crack widths at the steel level can be seen in Figs. 61 and 62 for beams FA 1 - 0, FA 2 - 0 and FA 4 - 0. These figures show that the crack widths increased with the number of load repetitions.

However, a stabiiised condition was reached within one million cycles for beam FA 1 - 0, 1.7 million cycles for beam FA 2 - 0 and six hundred thousand cycles for beam FA 4 - 0.

An examination of Figs. 61 and 62 shows that, in some cases, a reduction in the crack width was observed. This could be due to the formation of new cracks which tended to reduce the width of adjacent cracks.

Col. 6 of table (13) shows that even after three million repetitions of load the maximum crack width at the steel level did not exceed 0.2mm. However, the maximum crack widths at the bottom edge of the beams, as given in col. 8 of table (13), were 0.2mm in beam FA 1 - 0, 0.28mm in beam FA 2 - 0 and 0.24mm in beam FA 4 - 0.

The average crack width, as can be seen in cols 7 and 9 of table (13), did not exceed a value of 0.2mm. Cols. 10 and 11 of table (13) show that the ratios

of the maximum crack width at the working moment after three million repetitions to that at the first cycle of loading ranged between 1.25 and 1.43 for the cracks at the steel level and between 1.2 and 1.43 for the cracks at the bottom edge of the beams. In a previous investigation increases in crack width ranged between 20 and 25% in normal weight concrete members tested under fatigue loading were observed (97).

At the level of the working moment, the maximum crack width in the ordinary beams after three million cycles did not exceed a value of 0.3mm. This may indicate that the beams had satisfied the limit state of cracking even after three million cycles of loading.

(b) Composite Beams

When the beams were first loaded up to their working moment no cracks were observed at their soffits. This was mainly because the f.r.c. channels did not crack in the first cycle of loading. At the interface (level of the steel) beam FA 1 - C did not show any crack whereas beam FA 2 - C had a maximum crack width of 0.04mm under the working moment.

Figs. 61 and 62 show the variation in the maximum and average crack widths in relation to the number of load repetitions for beams FA 1 - C and FA 2 - C. For both beams most of the increase in the crack widths occurred within 1.5 million repetitions. It is worth pointing out here that most of the increase in the deflection as mentioned in 8.2.5.2. also occurred within the same number of repetitions. This indicated a direct relation between the deflection and cracking behaviour in composite beams subjected to fatigue loading.

One of the major factors which could have affected the crack widths in the concrete was the formation of cracks in the f.r.c. channels during the process of repeated loading. This effect, however, was not significant compared with that observed in beams tested under static test only. It can be seen in Figs. 61 and 62 that when the channels cracked the crack width in concrete did not increase excessively. This could be as mentioned in 8.2.5.2. due to the fact that the f.r.c. channels cracked at the level of the working moment where the stresses in the f.r.c. channels were relatively low. The maximum crack width observed at the time when cracks formed did not exceed a value of 0.2mm.

Examination of Figs. 61 and 62 shows that at some stages a reduction in the crack width was observed. This as explained in case of the ordinary beams could also be due to the formation of new cracks which tended to reduce the width of adjacent cracks.

Col. 6 of table (13) shows that the values of the maximum crack widths at the steel level after three million cycles were 0.15mm in beam FA 1 - C and 0.18 in beam FA 2 - C. The values for the average crack widths given in col. 7 of table (13) were 0.06 in beam FA 1 - C and 0.1 in beam FA 2 - C. This clearly indicates that the widths of the cracks measured at the steel level even after three millions of cycles were not excessive but well within the recommended limits.

Cracks at the bottom edge of the beams (on the f.r.c. channels) observed after three million cycles' had a maximum value of 0.32mm in beam FA 1 - C and 0.38mm in beam FA 2 - C; the average value were 0.27mm in beam FA 1 - C and 0.26mm in beam FA 2 - C. The remaining crack widths at the bottom edge of beams FA 1 - C and FA 2 - C as given in col. 12 of table (13) were 0.1mm and 0.14mm respectively.

To study the crack formation in the confined concrete a similar exercise to that carried out for the composite beams tested only under static loading as explained in 7.7.3.2. was carried out for the composite beam FA 2 - C. This was carried out after the beam FA 2 - C had been subjected to three million cycles. The observations and results obtained were similar to those explained in 7.7.3.2(d)

(c) Comparison Between Ordinary and Composite Beams

At the first cycle of loading the composite beams FA 1 - C and FA 2 - C did not show any cracks at their soffits, while the corresponding ordinary beams FA 1 - 0 and FA 2 - 0 had maximum crack widths, at the working moment, equal to 0.14mm and 0.22mm respectively. Similarly cracks at the level of the steel were much greater in the ordinary beams compared with those in the composite beams.

Figs. 61 and 62 show the cracking behaviour of the ordinary and composite beams which were tested under fatigue loading. Examination of these figures shows that the composite beams had smaller crack widths at the level of the steel within a range of 1.5 million cycles. Thereafter beam FA 1 - C showed a slightly

greater maximum crack width than that in the corresponding beam FA 1 - 0, whereas beam FA 2 - C showed a lower maximum crack width than the corresponding beam FA 2 - 0 up to three million cycles. The average crack widths in the composite beams were lower than those in the corresponding ordinary beam up to three million cycles.

The crack widths observed at the bottom edge of the composite beams, after the f.r.c. channel had cracked, were greater than those in the corresponding ordinary beams (see cols. 8 and 9 of table (13)). However, the actual crack widths in the confined concrete could be lower than those measured on the f.r.c. channel as explained in 7.7.3.2(d)

The remaining crack widths after three million cycles as given in col. 12 of table (13) in the composite beams did not differ significantly from those observed in the corresponding ordinary beams.

8.3 Sustained Loading Tests

The sustained load for the test beams was maintained for a minimum period of 500 days. The periods of sustained loading for the various beams are given in table (6).

8.3.1. Time-dependent Flexural Strain Distribution

(a) Ordinary Beams

The flexural compressive strains in concrete in the beams tested under sustained loading increased at a much higher rate than the tensile strain in the steel. This resulted in an increase in the neutral axis depth with the passage of time. At a later stage in the sustained loading period a slight reduction in the tensile strains at the level of the steel was observed.

Another explanation for the variation of the neutral axis depth given was that due to plastic flow of concrete, the compressive stresses in the concrete reduced. This necessitates that the neutral axis depth should increase in order to provide a greater area of concrete in compression (98).

A typical flexural strain distribution for a beam tested under sustained loading is shown in Fig. 63. A similar pattern for the time-dependent strain distribution for conventionally reinforced and prestressed concrete beams has also

been reported by many investigators (64) (73) (96) (99).

The initial (at the first cycle) and final (at the end of sustained loading) values of the maximum flexural compressive strain in concrete at the working moment are given in cols. 3 and 4 of table (14). The ratios of the final to initial values (as given in col. 5 of table (14)) were 3.5 for beam SU 1 - 0 and 2.34 for beam SU 2 - 0. The ratio for beam SU 1- 0 was greater than that of beam SU 2 - 0; this was mainly due to the lower initial value of beam SU 1 - 0 and also to the fact that the increase in the compressive strain in concrete did not differ significantly from that of beam SU 2 - 0. The increases in the maximum flexural compressive strain in the concrete are given in col. 6 of table (14).

The shrinkage strains measured on the sides of the beams (as explained in 6.7.1 (e)) after 500 days of loading were 410×10^{-6} for beam SU 1 - 0 and 350×10^{-6} for beam SU 2 - 0. This indicated that the shrinkage strains formed 45% and 37% of the respective increase in the flexural compressive concrete strains in beams SU 1 - 0 and SU 2 - 0 respectively. The values are given in cols. 6, 7 and 8 of table (14).

Fig. 63 shows the increase in the neutral axis depth with the passage of time. After 500 days of loading the neutral axis depths were 62% and 58% greater than the initial values in beams SU 1 - 0 and SU 2 - 0 respectively. The values of the neutral axis depth for beam SU 2 - 0 can be seen in Fig. 63.

(b) Composite Beams

The behaviour of the composite beams under sustained loading was basically similar to that of the ordinary beams.

A typical time-dependent flexural strain distribution for a composite beam is shown in Fig. 64, where it can be seen that the compressive strains in the concrete and the neutral axis depth were increased with the passage of time. The variation of the tensile strain in the f.r.c. channels with the passage of time is discussed in 8.3.2.

The values of the maximum flexural compressive strains in the concrete are given in cols. 3 and 4 of table (14). The ratios of the final to initial values were 3.55 and 2.82 for beams SU 1 - C and SU 2 - C respectively. The ratio for beam SU 1 - C was greater than that of beam SU 2 - C; this was mainly due to the

relatively lower initial value of beam SU 1 - 0.

The shrinkage strain in concrete measured on the sides of the beams (as explained in 6.7.1(e) after 500 days are given in col. 7 of table (14). This indicates that the shrinkage strains formed 41% and 42% of the respective increase in the flexural compressive strains in beams SU 1 - C and SU 2 - C respectively. The values can be seen in cols. 6, 7 and 8 of table (14).

As regards the neutral axis depth the final values were 28% and 48% greater than the initial values for beams SU 1 - C and SU 2 - C respectively. The lower percentage for beam SU 1 - C was mainly due to its greater initial value of the neutral axis depth.

A major factor which might have affected the flexural strain distribution in beam SU 2 - C was the formation of a crack in the f.r.c. channel. When the channel cracked the neutral axis depth decreased, consequently the strain values were affected. This can be seen in the case of beam SU 2 - C, where the increase in the maximum flexural compressive strain in beam SU 2 - C was greater than that of beam SU 1 - C. The values are given in col. 6 of table (14).

(c) Comparison Between Ordinary and Composite Beams

When the beams were first loaded, the composite beams showed lower flexural compressive strains in the concrete and greater values for the neutral axis depths than those observed in the corresponding ordinary beams. The values of the initial maximum flexural compressive strains are given in col. 3 of table (14).

After 500 days of sustained loading, beam SU 1 - C maintained a lower value for the maximum compressive strain in the concrete than the corresponding ordinary beam SU 1 - 0, whereas beam SU 2 - C had a slightly greater value than the corresponding ordinary beam SU 2 - 0, the values can be seen in col. 4 of table (14). This could be mainly due to the shrinkage strain of beam SU 2 - C was greater than that of beam SU 2 - 0 (col. 7 of table (14)). Additionally the formation of a crack in the f.r.c. channel of beam SU 2 - C might also have contributed to the increase in the flexural compressive strain.

The values of the neutral axis depth for the ordinary and composite beams after 500 days were found to be nearly the same. The final values of the neutral axis depths were 178mm and 182mm for beams SU 1 - 0 and SU 2 - 0 respectively;

for beams SU 2 - 0 and SU 2 - C the final values are given in Figs. 63 and 64. These are 174mm and 178mm for beams SU 2 - 0 and SU 2 - C respectively.

8.3.2 Variations of Tensile Strains in the f.r.c. Channels

When the beams were first loaded the total maximum tensile stresses induced in the f.r.c. channels including the stress due to selfweight of the beam at the level of the working moment were 4.3 N/mm^2 and 10.2 N/mm^2 for beams SU 1 - C and SU 2 - C respectively. The corresponding values of strains in the f.r.c. channels were 311 x 10^{-6} and 940 x 10^{-6}. These values agree well with those obtained at the first static test in the f.r.c. channels for the corresponding beams FA 1 - C and FA 2 - C which were tested under fatigue loading as discussed in 8.2.3.

The initial maximum tensile stresses in the f.r.c. channels expressed as percentages of a nominal tensile strength equal to 15 N/mm^2 were 29% and 68% in beams SU 1 - C and SU 2 - C respectively.

The variations in the maximum tensile strain in the f.r.c. channels with the passage of time for beams SU 1 - C and SU 2 - C are shown in Fig. 65. It can be seen that the tensile strains in the f.r.c. channels increased at a diminishing rate as time elapsed. Most of the increase in the tensile strains occurred during the first 100 days of loading, after which the change was not appreciable. A slight reduction, however, was observed in the tensile strains after a period of one year. This could be due to the increase in the neutral axis depth caused by the creep and shrinkage as discussed earlier.

After eight months of sustained loading a fine crack of 0.16mm width was observed in the f.r.c. channel of beam SU 2 - C. The maximum measured tensile strain in the f.r.c. channel at the time of cracking was 1300 x 10^{-6}. This, however, is lower than the maximum tensile strain (1800 x 10^{-6}) of the f.r.c. channel as measured by direct tensile test (see Fig. 8). The reasons which might have caused the channel to crack before reaching its maximum tensile strain are discussed in 7.5. No more cracks appeared in the f.r.c. channel even after a period of 500 days of sustained loading. This behaviour may be explained by the fact that most of the increase in the tensile strain occurred during the first 100 days as mentioned earlier. Beam SU 1 - C did not show any crack on the

f.r.c. channel for the period of the sustained loading test.

The formation of a crack in the f.r.c. channel of beam SU 2 - C was mainly due to the high initial tensile stress which was equal to 68% of the tensile strength of the channel. In addition the shrinkage strain which occurred in the concrete might have also contributed to the development of cracking in the f.r.c. channel.

8.3.3 Variations of the Steel Stresses

(a) Ordinary Beams

The steel stresses in beams tested under sustained loading could mainly be affected by the movement of the neutral axis depth. Due to creep of the concrete the neutral axis depth dropped, and consequently the lever arm of the steel was reduced. This resulted in an increase in the steel stresses for the same level of moment. Fig. 66 shows the increase in the steel stress as time elapsed. The values in this graph were calculated using the equation of compatibility for moments (equation 4.18) based on the experimental results obtained as explained in 4.5.2. The value β for centroid of the compression stress distribution was based on the initial stress distribution for the beams when first loaded to their working moment. The relationship between β and the maximum compressive strain in the concrete is explained in 4.3.3. The only variable used in the equation was the neutral axis depth. From the figure it can be seen that the steel stresses increased at a diminishing rate with the passage of time.

The initial and final values for the steel stresses are given in cols. 9 and 10 of table (14). This shows that the increases in the steel stress after 500 days of sustained loading are 11.8% and 11.4% of the initial values for beams SU 1 - 0 and SU 2 - 0 respectively.

(b) Composite Beams

The effect of sustained loading on the steel stresses in the composite beams is basically similar to that in the ordinary beams discussed earlier. Furthermore the formation of cracks in the f.r.c. channel could also increase the local tensile steel stresses in the vicinity of these cracks. In Fig. 66 it can be seen that the stresses in the steel increased with the passage of time. In calculating the steel

stresses equation 4.20 for the compatibility of moment was used taking into consideration the experimental results obtained as explained in 4.6. The values used for the centroid of the compressive stress distribution and the tensile stresses in the f.r.c. channel were those obtained when the beams were first loaded to their working moments.

In cols. 9 and 10 of table (14) the initial and final values of the steel stresses are given. This shows that the increases in the steel stresses after 500 days of loading are 8% and 12.4% of the initial values for beams SU 1 - C and SU 2 - C respectively. It is important to point out that the contribution of the f.r.c. channel was included in the calculation of the steel stresses at all the stages. As mentioned earlier beam SU 2 - C had the f.r.c. channel cracked after eight months of sustained loading. Without considering the contribution of the f.r.c. channel the increase in the steel stress of beam SU 2 - C would be equal to 33% of the initial values.

(c) Comparison Between Ordinary and Composite Beams

From Fig. 66 it can be seen that during the period of sustained loading the steel stresses in the composite beams are lower than those in the corresponding ordinary beams. After 500 days of loading, beam SU 1 - C had a steel stress 8.8% lower than that in the corresponding beam SU 1 - 0; beam SU 2 - C had a steel stress 15.7% lower than that in the corresponding beam SU 2 - 0. If the contribution of the f.r.c. channel is not considered in the calculation, e.g. for beam SU 2 - C where the channel cracked, the stresses in the ordinary and composite beams will be equal.

8.3.4. Limit States of Serviceability

8.3.4.1. Limit State of Deflection

(a) Ordinary Beams

Deflection under sustained loading is mainly affected by the variation taking place with the passage of time in the flexural compressive strain and the neutral axis depth.

The increase in deflection under sustained loading for beams SU 1 - 0 and SU 2 - 0 is shown in Fig. 67. For both beams it can be seen that with the passage

of time the deflection increases at a diminishing rate. The initial and final values of deflection are given in cols. 12 and 13 of table (15). It should be remembered that the total deflection for a beam is equal to 7.7 times the value given in table (15). This is explained in 6.5.1, also see appendix (G).

The ratios of final to initial deflection for beams SU 1 - 0 and SU 2 - 0 as given in col. 15 of table (15) were 2.4 and 1.42 respectively. The greater ratio of beam SU 1 - 0 was mainly due to its greater rate of increase in the flexural compressive strain in concrete, which consequently led to a greater rate of deflection.

In a previous investigation (36) it was found that after 25 months of sustained working load the ratios of final to initial deflection ranged between (2 - 2.33) for lightweight concrete beams and between (2.34 - 3.09) for normal weight concrete beams. In other investigations ratios for final to initial deflection for various periods of sustained loading for normal weight concrete were reported as follows:-

3 for a period of two years (99), 3.14 to 3.94 for a period of about five years (100), 2.15 for a period of five months (101).

Factors which could have affected these ratios were the level of steel stress, percentage of steel and the surrounding temperature and humidity for the beams tested.

After 500 days of sustained loading the beams were unloaded and the immediate remaining deflections at zero load were measured. These values are given in col. 14 of table (15). The immediate recoveries were 18% and 50% of the corresponding final deflection at the working moment for beams SU 1 - 0 and SU 2 - 0 respectively.

Col. 13 of table (15) shows that the deflection of beam SU 1 - 0 did not reach the limit $L/_{250}$ which for the test beam equal to $\frac{18}{7.7} = 2.34\text{mm}.$ Beam SU 2 - 0 however marginally exceeded this value.

This indicates that the beams had satisfied the limit state of deflection even after 500 days of sustained loading.

(b) Composite Beams

The time-dependent deflections for the composite beams are shown in Fig. 67. Similar to the behaviour of the ordinary beams the deflection of the composite beams

increased at a decreasing rate with the passage of time. One of the major factors which could have affected the increase in deflection of beam SU 2 - C was the formation of a crack in the f.r.c. channel after eight months of sustained loading. However, it can be seen from Fig. 67 that the formation of a crack in the f.r.c. channel did not have an immediate effect on the deflection behaviour. This was probably due to the fact that the channel cracked at the level of the working moment where the stresses in the channel were relatively low and that the crack width in the f.r.c. channel was very small (0.16mm).

The values of deflection at the level of the working moment obtained at the first test and after 500 days of sustained loading are given in col. 12 and 13 of table (15). The ratios of final to initial deflection for beams SU 1 - C and SU 2 - C were 3.5 and 2.0 respectively. The greater ratio of beam SU 1 - C could be due to its greater rate of increase in the flexural compressive strain in the concrete which led to a consequent increase in deflection (see col. 5 of table (14)).

When the beams were unloaded after the sustained loading period the remaining deflections indicated recoveries of 25% and 50% of the respective final deflection for beams SU 1 - C and SU 2 - C respectively. The final deflectionsof the composite beams (as given in col. 13 of table (15)) when compared with the recommended limit $L/250$ (i.e. 2.34mm) indicated that the composite beams had satisfied the limit state of deflection even after 500 days of sustained loading.

(c) Comparison Betwcen Ordinary and Composite Beams

The deflections at the level of the working moment when the beams were first loaded are given in col. 12 of table (15). The ratios of the deflection for the ordinary beams to that of the corresponding composite beams were 1.78 for beams SU 1 - 0 and SU 1 - C, and 1.46 for beams SU 2 - 0 and SU 2 - C.

A direct comparison can be seen in Fig. 67 between the time-dependent deflection for ordinary and composite beams. This figure shows that the composite beams had a greater stiffness in the early stages of sustained loading. This behaviour was maintained by beam SU 1 - C compared with beam SU 1 - 0 up to the end of the sustained loading period. However, the greater stiffness for beam SU 2 - 0

in relation to beam SU 2 - 0 gradually diminished with the passage of time. The main factors which could have contributed to this behaviour were the cracking of the f.r.c. channel and the greater shrinkage of beam SU 2 - C compared with beam SU 2 - 0. The shrinkage strain for beam SU 2 - C as given in col. 7 of table (14) was 1.4 times that for beam SU 2 - 0.

Another factor which contributed to the diminishing of the greater flexural rigidity of the composite beams in relation to the ordinary beams was the greater rate of reduction in the tension stiffening effect of the concrete with time in the composite beams. When the composite beams are first loaded the height of travel of the cracks is limited, hence the area of concrete between the neutral axis level and the level of the tips of the cracks forms a major part in the tension stiffening effect of the concrete. With the passage of time. the neutral axis drops, resulting in a decrease in the uncracked concrete area in the tensile zone. This will lead to a reduction in the tension stiffening effect of the concrete.

The tension stiffening effect resulting from the concrete between flexural cracks may be of the same magnitude in the ordinary and composite beams.

After 500 days of loading the ratios of deflection of the ordinary beams to that of the corresponding composite beams were 1.22 for beams SU 1 - 0 and SU 1 - C, and 1.03 for beams SU 2 - 0 and SU 2 - C.

8.3.4.2. Limit State of Cracking

(a) Ordinary Beams

Many investigators reported that crack widths in prestressed and conventionally reinforced concrete beams tested under sustained loading were increased initially with the passage of time, thereafter a stabilised condition could be reached (64) (73) (102). A similar behaviour for the variation of the crack widths with the passage of time is also observed in the present investigation. This is shown in Figs. 68 and 69, where the maximum and average crack widths at the steel level are plotted against time. The initial and final values of the crack widths are given in table (15).

From the figures it can be seen that most of the increase in the crack widths occurred during a period of 200 days, thereafter no appreciable change was

observed. At some stages a slight reduction in the crack widths was observed. This could be due to the formation of new cracks which tended to reduce the width of adjacent cracks.

However, it was observed that 90% of the total number of cracks was formed during the first month of loading.

The ratios of final to initial maximum crack width at the steel level were 2 and 2.2 for beams SU 1 - 0 and SU 2 - 0 respectively. The ratios of final to initial maximum crack width at the bottom edge of the beams were 1.83 and 1.4 for beams SU 1 - 0 and SU 2 - 0 respectively.

The maximum crack width for both beams after 500 days of loading, as given in col. 8 of table (15), did not exceed 0.22mm. This value is lower than a recommended maximum crack width of 0.3mm by CP110. This indicated that the beams had satisfied the limit state of cracking under sustained loading.

(b) Composite Beams

The composite beams when first loaded to their working moment showed no signs of cracking at their soffits.

The concrete at the level of the interface (at the steel level) did not crack in beam SU 1 - C whereas a maximum crack width of 0.08 was observed in beam SU 2 - C.

Similar to the behaviour of the ordinary beams the width of cracks increased with the passage of time for a period of about 240 days, after which no practical change was observed; this is shown in Figs. 68 and 69.

After 500 days of sustained loading the maximum crack width observed at the interface was 0.1mm for beam SU 1 - C which originally had no cracks when first loaded. Beam SU 2 - C, however, had an initial crack width of 0.08mm, which then increased to 0.14mm after 500 days of sustained loading.

The maximum and average crack widths are given in table (15). As previously mentioned in 8.3.2, after eight months of sustained loading the f.r.c. channel of beam SU 2 - C cracked. The width of the crack in the f.r.c. channel when first observed was 0.16mm; after 500 days of sustained loading the crack width reached 0.2mm. This increase could be due to an increase in the crack width of the confined concrete and also due to the increase in the curvature of the member.

Again the important consideration as previously mentioned in 8.3.2 is that the cracking of the f.r.c. channel did not significantly affect the cracks in the concrete as it did in beams tested under static load only.

The composite beams after a period of 500 days of loading did not become unserviceable with regard to the limit state of cracking. This was due to the fact that no cracks formed at the soffit of beam SU 1 - C whereas the maximum crack width observed in the f.r.c. channel of beam SU 2 - C was 0.2 mm.

Similar to the behaviour of ordinary beams, 90% of the final number of the cracks were formed within the first month of loading.

(c) Comparison Between Ordinary and Composite Beams

The maximum and average crack widths as can be seen in Figs. 68 and 69 in the composite beams are considerably less than those in the corresponding ordinary beams. This behaviour was maintained during the 500 days of the sustained loading period.

After 500 days of loading the ratios of the maximum crack width at steel level in the ordinary beams to that in the corresponding composite beams were 2 for beams SU 1 - 0 and SU 1 - C, and 1.6 for beams SU 2 - 0 and SU 2 - C.

The ratios of the average crack width in the ordinary beams to that in the corresponding composite beams were 1.7 for beams SU 1 - 0 and SU 1 - C, and 1.9 for beams SU 2 - 0 and SU 2 - C. When the beams were unloaded after 500 days of sustained loading the remaining maximum crack widths in the composite beams were much smaller than those in the corresponding ordinary beams. The values are given in cols. 10 and 11 of table (15).

In Fig. 70 a typical cracks pattern for ordinary and composite beams subjected to sustained loading is shown. This shows that the height of travel of the cracks in the composite beam was lower than that in the ordinary beams. This behaviour for the composite beams is of great value since it reduces the cracked concrete area in the tensile zone.

CHAPTER NINE

CONCLUSIONS AND SUGGESTIONS FOR FUTURE WORK

9.1 Conclusions

The Conclusions drawn from the present investigations are as follows:

(1) The prediction of the stresses in the steel and the f.r.c. channels, ultimate strengths, deflections and width of cracks can be made to a sufficient degree of accuracy by the methods suggested in this thesis.

(2) The bond between the f.r.c. channels and the concrete was very good

(3) The f.r.c. channels did not crack up to and well above the level of the working moments, the exception being one beam containing "Kam 60" steel.

(4) Adequate warning of impending failure was obtained for all the beams tested.

(5) There was a considerable reduction in width of cracks and deflections of composite beams tested under short term, fatigue and sustained loading as long as the f.r.c. channels did not crack.

(6) Deformed steel bars had a better control on flexural cracking than did mild steel bars.

(7) There was no significant change in the steel stresses for ordinary beams subjected to fatigue loading, whereas a maximum increase of 22% was obtained in the composite beams after the application of 3×10^6 cycles.

(8) There were no significant increases in the steel stresses for the beams tested under sustained loading for a period of 500 days.

(9) Fatigue loading did not greatly affect the ultimate strength of the beams tested.

(10) Fatigue loading rather than sustained loading was a critical condition for the cracking of the f.r.c. channels.

(11) Sustained loading rather than fatigue loading was a critical condition for the limit state of deflection.

(12) Deflection under short-term, fatigue and sustained loading was found to be a critical factor in the design of the beams.

9.2 Advantages of Using f.r.c. Channels at the Tensile Sides of Flexural Concrete Members

The use of f.r.c. channels in the composite beams resulted in the following advantages:

(1) Full utilization of the tensile properties of concrete.

(2) Better control on shrinkage cracks.

(3) Lower flexural compressive strains in concrete and greater neutral axis depth.

(4) A reduction in the steel stresses for the same level of load.

(5) A considerable reduction in deflection and crack width, thus allowing a more efficient use of the high-strength steel.

9.3 Suggestions for Future Work

(1) The present investigation used a span to depth ratio of 17 (maximum permitted in CP110 for simply supported lightweight concrete members reinforced with 1% of a steel of 410 N/mm^2 nominal yield stress and no compressive steel.

It was found that for some beams containing high strength steel the limit state of deflection $L/250$ was exceeded.

It is therefore suggested that beams with a span to depth ratio lower than 17 should be investigated. This would result in a lower amount of deflection under load, thus allowing better use of the high strength steel.

(2) The present investigation was carried out using rectangular shaped beams. It is therefore suggested that the effect of the geometrical shape on the structural behaviour should be investigated.

In this respect, a composite lightweight concrete T beams with normal weight concrete flange can be used. The use of normal weight concrete flange will help to a great extent in reducing the amount of deflection under load.

At this point it would be interesting to use f.r.c. channels on the lightweight concrete web. The good bond achieved between the f.r.c. channel and the lightweight concrete will ensure the restraint action of the f.r.c. channels, thus enabling high-strength steel to be used.

(3) The present investigation has shown that composite beams exhibited a stiffness greater than that of ordinary beams for levels lower than the cracking moments of the f.r.c. channels.

One of the factors which might have contributed to the cracking of the f.r.c. channel was the formation of cracks in the confined concrete. These cracks make an important contribution to the reduction in the flexural rigidity of the composite beams.

A study is therefore suggested regarding the formation of the cracks in the confined concrete.

(4) In the fatigue loading tests of the present investigation, the f.r.c. channels cracked after a few hundred thousand load repetitions. A study is therefore required into the effect of fatigue loading on f.r.c. units with various ranges of applied tensile stresses. A relationship should be established between the number of repetitions and applied tensile stresses at which cracking occurs.

Similarly the tensile creep and the consequent formation of cracks in the f.r.c. units, employing various levels of stress, should also be investigated.

Following this, fatigue and sustained loading tests should be carried out on composite beams. The effect of long-term weathering and shrinkage should also be examined.

LIST OF REFERENCES

1. Hognestad, E
Development of High-Strength Steel
Journal of Metals, June 1966.

2. Abeles, P.W. and Gill, V.L.
High-Strength Strand Reinforcement for Concrete
Concrete, April 1969.

3. Ramaswamy, G.S., Chandre, R. and Naraynan, R.
Savings in Reinforced Concrete Structures by Using Ultimate Strength Design Procedure and High Strength Deformed Bars.
Indian Concrete Journal. October 1967.

4. Clark, L. A.
The Flexural Strength of Concrete Beams Reinforced with Very High Strength Steel.
PhD. Thesis. University of Sheffield, 1968.

5. British Standards Institution. Code of Practice - CP110
The Structural Use of Concrete.
Part 1. November 1972.

6. Granholm, H.
Kam 40, Kam 60, Och Kam 90.
Trans of Chalmers, University of Technology, No. 213.
Gothenberg, Sweden, 1959.

7. American Iron and Steel Institute
Committee of Concrete Reinforcing Bar Producers.
High Strength Reinforcing Bars, Vol. 1, 1964, revised edition.

8. Short, A.
The Use of Lightweight Concrete for Reinforced Concrete Construction.
R.C.R., September 1959.

9. Teychenne, D.C.
Structural Concrete Made with Lightweight Aggregates.
Concrete, April 1967.

10. Manual Lightweight Concrete
C.E.B., Bulletin d Information No. 85.
Second draft Cand C.A. - May 1972.

11. Shideler, J.J.
Lightweight-Aggregate Concrete for Structural Use.
A.C.I. Journal, October 1957.

12. Hanson, J.A.
Replacement of Lightweight Aggregate Fines with Natural Sand in Structural Concrete.
A.C.I. Journal, July 1964.

13. Baron-Hay, J.K.
A Study of Physical Properties of Structural Quality of Lightweight Aggregate (Aglite and Terlite).
PhD. Thesis, University of London, July 1960

14. Zunz, G.J.
Some Examples of When and How Lightweight Concrete be Used.
I.C.L.C., May 1968.

15. Skoyles, E.R.
The Economics of Lightweight Aggregate Structural Concrete
B.R.E., CP7/73, March 1973.

16. Parrott, L.J.
Selection of Constituent Properties for Workable Concrete.
London, C and CA., Technical Report 417, May 1969.

17. Abeles, P.W.
Introduction to Prestressed Concrete
Vol. 1, Concrete Publication Ltd., London, 1964.

18. British Standards Institution, Code of Practice CP114
The Structural Use of Reinforced Concrete in Building
reset and reprinted, 1965.

19. Porter, II. F.
Preperation of Concrcte From Selection of Materials to Final Disposition.
Proceedings of the National Association of Cement Users.
A.C.I., Vol. 6, 1910, p 296.

20. Romualdi, J. P. and Mandel, J. A.
Tensile Strength of Concrete Affected by Uniformly Distributed and Closely Spaced Short Lengths of Wire Reinforcement.
A.C.I. Journal, June 1964.

21. Hughes, B. P.
Advances in Concrete
proceedings of a symposium held at the University of Birmingham, September 1971.

22. Hannant, .D. J.
Steel Fibre Reinforced Concrete
Prospects for fibre reinforced construction materials
B.R.E., Department of the Environment, 1972

23. Swamy,, R.N.
The Technology of Steel Fibre Reinforced Concrete for Practical Applications.
Proceedings of I.C.E., May 1974.

24. Austerberry, R.
The Use of Fibres as Reinforcement in Concrete
MSc. Thesis, 1972, University of Salford.

25. McCurrich, L.H. and Adams, M.A.J.
Fibres in Cement and Concrete
Concrete, April 1973.

26. Swamy , R.N.
Delft Conference on Fibre Reinforced Materials
Concrete, December 1973.

27. Fibre Reinforced Concrete
Conference on Properties and Applications of Fibre Reinforced Concrete and Other Fibre Reinforced Building Materials.
Delft, September 1973

28. Allen, H. G.
The Purpose and Methods of Fibre Reinforcement.
Prospects for Fibre Reinforced Construction Materials.
B.R.E., Department of the Environment, 1972.

29. Steel, B.R.
Glass Fibre Reinforced Cement.
Prospects for Fibre Reinforced Construction Materials.
B.R.E., Department of the Environment, 1972.

30. Hanson, J.A.
Shear Strength of Lightweight Reinforced Concrete Beams
Journal of A.C.I. Proc., September 1958.

31. Hanson, J.A.
Tensile Strength and Diagonal Tension Resistance of Structural Lightweight Concrete
A.C.I. Journal, July 1961.

32. Welch, G.B. and Patten, B.J.F.
Structural Lightweight-Aggregate Concrete.
Constructional Review. February 1964.

33. Evans, R.H. and Hardwick, T.R.
Lightweight Concrete with Sintered Clay Aggregate.
R.C.R., June 1960.

34. Richart, F. and Jensen, V.
Tests of Plain and Reinforced Concrete Made With Haydite Aggregate.
Engineering Experiment Station, University of Illinois, 1931.

35. Evans, R.H. and Orangun, C.O.
Behaviour in Flexural of Reinforced Lightweight-Aggregate (Lytag) Concrete Beams.
Civil Engineering and Public Works Review, May 1964.

36. Evans, R.H. and Paterson, W.S.
Long-Term Deformation Characteristics of Lytag Lightweight-Aggregate Concrete.
Paper presented at a joint meeting of the Institution of Structural Engineers and the Concrete Society.
London, January 1967.

37. European Committee for Concrete
Information Bulletin No. 24, Part 1.
Proceedings of the fifth working session. Vienna, April 1959.

38. Roberts, N.P.
The Use of Deformed Bars as Reinforcement in Lightweight Concrete.
One-day symposium on structural lightweight concrete.
June 1962, Brighton.

39. Kanoh, Y.
The Long-Term Deflection of Reinforced Concrete Beams made with Artificial Lightweight Aggregate.
I.C.L.C. Vol. 2, London, May 1968.

40. Swamy, R.N. and Ibrahim, A.B.
Deflection Characteristics of Structural Lightweight Reinforced and Prestressed Concrete Beams.
Deflection of concrete structures, A.C.I. sp 43-15, April 1974.

41. Romualdi, J.P. and Batson, G.B.
Behaviour of Reinforced Concrete Beams With Closely Spaced Reinforcement.
A.C.I. Journal, June 1963.

42. Biryukovich, K.L., Biryukovich, Yu. L. and Biryukovich, D.L.
Steklotsement, Budivelnik, kiev,
Glass Fibre-Reinforced Cement,
Translated by G.L. Cairns, CERA Translation No. 12,
Civil Engineering Research Association, London 1965.

43. Taylor, R.
An Idea for a New Structural Material. Composite Reinforced Concrete.
Engineering, London, December 1971.

44. Kaar, P.H. and Mattock, A.H.
High Strength Bars as Concrete Reinforcement, Part 4, Control of Cracking.
Journal of the P.C.A. Research and Development Laboratories.
January 1963.

45. Hognestad, E.
High Strength Bars as Concrete Reinforcement.
Part 2, Control of Flexural Cracking.
Journal of the P.C.A. Research and Development Laboratories.
January 1962.

46. Nervi, P.L.
Ferro-Cement: 'Its Characteristics and Potentialities".
(In Italian), L'Ingegnere (Rome), No. 1, 1951.

47. Romualdi, J.P., Frasier, J.T. and Irwin, G.R.
Crack Extension Force Near a Riveted Stiffener.
Report 4956, U.S. Naval Research Laboratory, 1957.

48. Broms, B.B. and Shah, S.P.
Discussion of Reference (41) and (51)
Proceedings, A.S.C.E., Vol. 90, E.M.1., February 1964.

49. Abeles, P.W.
Discussion of Reference (41) and (51)
Proceedings A.S.C.E., Vol. 90, E.M.1., February 1964.

50. Kar, J.N. and Pal, A.K.
Strength of Fibre-Reinforced Concrete
Structure Division, Proceedings of A.S.C.E., May 1972.

51. Romualdi, J.P. and Batson, G.B.
Mechanics of Crack Arrest in Concrete
Proceedings, A.S.C.E., June 1963.

52. Untraur, R.E. and Works, R.E.
Discussion of Reference (20)
A.C.I. Journal, December 1964.

53. Abolitz, A.L.
Discussion of Reference (20)
Journal of A.C.I., December 1964.

54. Agbim, C.C.
Discussion of Reference (20)
A.C.I. Journal, December 1964.

55. Shah, S.P. and Rangan, B.V.
Fibre Reinforced Concrete Properties.
A.C.I. Journal, February 1971.

56. Swamy, R.N. and Lankard, D.R.
Some Practical Applications of Steel Fibre Reinforced Concrete
Proceedings of I.C.E., August 1974.

57. Hannant, D.J.
Steel Fibres and Lightweight Beams
Concrete. August 1972. Vol. 6.

58. Samarrai, M.A. and Elvery, R.H.
The Influence of Fibres Upon Crack Development in Reinforced Concrete Subject to Uniaxial Tension.
Magazine of Concrete Research, Vol. 26: No. 89, December 1974.

59. Taylor, R. and Burdon, P.
Tests On A New Form of Composite Construction.
I.C.E., Vol. 53. December 1972.

60. Durham, J.
The Tensile Strength of Fibre Reinforced Concrete
MSc. Dissertation, University of Salford, October 1971

61. O'Leary, D.C., Dave, N.J. and Saunders, J.
Steel Fibres in Partially Prestressed Composite Concrete Beams
A.C.I. Special Publication No. SP-44-27, Detroit 1974.

62. Dave, N.J., O'Leary, D.C., Al-Sanjary, K.A.A. and Saunders, J.
Asbestos and Glass Fibre Reinforced Cement Structural Concrete Composites, Parts I, II and III
Fibre Reinforced Concrete - Conference on Properties and Applications of Fibre Reinforced Concrete and Other Fibre Reinforced Building Materials. Delft, September 1973.

63. Dave, N. J., O'Leary, D.C. and Saunders, J.
The Structural Use of Fibrous Cement in Composite Concrete Construction
A.C.I. Special Publication No. SP 44-29, Detroit, 1974.

64. Dave, N.J.
Limited Prestressing As A Means of Economy in Structural Concrete.
PhD. Thesis, University of Leeds, July 1967.

65. Clark, L.A. and Eastwood, W.
The Flexural Strength of Concrete Beams Reinforced With Very High-Strength Steel.
The Structural Engineer. July 1970.

66. Kollek, J.J.
Fibres in Cement-Based Materials.
Advances in Concrete.
Proc. of a symposium held at the University of Birmingham, September 1971.

67. TAC Construction Materials Ltd.
Turner and Newall Limited.
Products Manual

68. Lytag
Lytag Structural Precast and Refractory Concrete
LYTAG Ltd.,

69. Nesbit, J.K.
Structural Lightweight-Aggregate Concrete
London, 1966.

70. British Standard 3797 : 1964.
Specification for Lightweight Aggregates For Concrete.

71. British Standard 882 & 1201 : 1965
Specification for Aggregates From Natural Sources For Concrete.

72. British Standard 812 : 1967.
Methods for Sampling and Testing of Mineral Aggregates, Sands and Filters.

73. Attisha, H. P.
High Tensile-Steel As Normal Reinforcement In Concrete
PhD. Thesis, University of Salford, May 1972.

74. Baker, A. L. L.
A Plastic Theory of Design for Ordinary Reinforced and Prestressed Concrete Including Moment Re-Distribution in Continuous Members.
Magazine of Concrete Research. June 1949.

75. Regan, P. E. and Yu, C.W.
Limit State Design of Structural Concrete.
London, 1973.

76. Rowe, R.E., Granston, W.B. and Best, B.C.
New Concepts In The Design of Structural Concrete.
The Structural Engineer, No. 12. Vol. 43. December 1965.

77. Anchor, R.D.
The Application of Limit State Design.
Concrete, March 1968.

78. Huges, B. P.
Limit State Theory for Reinforced Concrete.
Pitman Publishing, London 1971.

79. Baker, A. L. L.
The Ultimate Load Theory Applied To The Design of Reinforced and Prestressed Concrete Frames.
Concrete Publications Ltd., 1958.

80. Mayer, H.
Bauschaden Als Folge Der Durchbiegung Von Stanhlbeton Bauteilen.
Report No. 68. Materialprufungsamt Fur Das Bauwesen Der Technischen Hochschule Munchen, 1966.

81. Beeby, A.W. and Miles, J.R.
Proposals For The Control of Deflection In The New Unified Code For Structural Concrete.
B.R.E., May 1969.

82. Branson Dan, E.
Deflections of Reinforced Concrete Flexural Members.
A.C.I. Committee 435, June 1966.

83. Yu, W.W. and Winter, G.
Instantaneous and Long-Time Deflections of Reinforced Concrete Beams Under Working Loads.
A.C.I. Journal, July 1960.

84. Beeby, A.W.
Short-Term Deformations of Reinforced Concrete Members
C and C.A., TRA 408, March 1968.

85. Srinivasa, Rao, P. and Subrahmanyam, B.V.
Trisegmental Moment-Curvature Relationships For Reinforced Concrete Members.
A.C.I. Journal, May 1973.

86. A.C.I. Committee 224
Control of Cracking in Concrete Structures.
A.C.I. Journal, No. 12, December 1972.

87. Reis, E.E, John, J.R, Mozer, J.D., Bianchini, A.C. and Kesler, C.E.
Causes and Control of Cracking in Concrete Reinforced with High Strength Steel Bars. A Review of Research.
University of Illinois, Bulletin 479, 1965.

88. Base, G.D., Read, G.B., Beeby, A.W. and Taylor, H.P.J.
An Investigation of the Crack Control Characteristics of Various Types of Bars in Reinforced Concrete Beams.
Research Report No. 18, Part 1, C & C.A., London, December 1966.

89. British Standard 1881. Part 4 : 1970
Methods of Testing Concrete

90. Orangun, C.O.
Influence of Properties of Lightweight-Aggregate (Lytag) Concrete on Behaviour of Reinforced and Prestressed Concrete Members.
PhD. Thesis, University of Leeds, 1963.

91. Hajnal-Konyi, K.
Tests on Square Twisted Steel Bars and Their Applications As Reinforcement of Concrete.
The Structural Engineer, Vol. 21, No. 9, 1943.

92. Swamy, R.N. and Anand, K.L.
Influence of Steel Stress and Concrete Strength on the Deflection Characteristics of Reinforced and Prestressed Beams.
A.C.I. Publication. SP43-18, April 1974.

93. Sparks, P.R., Menzies, J.B.
The Deflection of Reinforced Concrete Beams Under Fluctuating Load With A Sustained Component.
The Structural Engineer, November 1973.

94. Abeles, P.W.
Static and Fatigue Tests of Partially Prestressed Concrete Constructions.
A.C.I. Journal, Vol. 26, No. 4, December 1954.

95. Bate, S.C.C.
A Comparison Between Prestressed Concrete and Reinforced Concrete Beams Under Repeated Loading.
I.C.E. Vol. 24, March 1963.

96. Garwood, T.G.
The Flexural Behaviour of "Class 3" Post-Tensioned Prestressed Concrete Beams Using Various Types of Untensioned Steel.
PhD Thesis, University of Salford, August 1972.

97. Snowdon, L.C.
The Static and Fatigue Performance of Concrete Beams with High Strength Deformed Bars
B.R.E., CP 7/71, March 1971.

98. Stevens, R.F., and Bryden-Smith, D.W.
Deformed Bars In Concrete.
Deflections of Reinforced Concrete Beams.
B.R.E., No. 225/70

99. Corely, W.G. and Sozen, M.A.
Time Dependent Deflections of Reinforced Concrete Beams.
A.C.I. Journal, Vol. 63, No. 3, March 1966.

100. Hajnal-Kony, K.
Tests on Beams with Sustained Loading.
Magazine of Concrete Research, March 1963.

101. Lutz, L.A., Sharma, N.K. and Gergely, P.
Increase in Crack Widths in Reinforced Concrete Beams Under Sustained Loading.
A.C.I. Journal, Vol. 64, September 1967.

102. Soretz, S.
Sustained Loading Tests.
RILEM Symposium on Bond and Crack Formation in Reinforced Concrete, Stockholm, 1957.

TABLE (1) DETAILS OF ORDINARY AND COMPOSITE BEAMS (STATIC TESTS)

Beam mark	Steel Reinforcement				Efective depth mm	Applied working moment KN.m	Applied ultimate moment KN.m
	Type	Number and size	Percentage	Nominal yield or 0.2% proof stress N/mm^2			
ST1-0 ST1-C	Mild Steel	2-16mm diameter	1.044	275	257	12.8	20.5
ST2-0 ST2-C	UNI 410	2-16mm. diameter	1.044	410	257	19.31	30.9
ST3-0 ST3-C	UNI 550	2-16mm. diameter	1.044	550	257	25.61	40.97
ST4-0 ST4-C	KAM 60	2-16mm. diameter	1.044	590	257	27.31	43.7
ST5-0	KAM 90	2-16mm. diameter	1.044	875	257	38.43	61.48
ST6-0	Lancs 60	2-16mm. diameter	1.044	410	257	19.31	30.9
ST7-0 ST7-C	Mild Steel	2-20mm. diameter	1.643	275	255	20.04	32.07
ST8-0	UNI 410	2-20mm. diameter	1.643	410	255	29.15	46.64
ST9-0	UNI 550	2-19.05mm. diameter	1.483	550	255.5	34.68	55.48
ST10-0 ST10-C	KAM 60	2-12mm. diameter	0.582	590	259	15.75	25.2
ST11-C	Mild Steel	3-12mm. diameter	0.874	275	259	10.75	17.2
ST12-C	UNI 410	3-12mm. diameter	0.874	410	259	16.44	26.3

Concrete Section: 150mm width x 300mm depth.

Nominal Concrete Cube Strength = 50 N/mm^2

Cover to main reinforcements = 35mm

TABLE (2) DETAILS OF ORDINARY AND COMPOSITE BEAMS (FATIGUE LOADING TESTS)

Steel Reinforcement					Effective depth mm	Applied working moment KN.m	Applied ultimate moment KN.m
Beam mark	Type	Number and size	Percentage	Nominal yield or 0.2% proof stress N/mm^2			
FA1-0 FA1-C	Mild Steel	2-16mm. diameter	1.044	275	257	12.8	20.5
FA2-0 FA2-C	UNI 410	2-16mm. diameter	1.044	410	257	19.31	30.9
FA4-0	KAM 60	2-16mm. diameter	1.044	590	257	25.61	40.97

TABLE (3) DETAILS OF ORDINARY AND COMPOSITE BEAMS (SUSTAINED LOADING TESTS)

Steel Reinforcement					Effective depth mm	* Working moment KN.m	Ultimate moment KN.m
Beam mark	Type	Number and size	Percentage	Nominal yield or 0.2% proof stress N/mm^2			
SU1-0 SU1-C	Mild Steel	2-16mm. diameter	1.044	275	257	14.95	23.3
SU2-0 SU2-C	UNI 410	2-16mm. diameter	1.044	410	257	21.45	33.7

*includesself weight of beam

Concrete Section: 150mm width x 300mm depth

Nominal Concrete Cube Strength = 50 N/mm^2

TABLE (4) MECHANICAL PROPERTIES OF f.r.c. UNITS (TENSILE AND BENDING TESTS)

Sample No.	Direct tensile tests size of sample (250 x 50 x 6) mm			Bending tests size of sample (240 x 30 x 6) mm		
	Initial tangent modulus of elasticity KN/mm^2	Maximum tensile stress N/mm^2	Maximum measured extensibility $\times 10^{-6}$	Initial* modulus of elasticity KN/mm^2	Modulus of rupture N/mm^2	Maximum measured deflection mm
1	11.75	18.40	1860	14.47	37.00	7
2	12.00	16.66	1760	12.24	29.40	7
3	13.50	16.12	1760	11.13	29.40	8.1
4	10.75	15.60	1700	17.23	35.80	6.2
5	11.25	14.93	1300	14.65	33.70	8.15
6	11.80	14.50	1250	18.10	33.70	6.15

*Obtained from the equation, deflection $= \frac{23}{216} \quad \frac{M}{EI} \quad L^2$

TABLE (5) TENSILE PROPERTIES OF STEEL BARS USED

Size of bars is 16mm diameter

Type of steel	Nominal yield or 0.2% proof stress N/mm^2	Observed yield or 0.2% proof stress N/mm^2	Ultimate tensile stress N/mm^2	Fracture stress N/mm^2	Modulus of elasticity KN/mm^2
Mild steel	275	280	465	360	200
Uni 410	410	425	581	476	210
Uni 550	550	590	712	515	225
Kam 60	590	655	925	911	200
Kam 90	875	870	915	890	225

TABLE (6) PROPERTIES OF CONCRETE

Beam mark	Properties at Testing Time								
	7 Days cube strength N/mm^2	Age of beams at testing time Days	Cube strength N/mm^2	Cylinder strength N/mm^2	Modulus of elasticity KN/mm^2	Direct tensile strength N/mm^2	Modulus of rupture N/mm^2	Air dry density Kg/m^3	Number of cycles or days
ST1-0	45.6	71	53.1	43.0	18.5	2.8	3.00	1760	3 cycles
ST1-C	45.6	34	54.2	47.5	17.4	1.70	2.50	1820	3 "
ST2-0	43.2	35	52.0	42.0	16.2	2.66	2.36	1820	3 "
ST2-C	43.3	34	52.0	40.5	17.6	3.00	4.20	1780	3 "
ST3-0	42.0	75	50.2	37.8	17.2	1.40	1.72	1750	3 "
ST3-C	46.2	35	52.7	40.8	18.3	2.80	3.36	1840	3 "
ST4-0	42.7	60	47.0	39.0	16.8	2.46	3.24	1700	3 "
ST4-C	44.4	41	54.6	45.0	18.2	1.81	2.80	1820	3 "
ST5-0	43.0	53	50.7	40.0	17.7	2.80	3.50	1750	3 "
ST6-0	46.6	35	47.0	42.0	15.2	2.70	2.55	1730	2 "
ST7-0	45.0	60	46.7	40.0	14.0	2.40	3.16	1680	3 "
ST7-C	51.0	37	54.2	-	-	1.13	1.4	1800	3 "
ST8-0	44.6	43	48.6	42.0	16.2	3.20	4.00	1760	3 "
ST9-0	43.0	68	47.5	32.0	-	1.8	3.74	1750	3 "
ST10-0	42.5	43	51.0	45.0	18.8	2.72	4.00	1780	3 "
ST10-C	53.0	35	58.5	48.6	18	0.84	2.0	1820	3 "
ST11-C	48.4	45	53.0	44.3	19	2.34	2.15	1780	3 "
ST12-C	46.2	44	48.2	-	-	2.50	3.5	1860	3 "
FA1-0	45.3	40	49.1	38.6	16.8	2.2	3.56	1790	2.96×10^6 "
FA1-C	44.7	41	53	40.8	17.2	2.1	3.30	1780	3.0×10^6 "
FA2-0	46.6	48	51.2	53.0	20.0	2.20	-	1675	3.0×10^6 "
FA2-C	45.4	30	54.6	43.6	18.8	0.98	2.28	1826	3.02×10^6 "
FA4-0	41.2	37	50.9	38.2	17.5	2.00	2.66	1800	3.04×10^6 "
SU1-0	44.1	31	59	46	19.2	1.14	1.60	1780	543 Days
SU1-C	-	37	58.0	44.8	19	1.06	2.22	1840	543 "
SU2-0	-	42	57.0	42	18.4	0.94	1.90	1860	528 "
SU2-C	-	35	53.0	41.5	17.4	0.96	1.78	1825	528 "

TABLE (7) STEEL STRESSES AND ULTIMATE MOMENTS (STATIC TESTS)

Beam mark	Type and percentage of steel	Working moment condition		At cracking moment of f.r.c. channel		Ultimate moment KN.m				Maximum measured compressive strain in concrete	
		Calculated steel stress N/mm^2	Reduction in steel stress %	Calculated steel stress N/mm^2	Reduction in steel stress %	Calculated (nominal strengths and partial safety factor	Calculated (actual strength without partial safety factors	Observed	Col. 9 / Col. 8	$\frac{M}{M_u}$	e_c%
1	2	3	4	5	6	7	8	9	10	11	12
ST1-0 ST1-C	M.S 1.044	173 156	9.8	214 190	11.2	20.50	32.64 32.9	39 40.5	1.19 1.23	0.54 0.74	0.075 0.109
ST2-0 ST2-C	UNI 410 1.044	240 207	13.75	310 260	16.1	30.90	39.2 39.18	45.75 46.5	1.17 1.19	0.82 0.97	0.210 0.385
ST3-0 ST3-C	UNI 550 1.044	310 263	15.16	370 306	17.3	40.95	58.15 58.63	57 55.5	0.98 0.95	0.96 0.95	0.271 0.390
ST4-0 ST4-C	KAM 60 1.044	330 333	-	261 229	12.3	43.70	58.2 59.3	64.5 65.85	1.11 1.11	0.90 0.87	0.238 0.254
ST5-0	KAM 90 1.044	457	-	-	-	61.48	74.7	84	1.12	0.79	0.221
ST6-0	Lancs 60 1.044	240	-	-	-	30.90	38.33	45	1.17	0.81	0.123
ST7-0 ST7-C	M.S 1.643	165 150	9	215 192	10.7	32.07	44.2 45.88	61.5 58.5	1.39 1.28	0.63 0.90	0.148 0.312
ST8-0	UNI 410 1.643	232	-	-	-	46.64	58.28	60	1.03	0.92	0.217
ST9-0	UNI 550 1.483	300	-	-	-	55.48	75.82	82.5	1.09	0.89	0.305
ST10-0 ST10-C	KAM 60 0.582	342 285	16.7	385 314	18.4	25.20	34.9 35.8	37.13 43.5	1.06 1.22	0.97 0.83	0.268 0.240
ST11-C	M.S. 0.874	166	-	-	-	17.20	28.76	27.45	0.95	0.82	0.170
ST12-C	UNI 410 0.874	216	-	-	-	26.30	32.73	45.3	1.38	0.83	0.211

TABLE (8) STRESSES AND CRACKING MOMENTS (f.r.c. channels)

Beam mark	Working moment KN.m	Observed cracking moment of f.r.c. channel KN.m	Experimental values at cracking moment of f.r.c. channel		Stress in f.r.c. channel due to self weight of beam N/mm^2	Total stress in f.r.c. channel (col. 7 + Col. 6) N/mm^2	$\frac{\text{Col. 3}}{\text{Col. 2}}$
			Strain x 10^{-6}	Stress N/mm^2			
1	2	3	4	5	6	7	8
ST1-C	12.8	16.5	800	8	0.53	8.53	1.29
ST2-C	19.31	25.5	1300	12.1	0.53	12.63	1.32
ST3-C	25.61	30.75	1700	14.5	0.53	15.03	1.2
ST4-C	27.31	21.0	1000	9.8	0.53	10.33	0.77
ST7-C	20.04	27	1100	9.6	0.48	10.13	1.35
ST10-C	15.75	18	1300	12.1	0.57	12.63	1.14
ST11-C	10.75	19.5	1100	10.6	0.46	11.13	1.81
ST12-C	16.44	23.55	1500	13.4	0.46	13.93	1.43

TABLE (9) SUMMARY OF DEFLECTIONS (STATIC TESTS)

Beam mark	Observed deflection (mm)		Calculated deflection at working moment (mm)		Col. (5) / Col. (2)	Span / deflection (working moment)
	At working moment	Remaining after first cycle	Based on experimental curvature	Proposed theoretical method		
1	2	3	4	5	6	7
ST1-0	7.6	2	6.8	7.93	1.04	592
ST1-C	5.4	1.22	5.5	5.6	1.04	833
ST2-0	12.2	2.39	13.2	12.53	1.03	369
ST2-C	9.6	1.82	9.65	10	1.04	469
ST3-0	18.4	2.92	20	17.33	0.94	245
ST3-C	15.0	2.55	14.4	15.2	1.01	300
ST4-0	17.6	2.88	18	18.7	1.06	256
ST4-C	18.4	4.1	21	18.0	0.98	245
ST5-0	27.2	3.95	23.6	27.42	1.00	165
ST6-0	12	2.39	12	12.53	1.04	375
ST7-0	9.6	1.83	9.6	10.04	1.05	469
ST7-C	9.0	1.42	9.7	9.2	1.02	500
ST8-0	15.2	2.52	14.4	15.15	1.00	296
ST9-0	21.2	2.85	20.4	19.84	0.94	212
ST10-0	14.2	3.24	15.2	14.4	1.01	317
ST10-C	9.2	1.76	10.1	9.2	1.00	489
ST11-C	4.2	0.8	4.2	4.4	1.05	1071
ST12-C	8.4	1.2	9.7	8.8	1.05	536

TABLE (10) SUMMARY OF CRACK WIDTHS (STATIC TESTS)

Beam mark	Cracking moment for concrete		Crack width at working moment (mm)						Remaining maximum crack width (mm)		Calculated design crack width by CP110 method (mm)		Calculated maximum crack width by the C & CA method (mm)	
			At steel level			At bottom edge of beam								
	Observed KN.m	Calculated KN.m	Maximum	Average	No. of cracks*	Maximum	Average	No. of cracks*	At steel level	At bottom edge of beam	At steel level	At bottom edge of beam	At steel level	At bottom edge of beam
1	2	3	4	5	6	7	8	9	10	11	12	13	14	15
ST1-0	3	3.46	0.13	0.08	12	0.15	0.09	13	0.09	0.1	0.05	0.08	0.09	0.17
ST1-C	12	11.87	0.03	0.02	6	0	0	0	0	0	-	-	-	-
ST2-0	6	3.46	0.14	0.12	13	0.18	0.11	14	0.06	0.06	0.1	0.16	0.13	0.24
ST2-C	13.4	11.87	0.08	0.05	5	0	0	00	0.02	0	-	-	-	-
ST3-0	4.5	3.46	0.2	0.1	13	0.26	0.17	16	0.06	0.1	0.15	0.23	0.18	0.32
ST3-C	12	11.87	0.1	0.08	10	0	0	0	0.04	0	-	-	-	-
ST4-0	3	3.46	0.18	0.09	12	0.22	0.18	14	0.05	0.1	0.17	0.24	0.2	0.36
ST4-C	12	11.87	0.21	0.09	6	0.24	0.24	5	0.02	0.1	-	-	-	-
ST5-0	**	3.46	0.2	0.14	14	0.3	0.22	16	0.08	0.1	0.28	0.37	0.24	0.44
ST6-0	4.5	3.46	0.12	0.11	16	0.16	0.1	14	0.06	0.08	0.1	0.16	0.13	0.24
ST7-0	4.5	3.94	0.12	0.05	12	0.2	0.12	14	0.05	0.1	0.07	0.11	0.09	0.18
ST7-C	15	13.4	0.02	0.02	4	0	0	0	0	0	-	-	-	-
ST8-0	**	3.94	0.14	0.07	12	0.2	0.12	14	0.08	0.1	0.11	0.18	0.13	0.24
ST9-0	3	3.69	0.14	0.11	16	0.24	0.19	16	0.05	0.08	0.15	0.24	0.15	0.28
ST10.0	3.75	3.06	0.18	0.1	11	0.22	0.14	14	0.08	0.1	0.15	0.23	0.21	0.4
ST10-C	12	10.5	0.04	0.03	7	0	0	0	0.01	0	-	-	-	-
ST11-C	12	11.3	0	0	0	0	0	0	0	0	-	-	-	-
ST12-C	12	11.3	0.06	0.04	5	0	0	0	0.02	0	-	-	-	-

* In constant moment zone (1.5 m long)

** Shrinkage cracks formed

TABLE (11) STEEL STRESSES AND ULTIMATE MOMENTS (FATIGUE LOADING TESTS)

Beam mark	Type and percentage of steel	Steel stress at working moment N/mm^2		$\frac{\text{Col. 4}}{\text{Col. 3}}$	Ultimate moment KN.m		$\frac{\text{Col. 7}}{\text{Col. 6}}$
		first cycle N/mm^2	3×10^6 cycle		(Calculated) actual values of strength without partial safety factors	(Observed)	
1	2	3	4	5	6	7	8
FA1-0	M.S	173.4	172.2	0.99	31.92	36.125	1.13
FA1-C	1.044	143.96	168.36	1.17	32.44	38.375	1.18
FA2-0	UNI 410	240.7	245.2	1.02	39.02	44.7	1.15
FA2-C	1.044	208	254.18	1.22	39.56	50.5	1.28
FA4-0	KAM 60	332.97	343.9	1.03	58.81	65.625	1.12
	1.044						

TABLE (12) SUMMARY OF DEFLECTIONS (FATIGUE LOADING TESTS)

Beam mark	Deflection (mm)				$\frac{\text{Col. 4}}{\text{Col. 2}}$
	first cycle		3×10^6 cycles		
	At working moment	Remaining	At working moment	Remaining	
1	2	3	4	5	6
FA1-0	7.52	1.42	11.66	5.3	1.55
FA1-C	5.78	1.1	11.4	4.6	1.97
FA2-0	13.48	2.87	17.64	5.2	1.31
FA2-C	8.82	0.8	16.47	5.6	1.87
FA4-0	18.46	3.2	22.55	5.4	1.22

TABLE (13) SUMMARY OF CRACK WIDTHS (FATIGUE LOADING TESTS)

Beam mark	Crack width at working moment (mm)										
	At First cycle				After 3×10^6 cycle						
	At steel level		At bottom edge of beam		At steel level		At bottom edge of beam		Ordinary beams		Remaining maximum crack width after 3×10^6 cycles
	Maximum	Average	Maximum	Average	Maximum	Average	Maximum	Average	Col. 6 / Col. 2	Col. 8 / Col. 4	
1	2	3	4	5	6	7	8	9	10	11	12
FA1-0	0.1	0.08	0.14	0.1	0.14	0.08	0.2	0.11	1.4	1.43	0.11
FA1-C	0	0	0	0	0.15	0.06	0.32	0.27	-	-	0.1
FA2-0	0.16	0.09.	0.22	0.19	0.2	0.11	0.28	0.19	1.25	1.27	0.12
FA2-C	0.04	0.02	0	0	0.18	0.1	0.38	0.26	-	-	0.14
FA4-0	0.14	0.09	0.2	0.12	0.2	0.11	0.24	0.15	1.43	1.2	0.1

TABLE (14) STEEL STRESSES AND COMPRESSIVE STRAINS IN CONCRETE (SUSTAINED LOADING TESTS)

Beam mark	Type and percentage of steel	Flexural strain in concrete x 10^{-6}		$\frac{\text{Col. 4}}{\text{Col. 3}}$	Col. 4 - Col. 3	Shrinkage after 500 days x 10^{-6}	$\frac{\text{Col. 7}}{\text{Col. 6}}$	Steel stress at working moment N/mm^2	
		At the first test (initial)	At the end of sustained loading (final)					initial	final
1	2	3	4	5	6	7	8	9	10
SU1-0	M.S	360	1262	3.5	902	410	0.45	170	190
SU1-C	1.044	312	1108	3.55	796	328	0.41	160.5	173.3
SU2-0	UNI 410	700	1640	2.34	940	350	0.37	243.9	271.8
SU2-C	1.044	640	1804	2.82	1164	490	0.42	203.7	229

TABLE (15) SUMMARY OF CRACK WIDTHS AND DEFLECTIONS (SUSTAIND LOADING TESTS)

Beam mark	Crack width of working moment (mm)								Remaining maximum crack width at end of sustained loading (mm)		Measured deflection at working moment (mm) **		Remaining deflection at the end of sustained loading (mm) **	Col. 13 / Col. 12
	At the first test (Initial)				At the end of sustained loading (Final)									
	At steel level		At bottom edge of beam		At steel level		At bottom edge of beam							
	Maximum	Average	Maximum	Average	Maximum	Average	Maximum	Average	At steel level	At bottom edge of beam	At the first test (Initial)	At the end of sustained loading (Final)		
1	2	3	4	5	6	7	8	9	10	11	12	13	14	15
SU1-0	0.1	0.07	0.12	0.1	0.2	0.1	0.22	0.15	0.1	0.12	0.82	1.97	1.62	2.4
SU1-C	0	0	0	0	0.1	0.06	0	0	0.02	0	0.46	1.61	1.2	3.5
SU2-0	0.1	0.08	0.16	0.11	0.22	0.13	0.22	0.13	0.1	0.1	1.72	2.45	1.23	1.42
SU2-C	0.08	0.06	0	0	0.14	0.07	*0.2	-	0.02	0.02	1.18	2.37	1.19	2

* one crack only

** the total deflection of a beam equal to 7.7 times the values given.

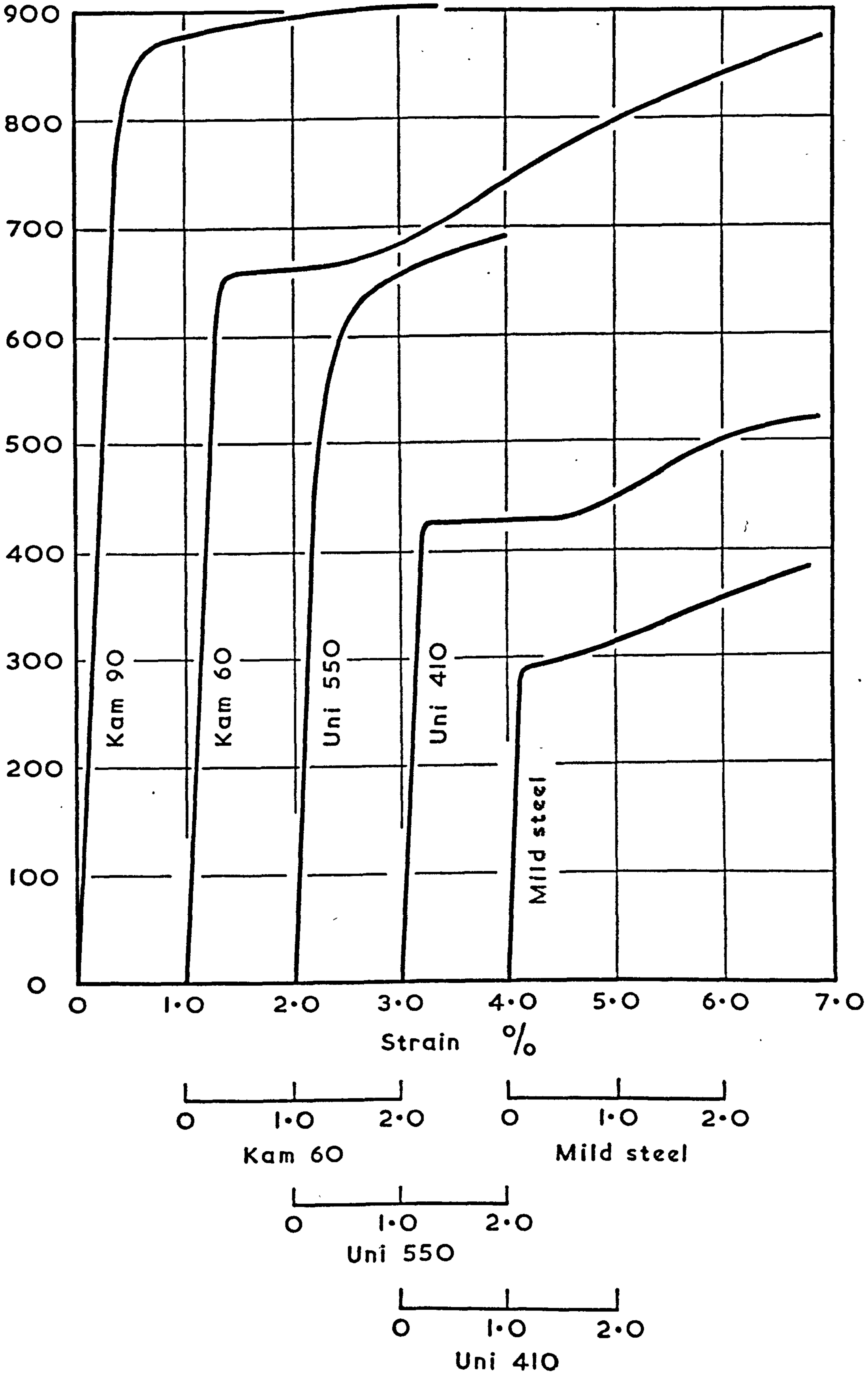

FIG. 1 TENSILE STRESS–STRAIN CHARACTERISTICS OF REINFORCEMENTS USED

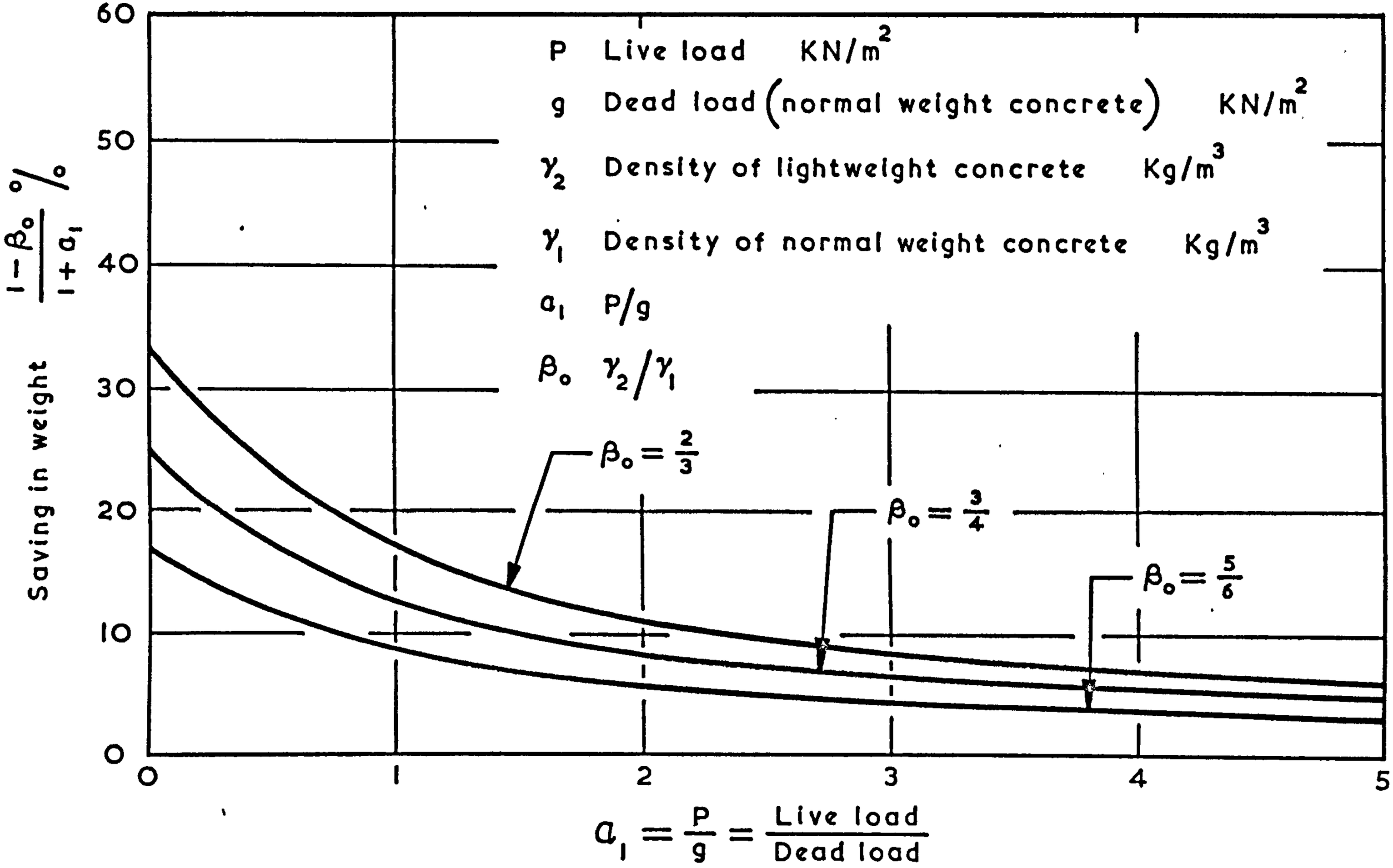

FIG. 2 RELATION BETWEEN SAVING IN WEIGHT FOR LIGHTWEIGHT CONCRETE AND THE RATIO OF LIVE LOAD TO DEAD LOAD FOR NORMAL CONCRETE

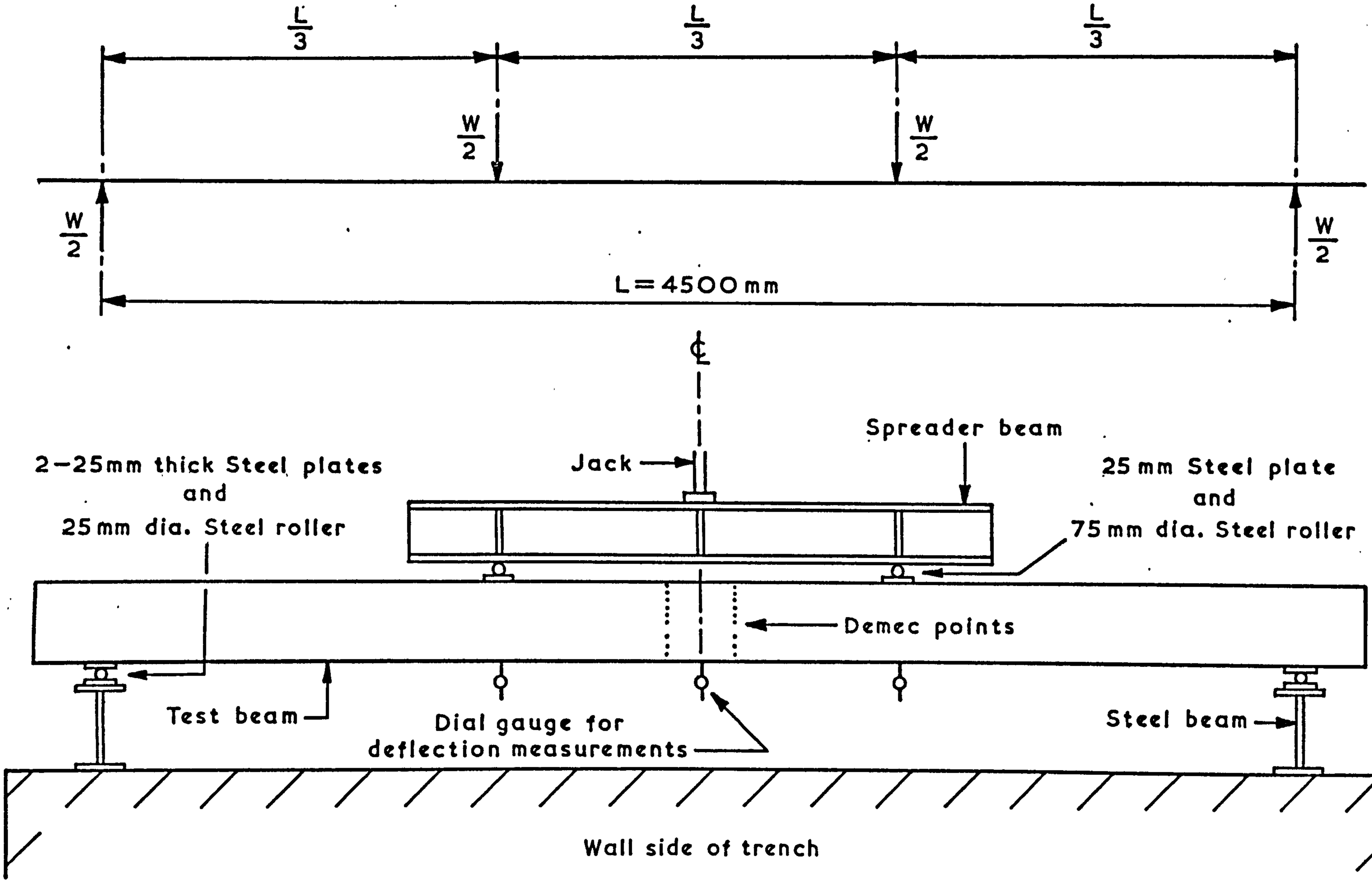

FIG. 3 ARRANGEMENTS FOR STATIC AND FATIGUE LOADING TESTS FOR ORDINARY AND COMPOSITE BEAMS

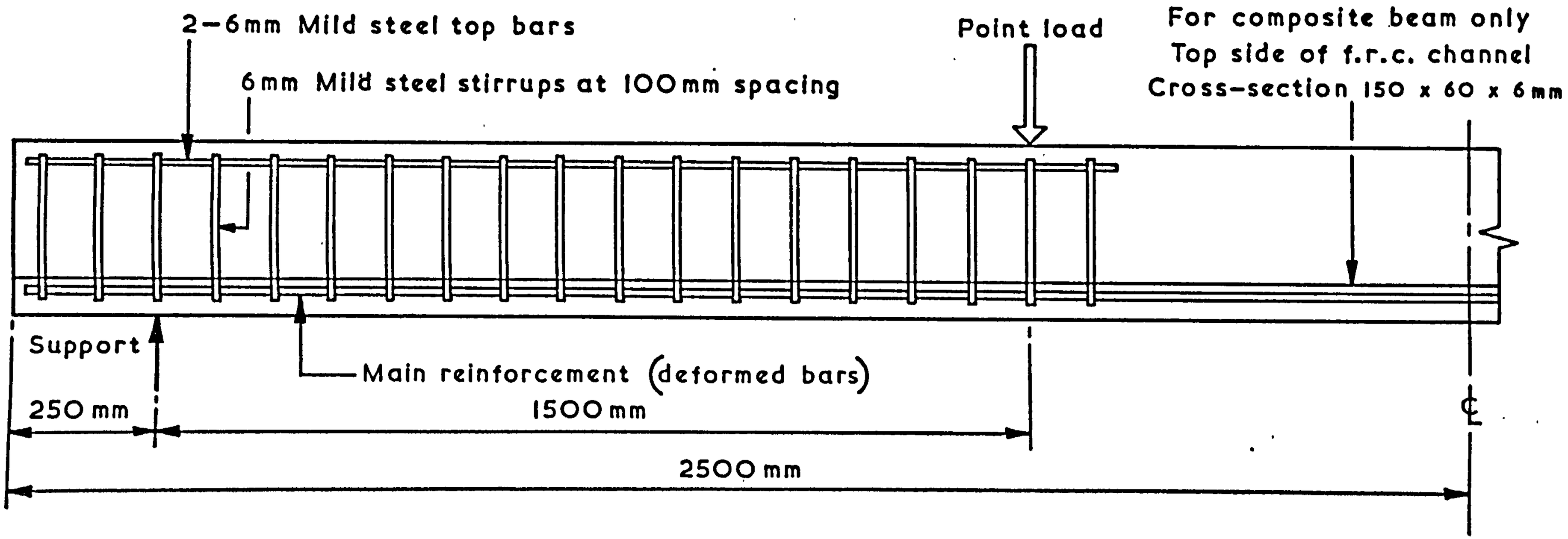

FIG. 4 DETAILS OF REINFORCEMENT IN ORDINARY AND COMPOSITE BEAMS (ELEVATION)

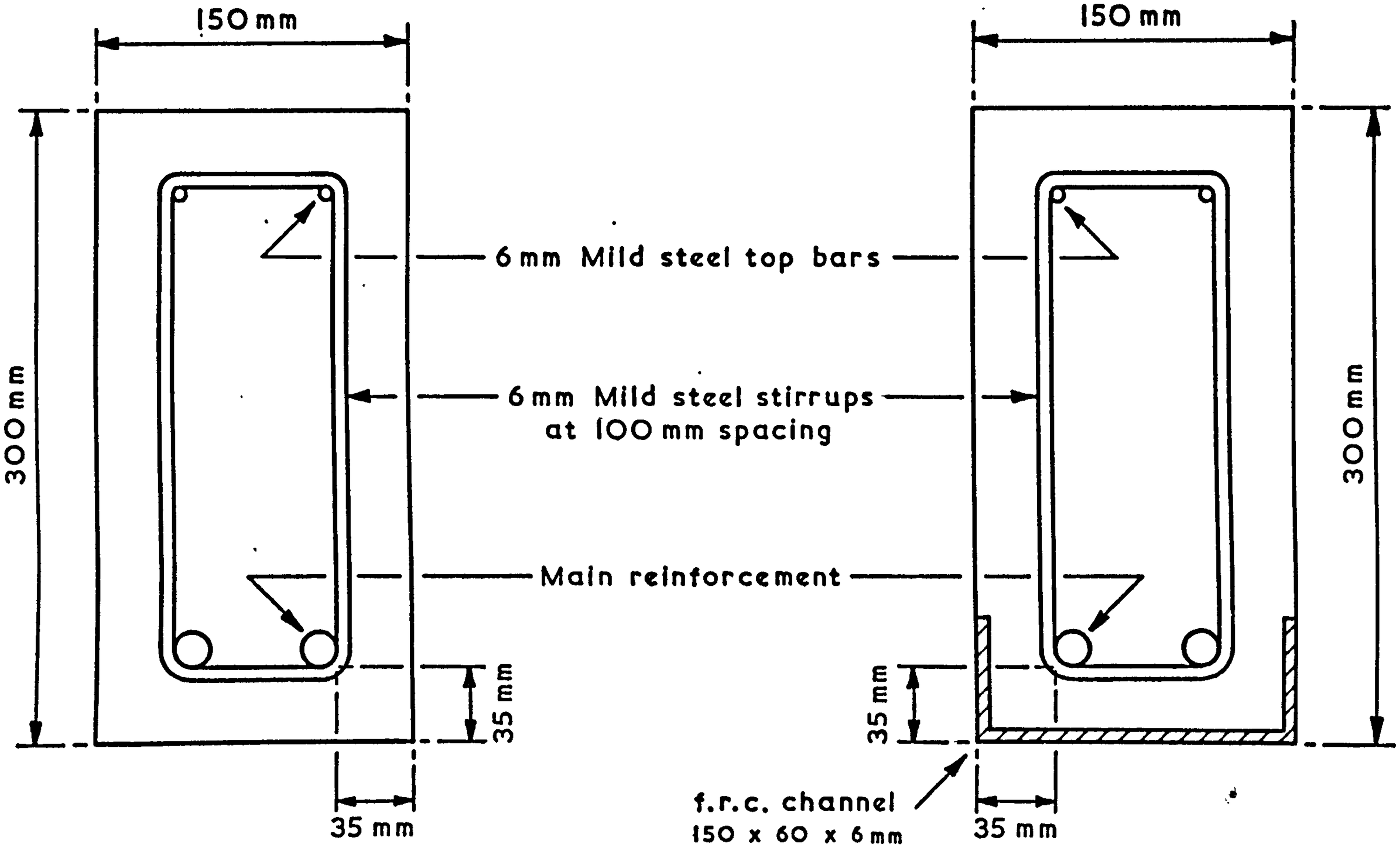

FIG. 5 DETAILS OF REINFORCEMENT IN ORDINARY AND COMPOSITE BEAMS (CROSS-SECTIONS)

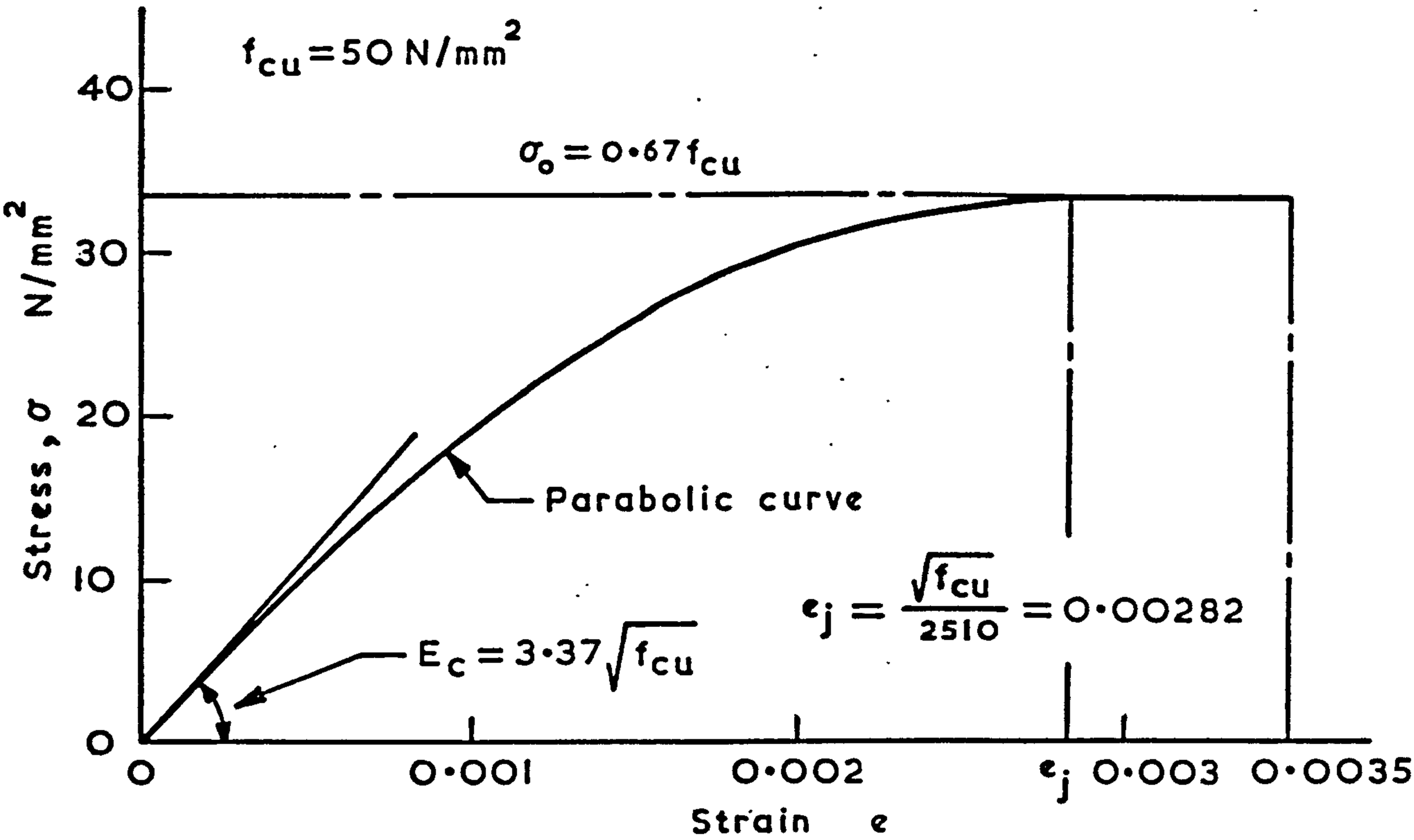

(a) Theoretical ultimate design stress–strain curve

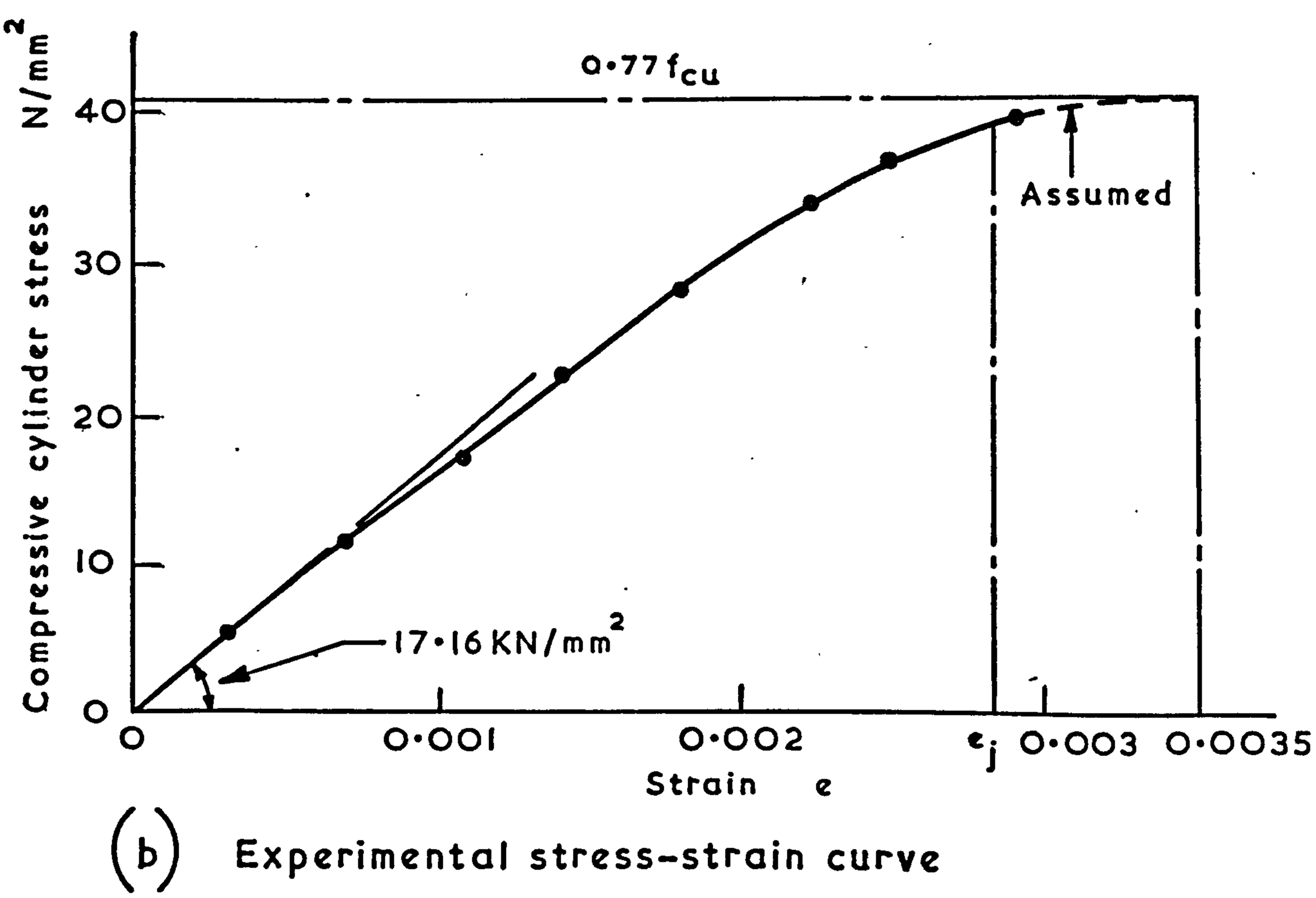

(b) Experimental stress–strain curve

FIG.6 THEORETICAL AND EXPERIMENTAL STRESS–STRAIN RELATIONSHIP FOR LIGHTWEIGHT CONCRETE IN COMPRESSION

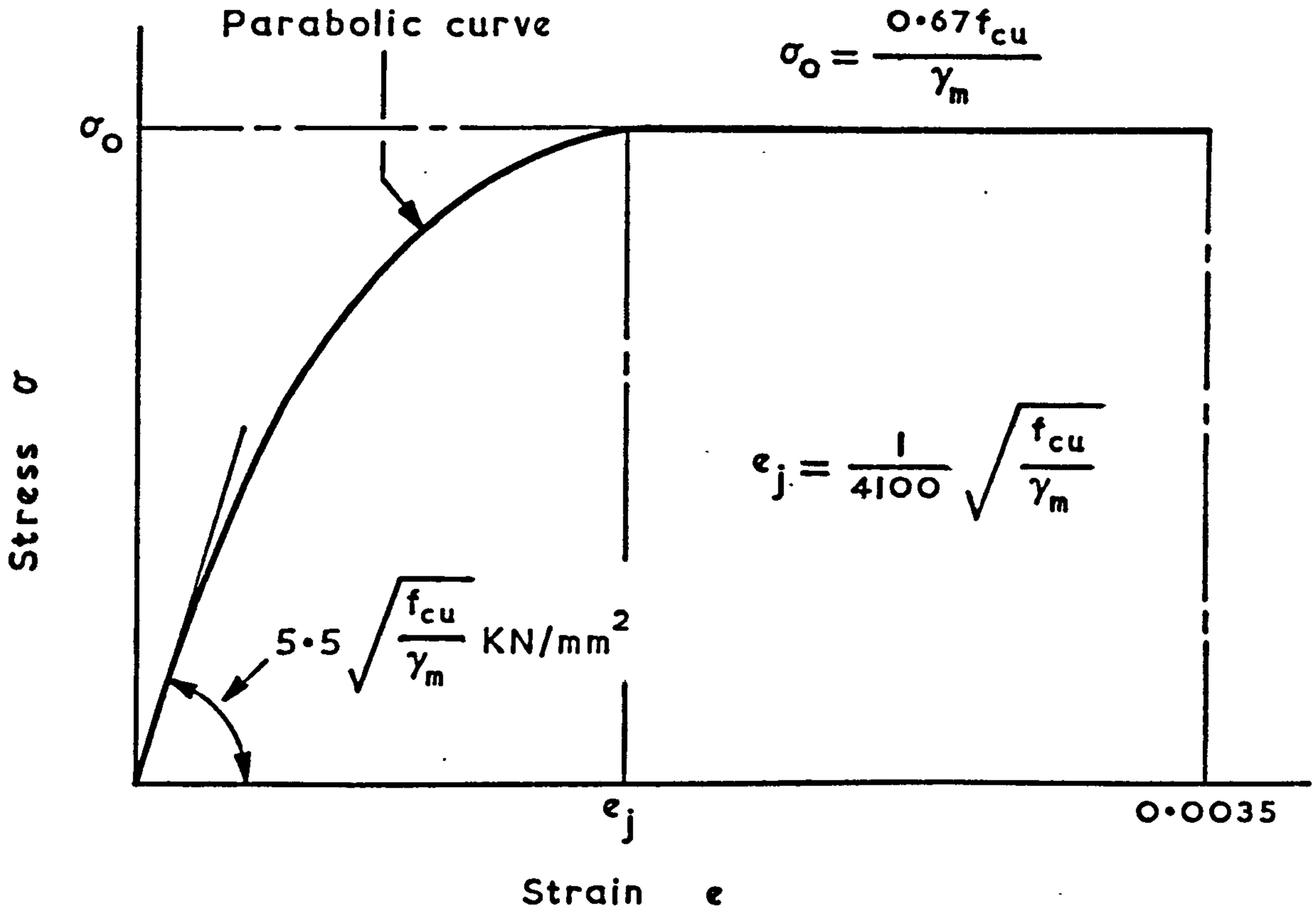

(a) Design stress-strain curve for normal weight concrete $(\gamma_m = 1{\cdot}5)$

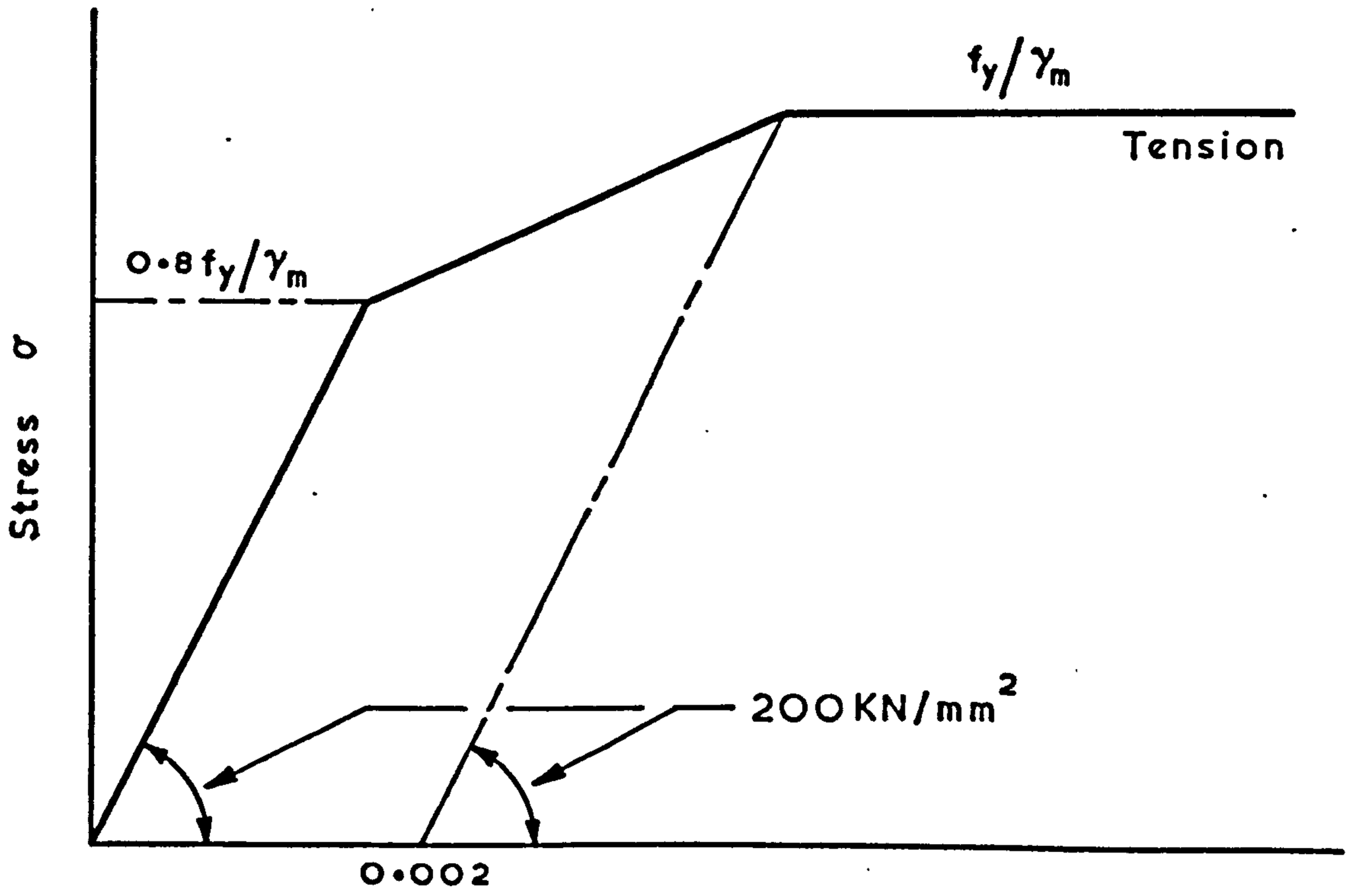

(b) Design stress-strain curves for reinforcements $(\gamma_m = 1{\cdot}15)$

FIG.7 DESIGN STRESS–STRAIN CURVES FOR CONCRETE AND STEEL AS PER B.S. CP110

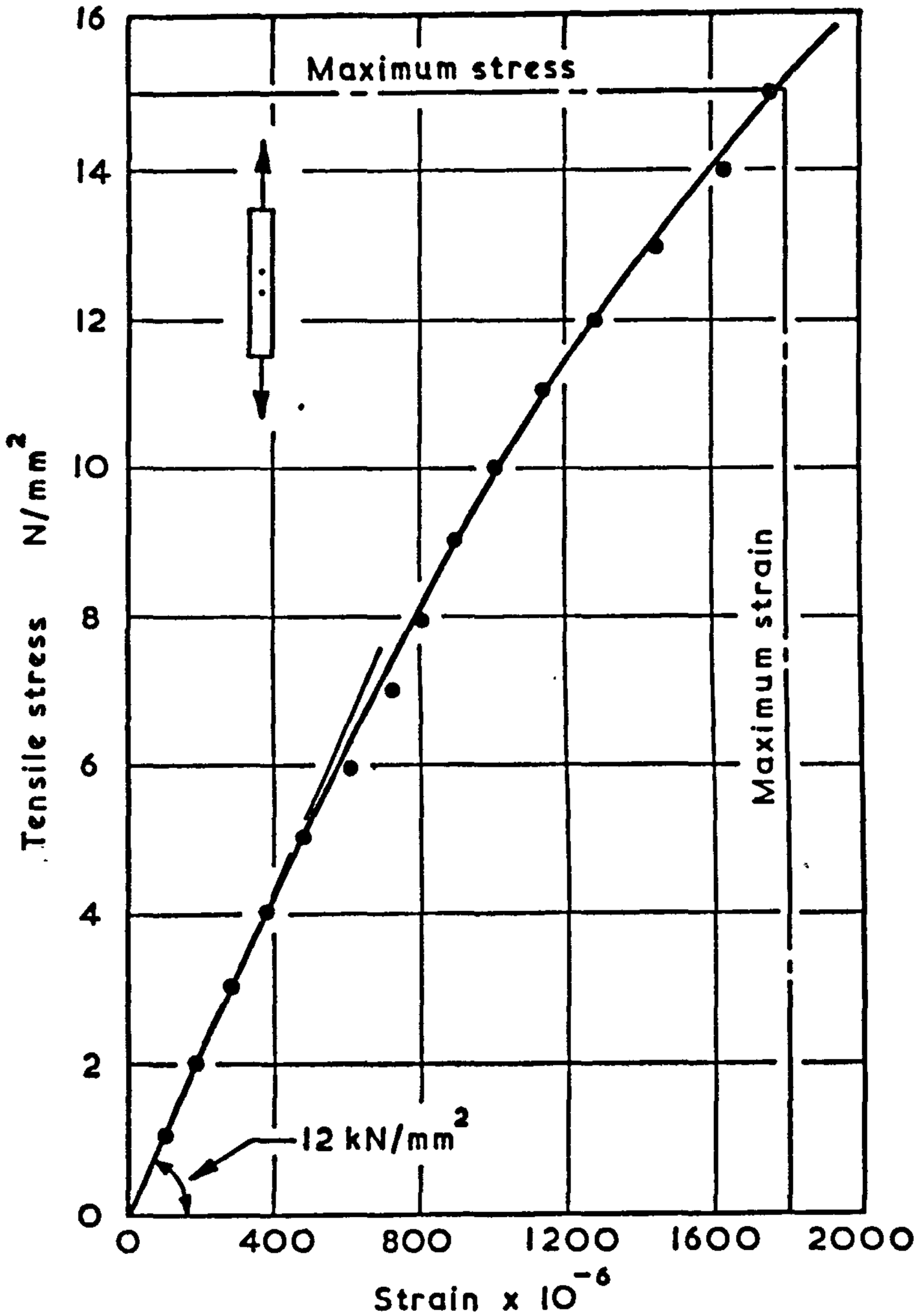

(a) Direct tensile properties (average of samples)

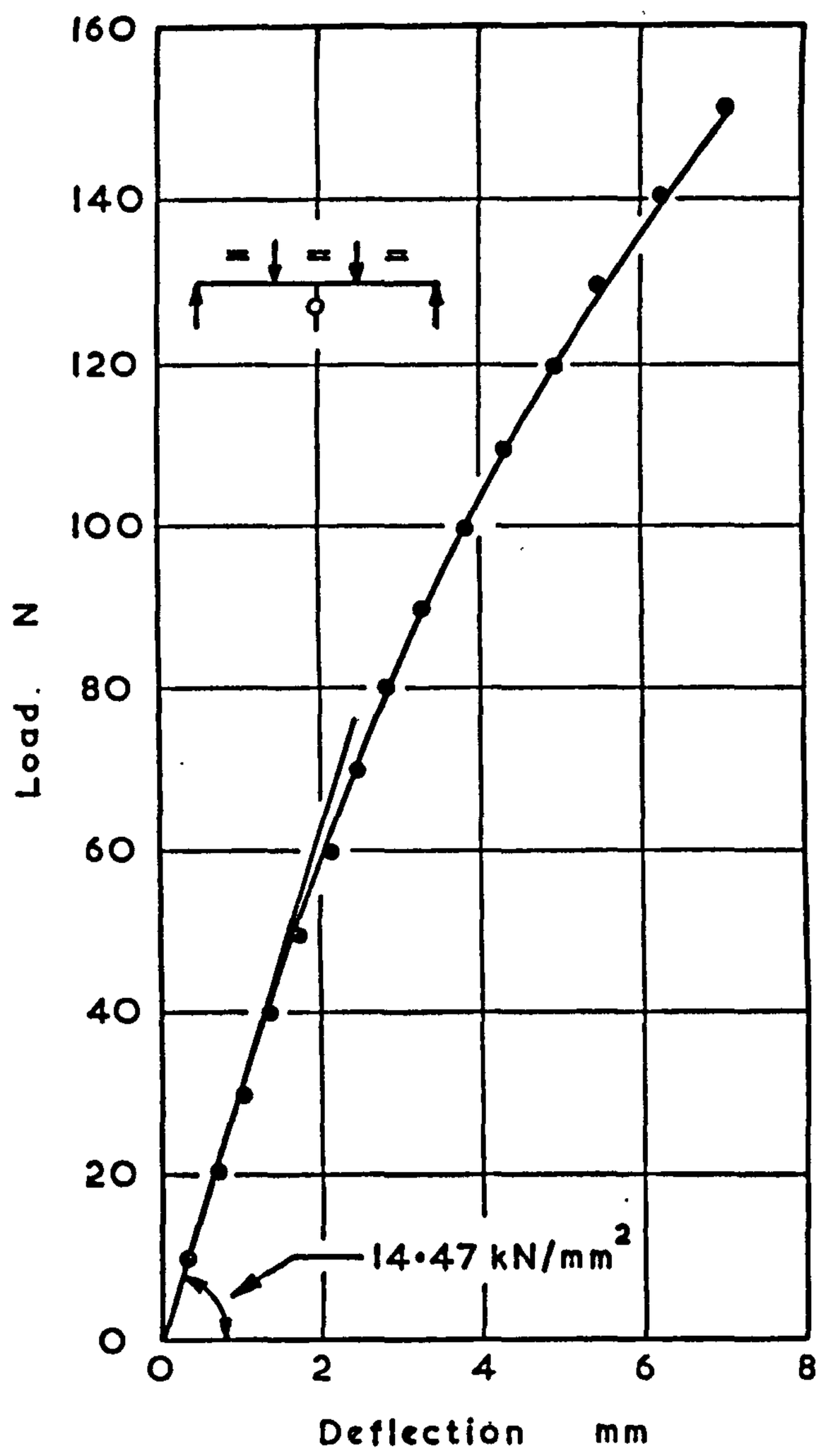

(b) Flexural properties (sample No. 1)

FIG. 8 DIRECT TENSILE AND FLEXURAL PROPERTIES OF f.r.c. UNITS

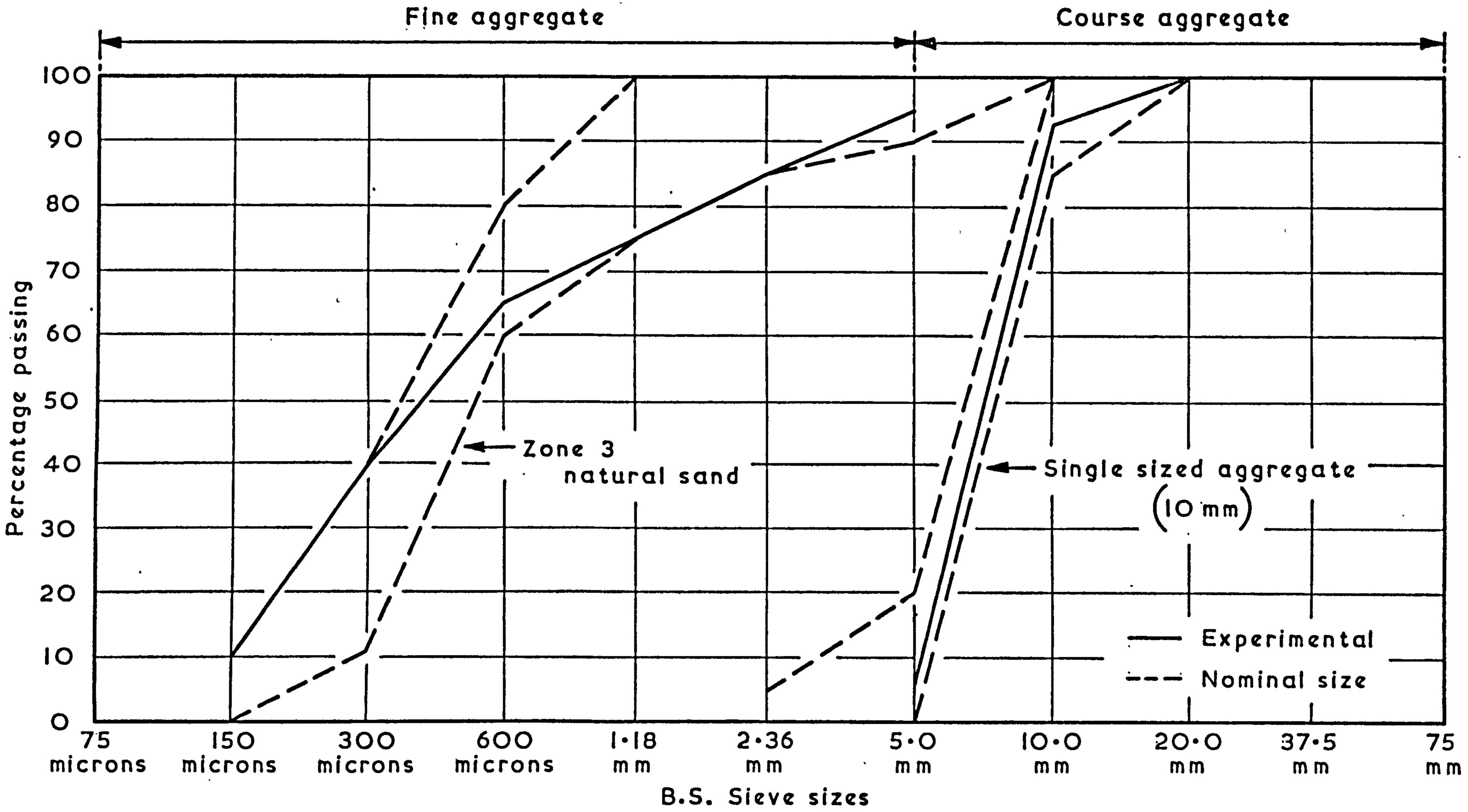

FIG.9 GRADING OF AGGREGATES USED

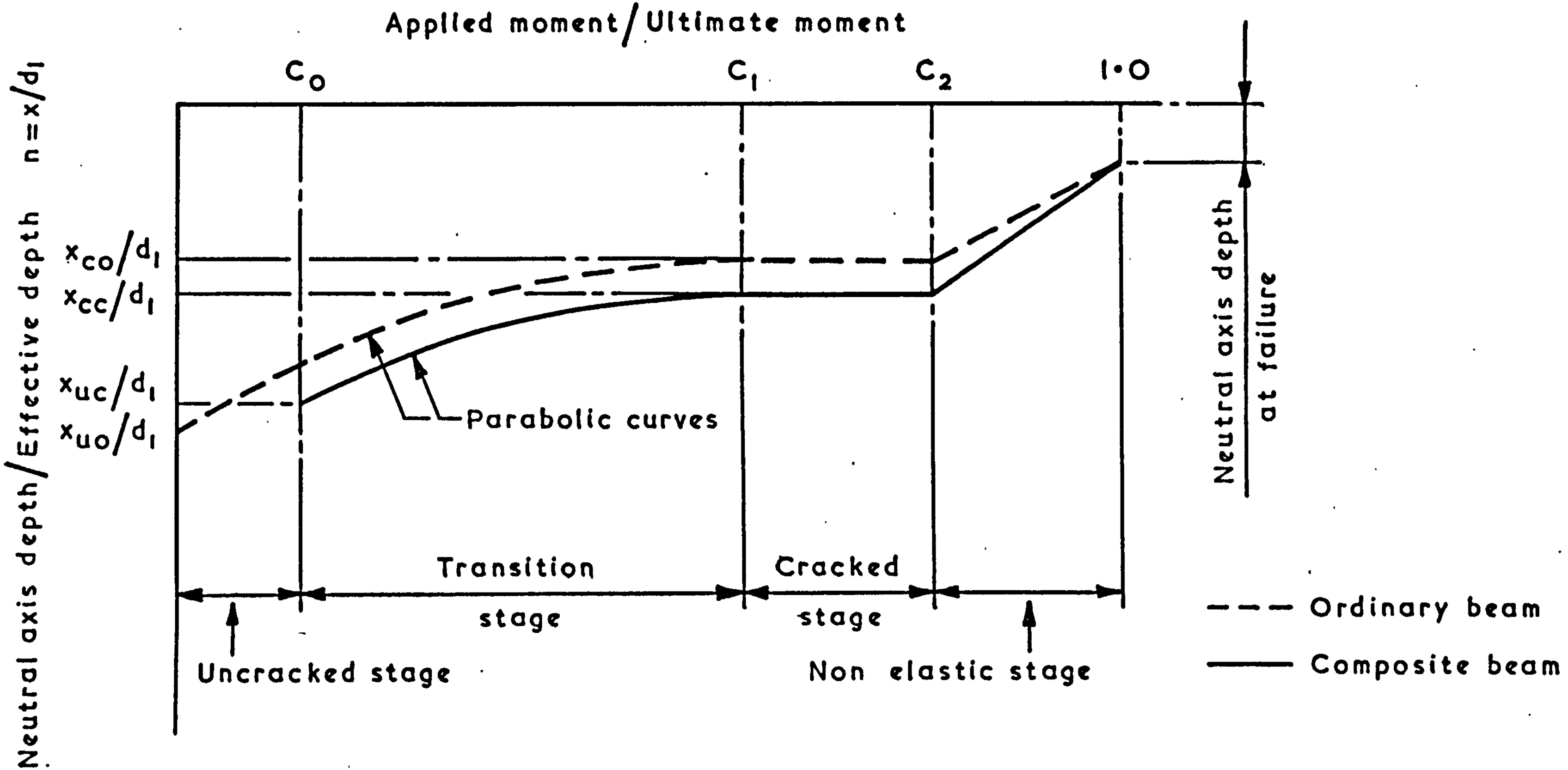

FIG.10 IDEALISED RELATIONSHIP BETWEEN THE LEVEL OF THE NEUTRAL AXIS DEPTH AND THE APPLIED MOMENT FOR ORDINARY AND COMPOSITE BEAMS

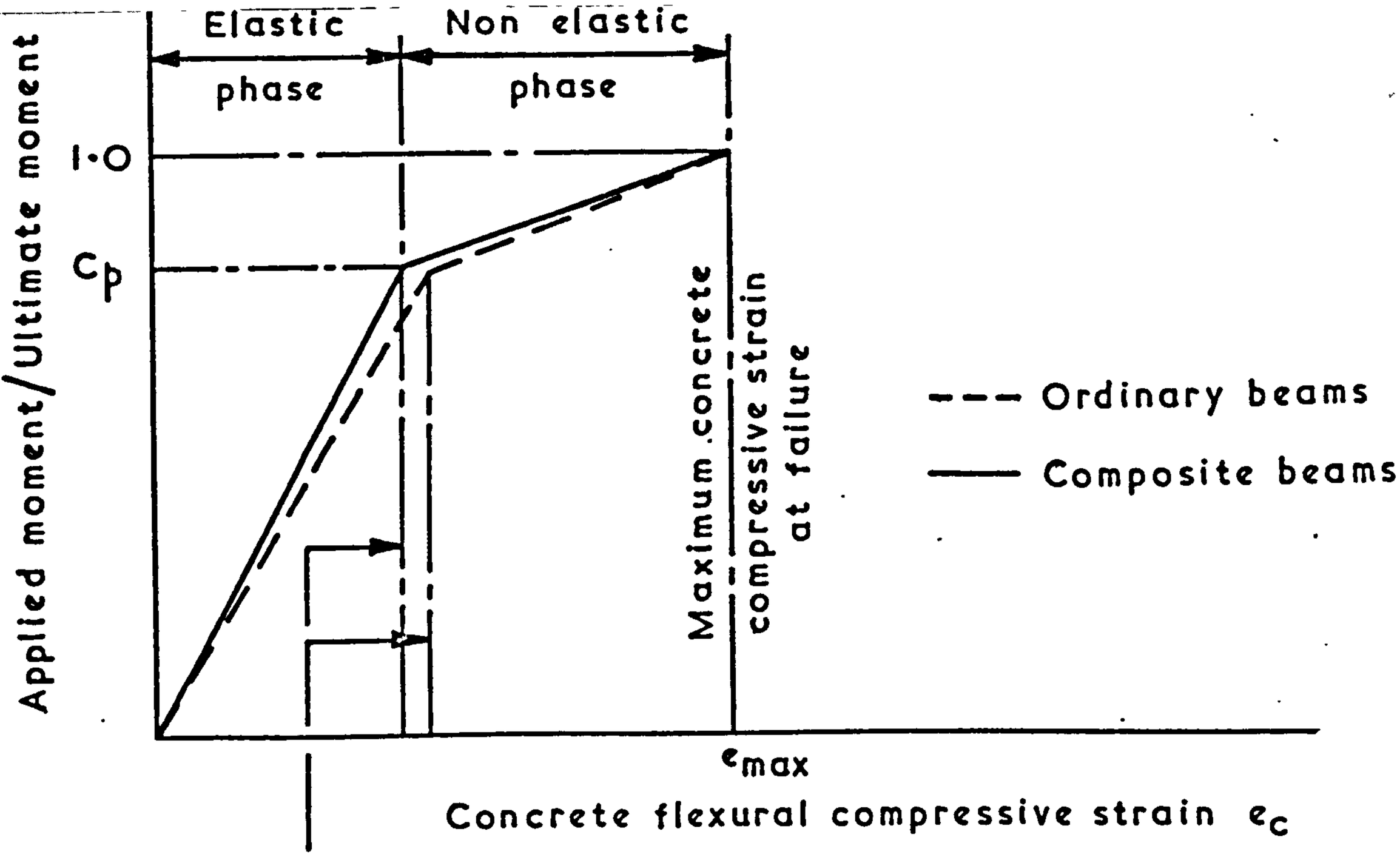

(a) Simplified bilinear relationship between applied moment and flexural compressive strain in concrete for ordinary and composite beams

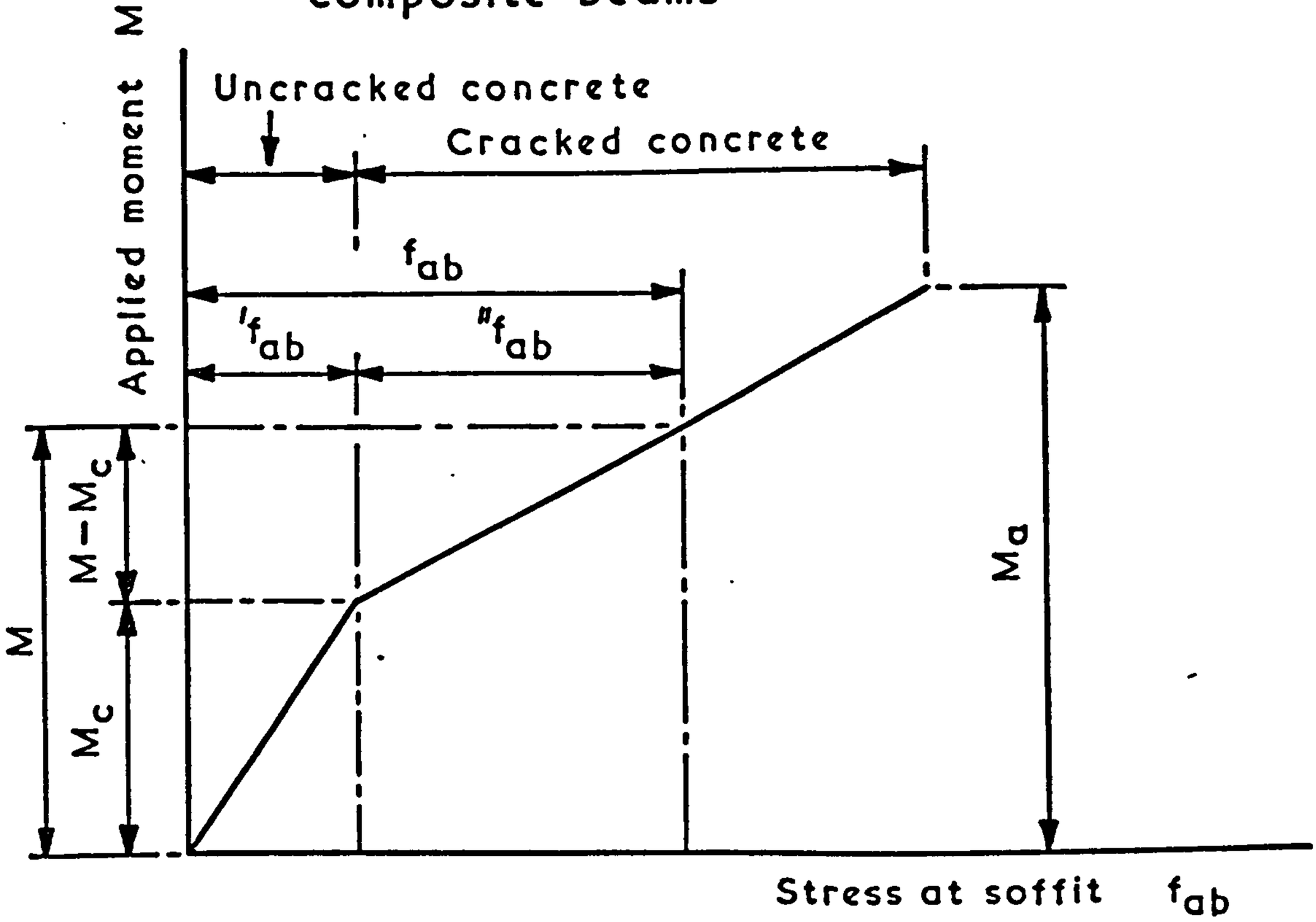

(b) Idealised relationship between applied moment and maximum stress in f.r.c. channel

FIG. 11 RELATIONSHIPS WITH APPLIED MOMENT FOR STRESS IN f.r.c. CHANNEL AND FLEXURAL COMPRESSIVE STRAIN IN CONCRETE

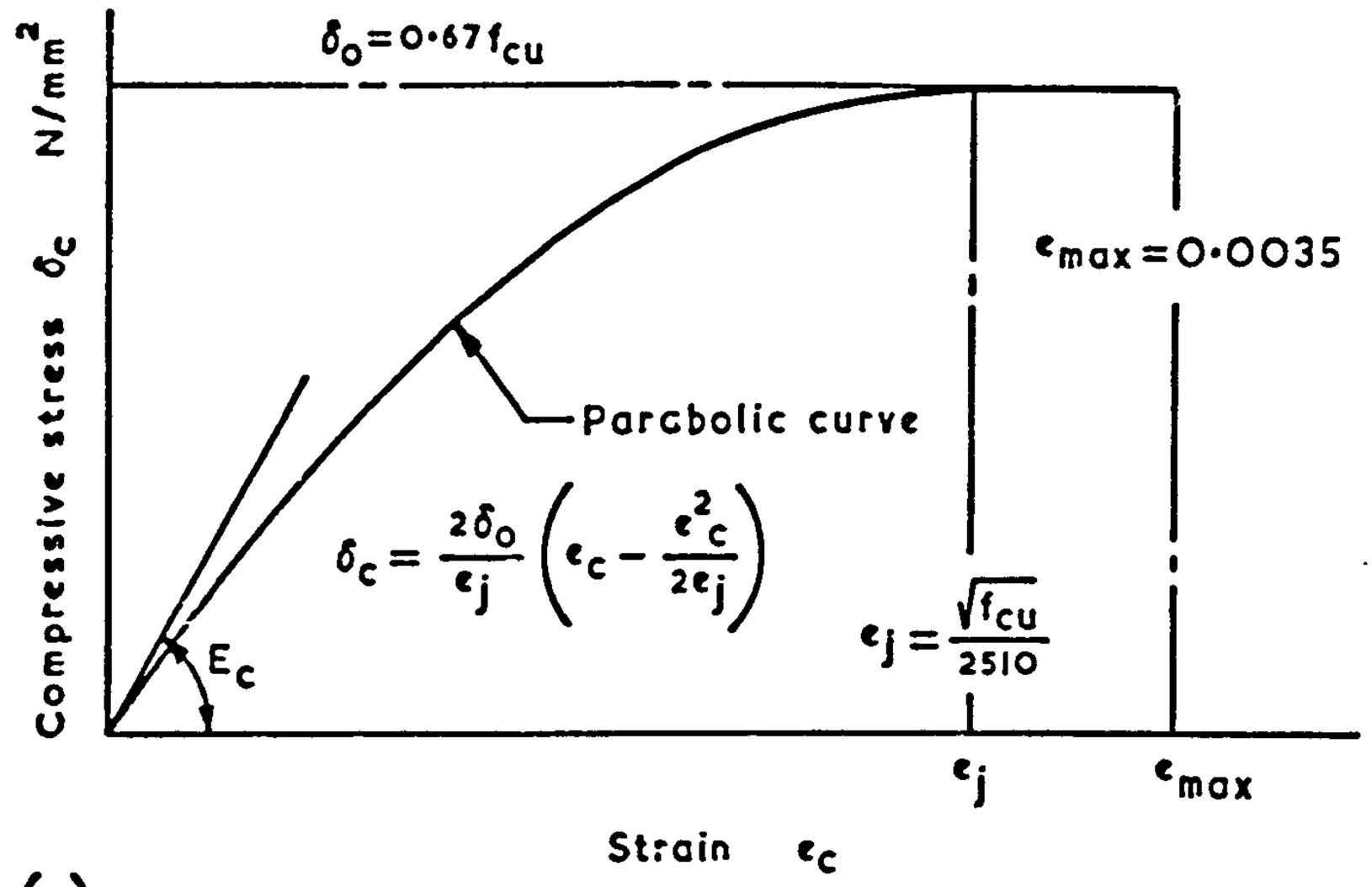

(a) Stress-strain relationship for lightweight concrete in compression

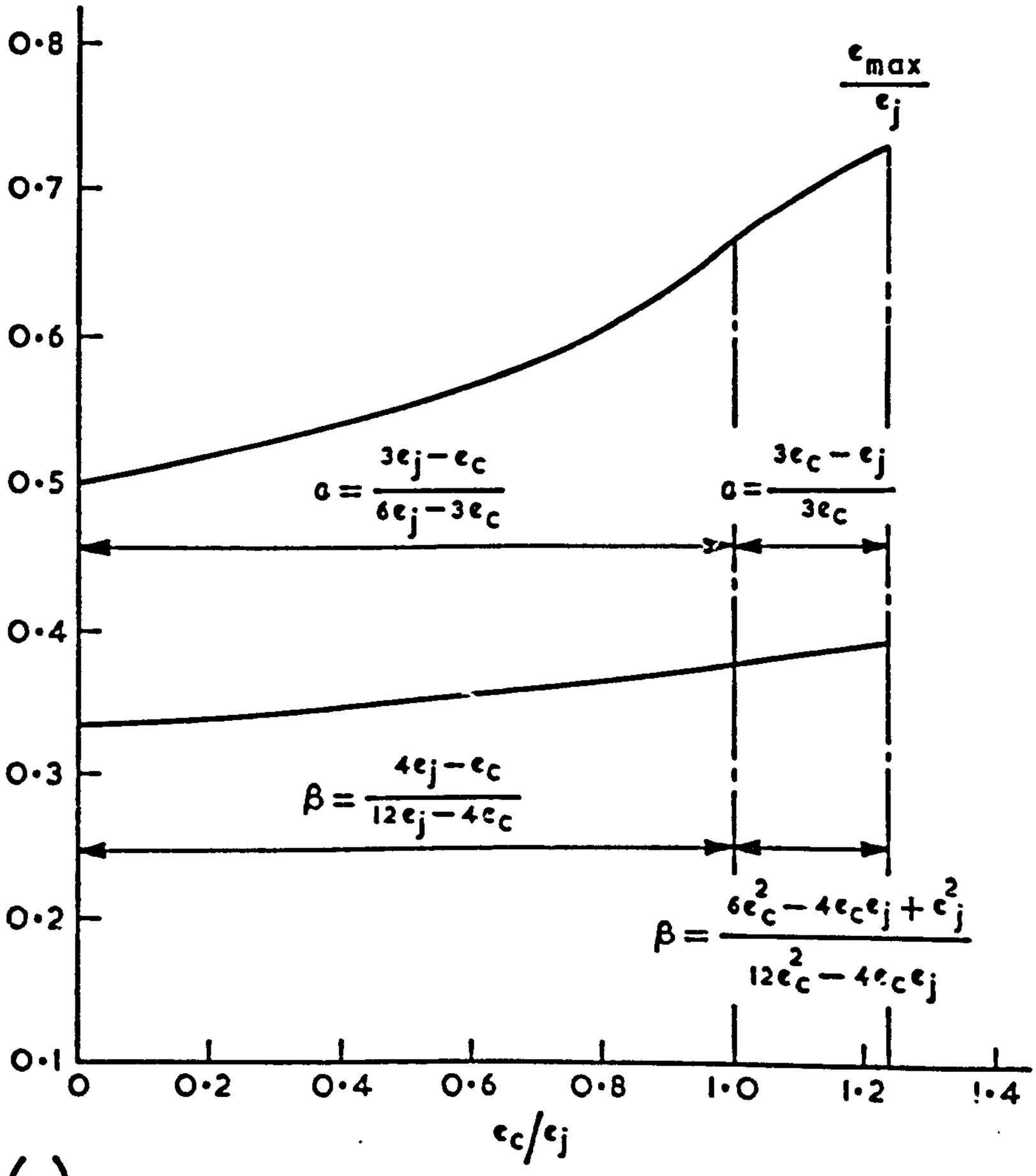

(b) Prediction of the coefficients α and β

FIG.12 CALCULATION OF CENTROID AND AREA FOR COMPRESSIVE STRESS DISTRIBUTION DIAGRAM IN CONCRETE

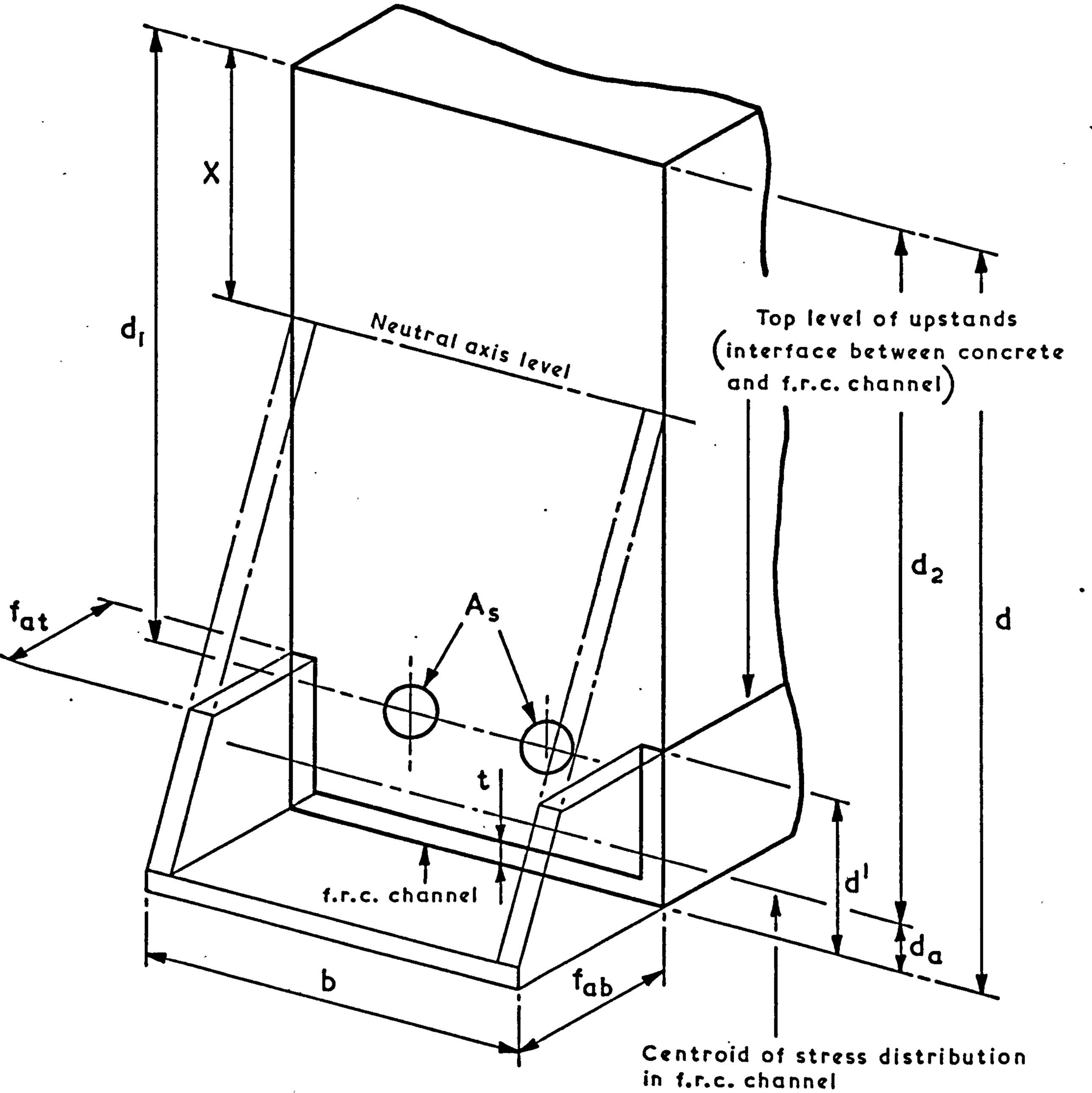

FIG.13 ASSUMED DISTRIBUTION OF TENSILE STRESSES IN f.r.c. CHANNEL FOR COMPOSITE BEAMS

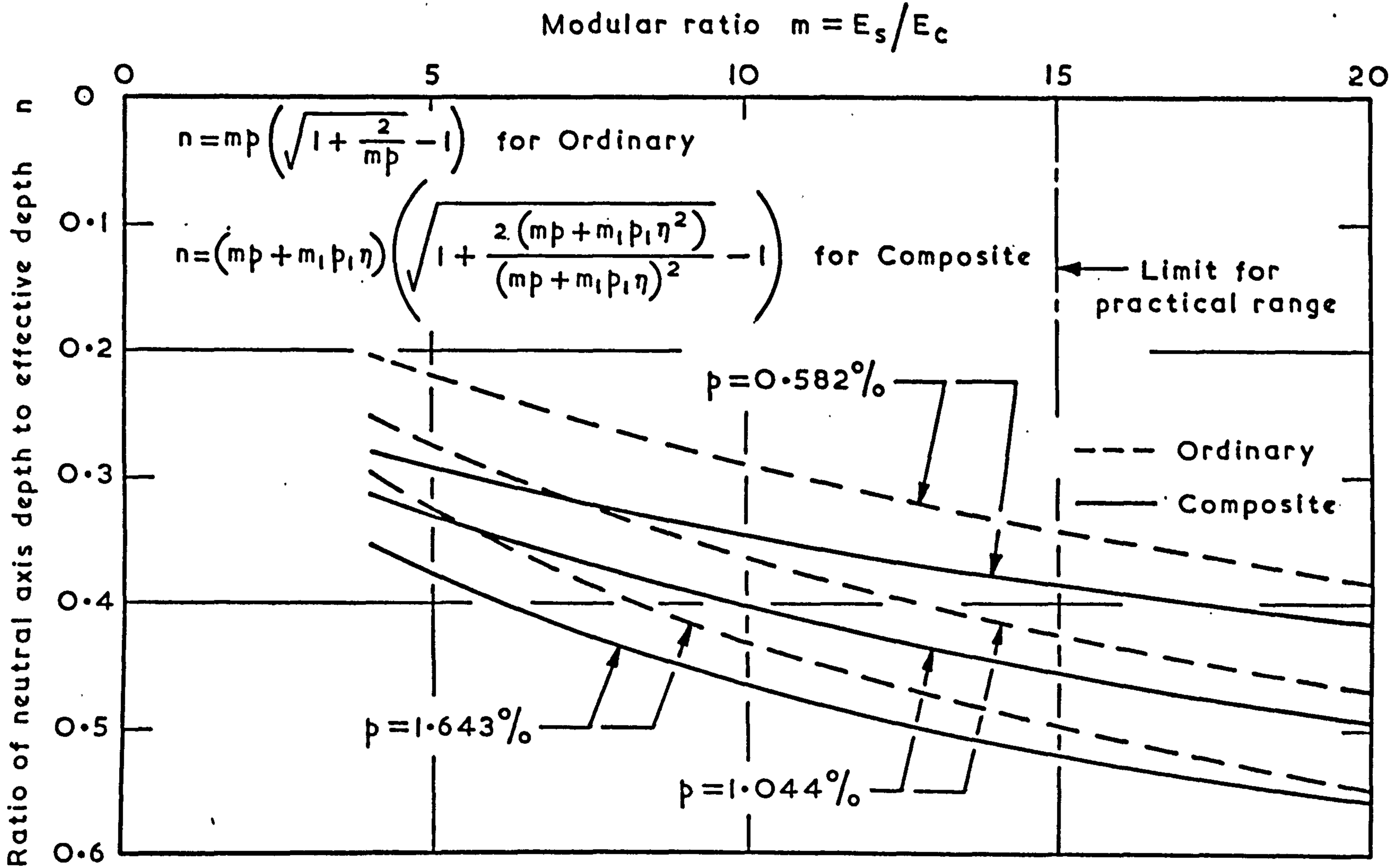

FIG.14 EFFECT OF MODULUS OF ELASTICITY OF CONCRETE ON LEVEL OF NEUTRAL AXIS DEPTH FOR CRACKED ORDINARY AND COMPOSITE SECTIONS

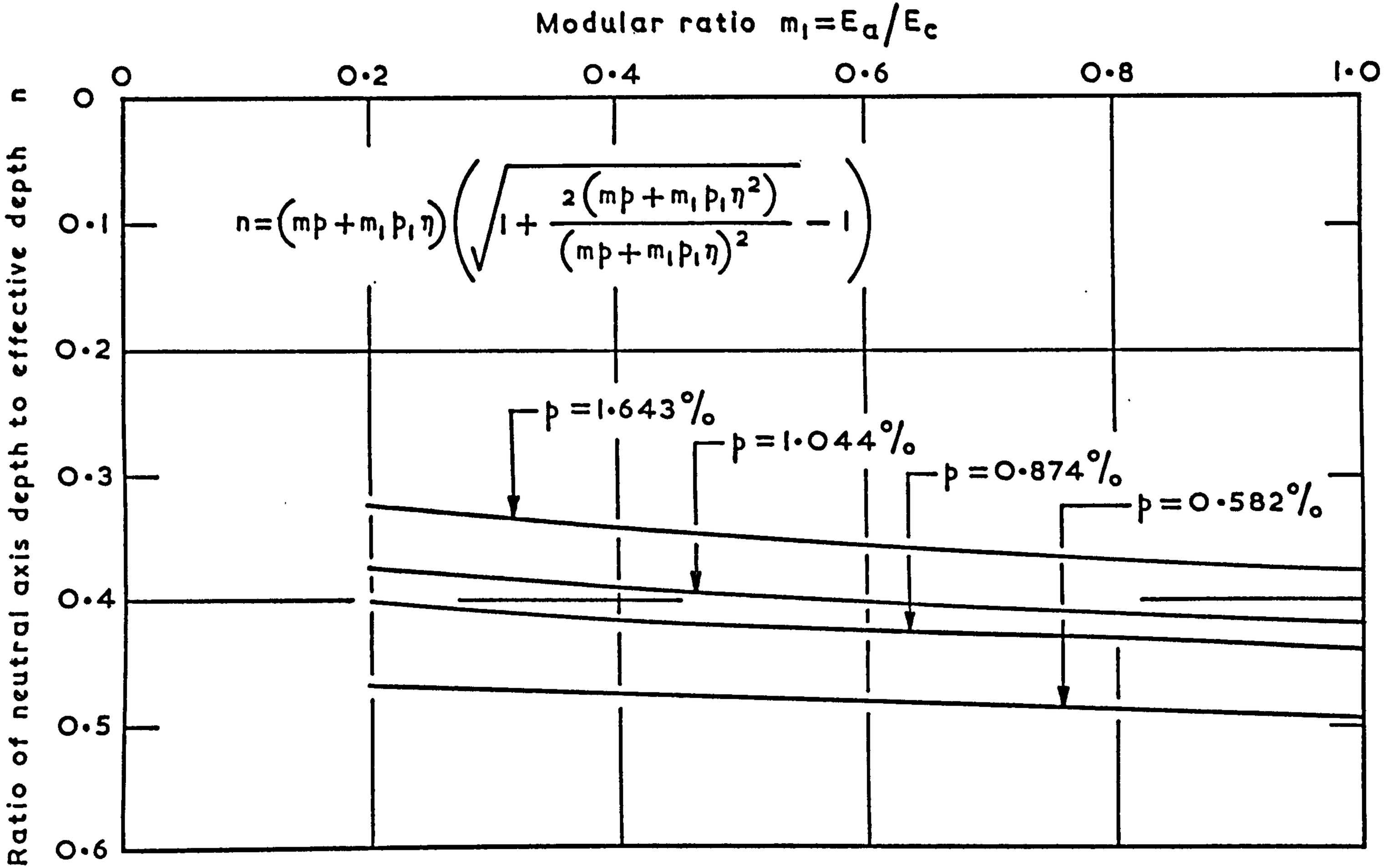

FIG. 15 EFFECT OF MODULUS OF ELASTICITY OF f.r.c. UNITS ON LEVEL OF NEUTRAL AXIS DEPTH FOR CRACKED COMPOSITE SECTIONS

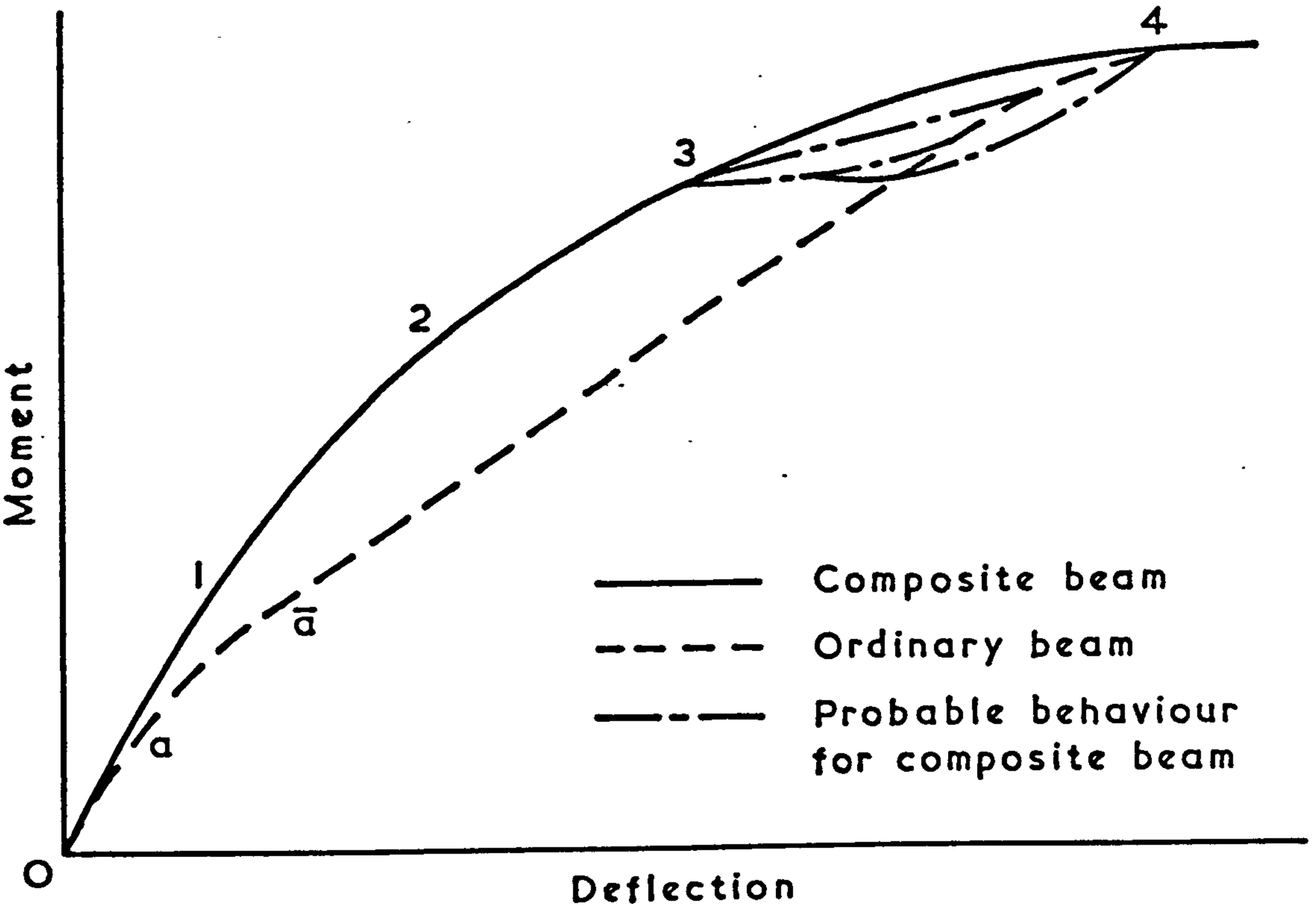

(a) Typical load-deflection behaviour for ordinary and composite beams

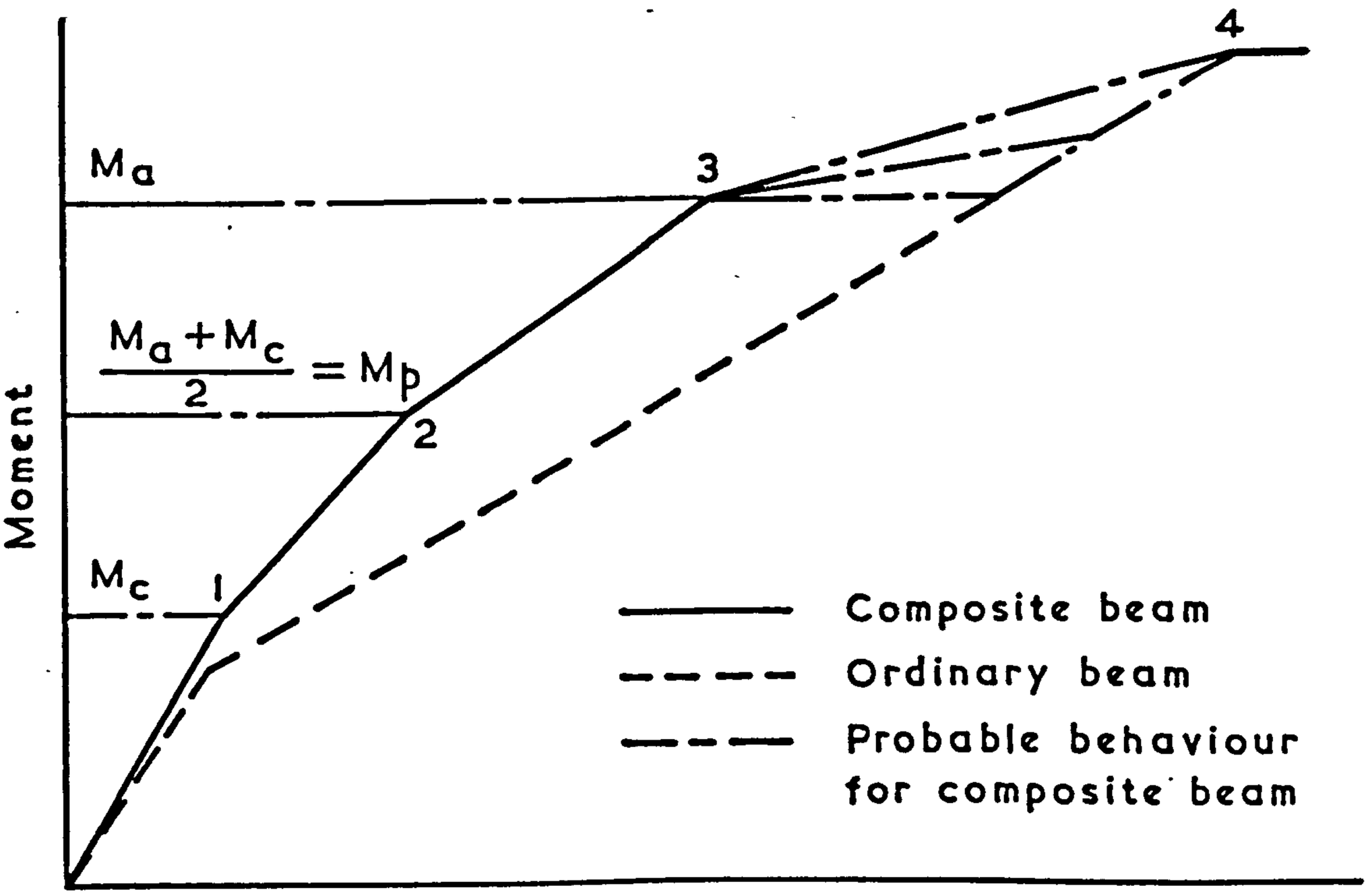

(b) Idealised moment-deflection relationship for composite beams

FIG. 16 LOAD—DEFLECTION BEHAVIOUR FOR ORDINARY AND COMPOSITE LIGHTWEIGHT CONCRETE BEAMS

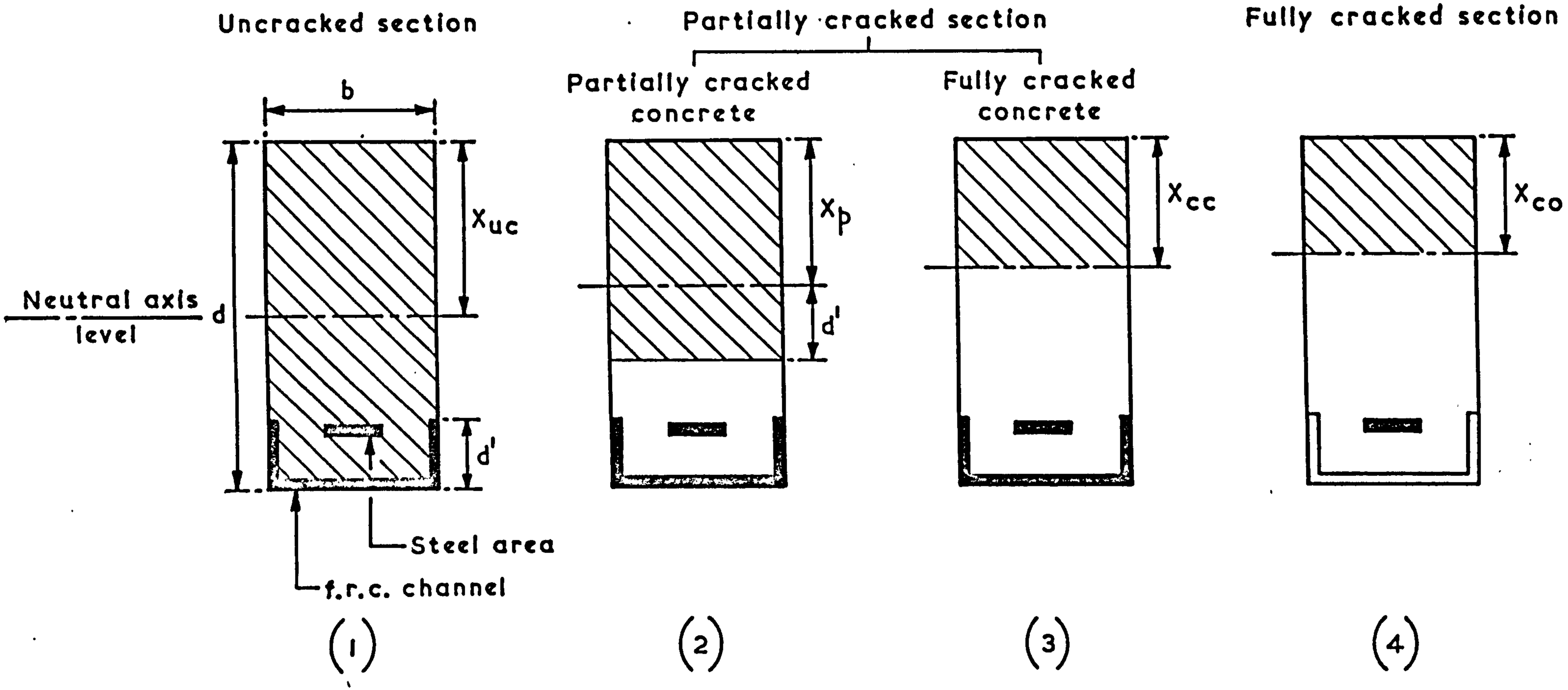

FIG.17 CROSS-SECTIONS ANALYSIS FOR THE DEFLECTION BEHAVIOUR OF COMPOSITE BEAMS

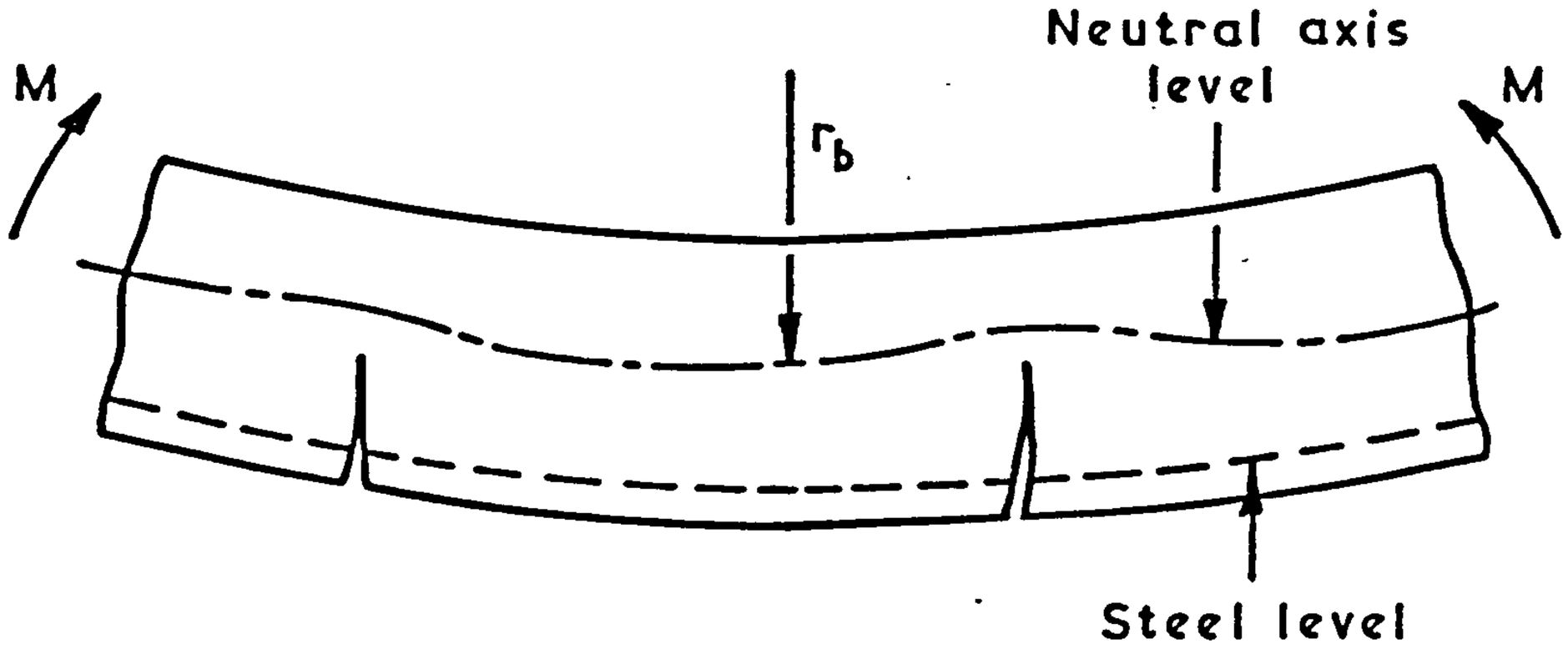

(a) Elevation of a cracked beam

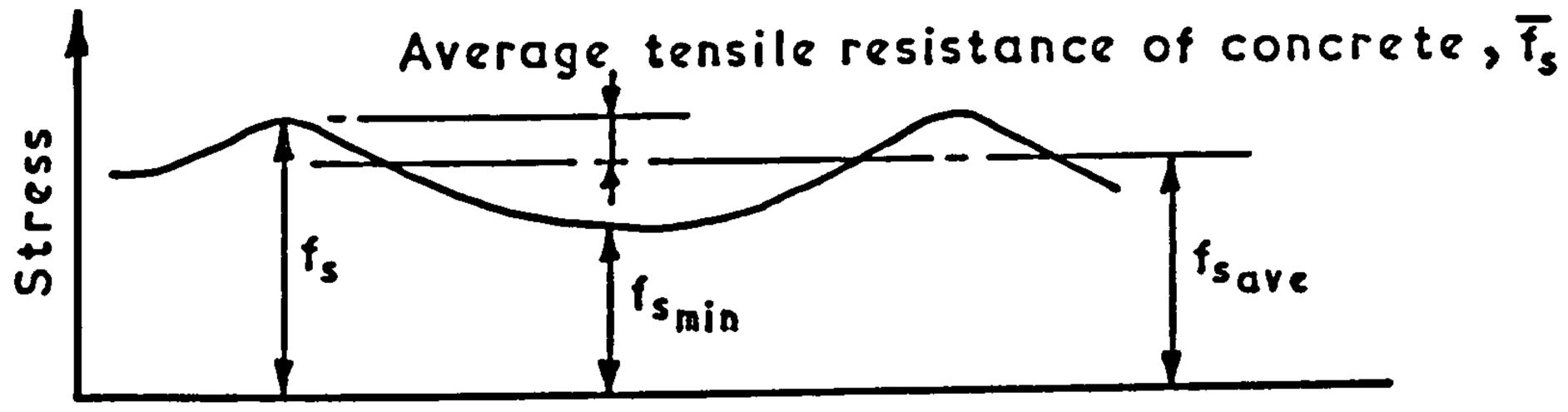

(b) Distribution of steel stress along a cracked beam

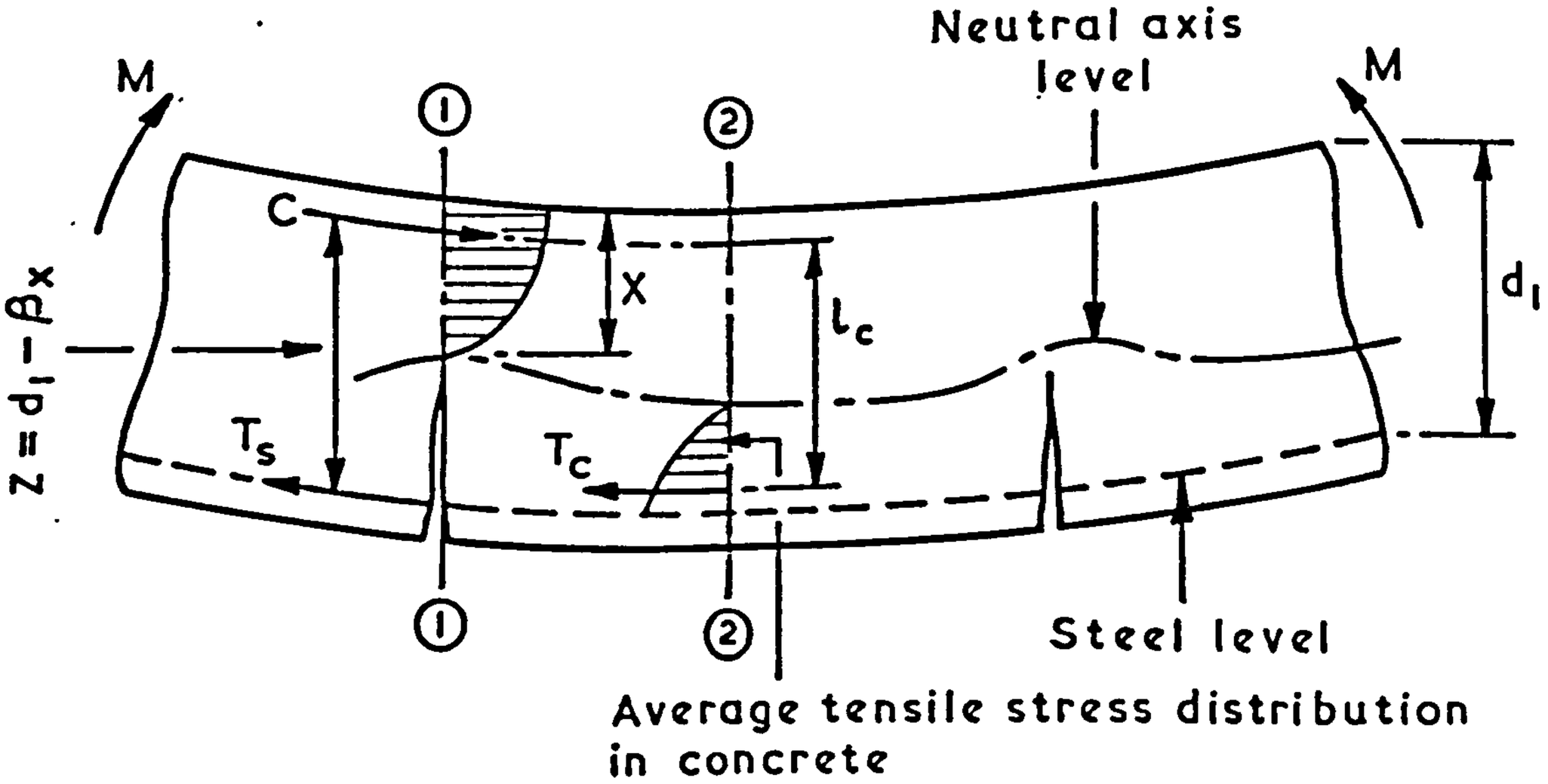

(c) Stress distribution at a cracked and uncracked concrete section

FIG. 18 ASSUMED STRESS DISTRIBUTION OF STRESS IN STEEL AND CONCRETE ALONG CRACKED ORDINARY BEAM

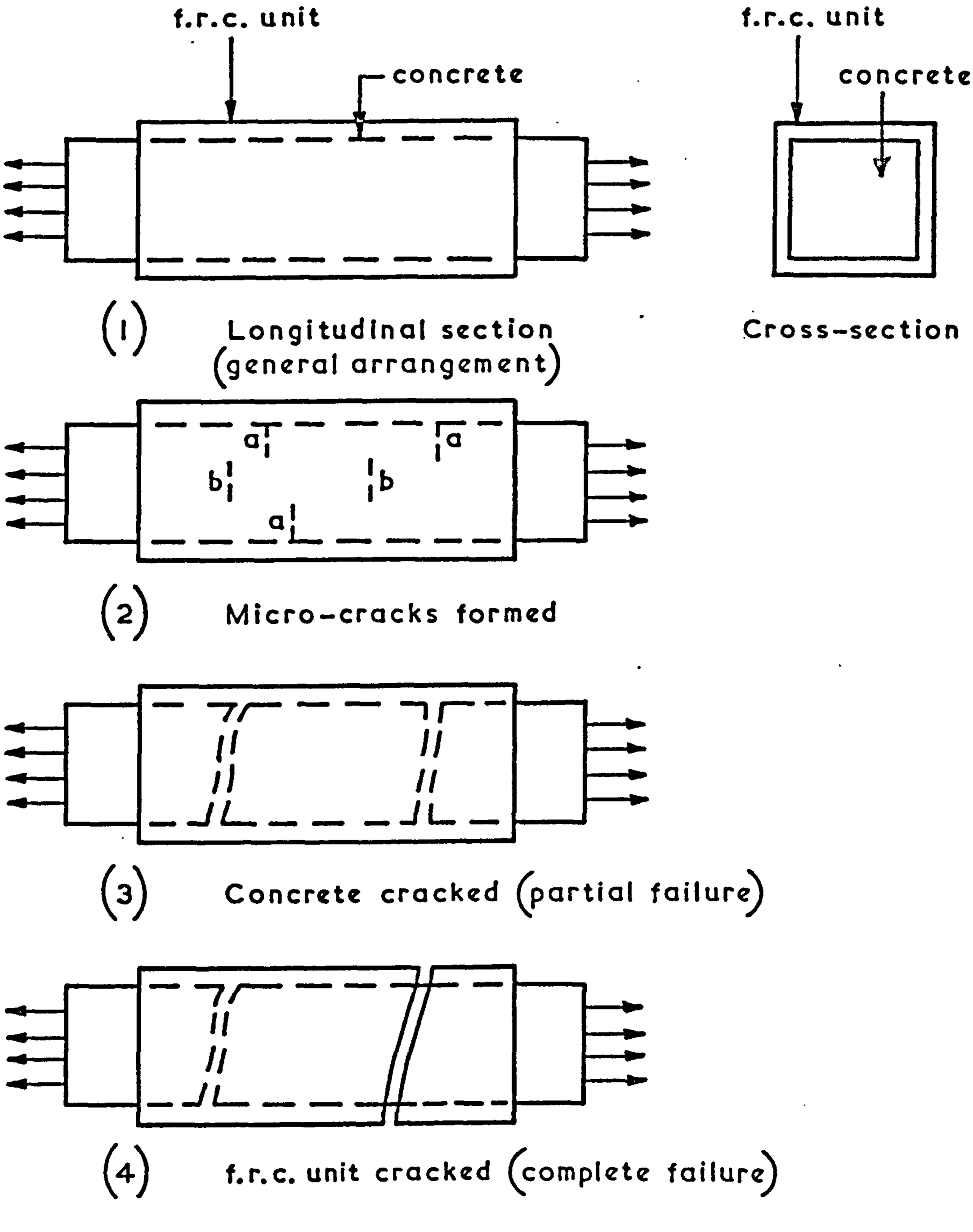

FIG. 19 CONCRETE PRISM CONFINED BY f.r.c. UNITS SUBJECTED TO DIRECT TENSION STRESS

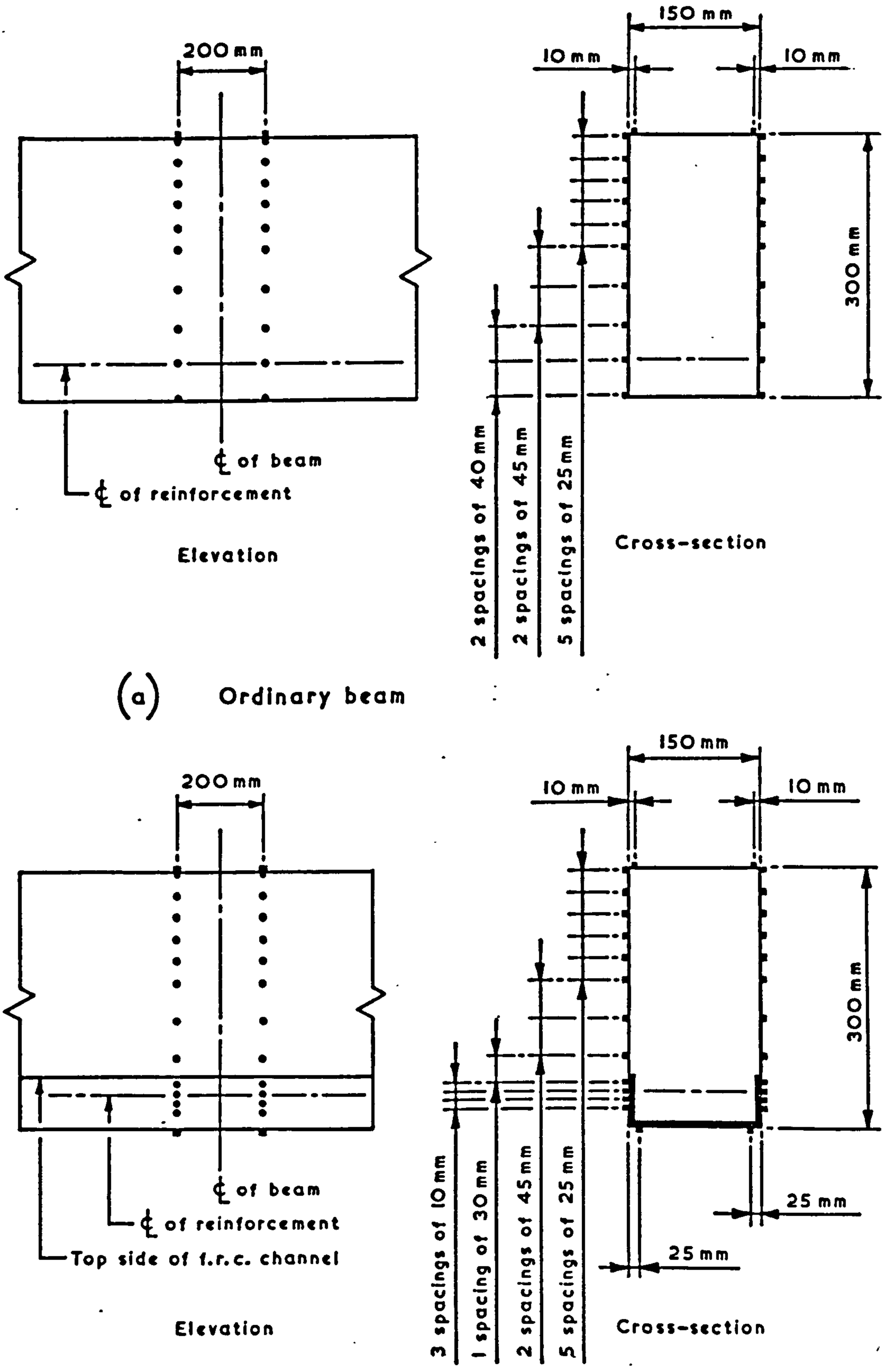

FIG.20 DEMEC LOCATIONS ON ORDINARY AND COMPOSITE BEAMS

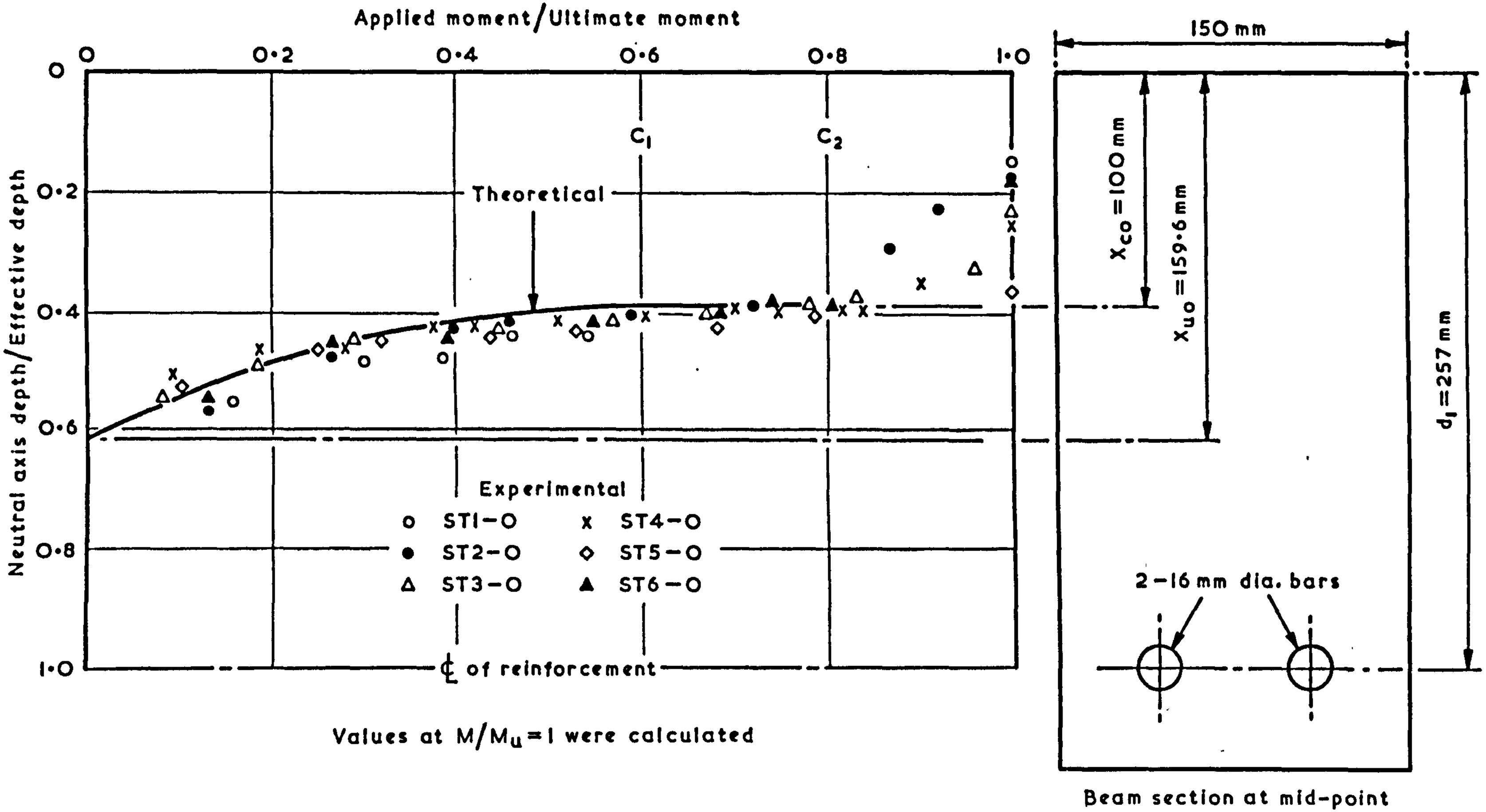

FIG. 21 PROPOSED RELATION OF NEUTRAL AXIS DEPTH WITH APPLIED MOMENT (ORDINARY BEAMS)

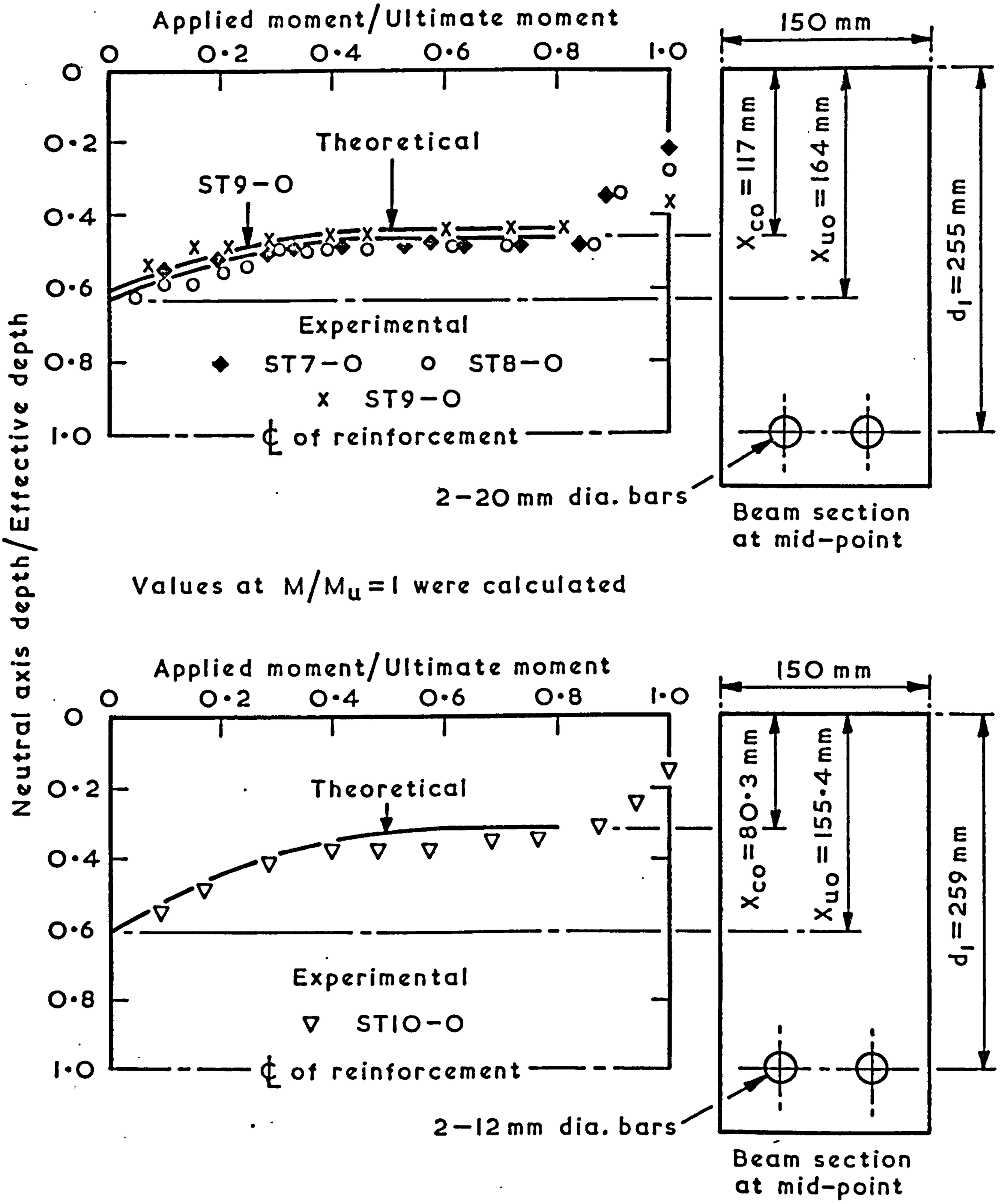

FIG. 22 PROPOSED RELATION OF NEUTRAL AXIS DEPTH WITH APPLIED MOMENT (ORDINARY BEAMS)

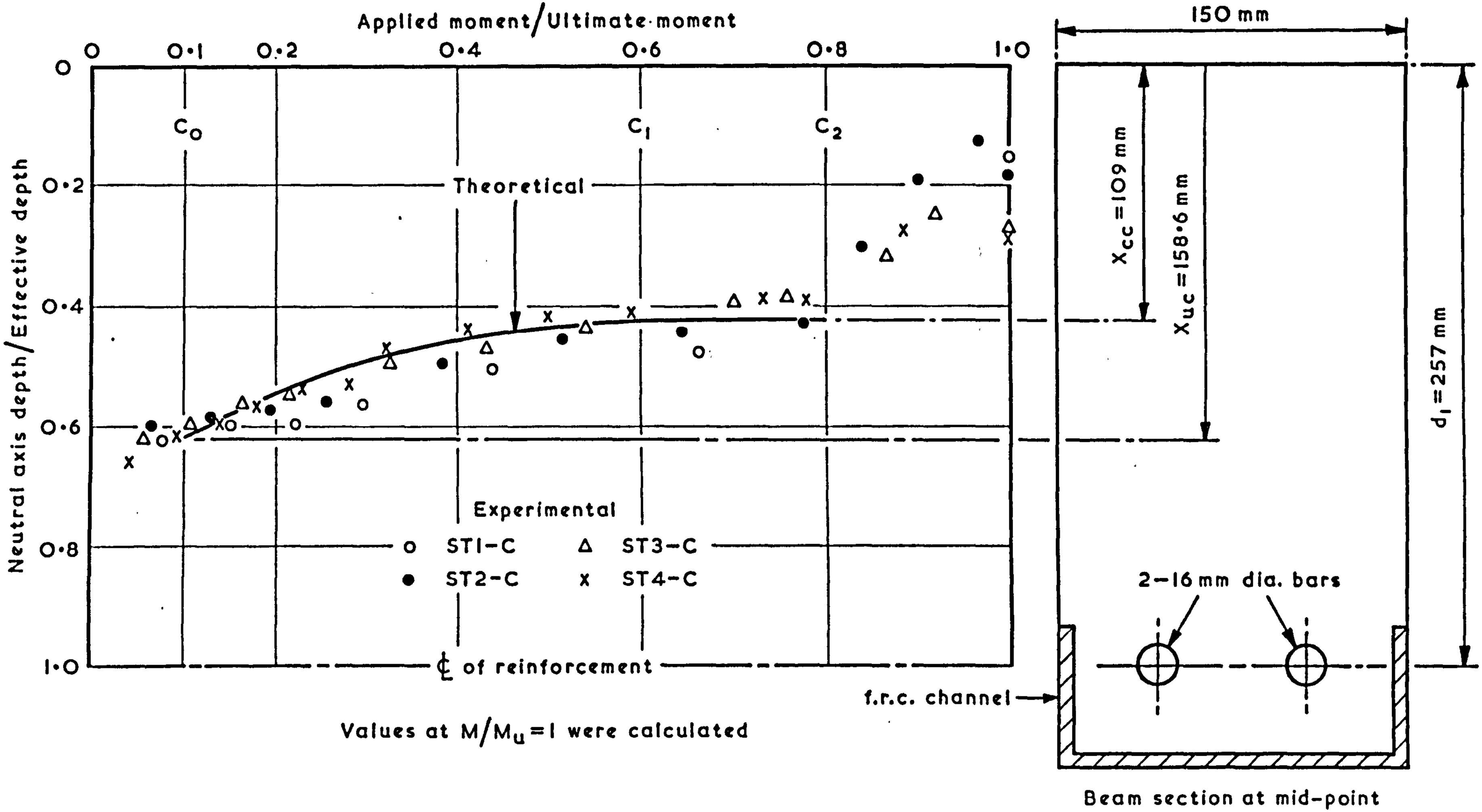

FIG.23 PROPOSED RELATION OF NEUTRAL AXIS DEPTH WITH APPLIED MOMENT (COMPOSITE BEAMS)

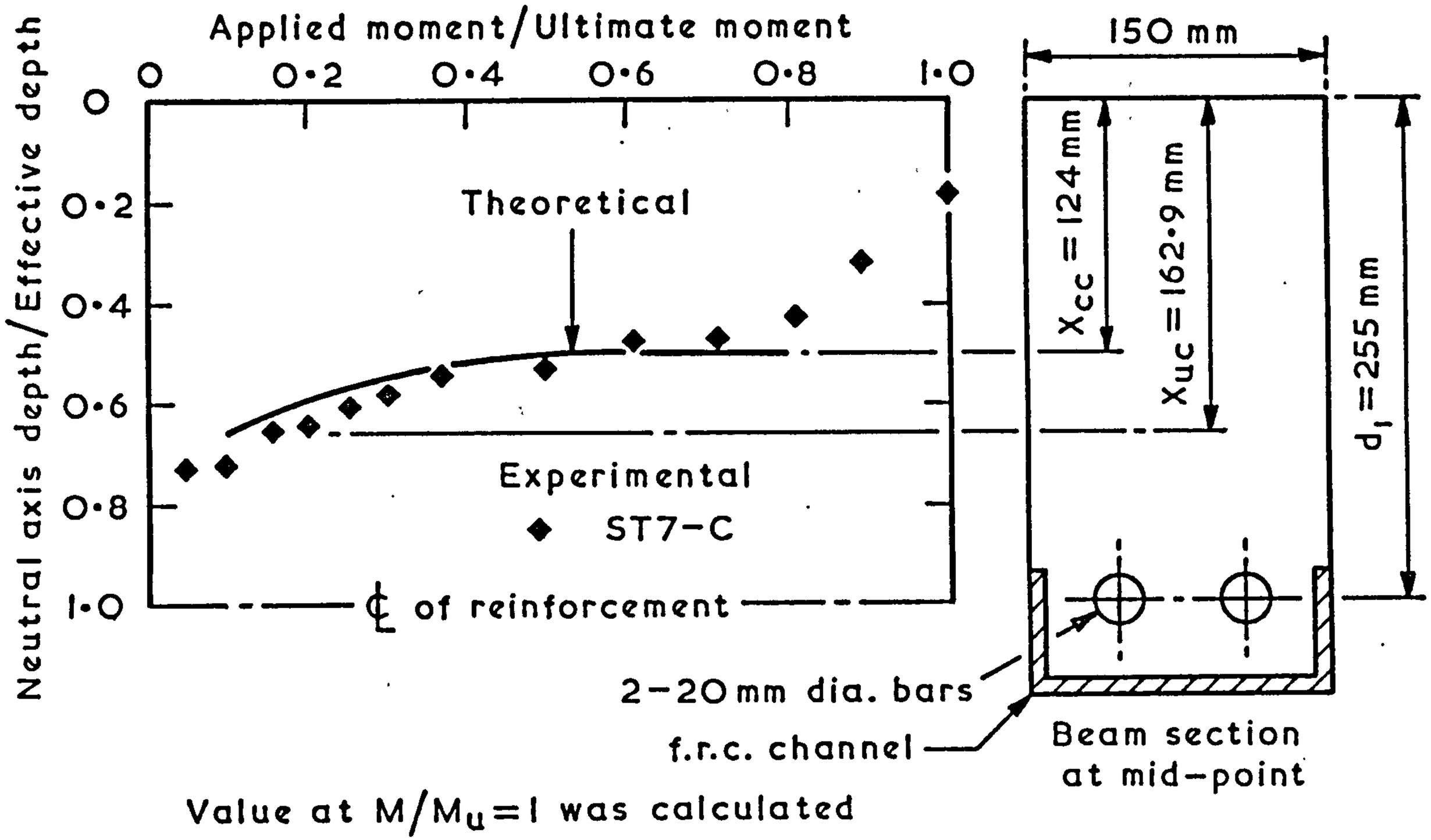

Value at $M/M_u = 1$ was calculated

FIG. 24 PROPOSED RELATION OF NEUTRAL AXIS DEPTH WITH APPLIED MOMENT (COMPOSITE BEAM)

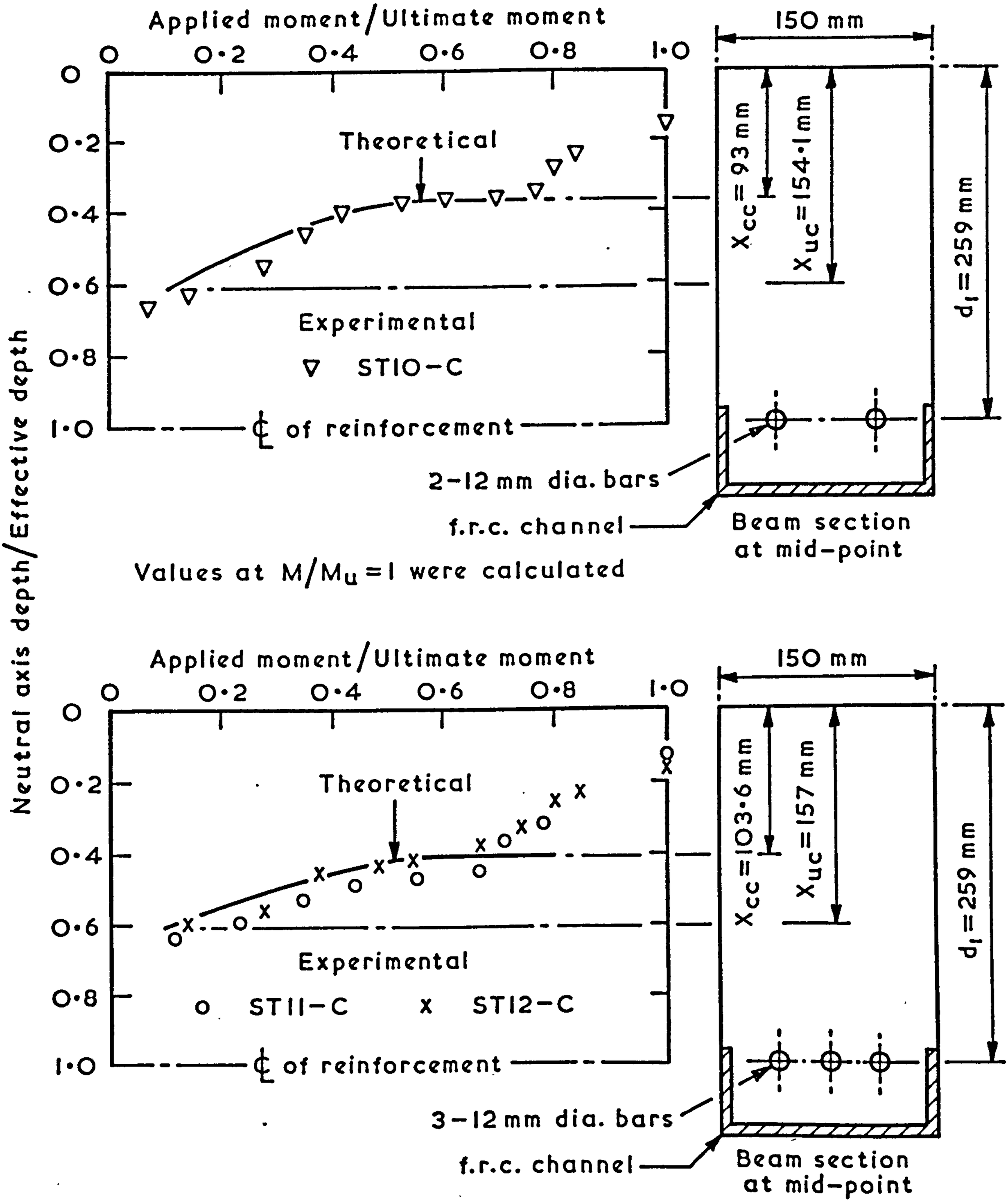

FIG. 25 PROPOSED RELATION OF NEUTRAL AXIS DEPTH WITH APPLIED MOMENT (COMPOSITE BEAMS)

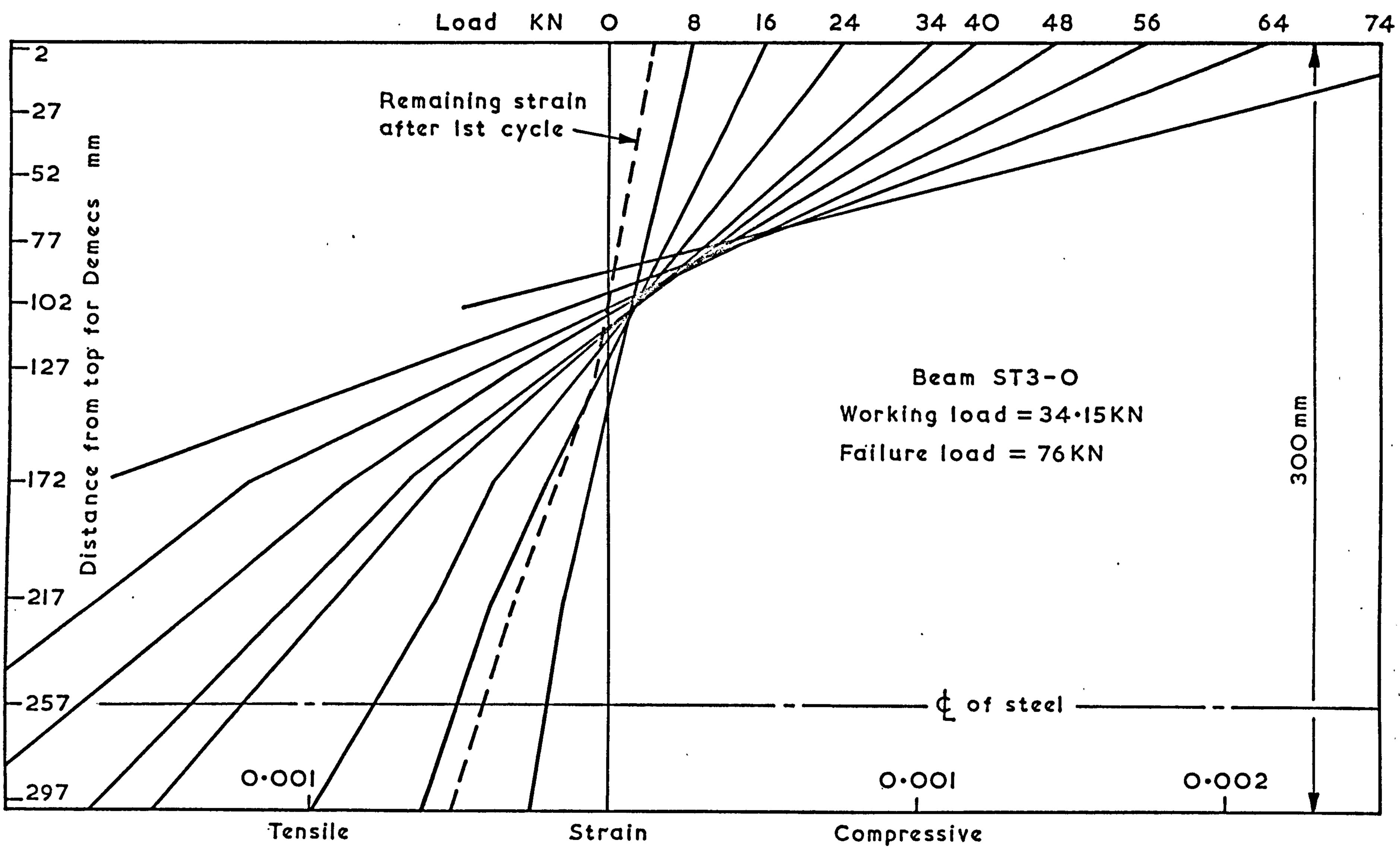

FIG. 26 FLEXURAL STRAIN DISTRIBUTION (ORDINARY BEAM)

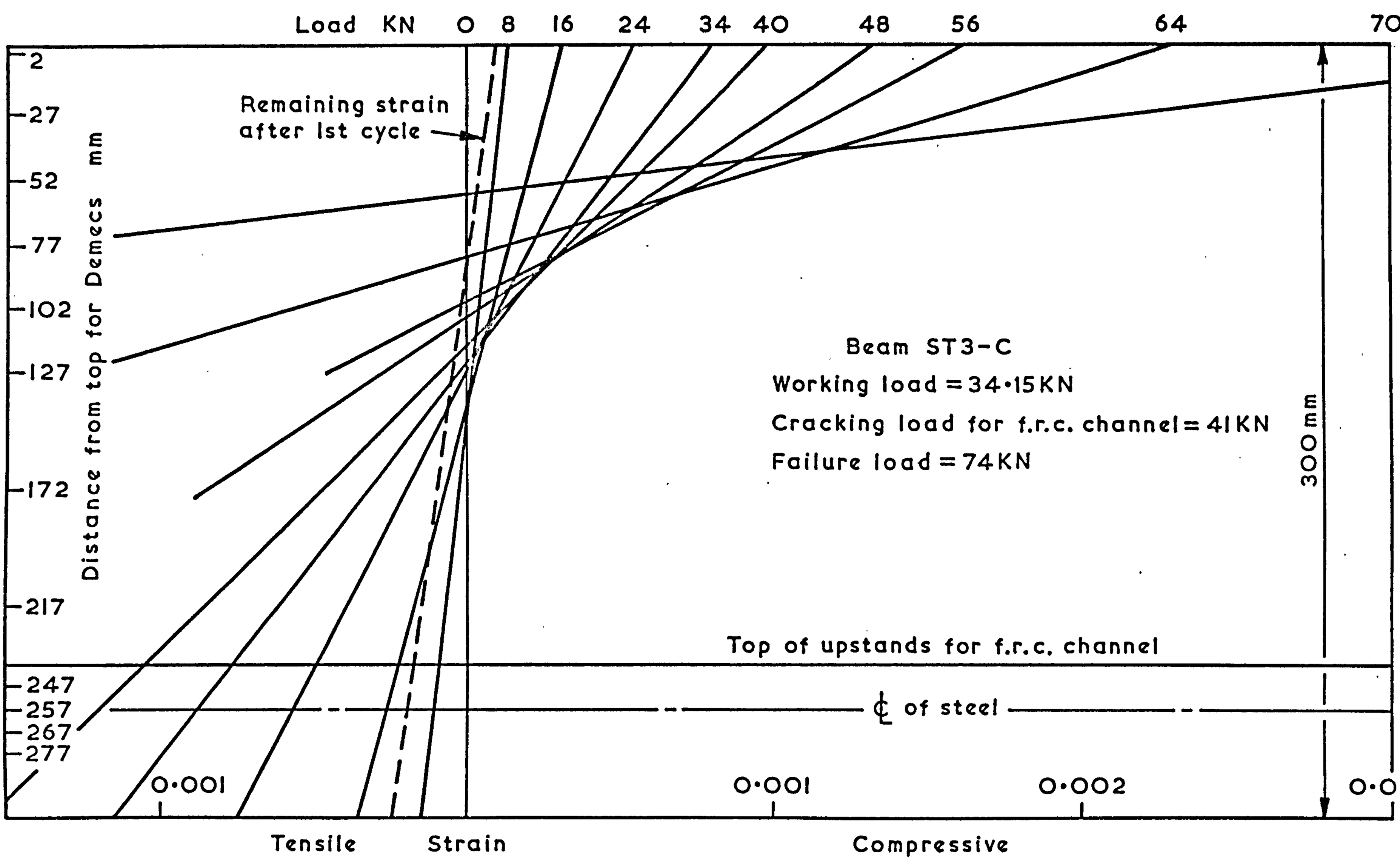

FIG. 27 FLEXURAL STRAIN DISTRIBUTION (COMPOSITE BEAM)

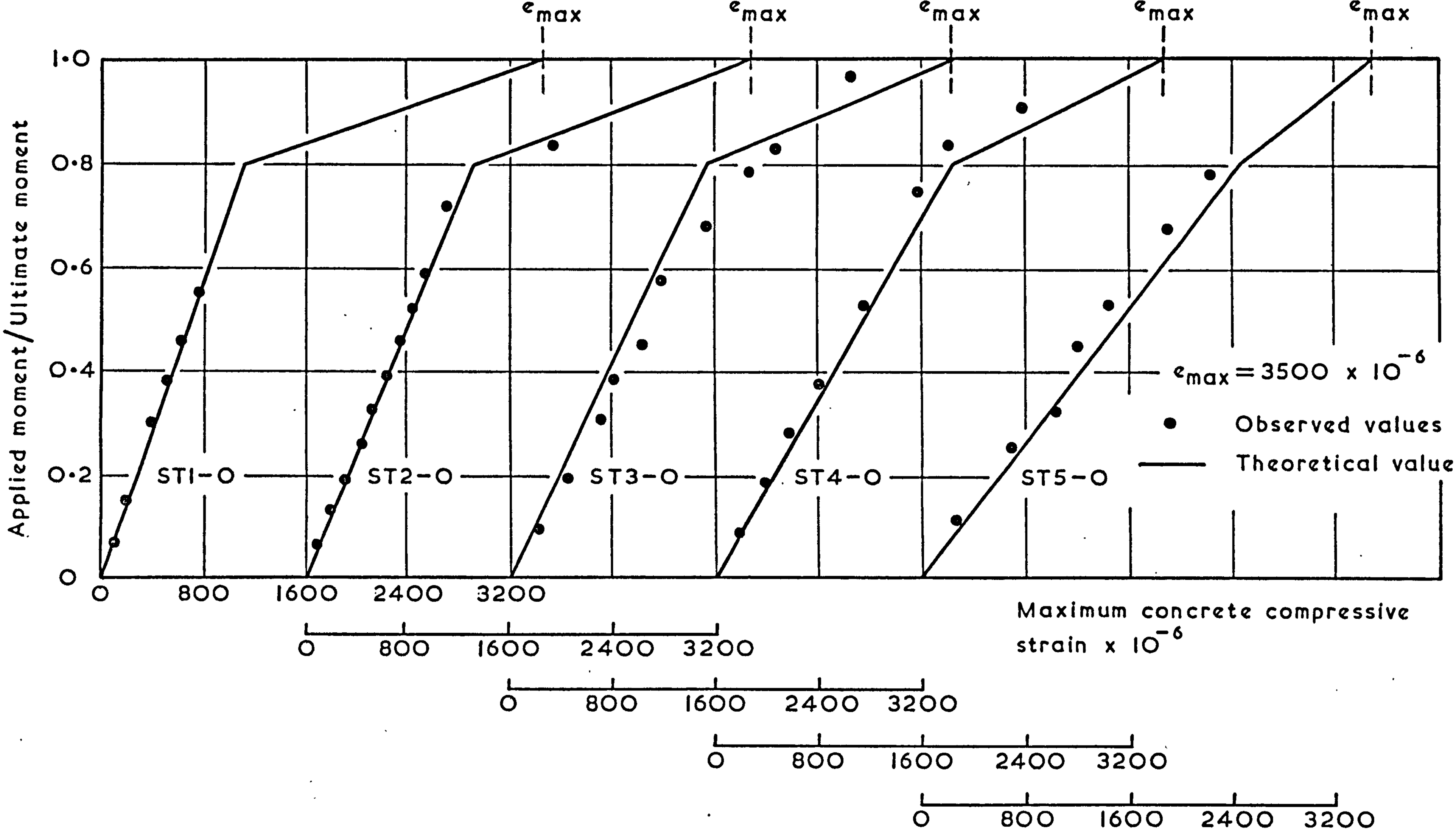

FIG. 28 VARIATION OF CONCRETE COMPRESSIVE STRAIN WITH APPLIED MOMENT (ORDINARY BEAMS)

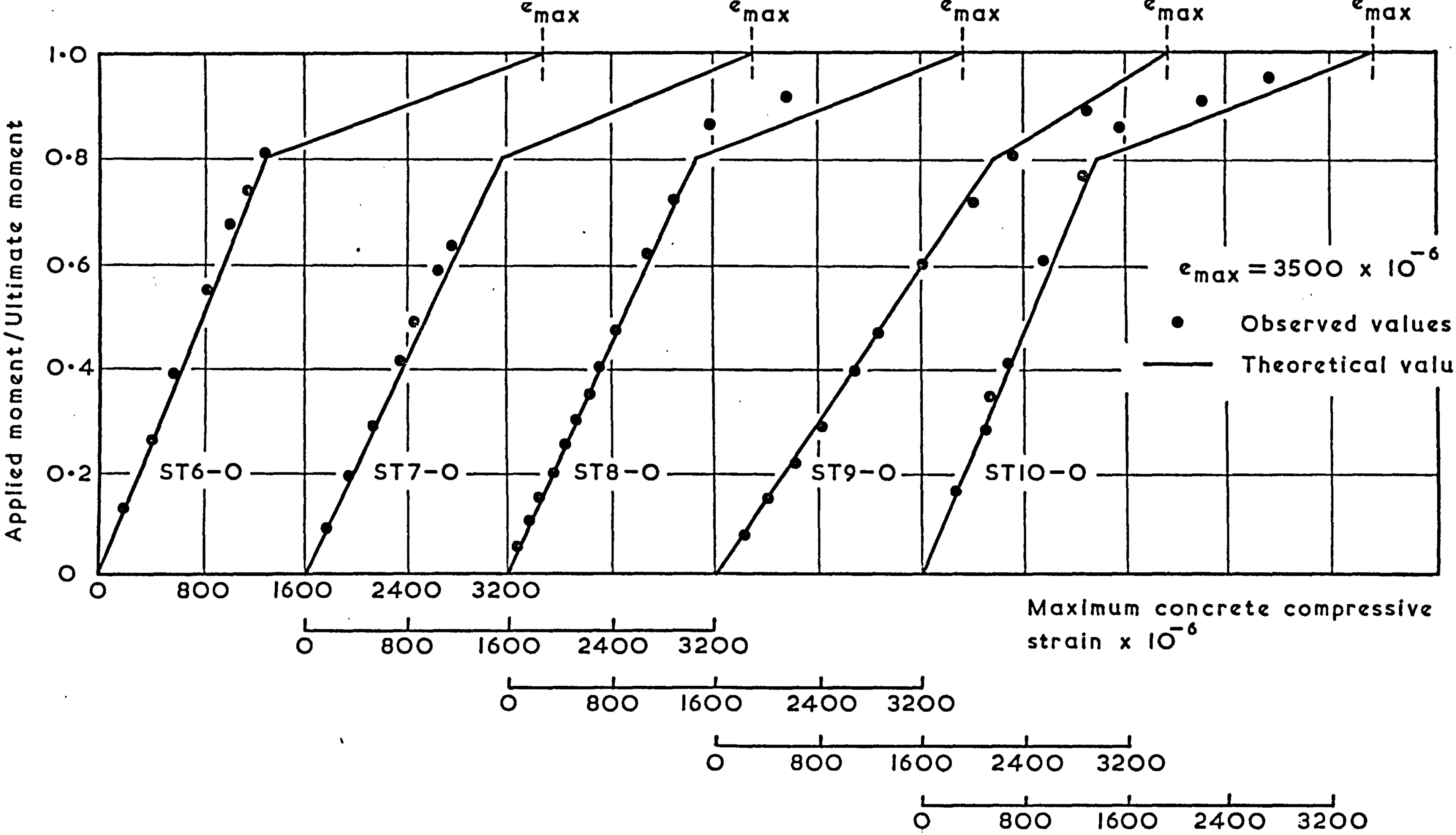

FIG.29 VARIATION OF CONCRETE COMPRESSIVE STRAIN WITH APPLIED MOMENT (ORDINARY BEAMS)

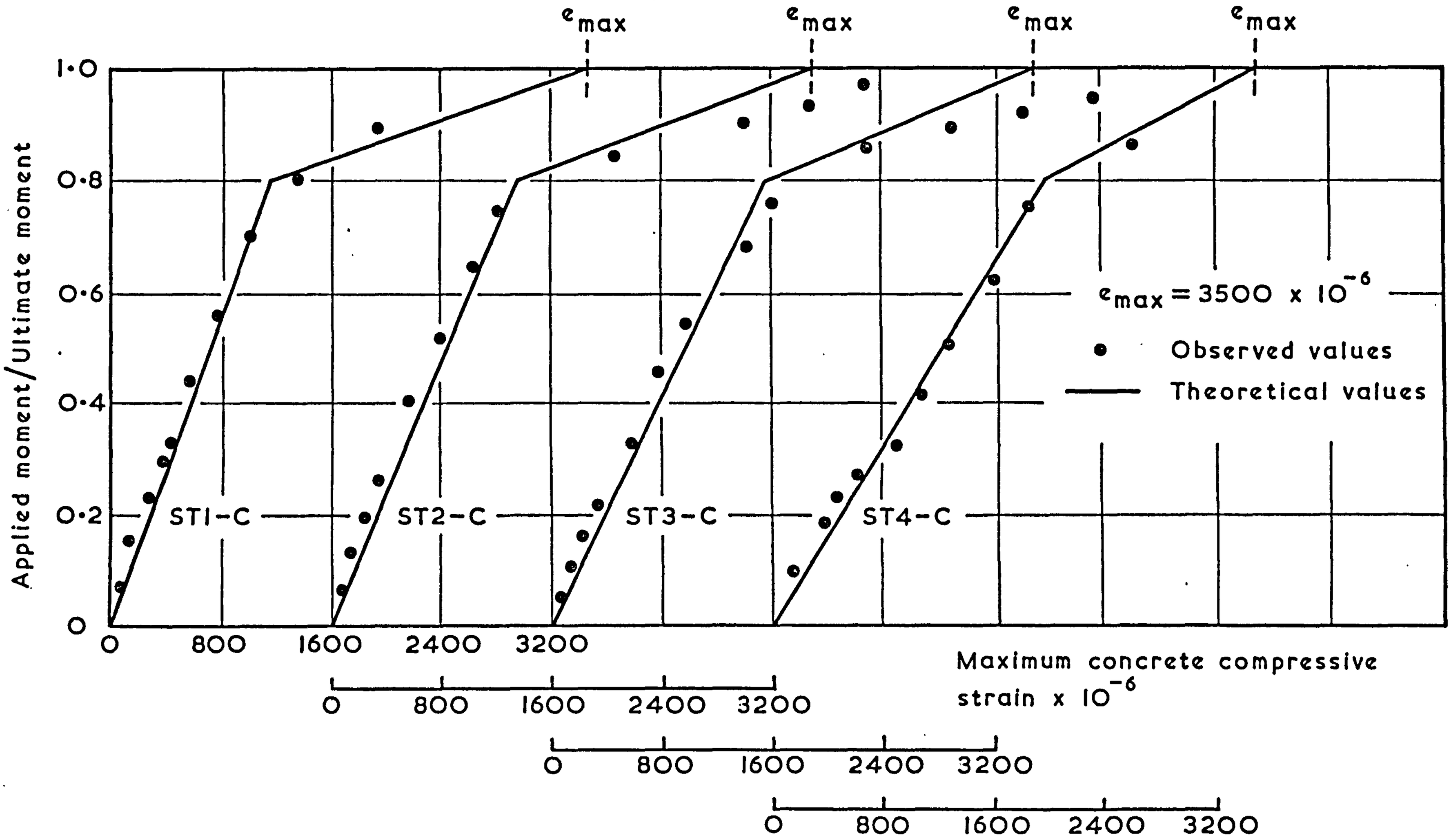

FIG.30 VARIATION OF CONCRETE COMPRESSIVE STRAIN WITH APPLIED MOMENT (COMPOSITE BEAMS)

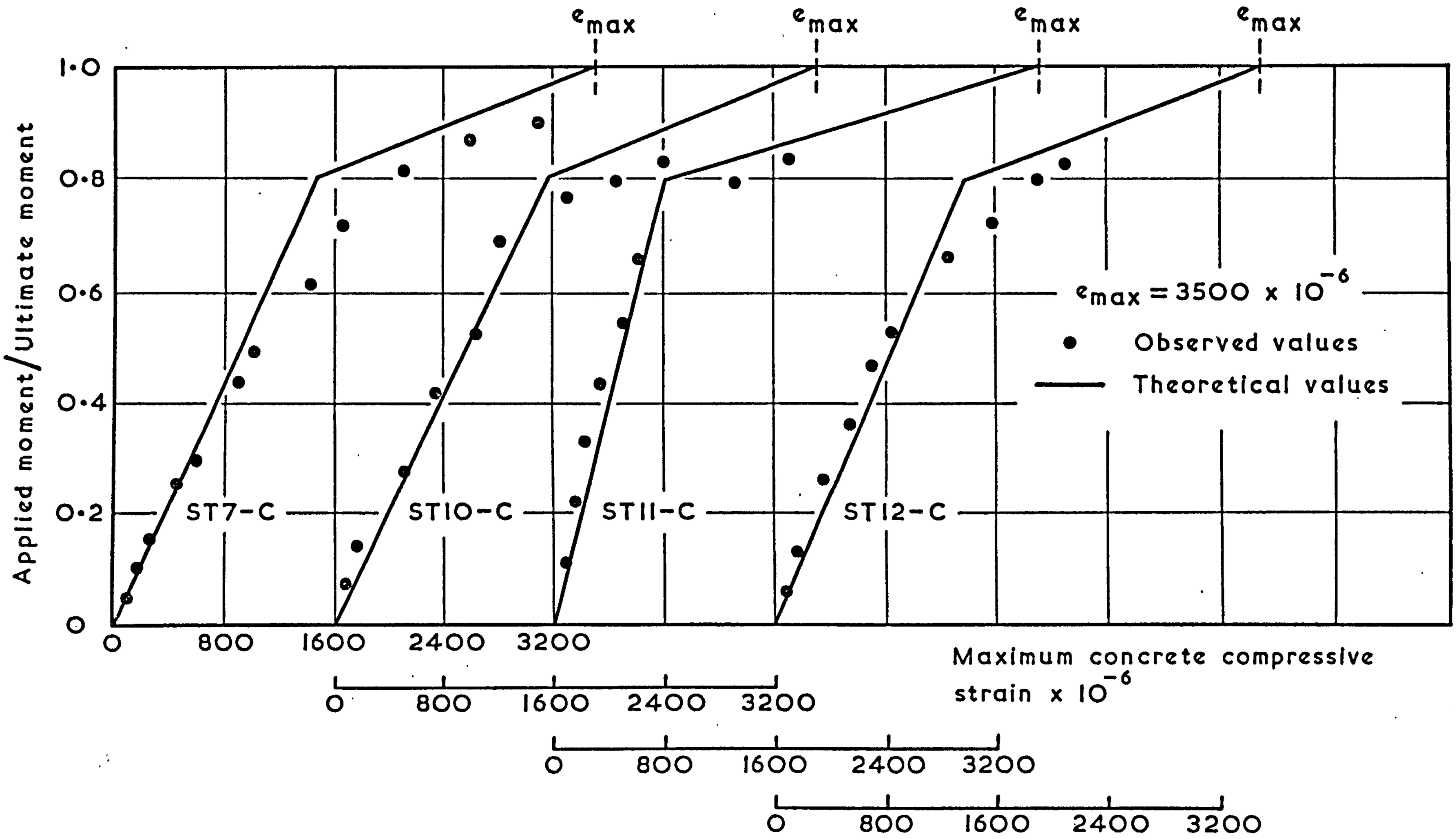

FIG.31 VARIATION OF CONCRETE COMPRESSIVE STRAIN WITH APPLIED MOMENT (COMPOSITE BEAMS)

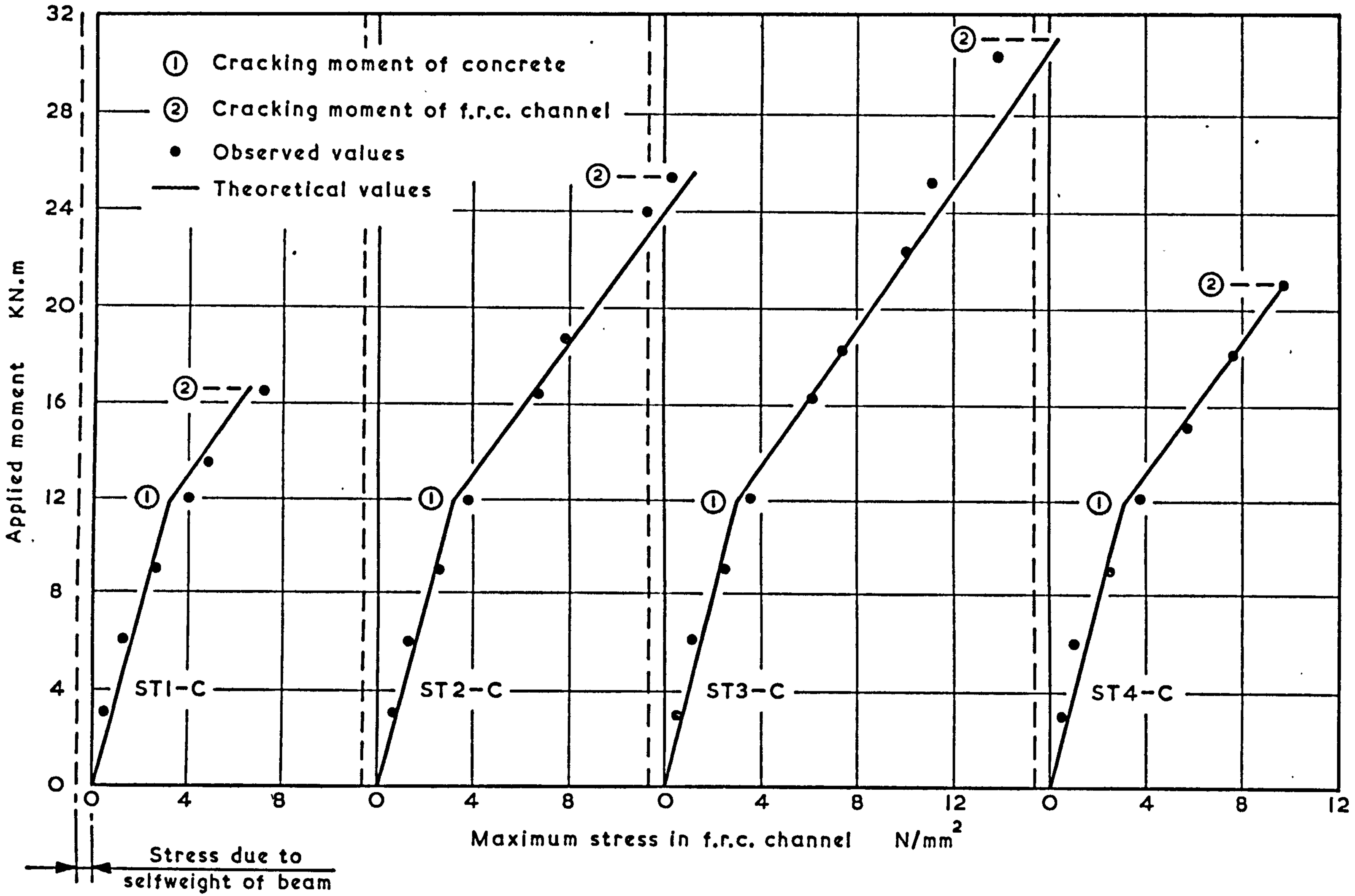

FIG. 32 VARIATION OF STRESSES IN f.r.c. CHANNELS WITH APPLIED MOMENT (COMPOSITE BEAMS)

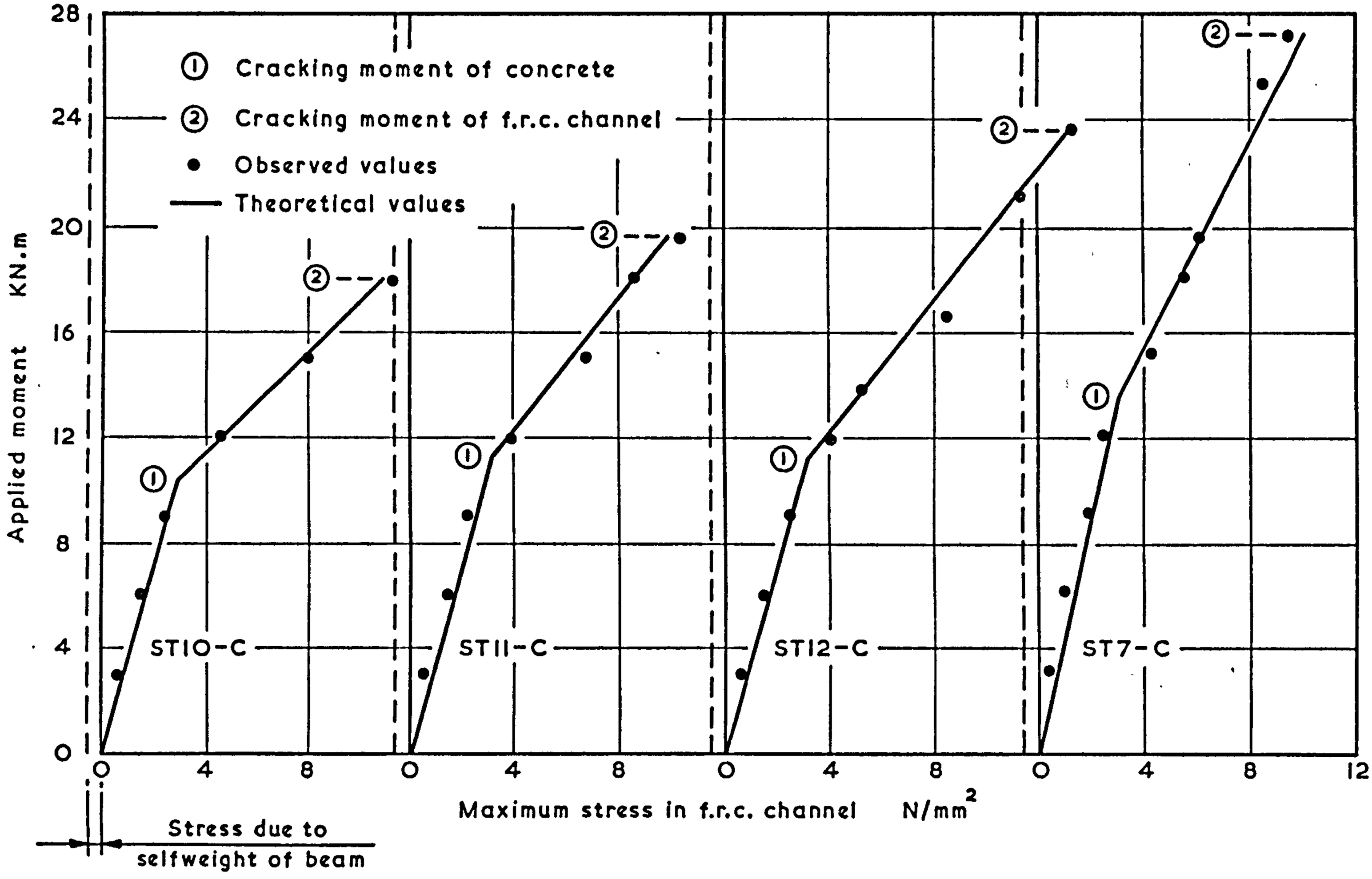

FIG.33 VARIATION OF STRESSES IN f.r.c. CHANNELS WITH APPLIED MOMENT (COMPOSITE BEAMS)

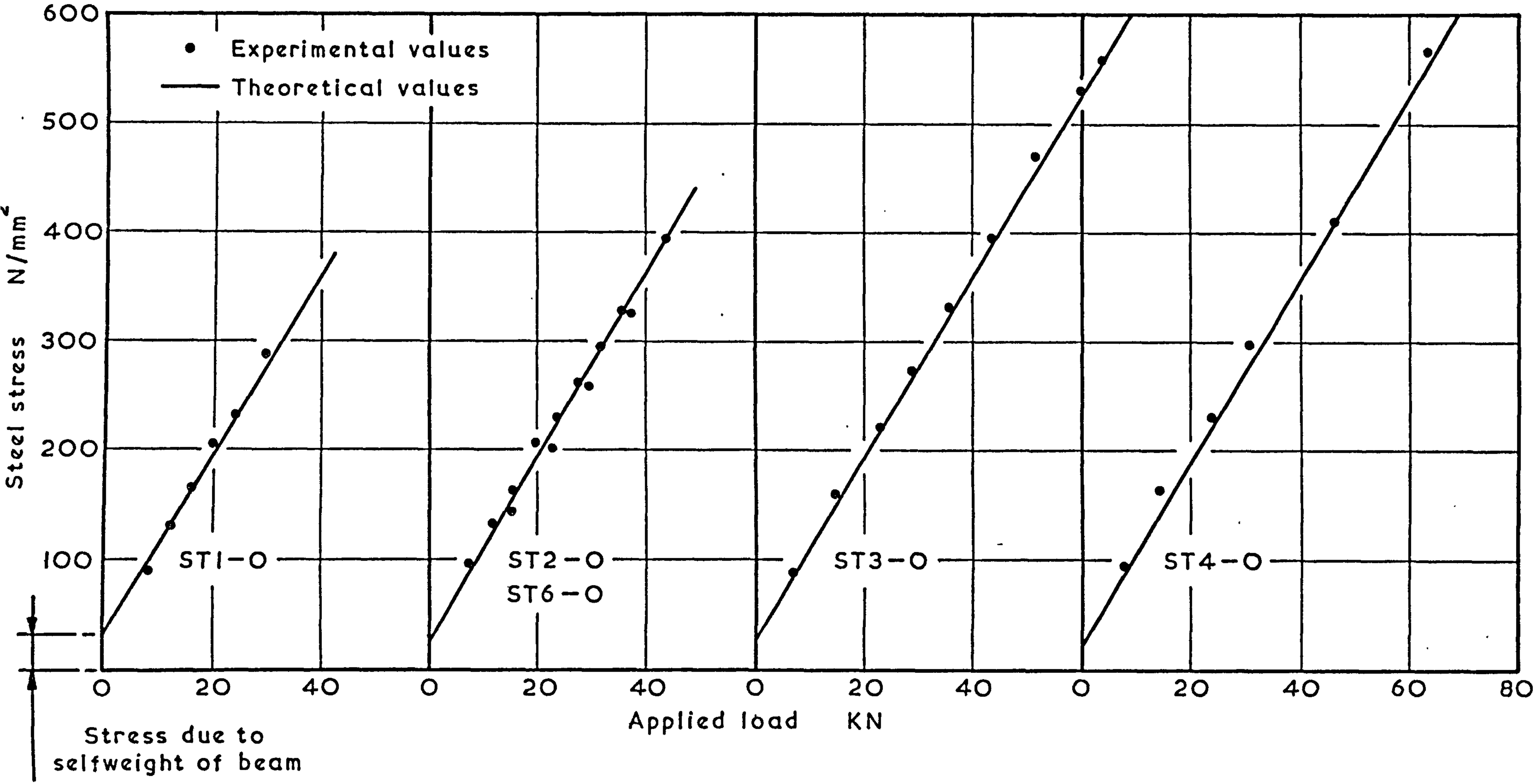

FIG. 34 VARIATION OF STEEL STRESS WITH APPLIED LOAD (ORDINARY BEAMS)

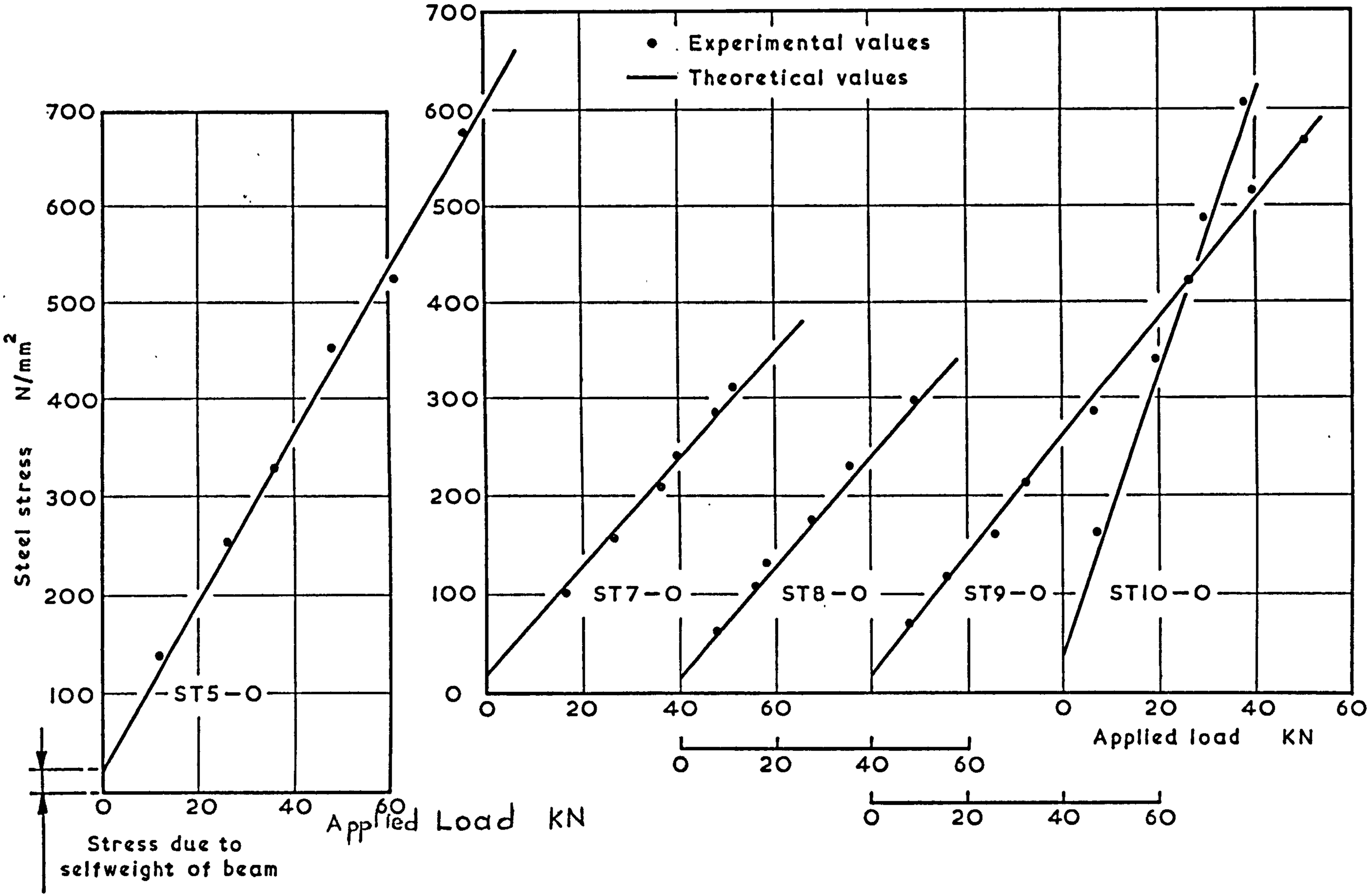

FIG. 35 VARIATION OF STEEL STRESS WITH APPLIED LOAD (ORDINARY BEAMS)

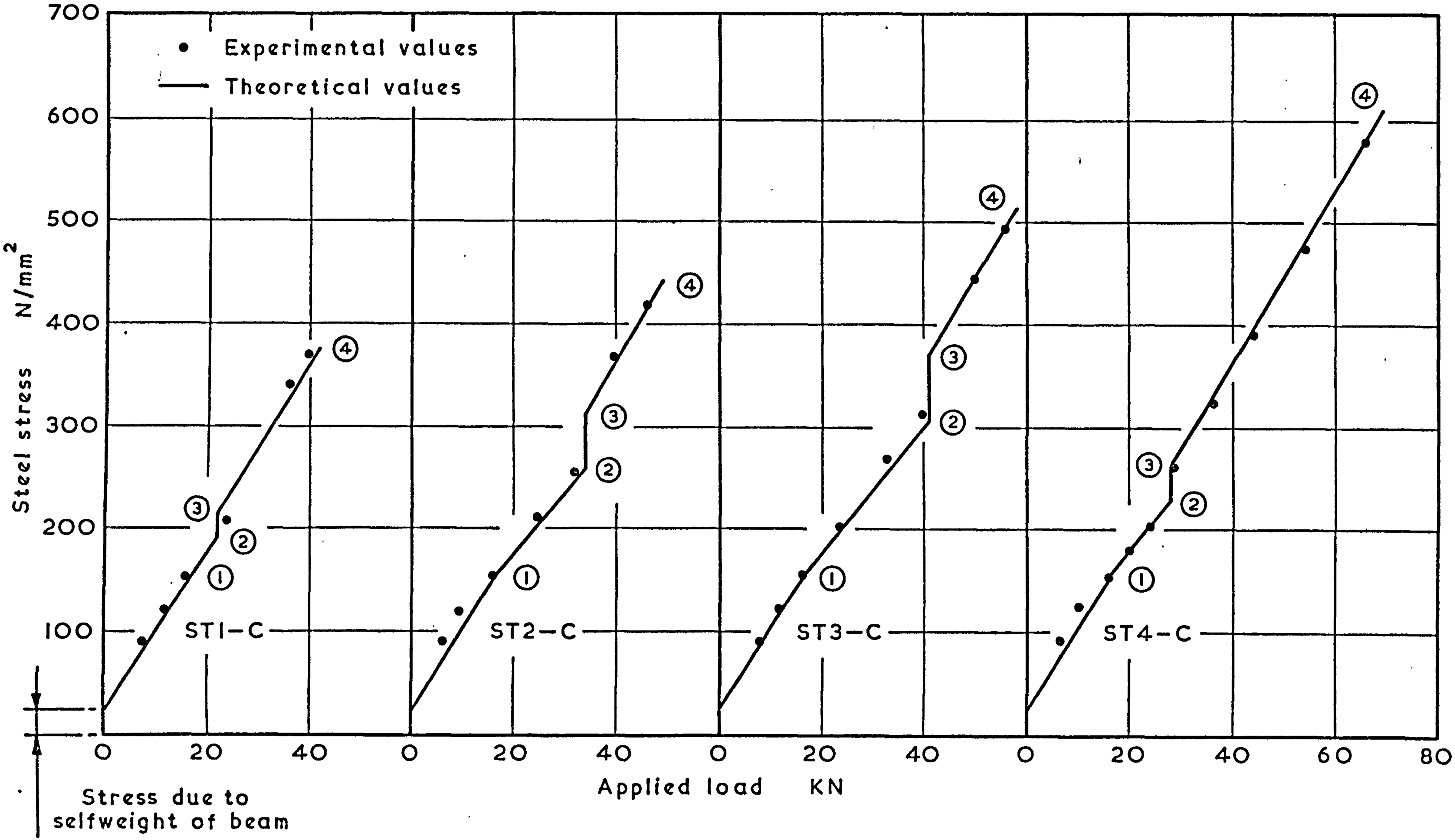

FIG.36 VARIATION OF STEEL STRESS WITH APPLIED LOAD (COMPOSITE BEAMS)

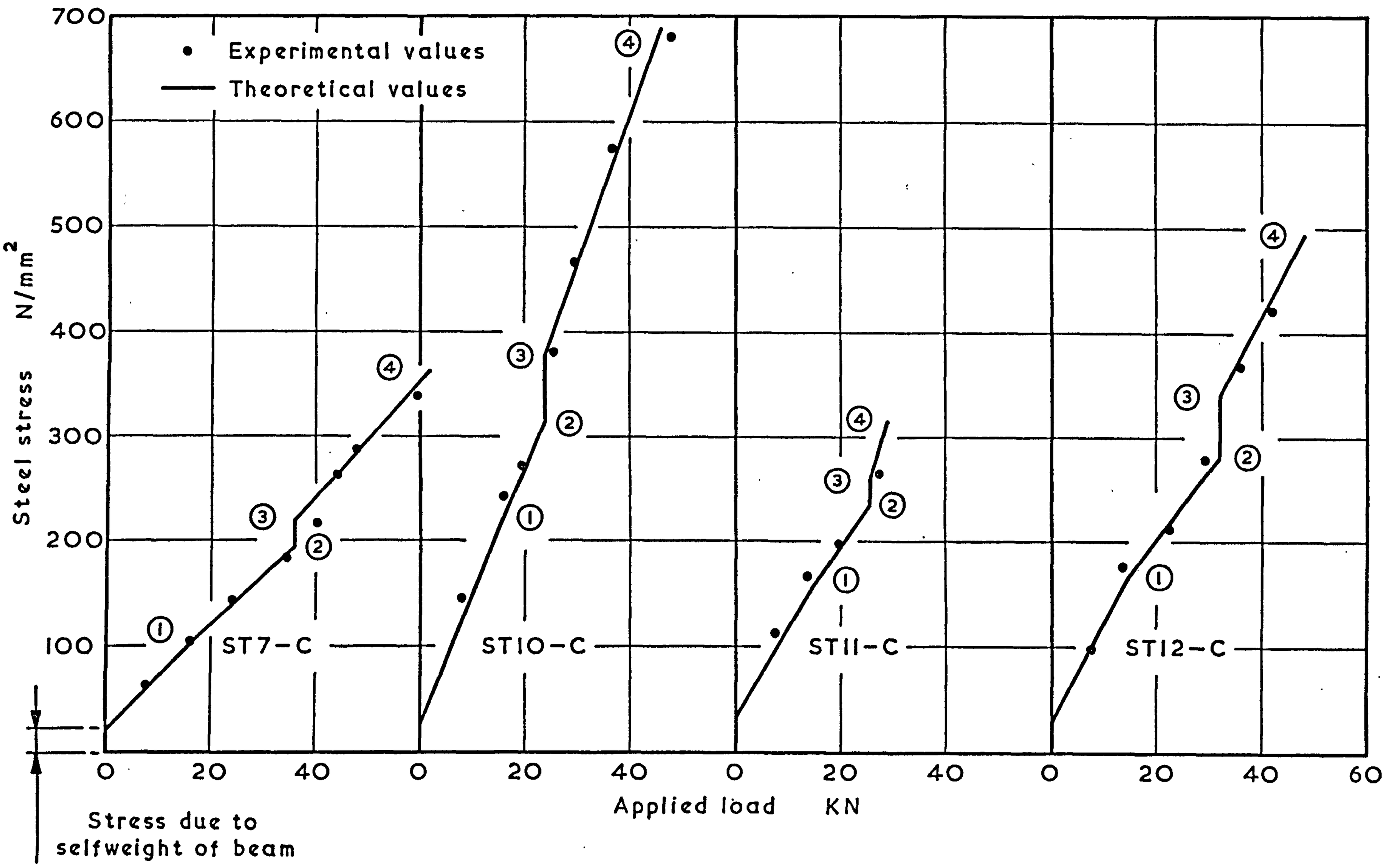

FIG. 37 VARIATION OF STEEL STRESS WITH APPLIED LOAD (COMPOSITE BEAMS)

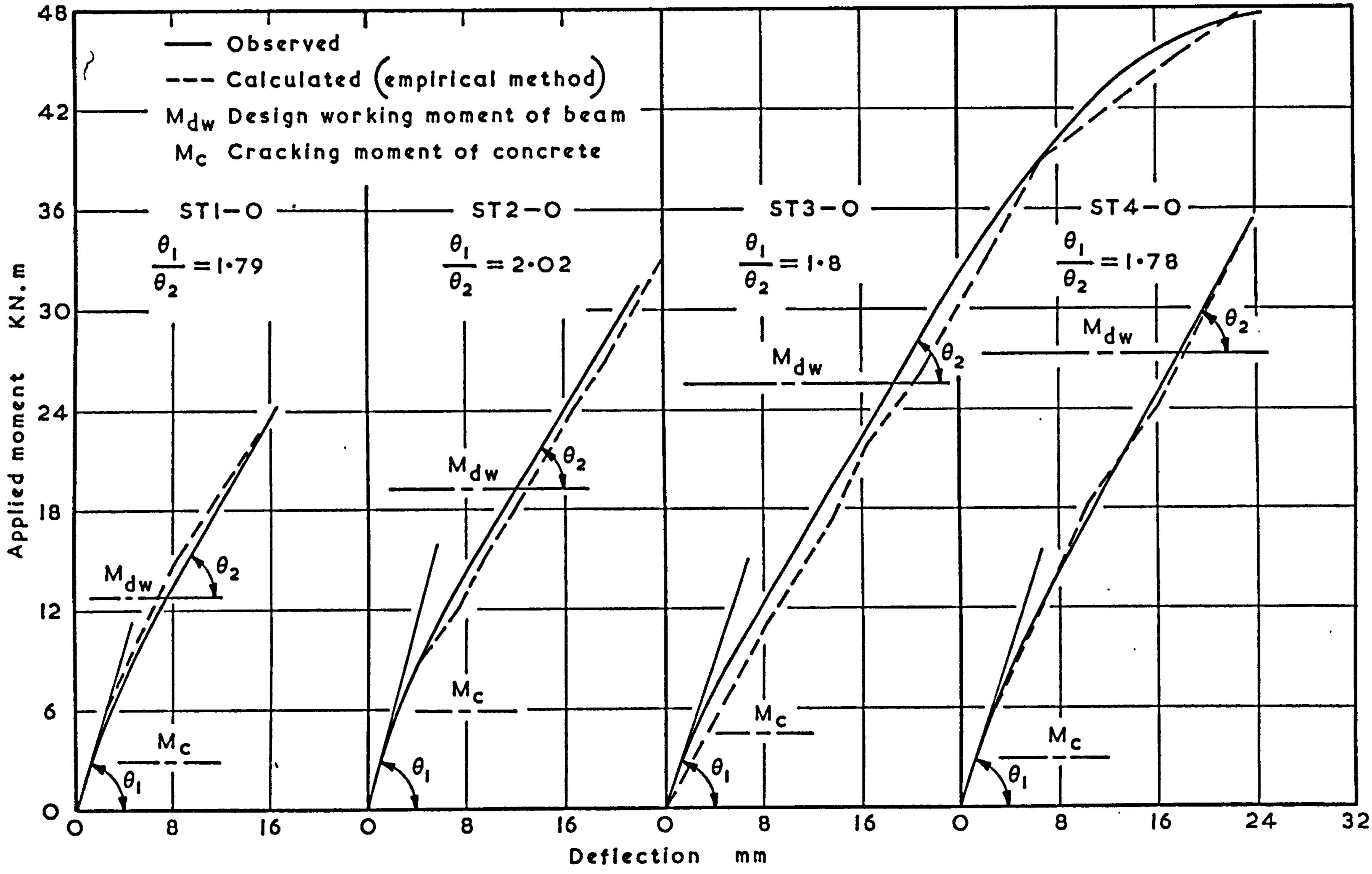

FIG.38 OBSERVED AND CALCULATED DEFLECTION (ORDINARY BEAMS)

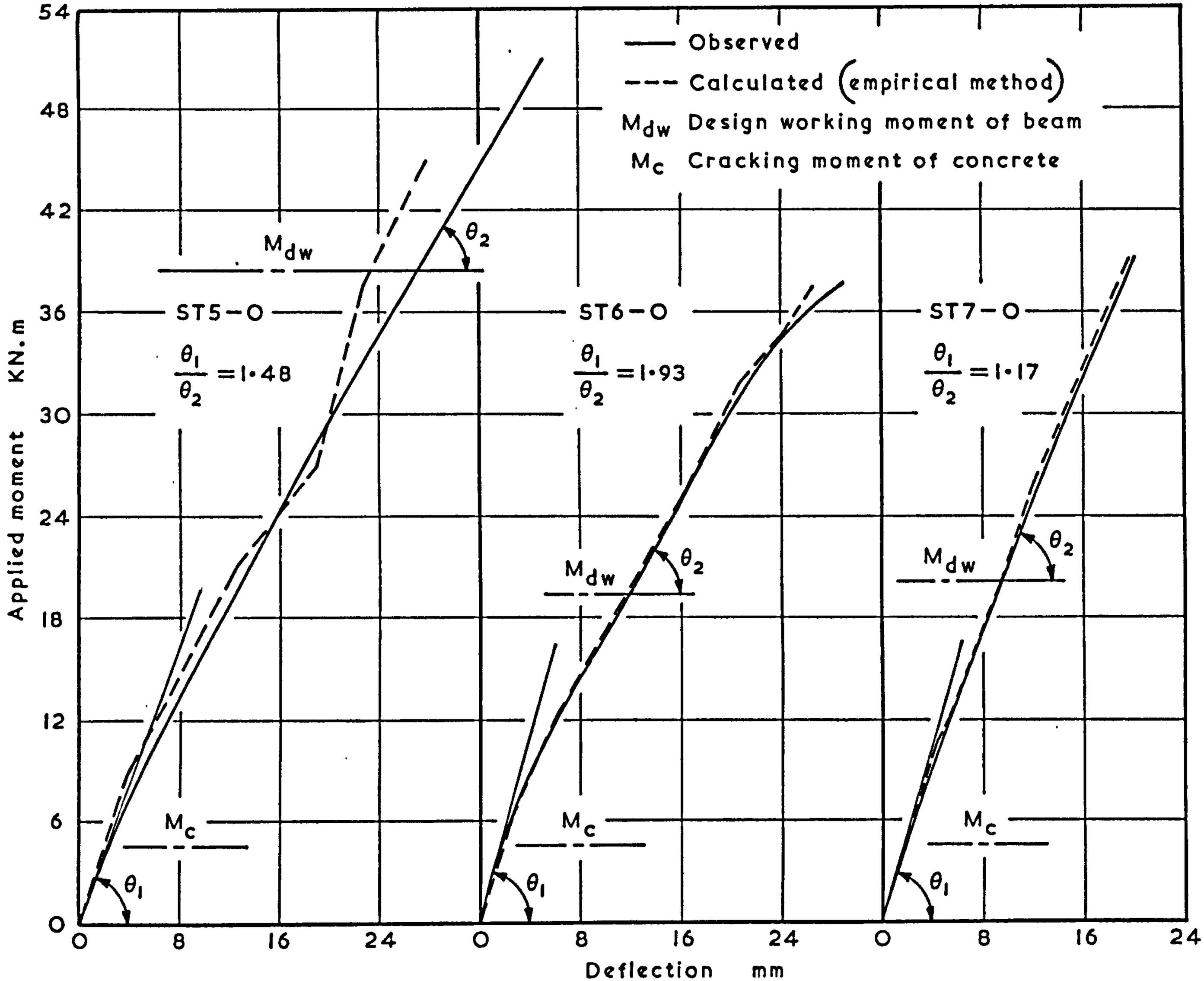

FIG.39 OBSERVED AND CALCULATED DEFLECTION (ORDINARY BEAMS)

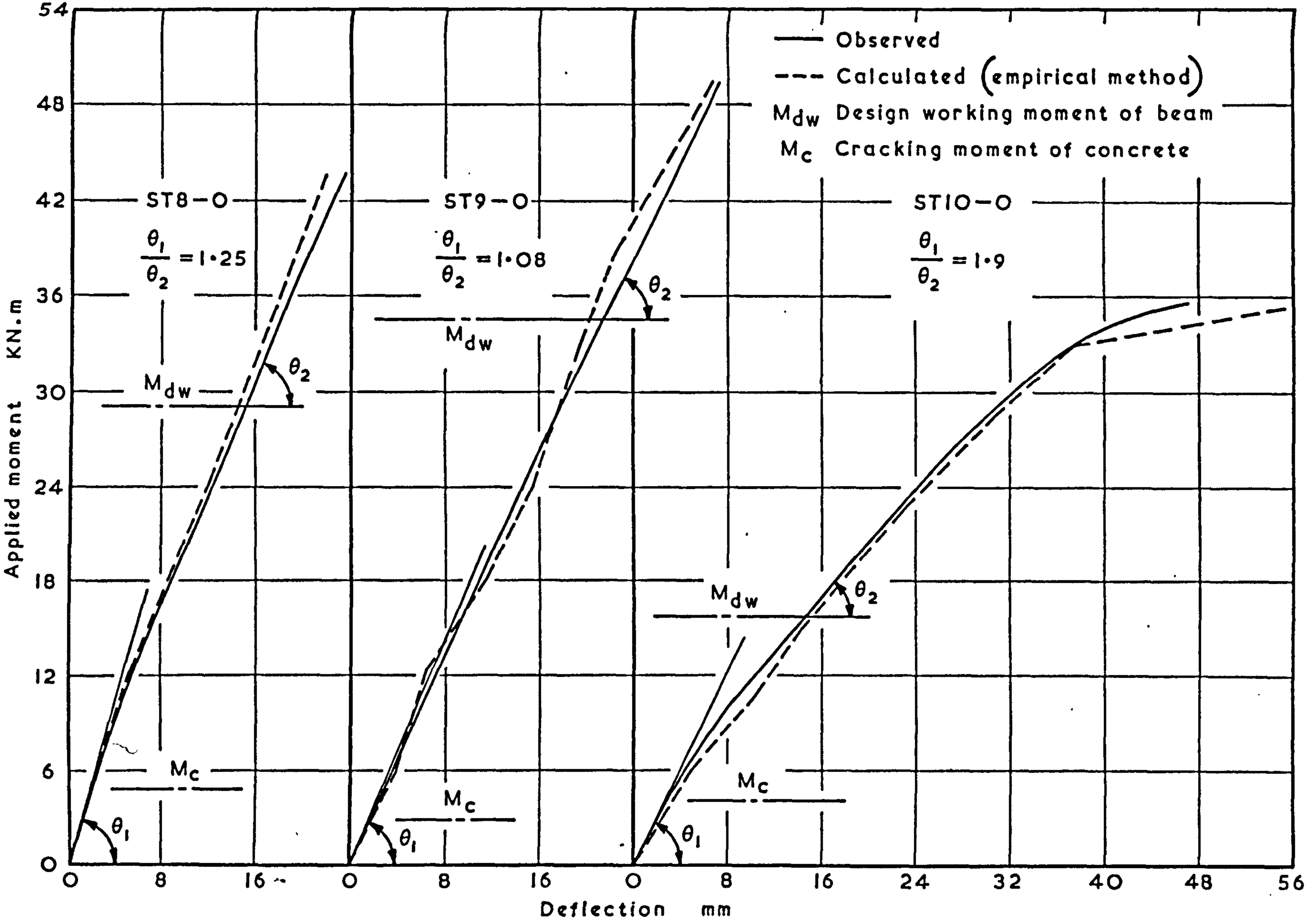

FIG.40 OBSERVED AND CALCULATED DEFLECTION (ORDINARY BEAMS)

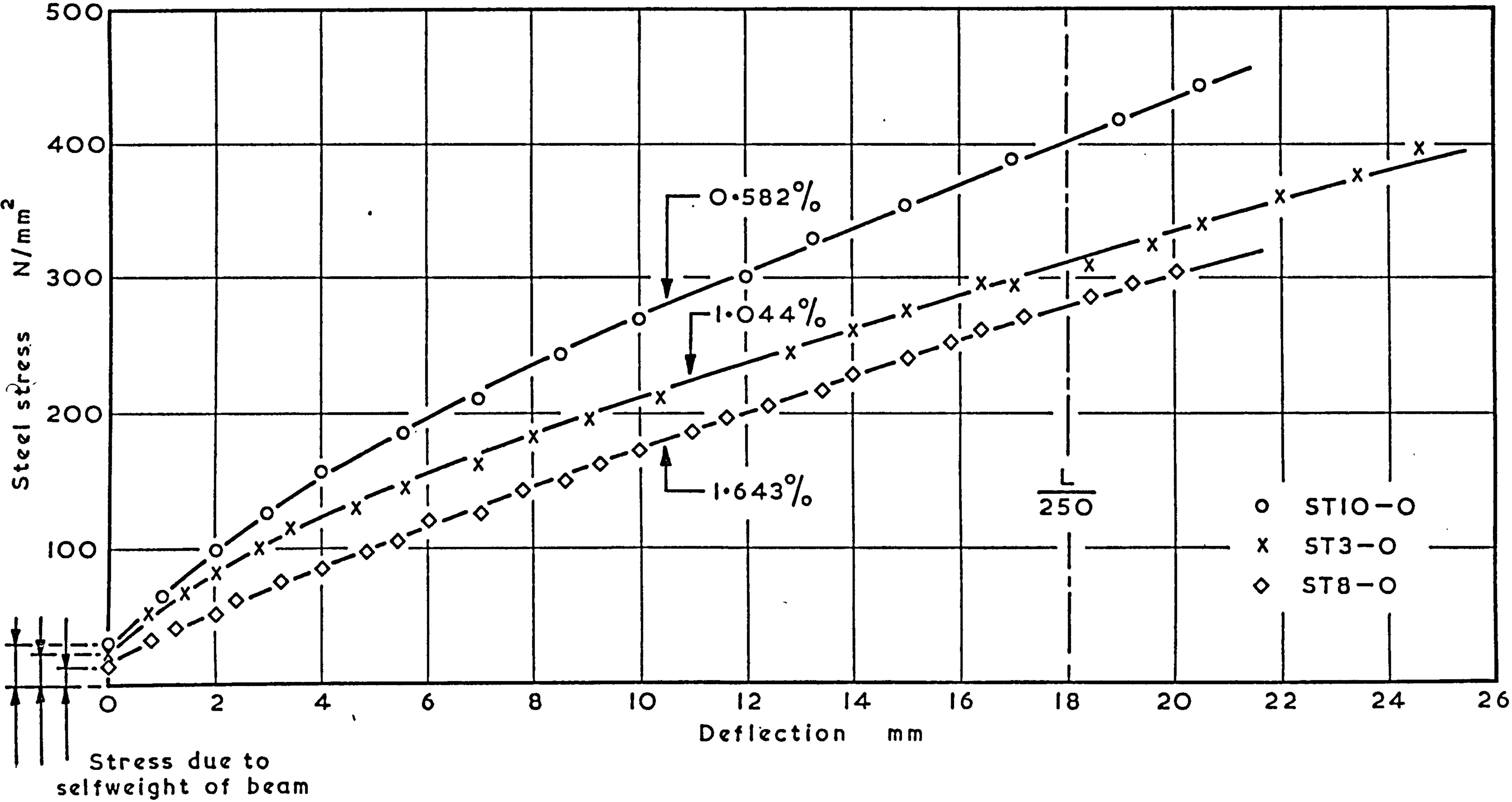

FIG. 41 RELATIONSHIP BETWEEN STEEL STRESS AND DEFLECTION FOR ORDINARY BEAMS (STATIC TEST)

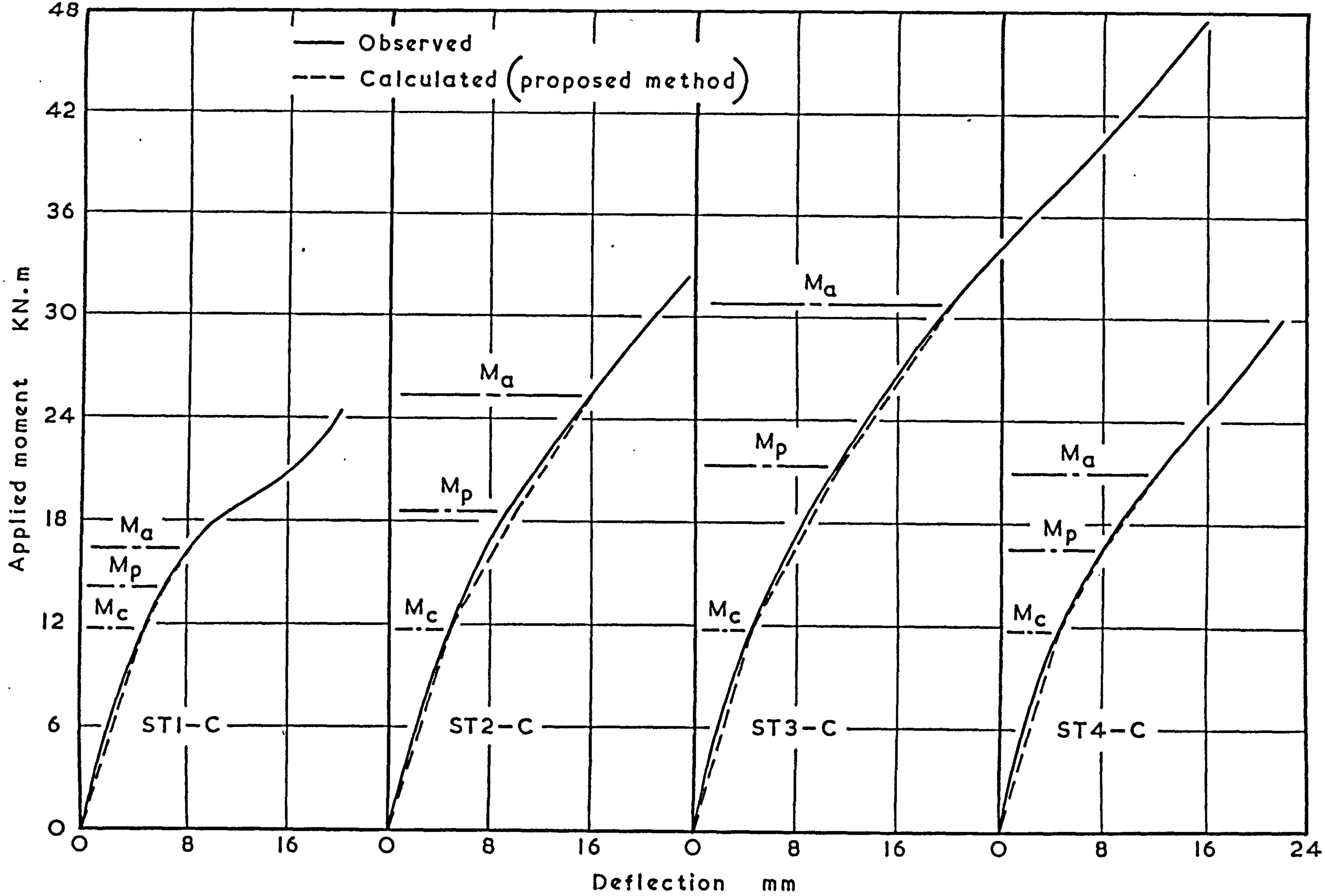

FIG.42 OBSERVED AND CALCULATED DEFLECTION (COMPOSITE BEAMS)

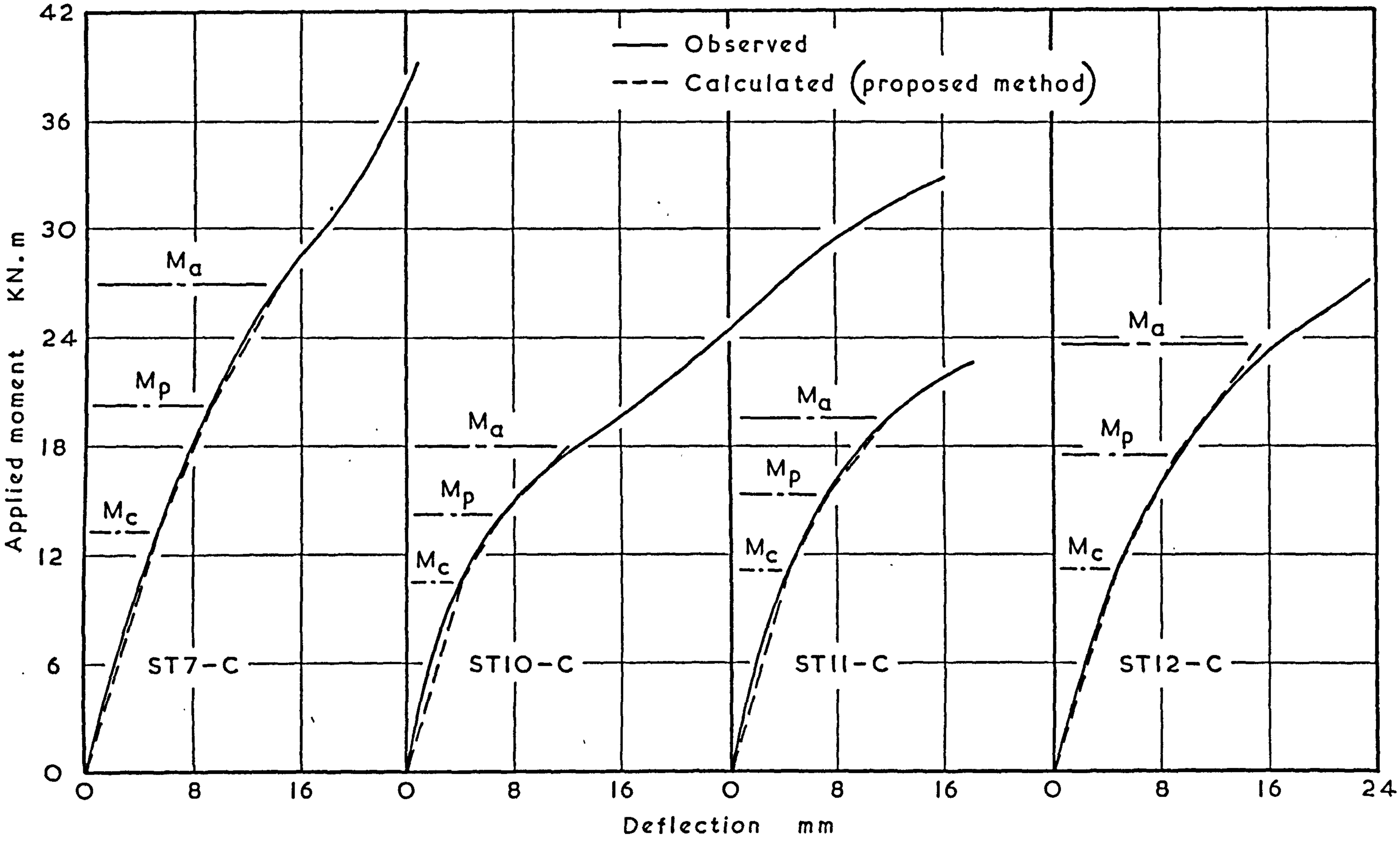

FIG.43 OBSERVED AND CALCULATED DEFLECTION (COMPOSITE BEAMS)

a_o = Deflection of ordinary beam at working moment

a_c = Deflection of composite beam at working moment

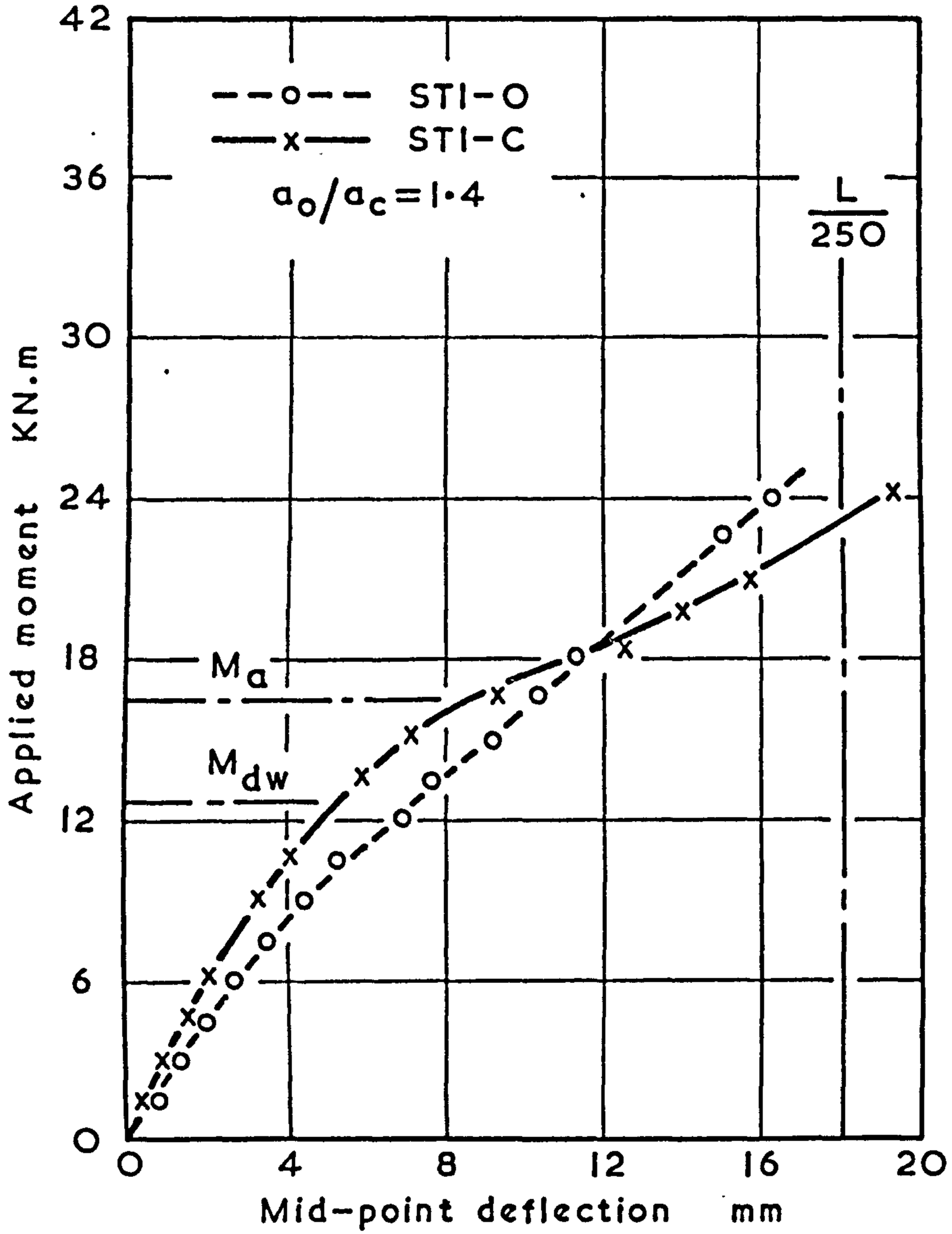

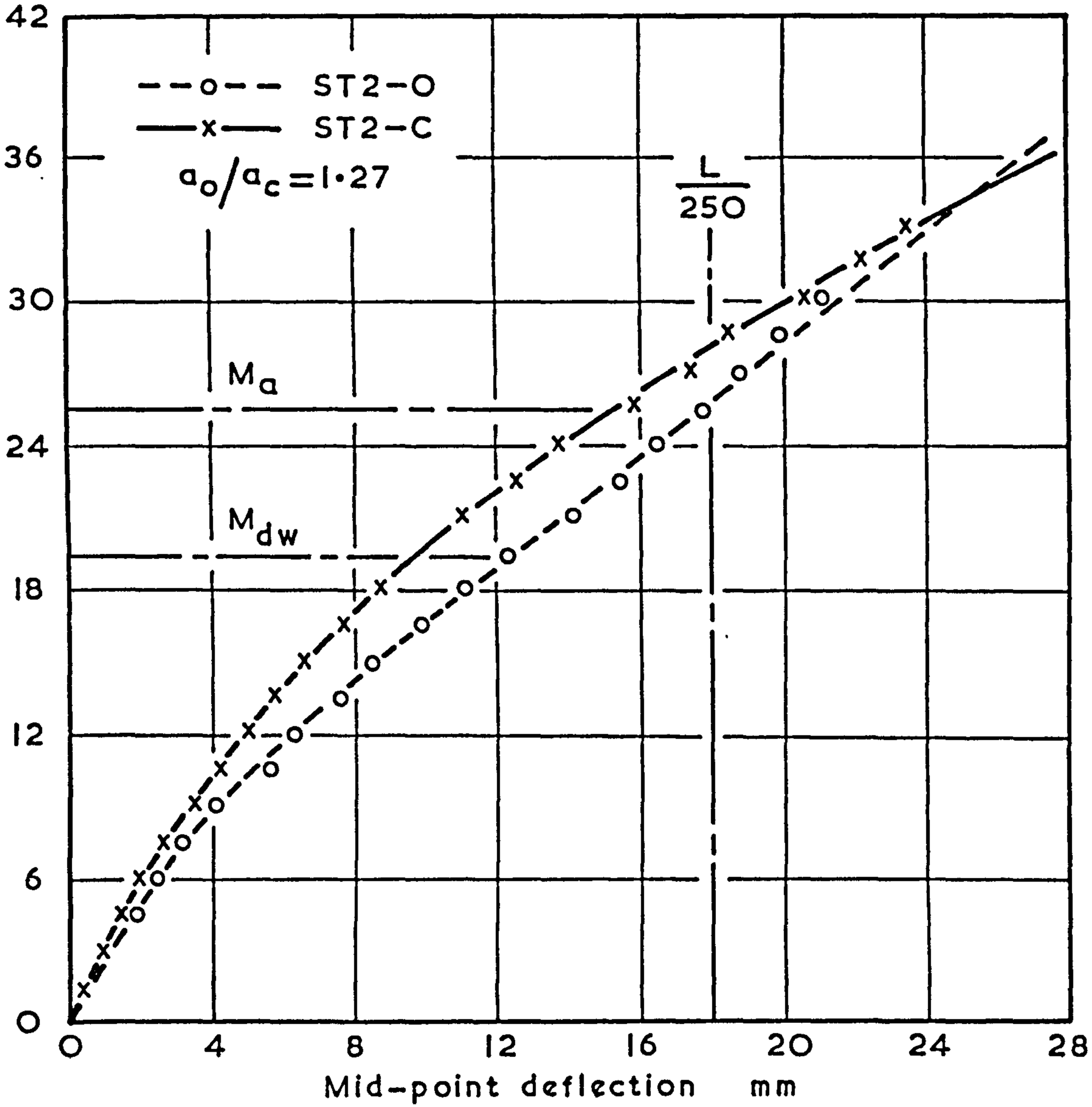

FIG. 44 COMPARISON BETWEEN DEFLECTION FOR ORDINARY AND COMPOSITE BEAMS

a_o = Deflection of ordinary beam at working moment

a_c = Deflection of composite beam at working moment

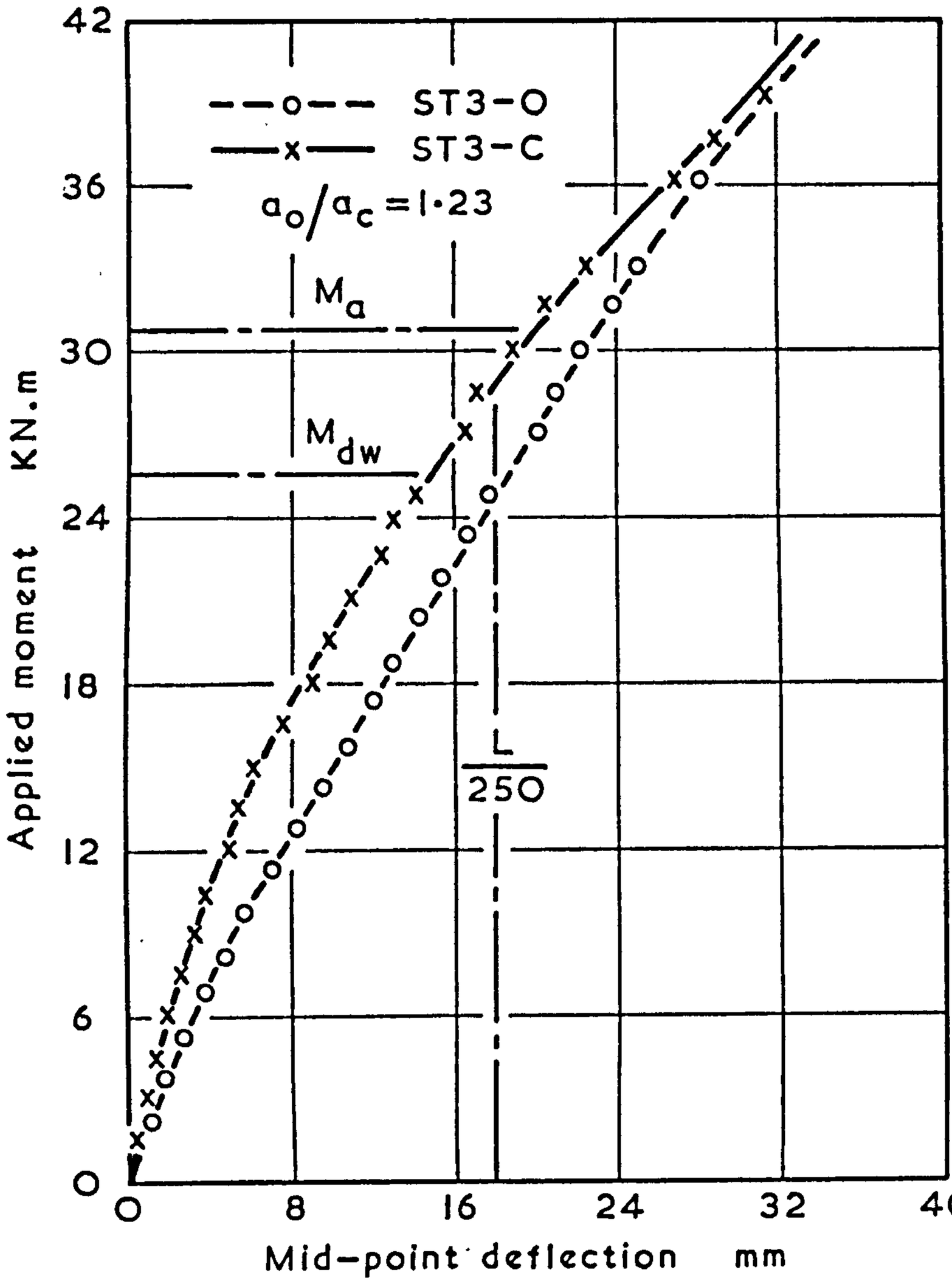

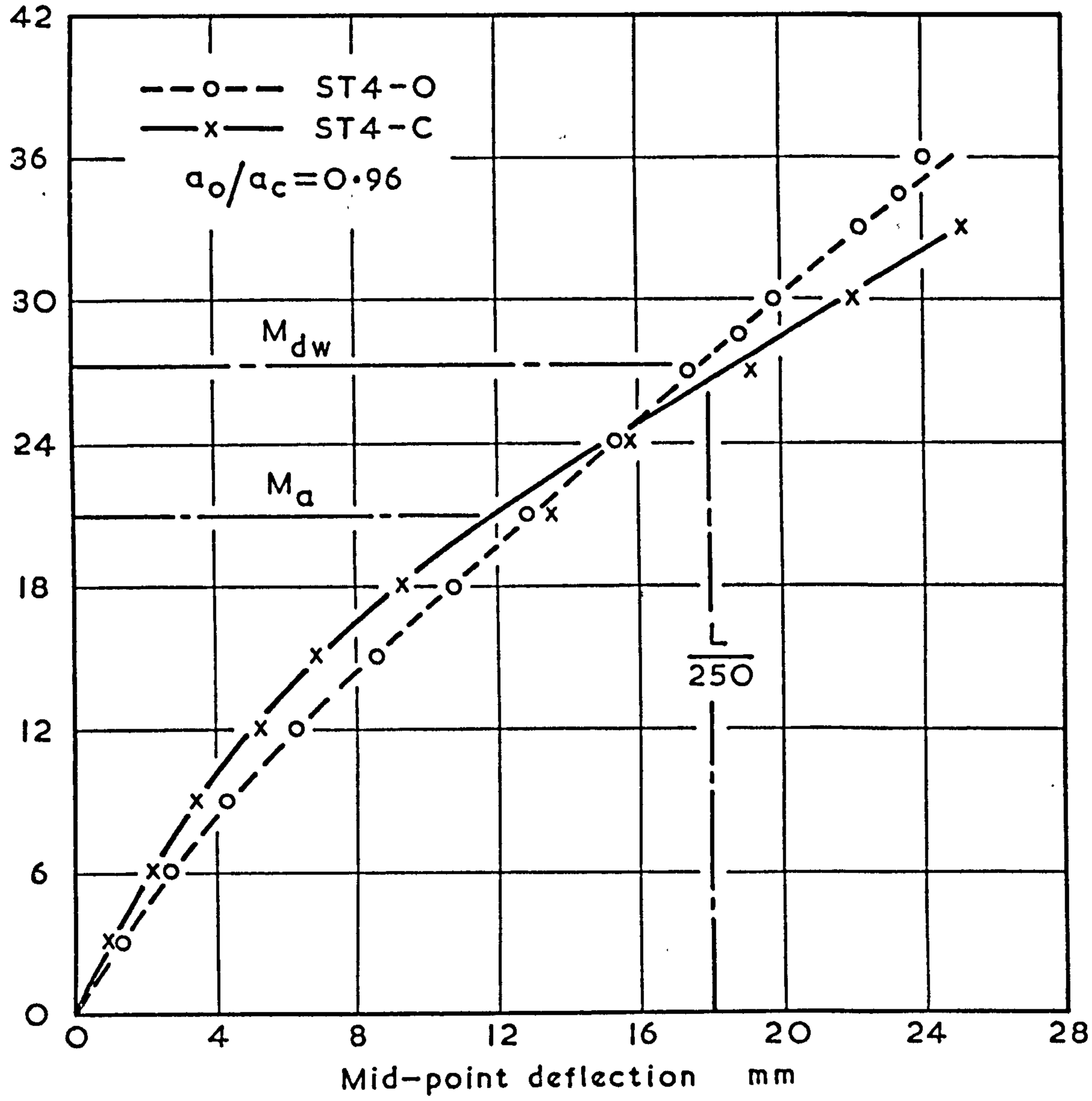

FIG. 45 COMPARISON BETWEEN DEFLECTION FOR ORDINARY AND COMPOSITE BEAMS

a_o = Deflection of ordinary beam at working moment

a_c = Deflection of composite beam at working moment

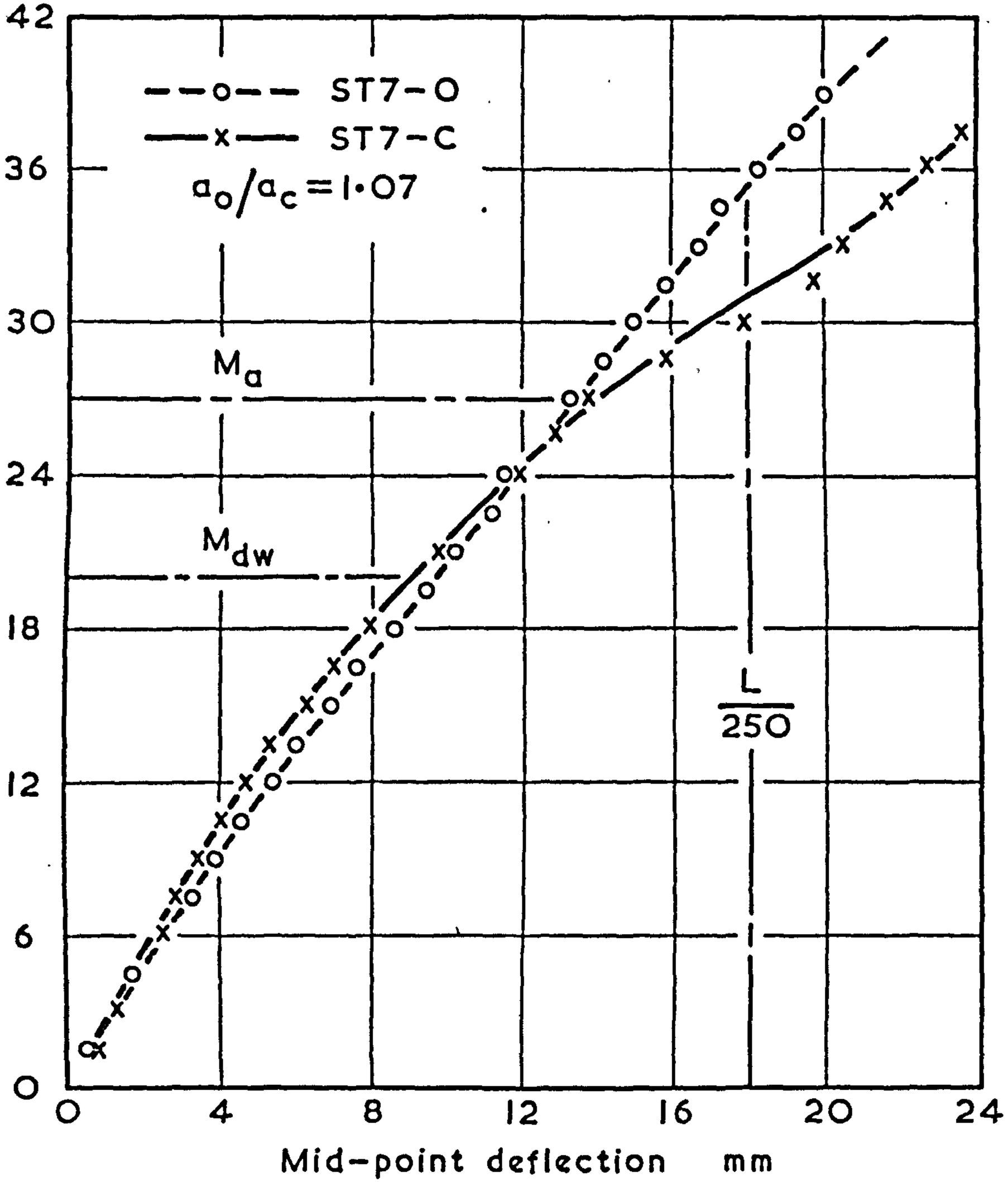

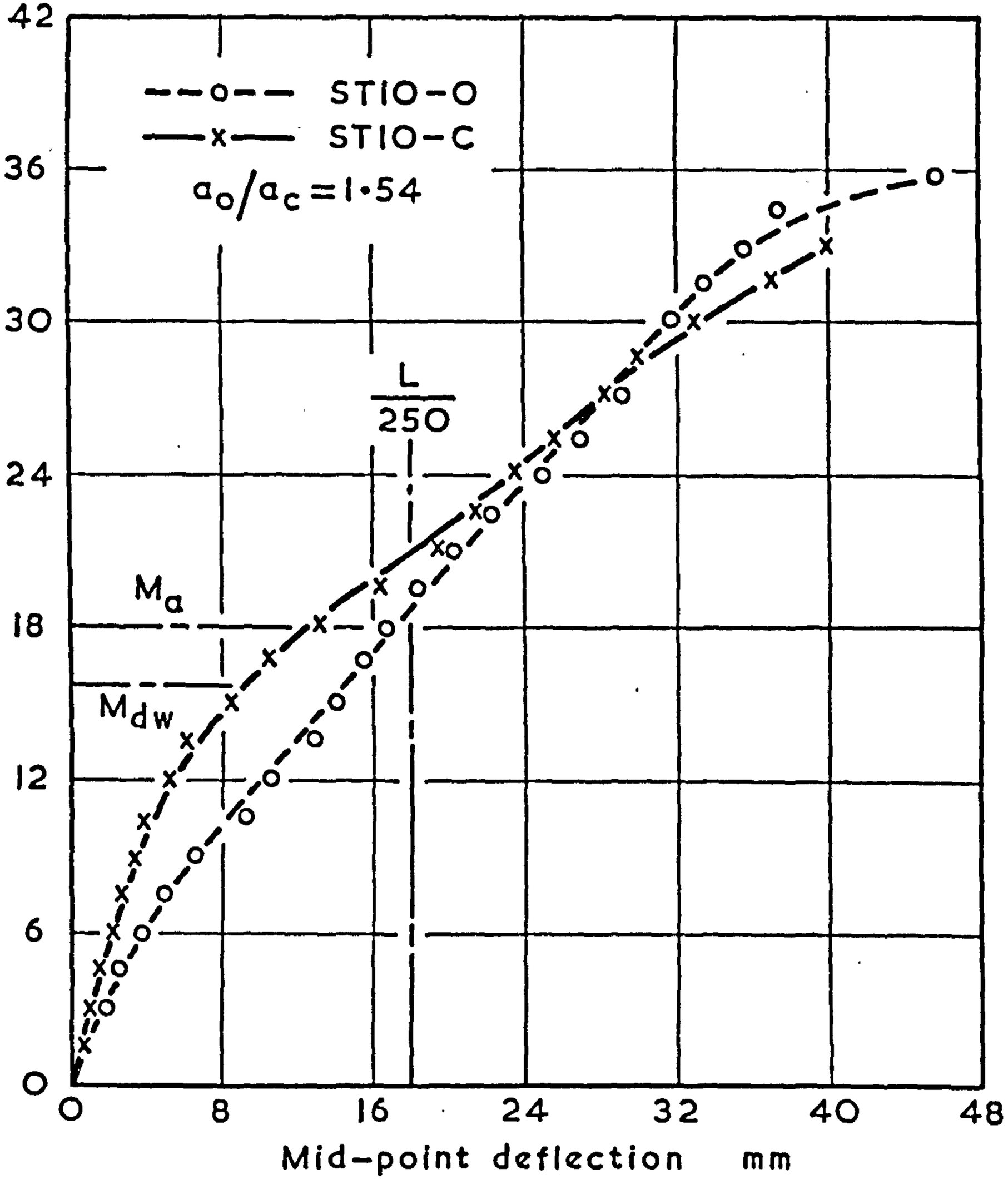

FIG. 46 COMPARISON BETWEEN DEFLECTION FOR ORDINARY AND COMPOSITE BEAMS

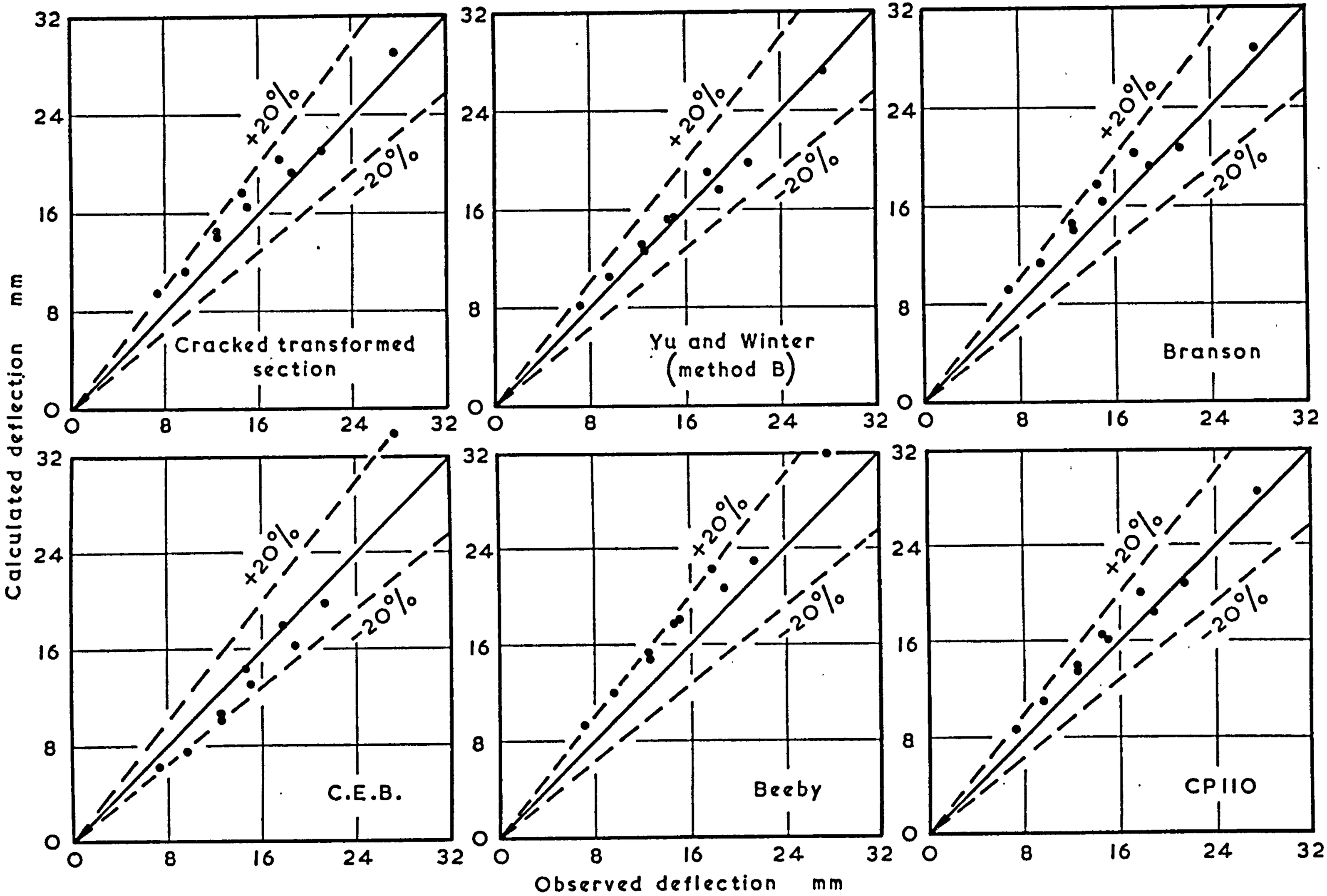

FIG. 47 OBSERVED AND CALCULATED DEFLECTION AT WORKING MOMENT FOR ORDINARY BEAMS

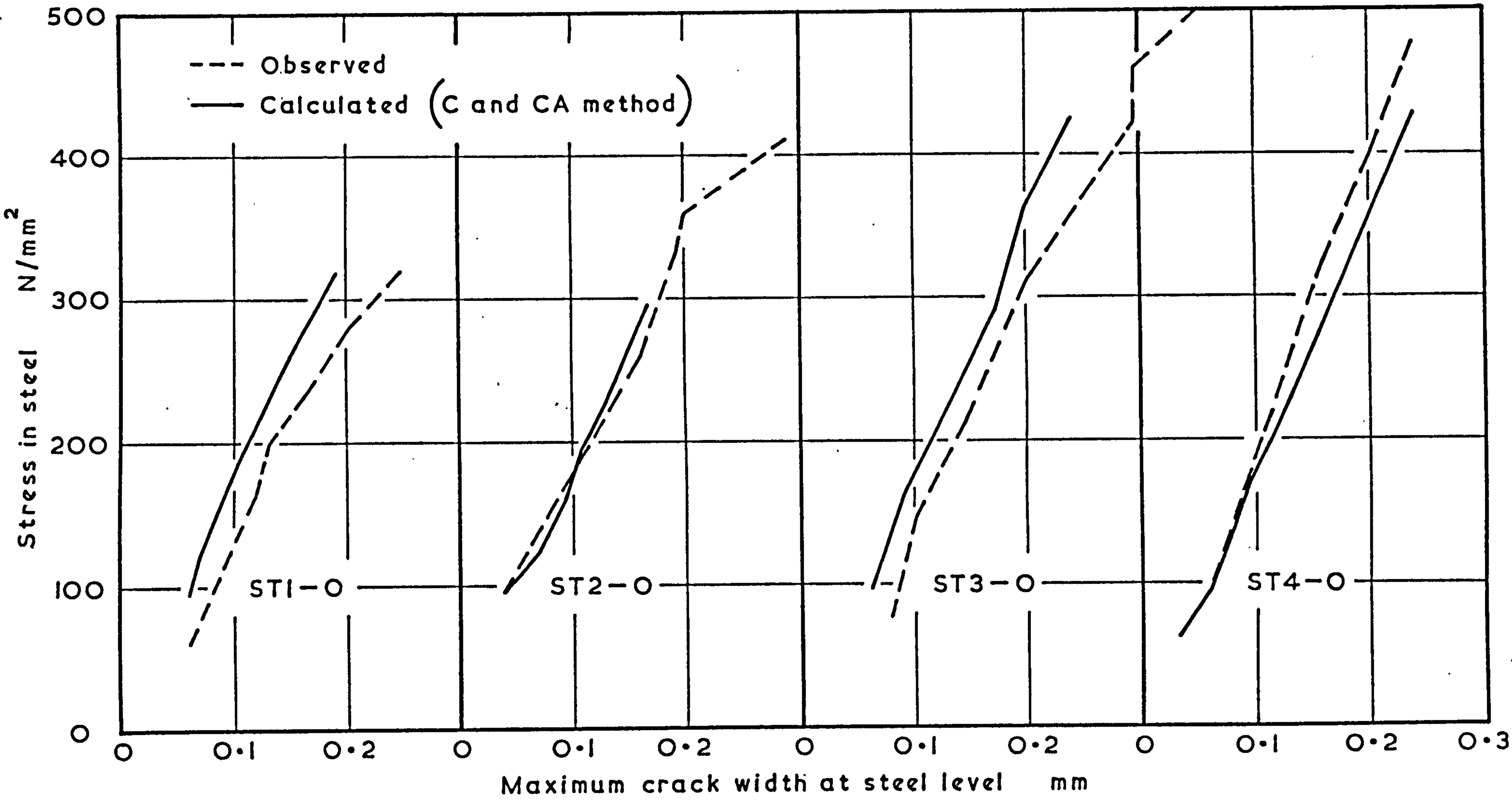

FIG.48 VARIATION OF MAXIMUM CRACK WIDTH WITH STRESS IN STEEL (ORDINARY BEAMS)

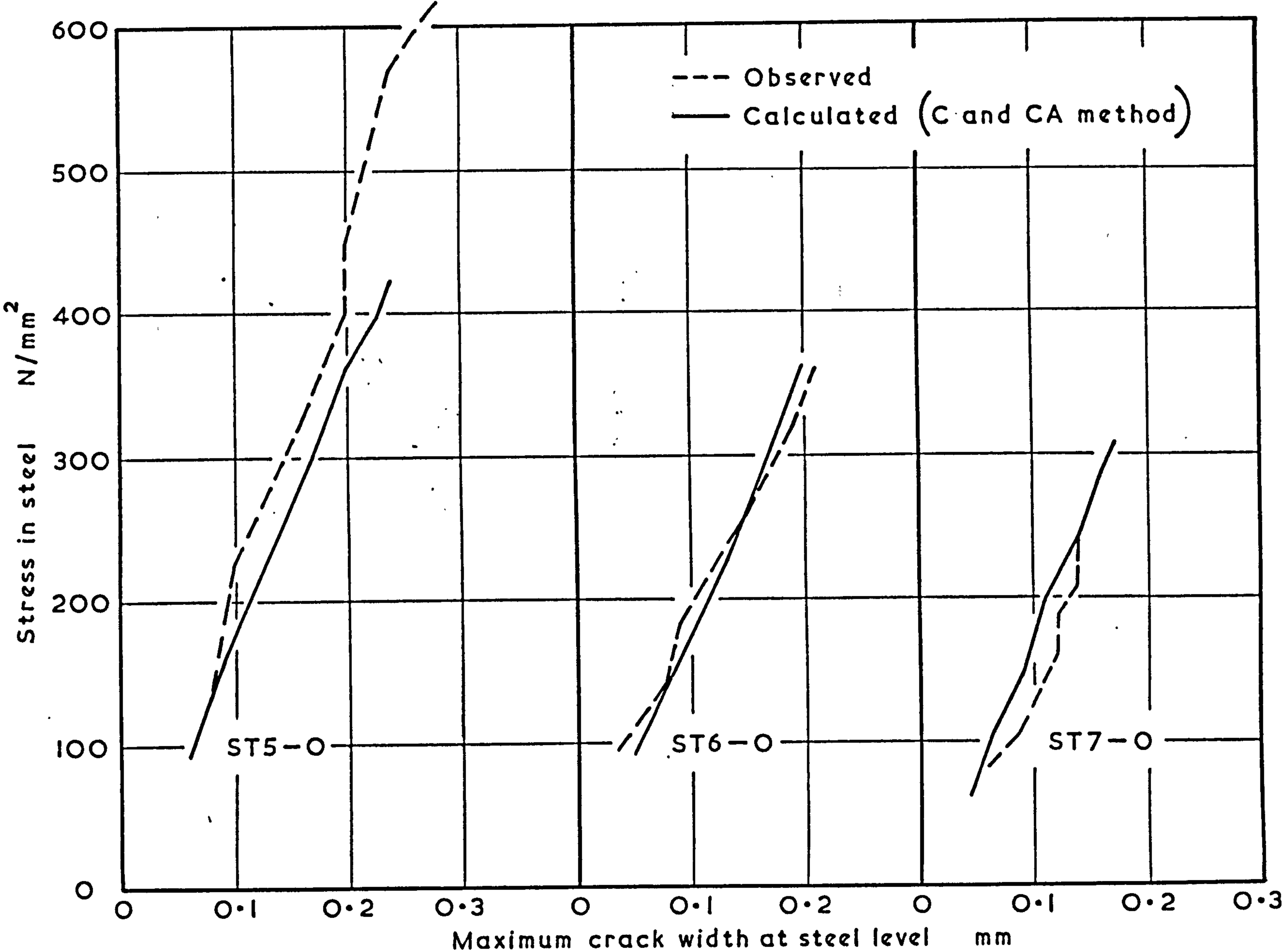

FIG. 49 VARIATION OF MAXIMUM CRACK WIDTH WITH STRESS IN STEEL (ORDINARY BEAMS)

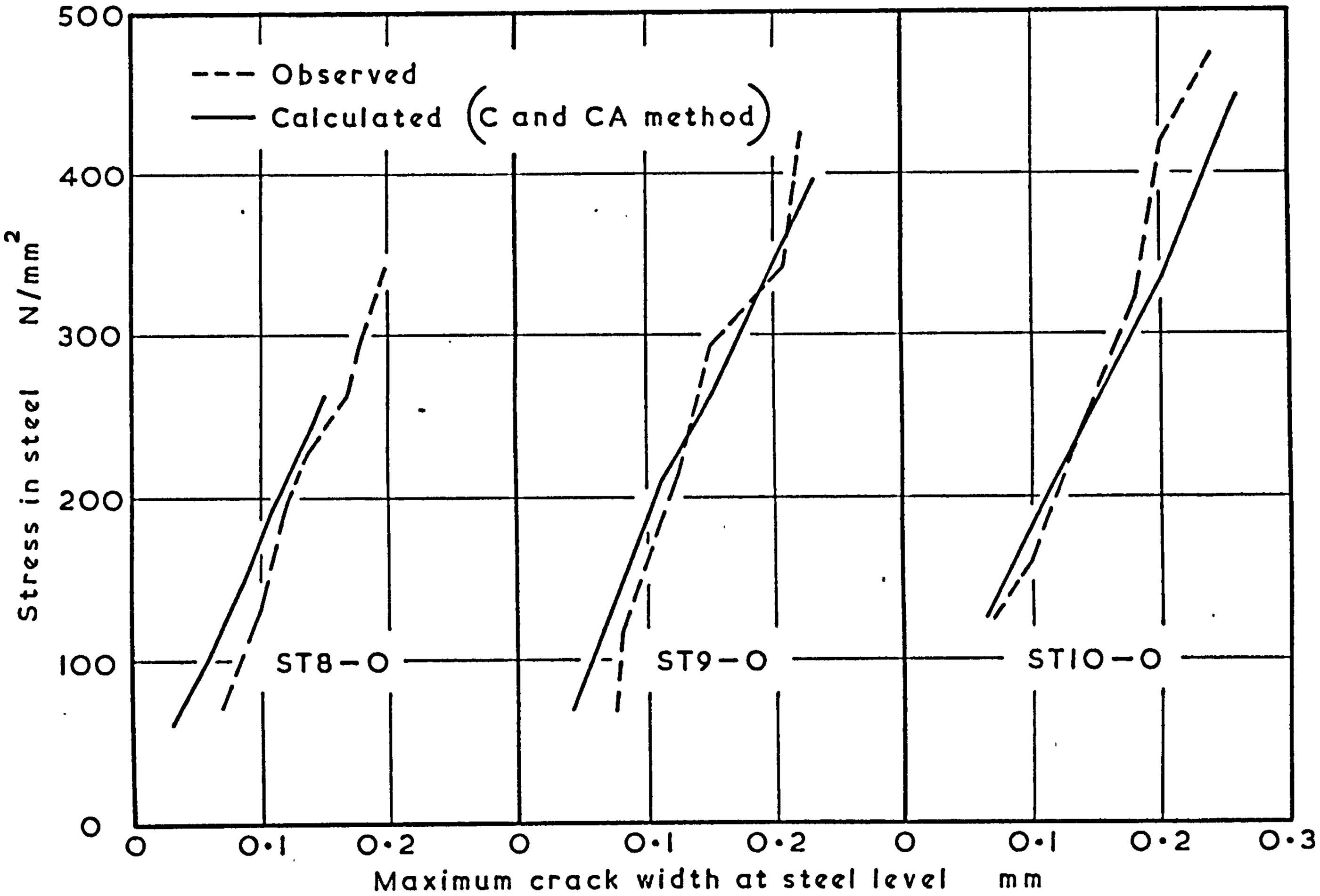

FIG. 50 VARIATION OF MAXIMUM CRACK WIDTH WITH STRESS IN STEEL (ORDINARY BEAMS)

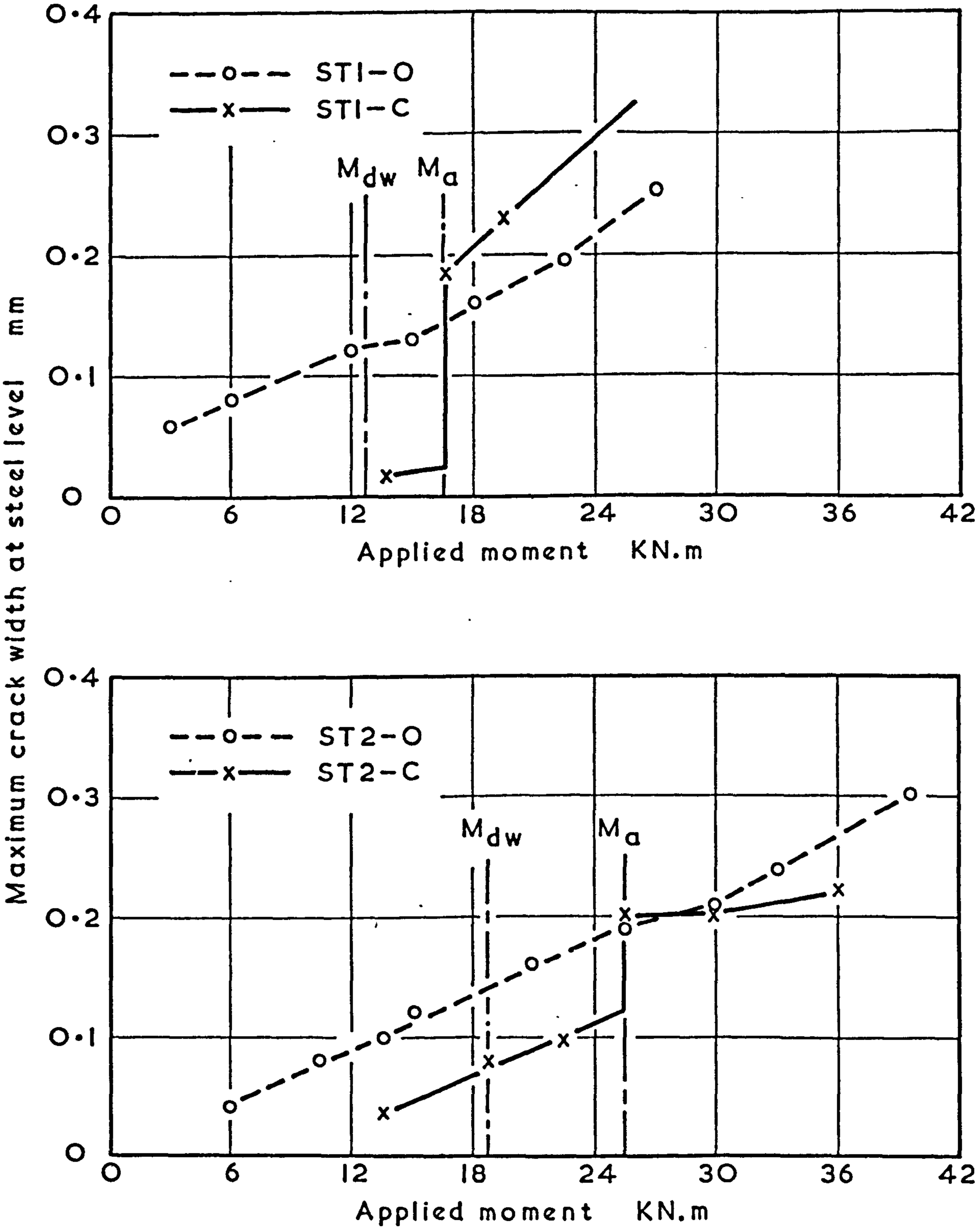

FIG. 51 COMPARISON BETWEEN CRACK WIDTHS FOR ORDINARY AND COMPOSITE BEAMS

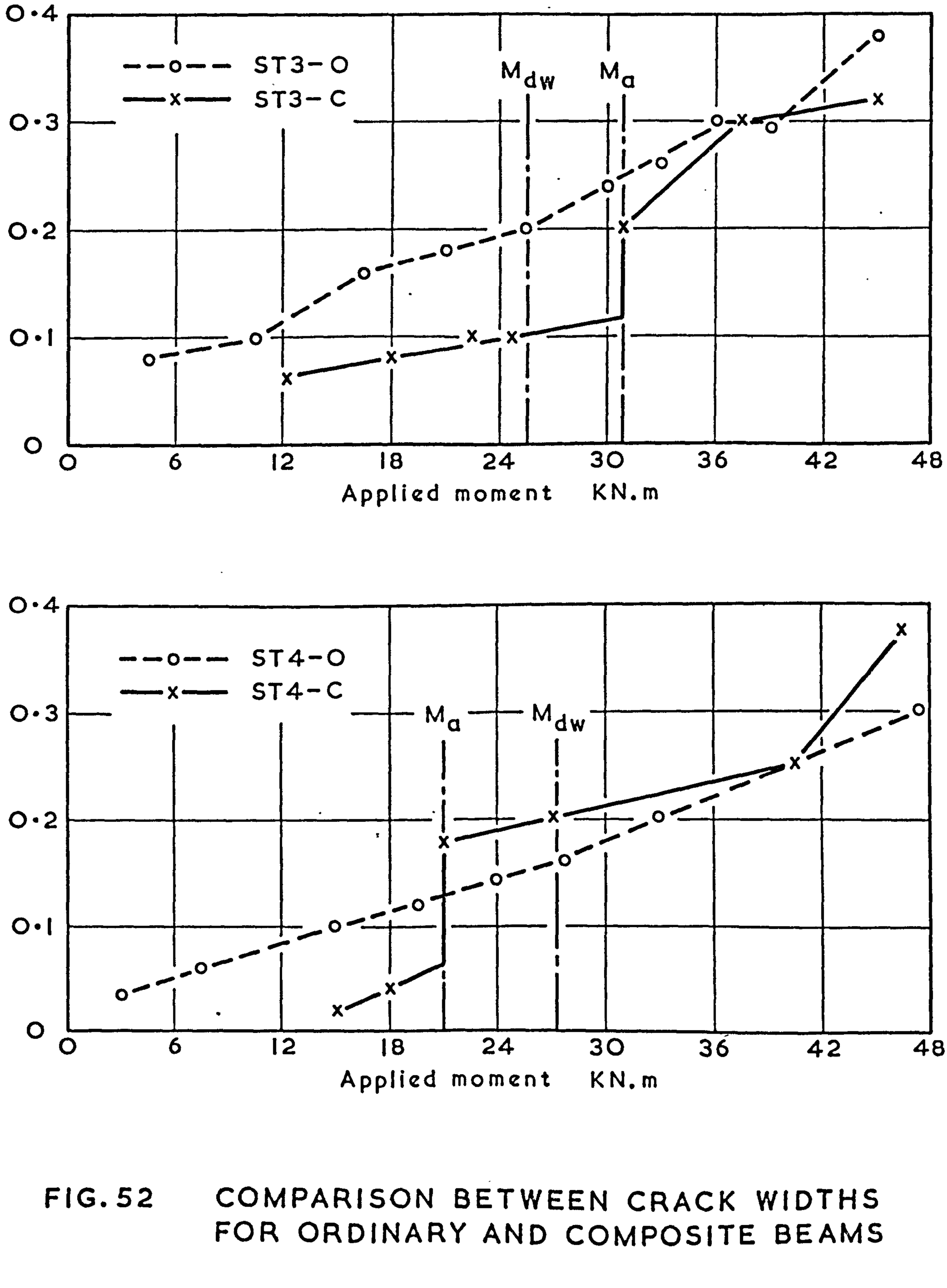

FIG. 52 COMPARISON BETWEEN CRACK WIDTHS FOR ORDINARY AND COMPOSITE BEAMS

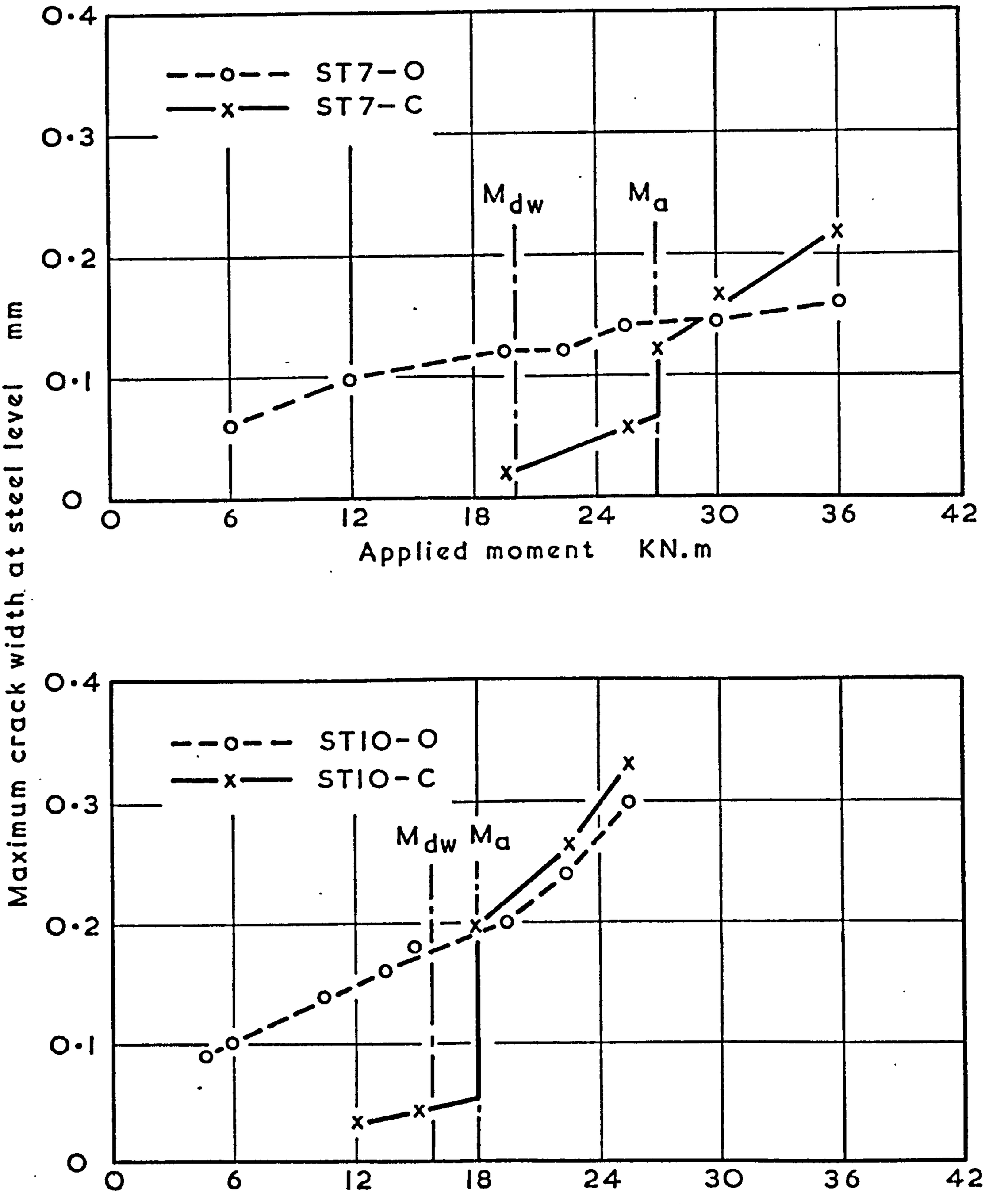

FIG. 53 COMPARISON BETWEEN CRACK WIDTHS FOR ORDINARY AND COMPOSITE BEAMS

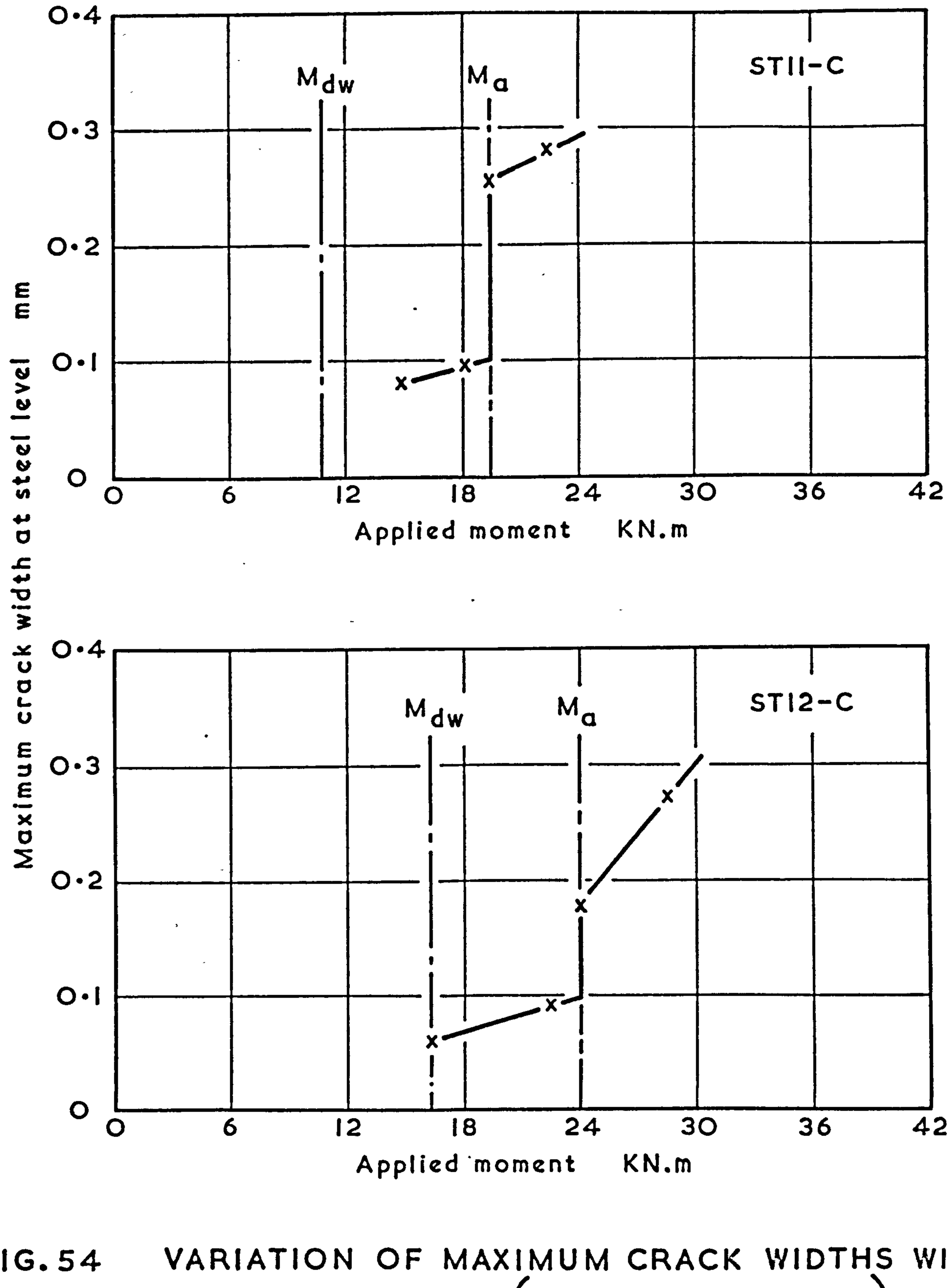

FIG. 54 VARIATION OF MAXIMUM CRACK WIDTHS WITH APPLIED MOMENT (COMPOSITE BEAMS)

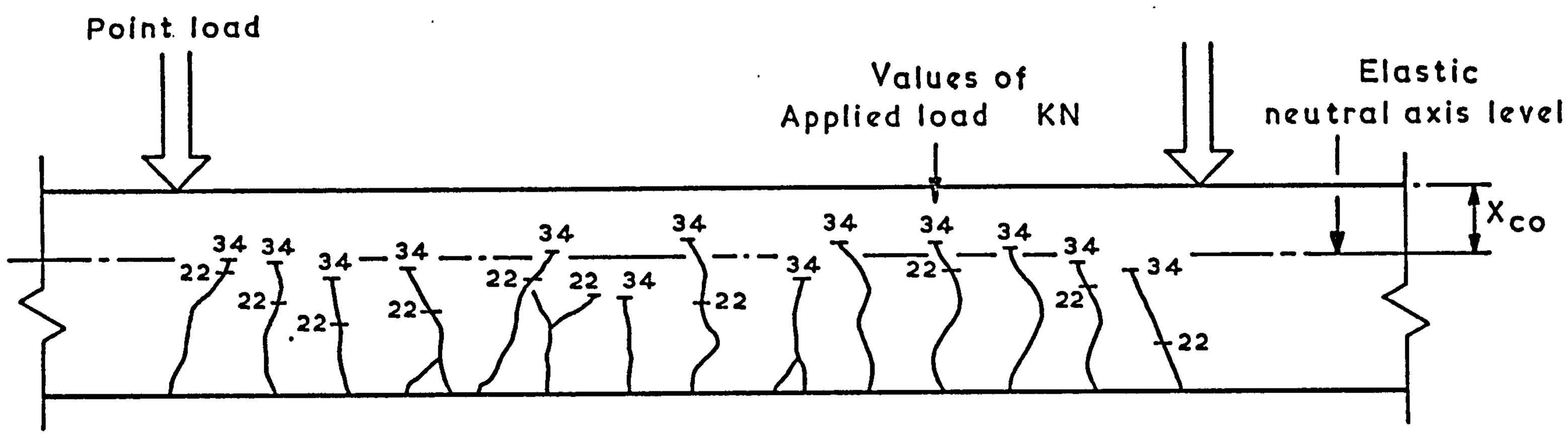

(a) Ordinary beam (ST3–O)

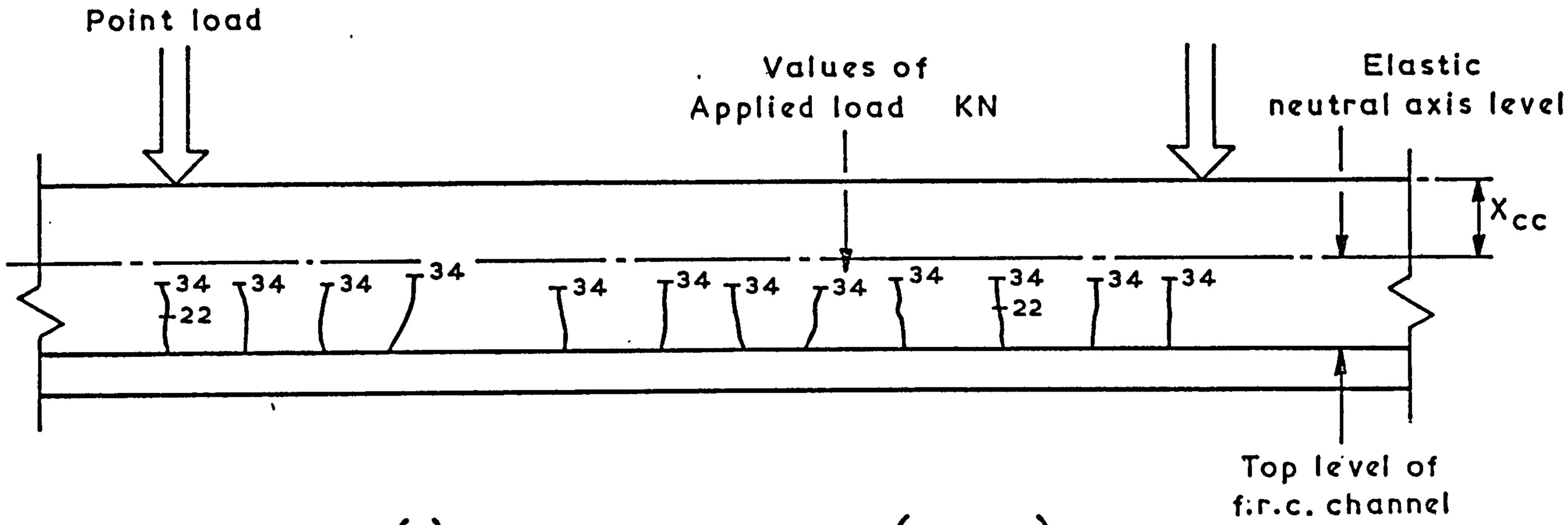

(b) Composite beam (ST3–C)

FIG. 55 CRACKS PATTERN AT WORKING MOMENT (STATIC TEST)

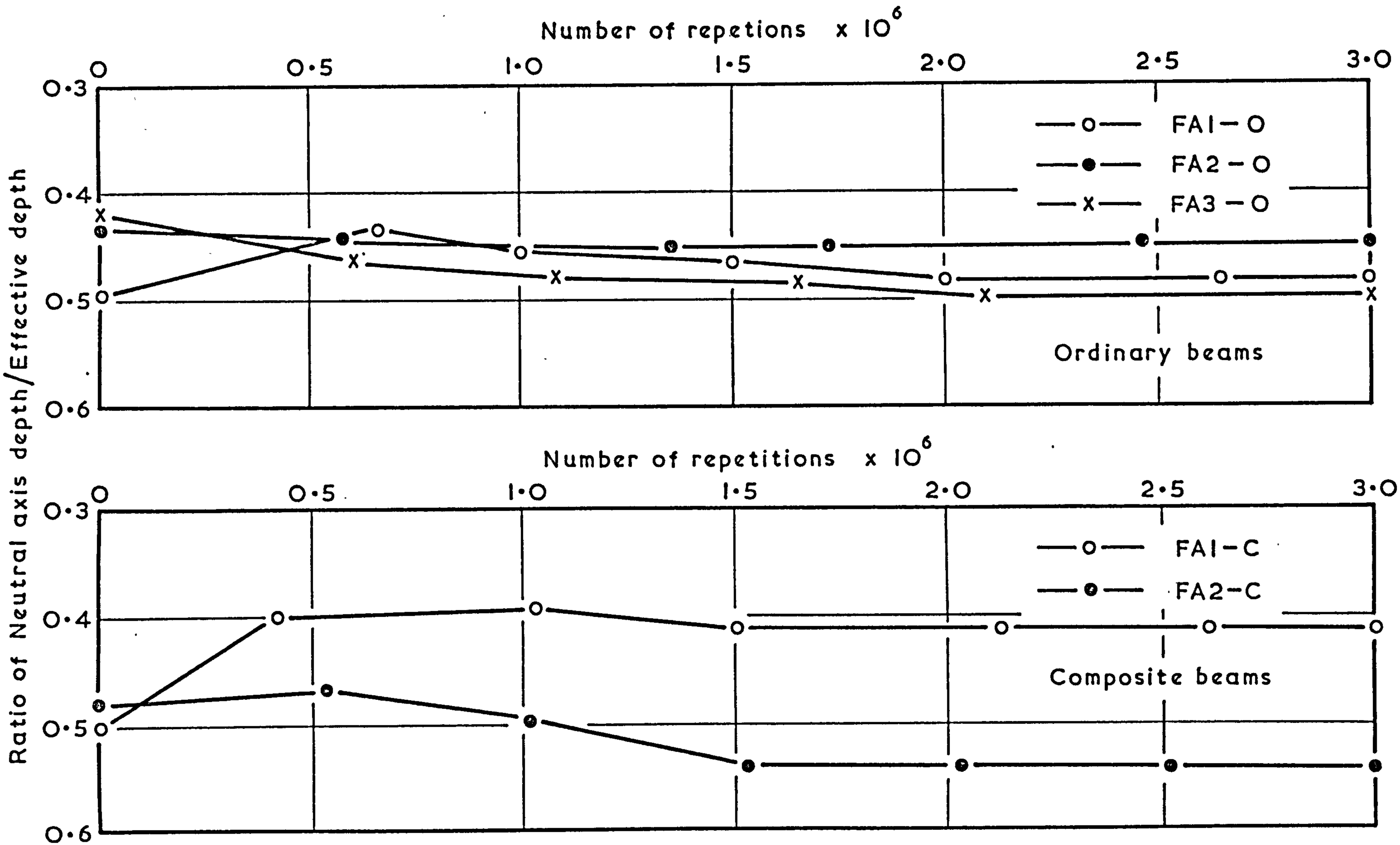

FIG. 56 EFFECT OF FATIGUE LOADING ON NEUTRAL AXIS DEPTH (ORDINARY AND COMPOSITE BEAMS)

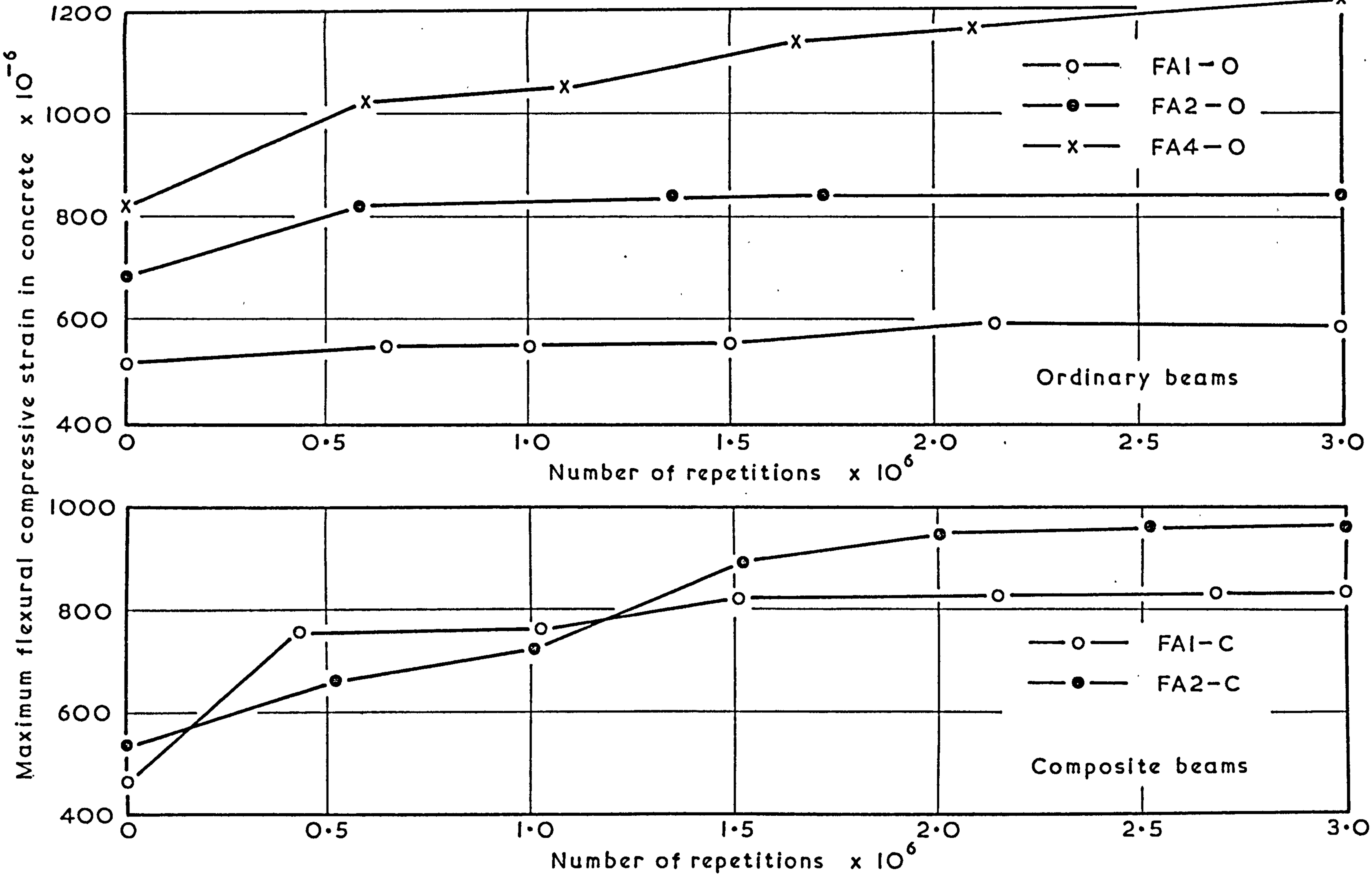

FIG. 57 EFFECT OF FATIGUE LOADING ON MAXIMUM FLEXURAL COMPRESSIVE STRAIN IN CONCRETE (ORDINARY AND COMPOSITE BEAMS)

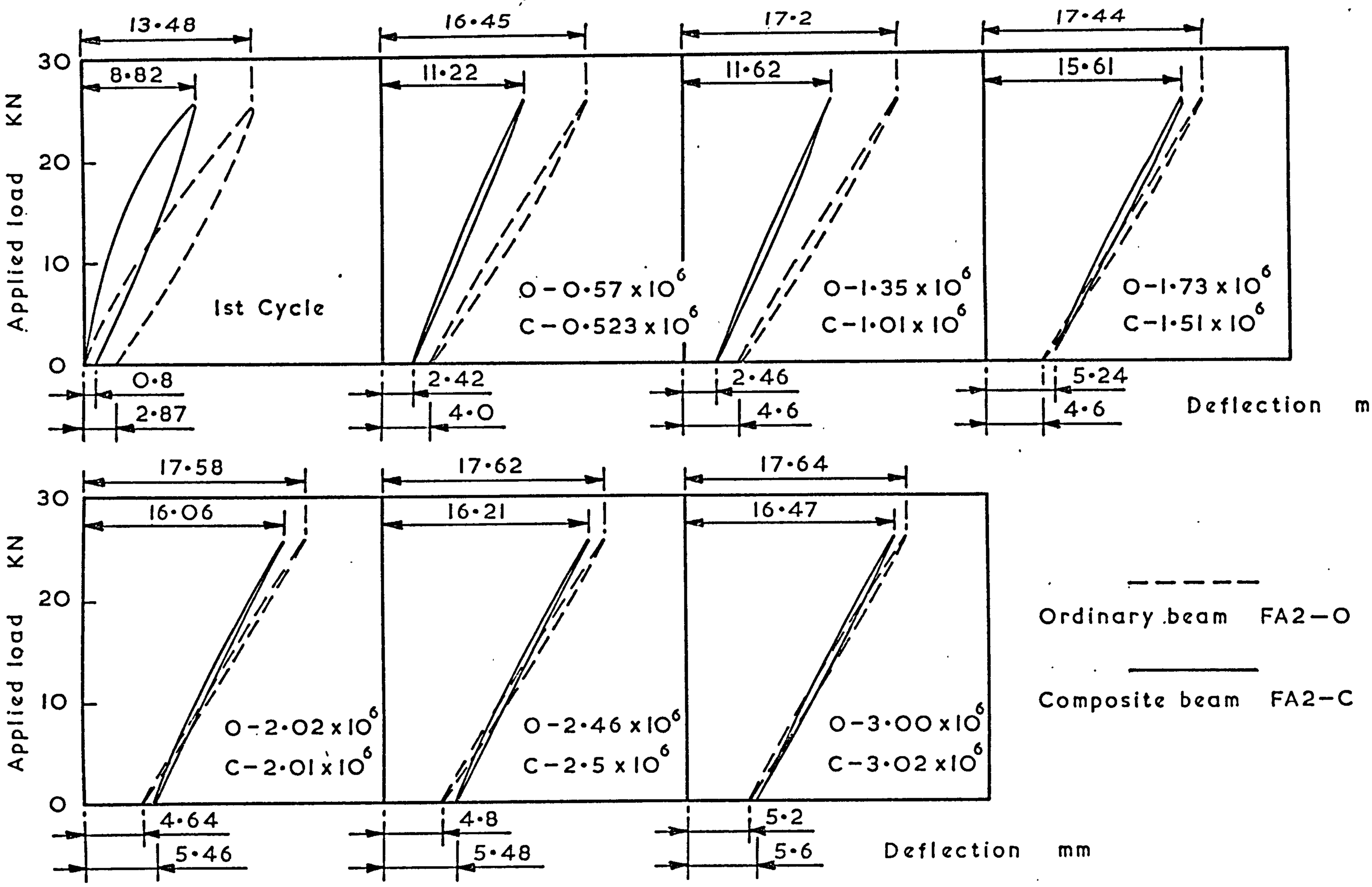

FIG. 58 EFFECT OF FATIGUE LOADING ON LOAD–DEFLECTION BEHAVIOUR (ORDINARY AND COMPOSITE BEAMS)

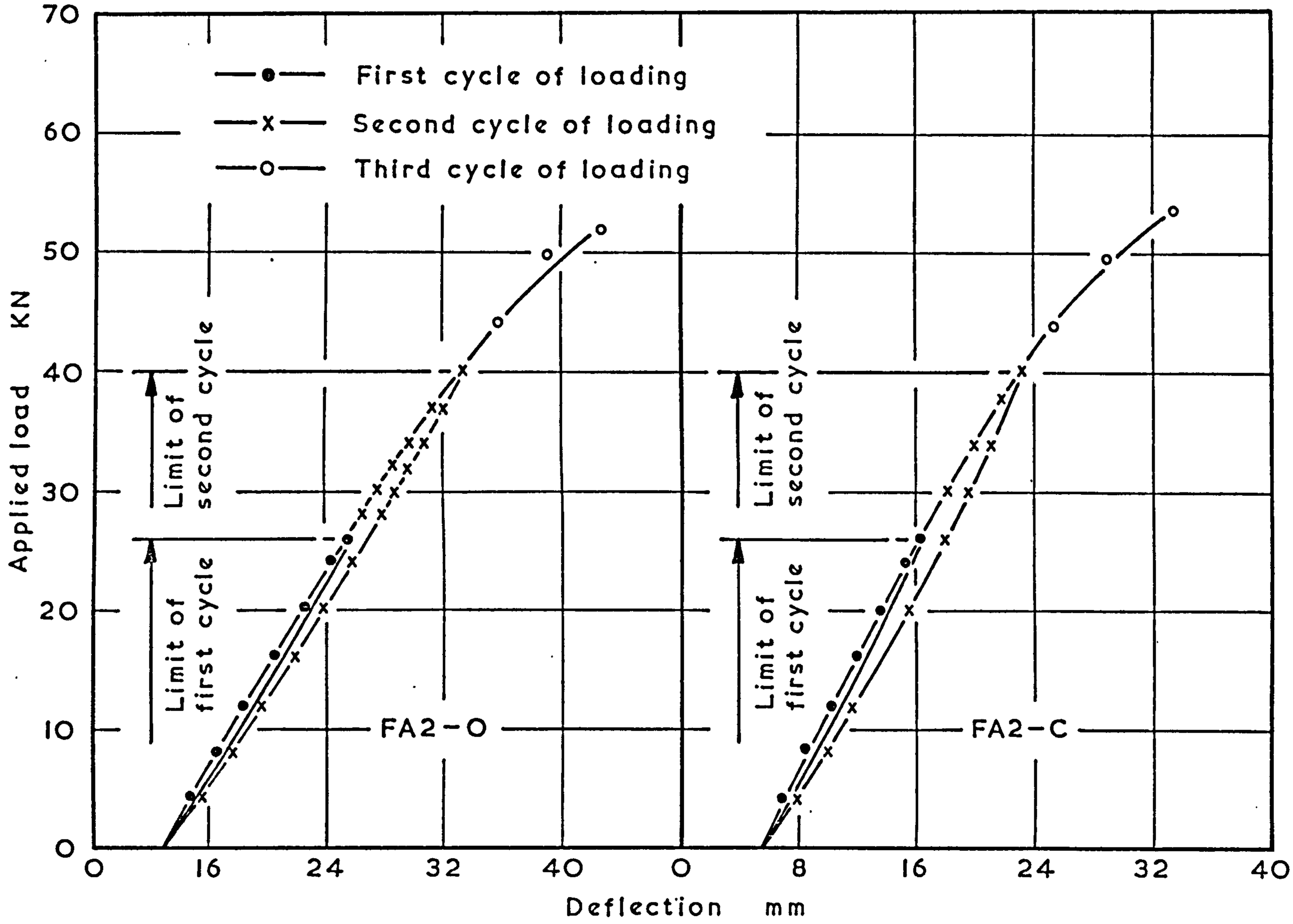

FIG.59 LOADING AND UNLOADING BEHAVIOUR OF BEAMS SUBJECTED TO PREVIOUS FATIGUE LOADING (ORDINARY AND COMPOSITE BEAMS)

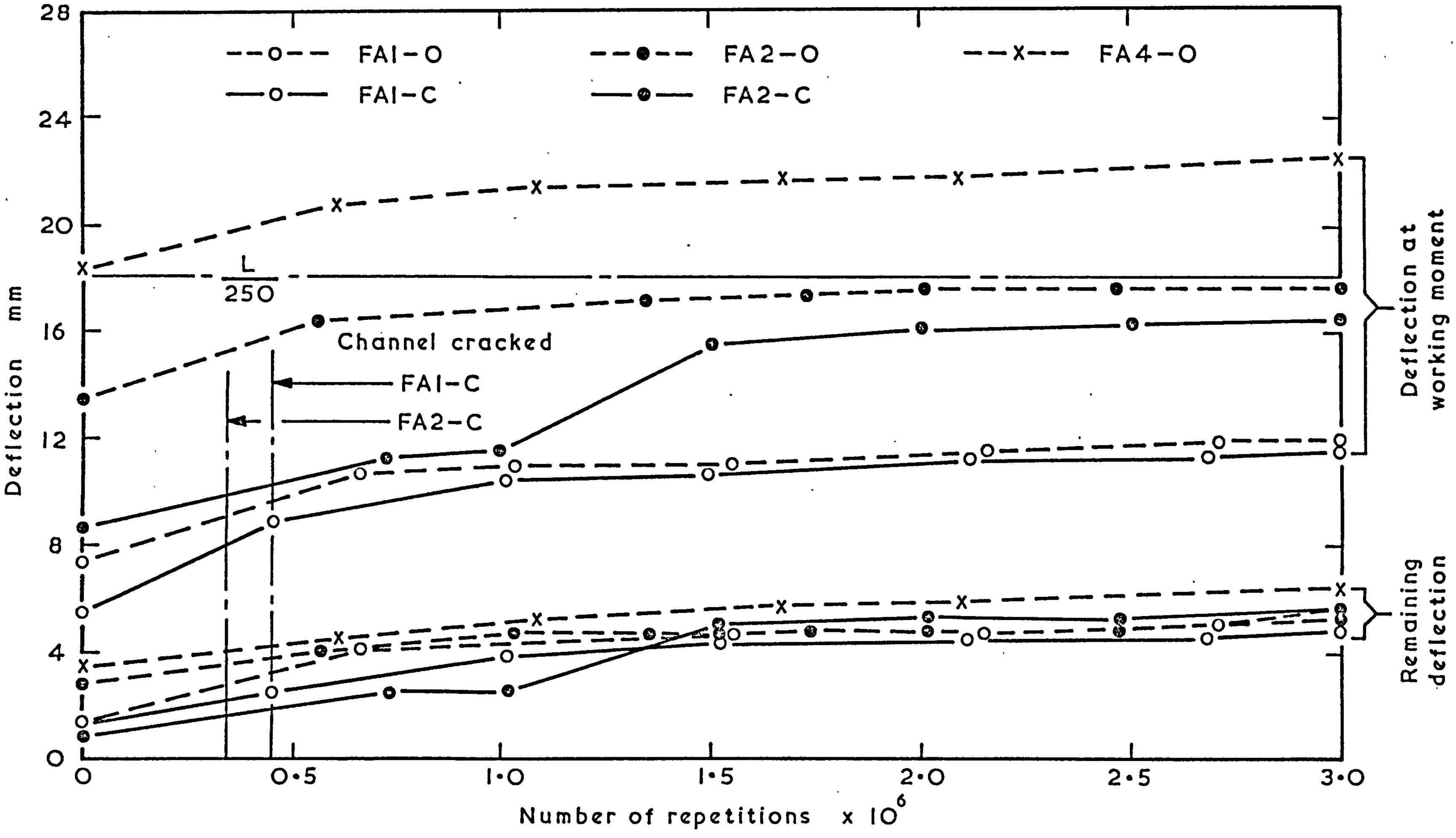

FIG.60 EFFECT OF FATIGUE LOADING ON DEFLECTIONS (ORDINARY AND COMPOSITE BEAMS)

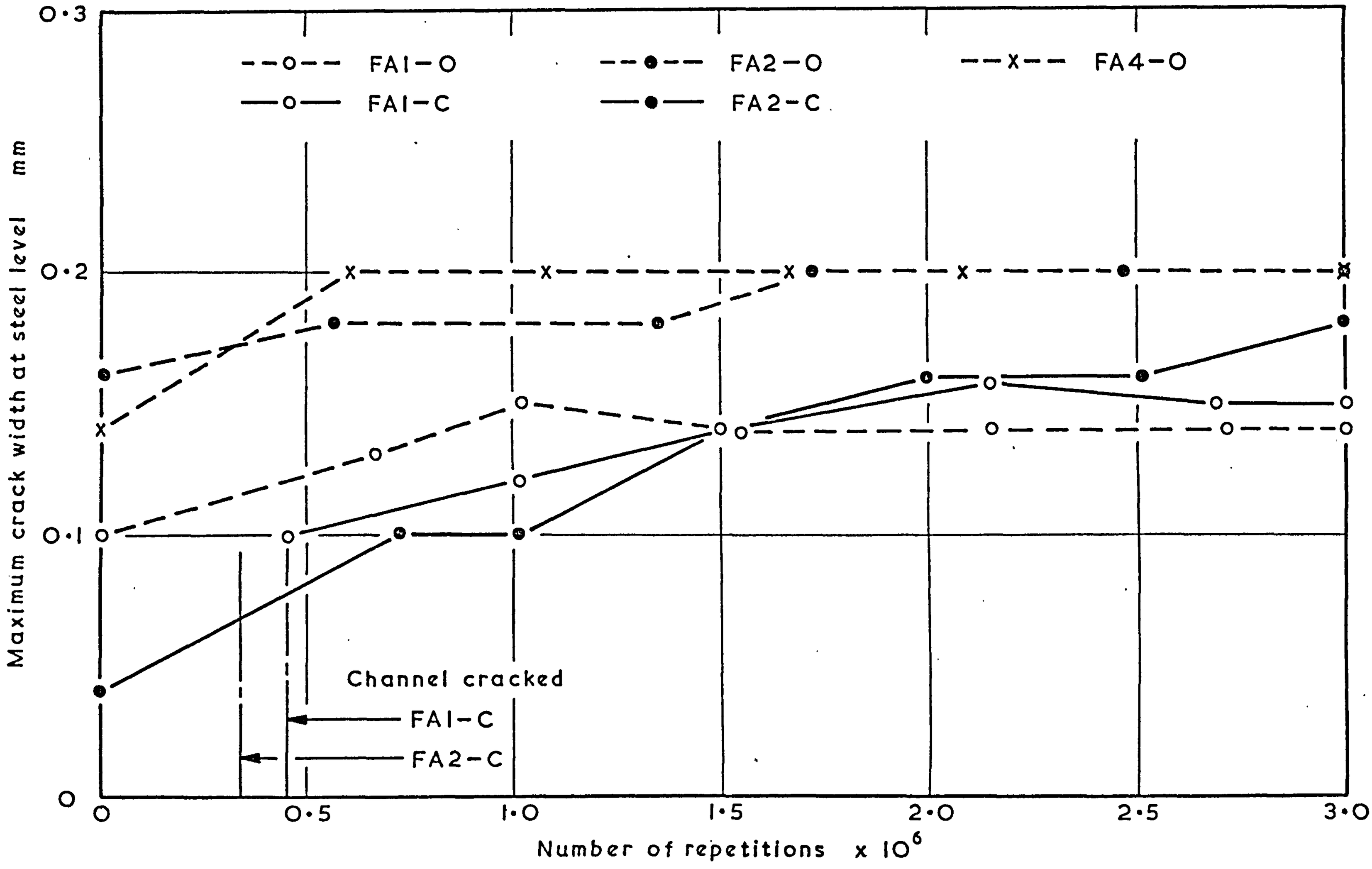

FIG.61 EFFECT OF FATIGUE LOADING ON CRACK WIDTHS AT WORKING MOMENT (ORDINARY AND COMPOSITE BEAMS)

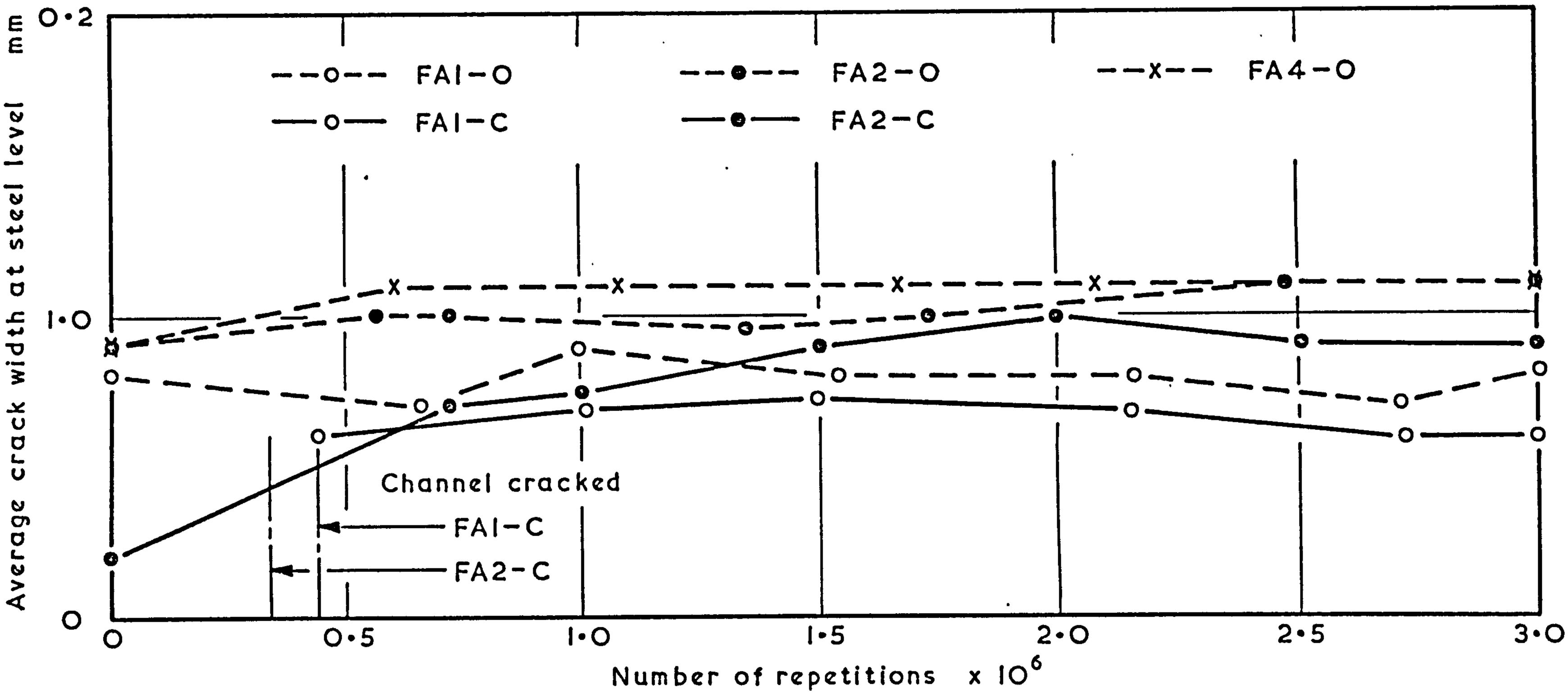

FIG.62 EFFECT OF FATIGUE LOADING ON CRACK WIDTHS AT WORKING MOMENT (ORDINARY AND COMPOSITE BEAMS)

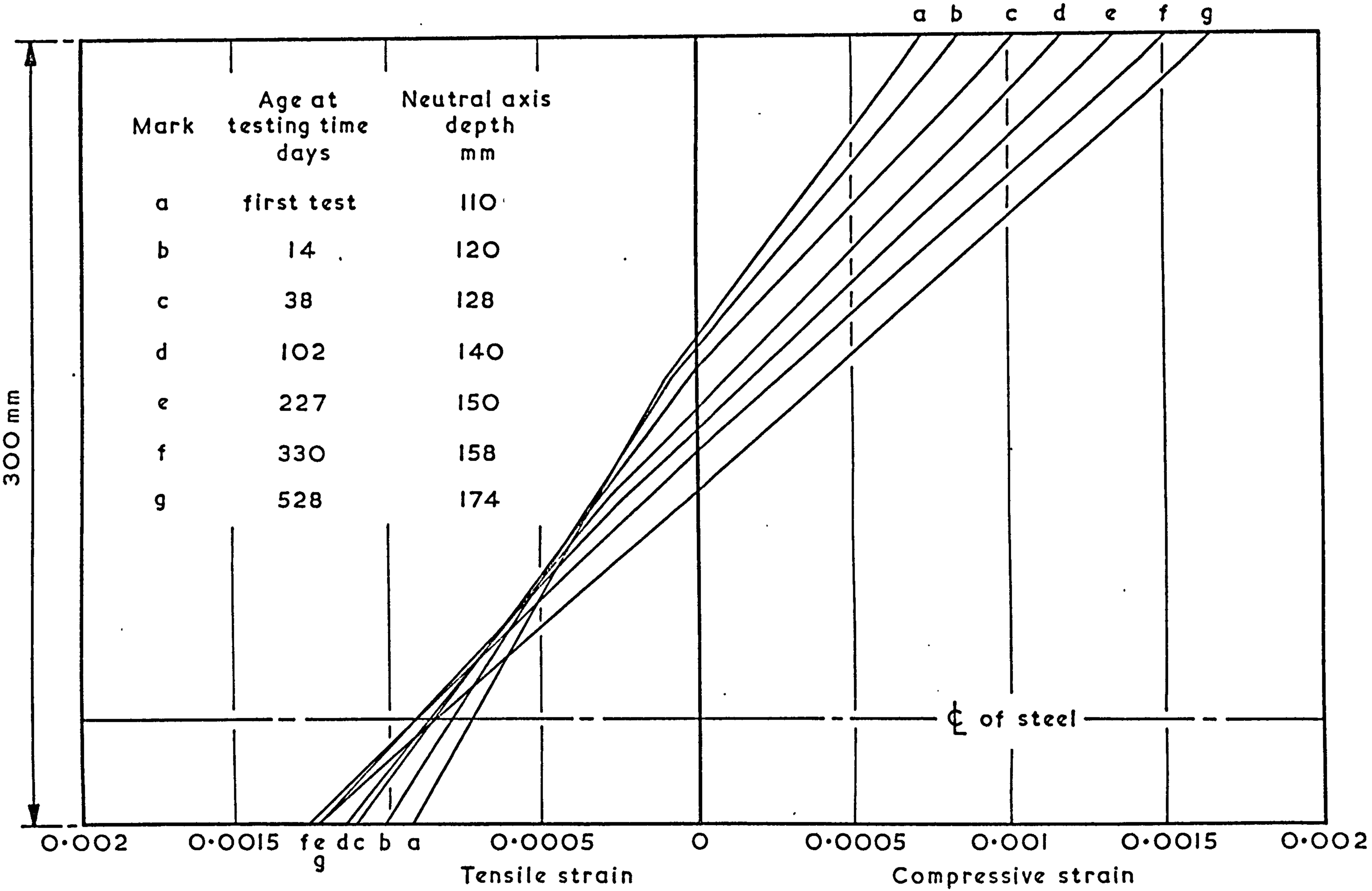

FIG.63 TIME-DEPENDENT FLEXURAL STRAIN DISTRIBUTION (ORDINARY BEAM SU2-O)

Mark	Age at testing time days	Neutral axis depth mm
a	first test	120
b	14	128
c	38	134
d	102	142
e	227	152
f	330	160
g	528	178

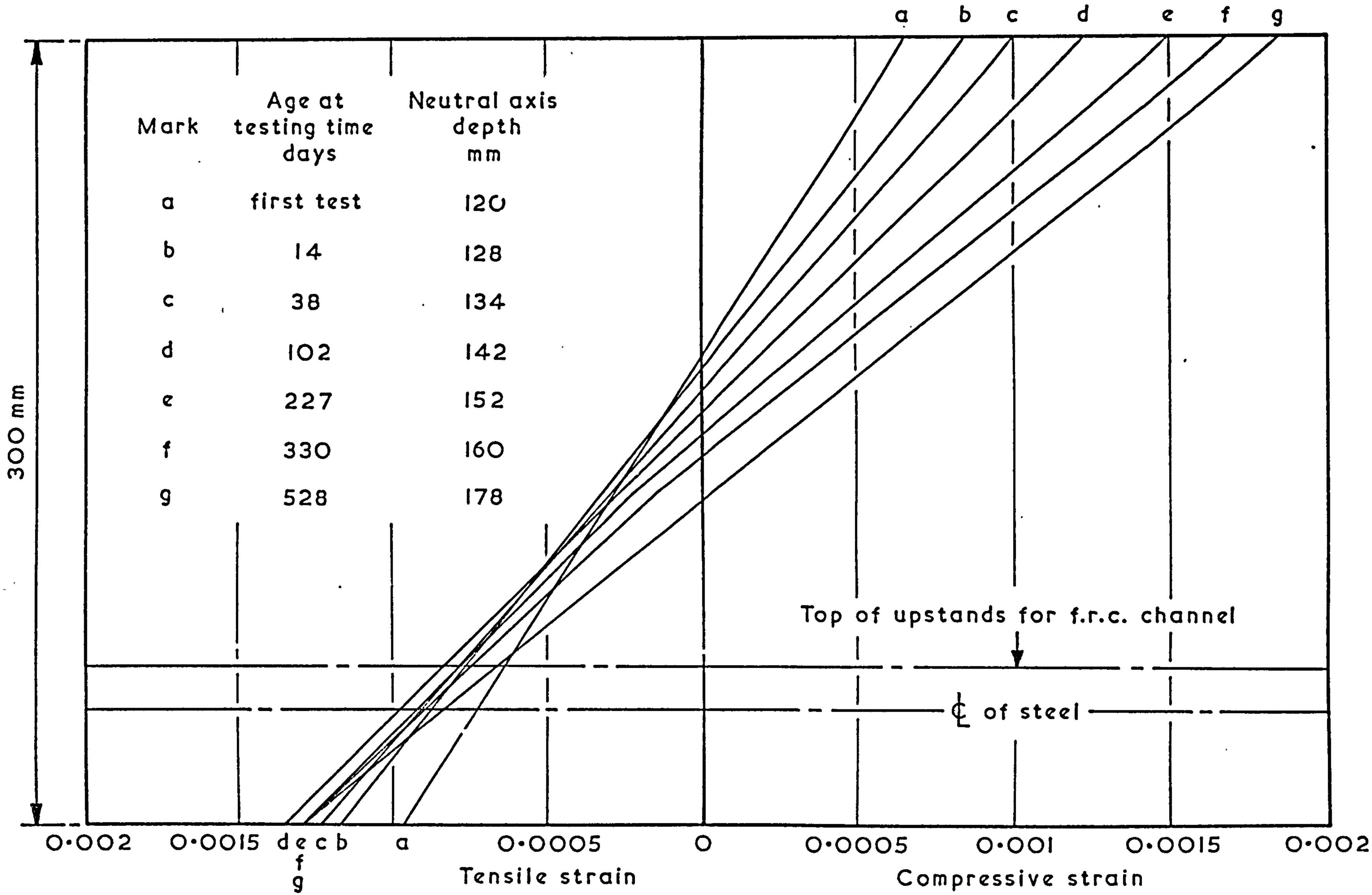

FIG.64 TIME-DEPENDENT FLEXURAL STRAIN DISTRIBUTION (COMPOSITE BEAM SU2-C)

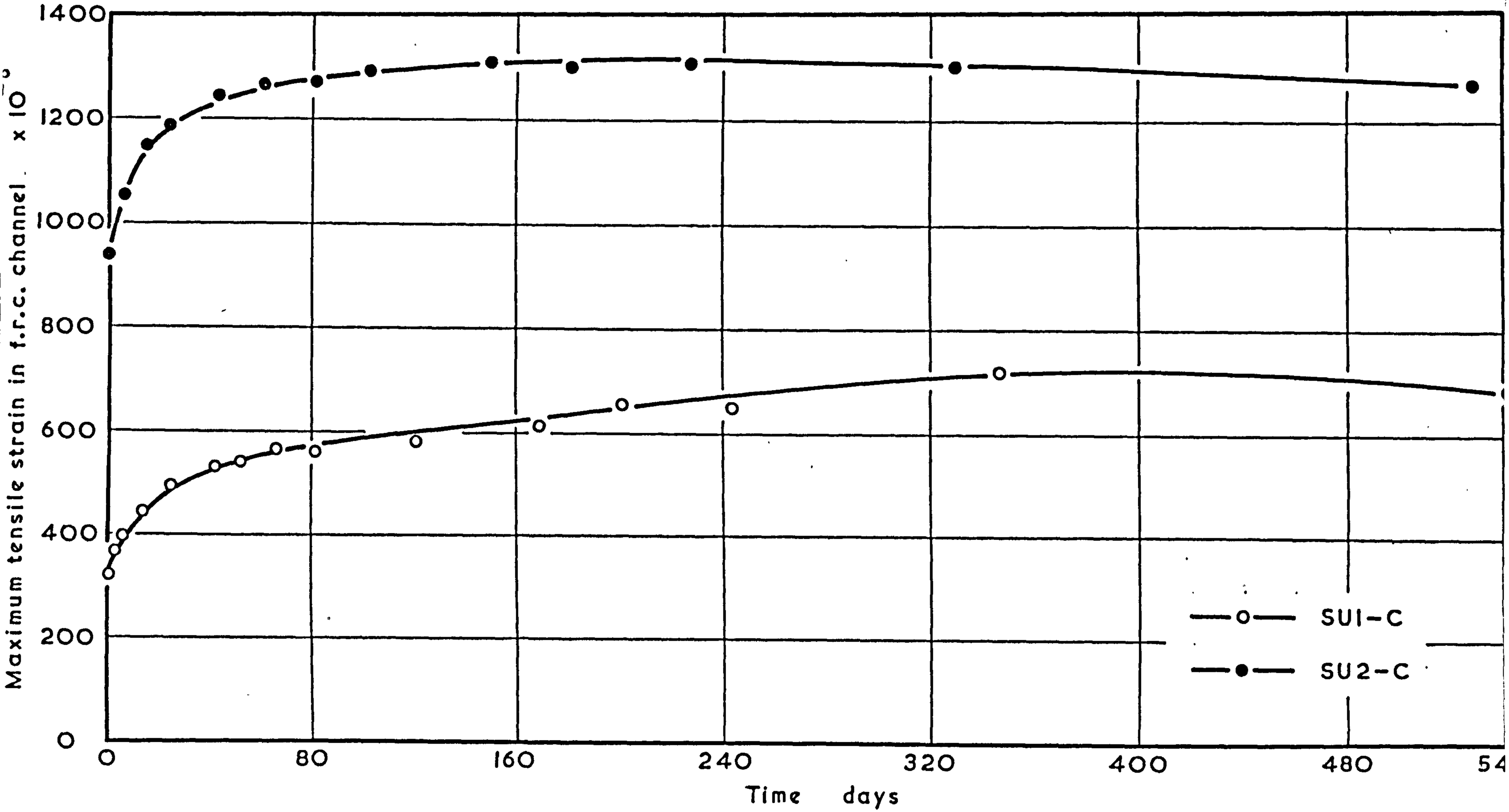

FIG.65 EFFECT OF SUSTAINED LOADING ON MAXIMUM TENSILE STRAIN IN f.r.c. CHANNELS

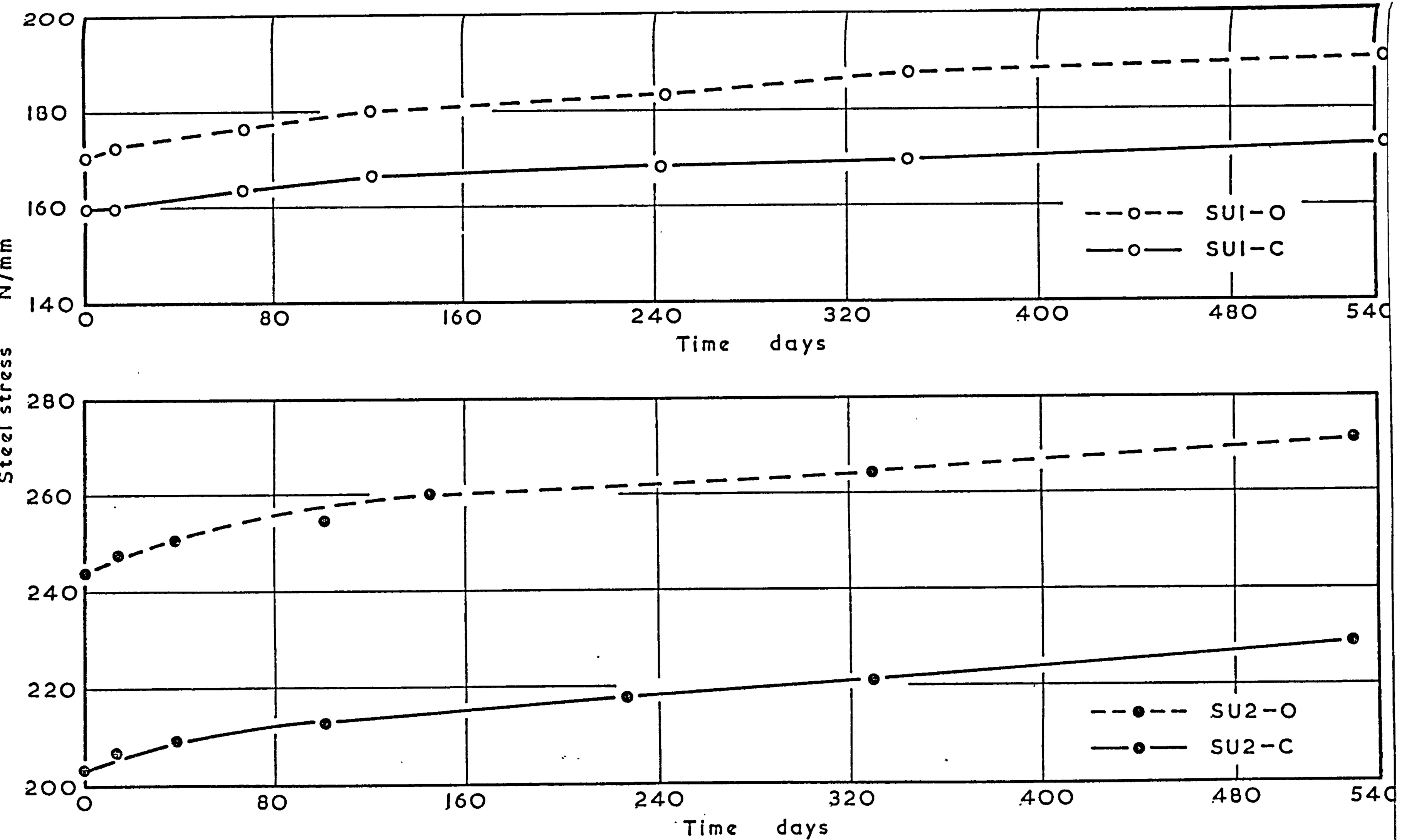

FIG.66 EFFECT OF SUSTAINED LOADING ON STEEL STRESSES (ORDINARY AND COMPOSITE BEAMS)

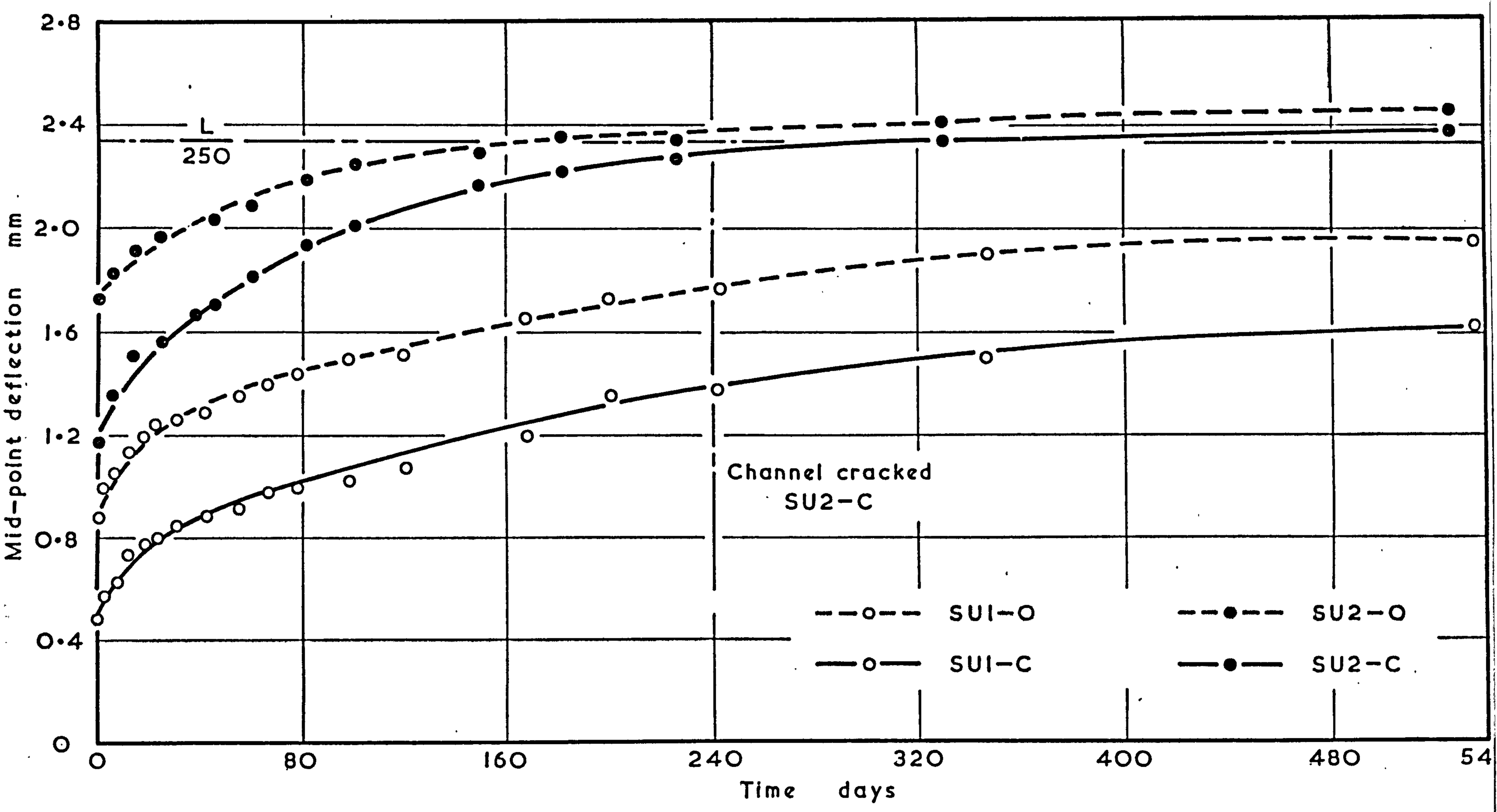

FIG. 67 EFFECT OF SUSTAINED LOADING ON DEFLECTION (ORDINARY AND COMPOSITE BEAMS)

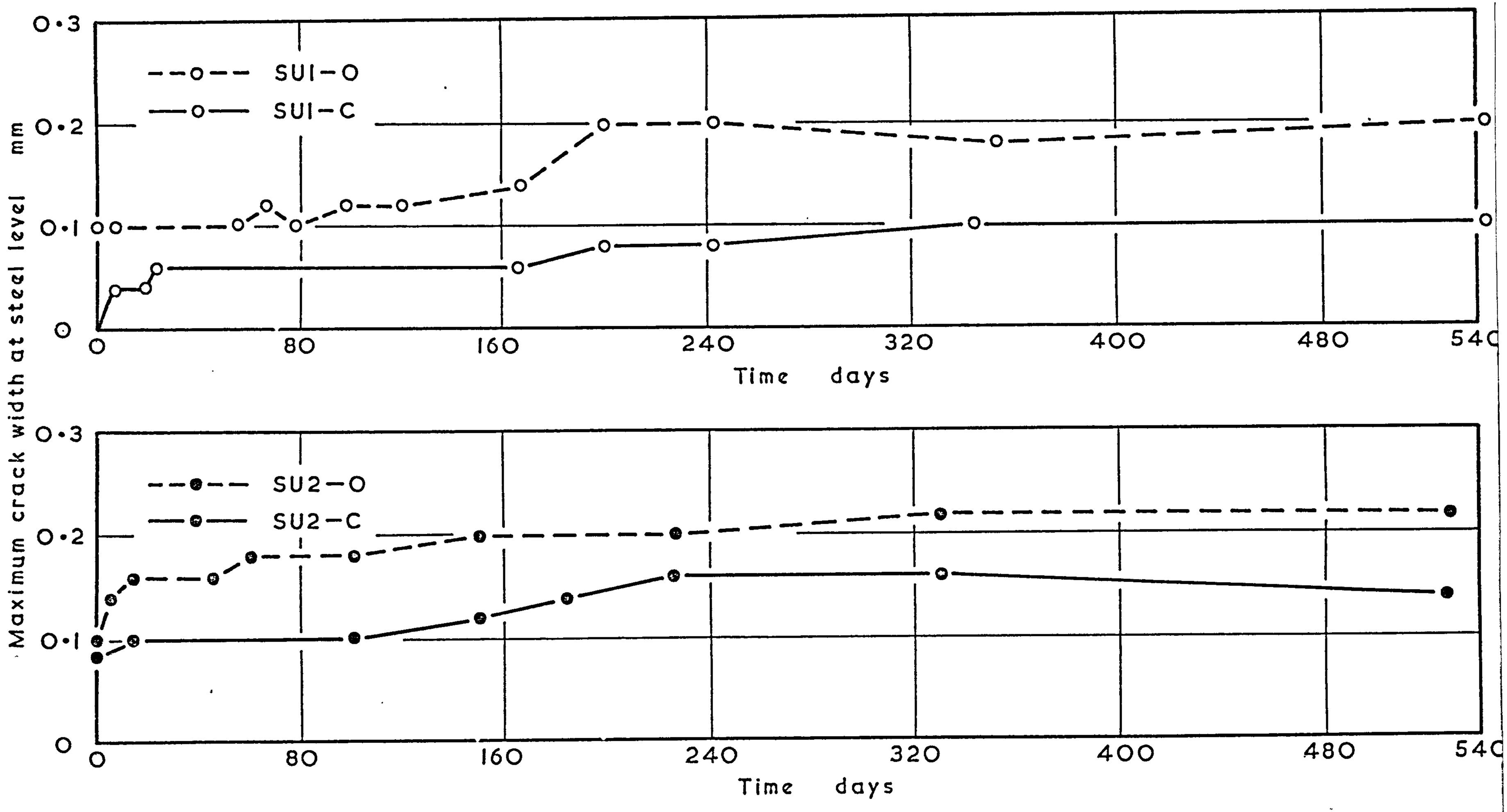

FIG.68 EFFECT OF SUSTAINED LOADING ON CRACK WIDTHS (ORDINARY AND COMPOSITE BEAMS)

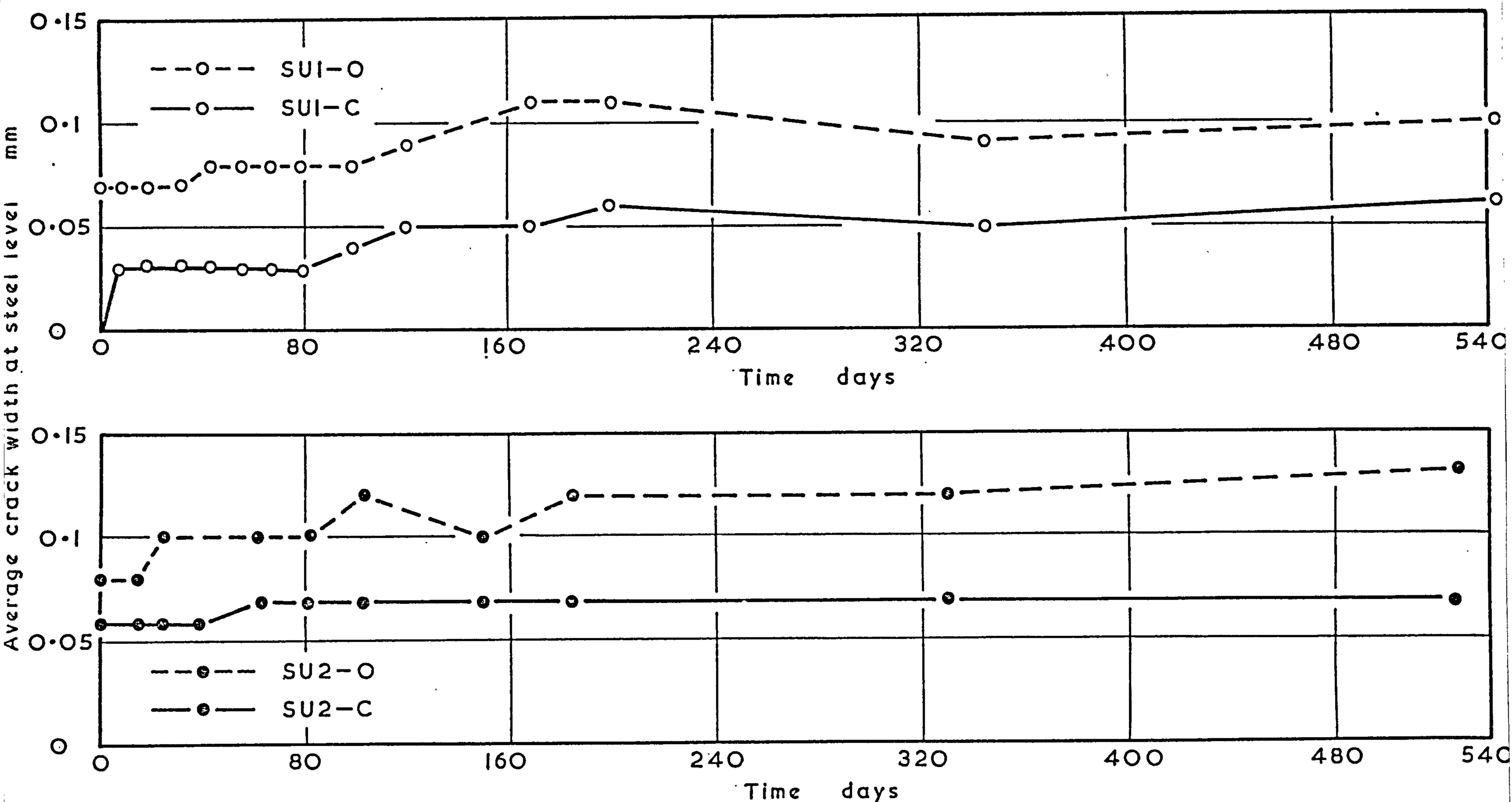

FIG.69 EFFECT OF SUSTAINED LOADING ON CRACK WIDTHS (ORDINARY AND COMPOSITE BEAMS)

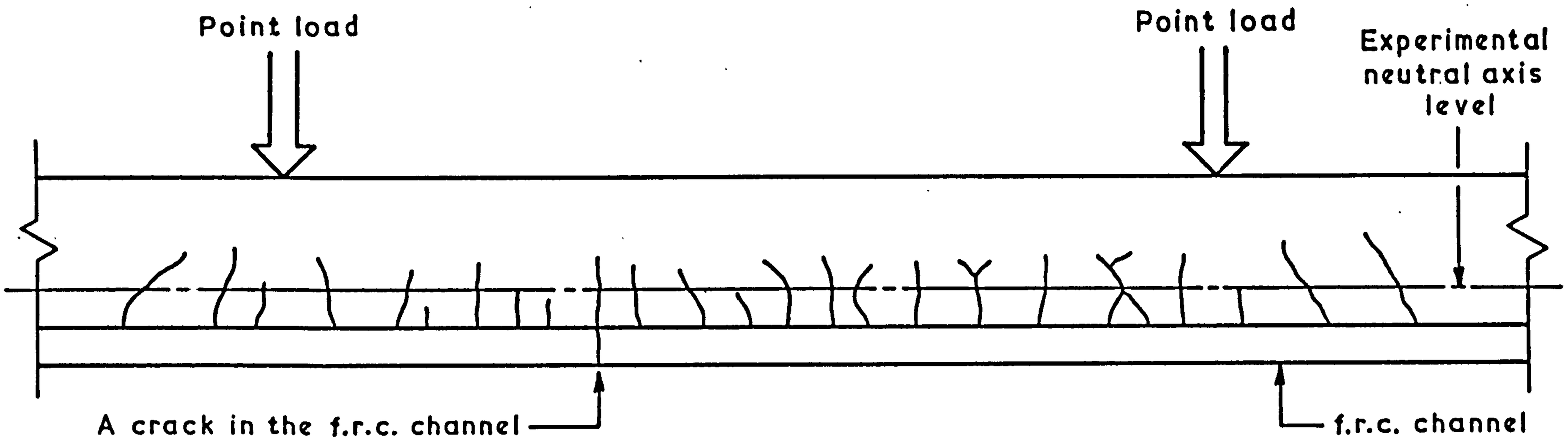

SU2-C

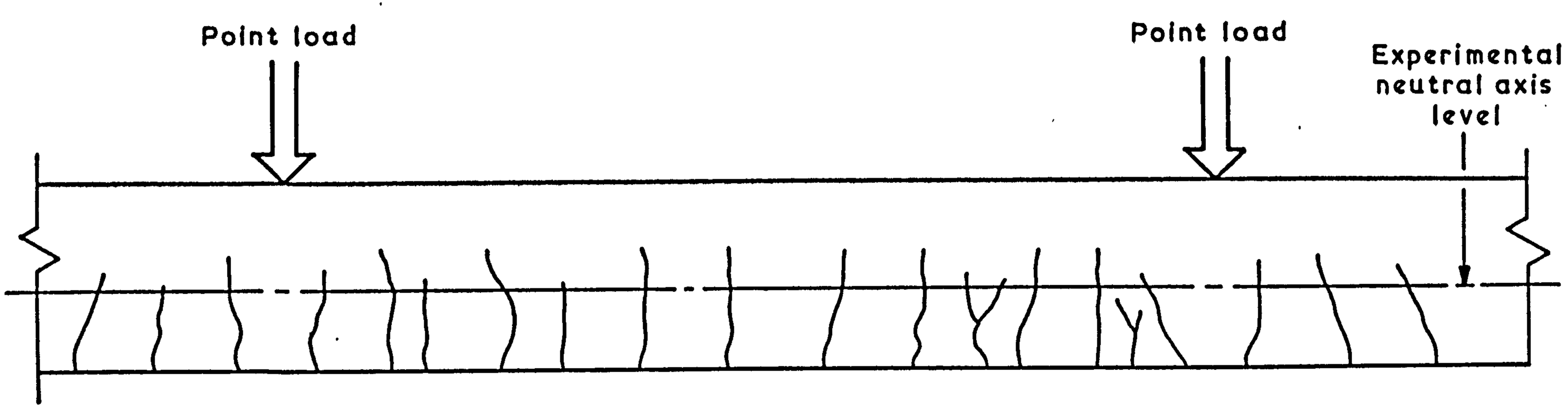

SU2-O

FIG.70 CRACKS PATTERN FOR ORDINARY AND COMPOSITE BEAMS AFTER 500 days OF SUSTAINED WORKING LOAD

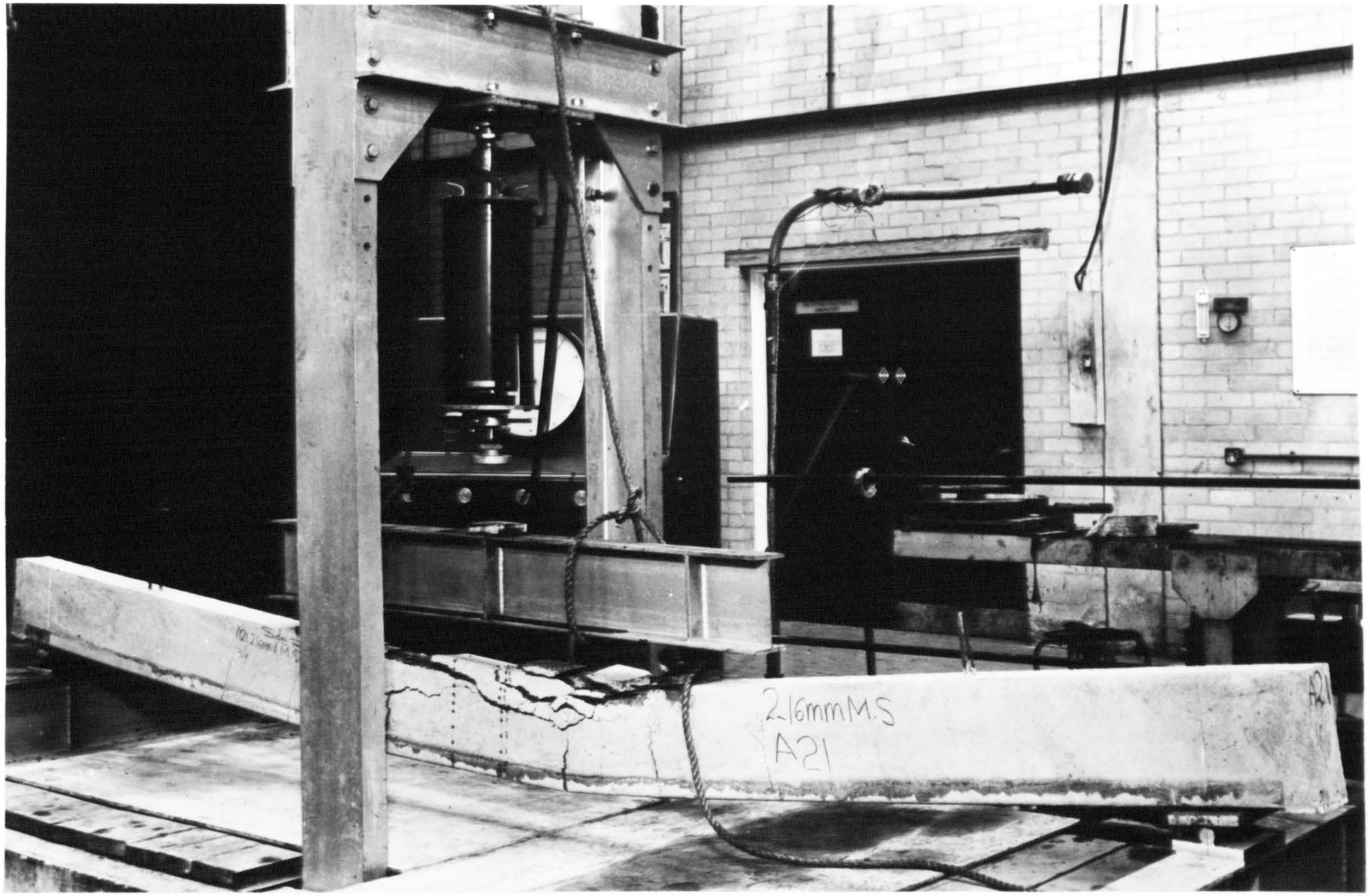

PLATE I COMPOSITE BEAM IN TEST RIG AFTER FAILURE (STI-C)

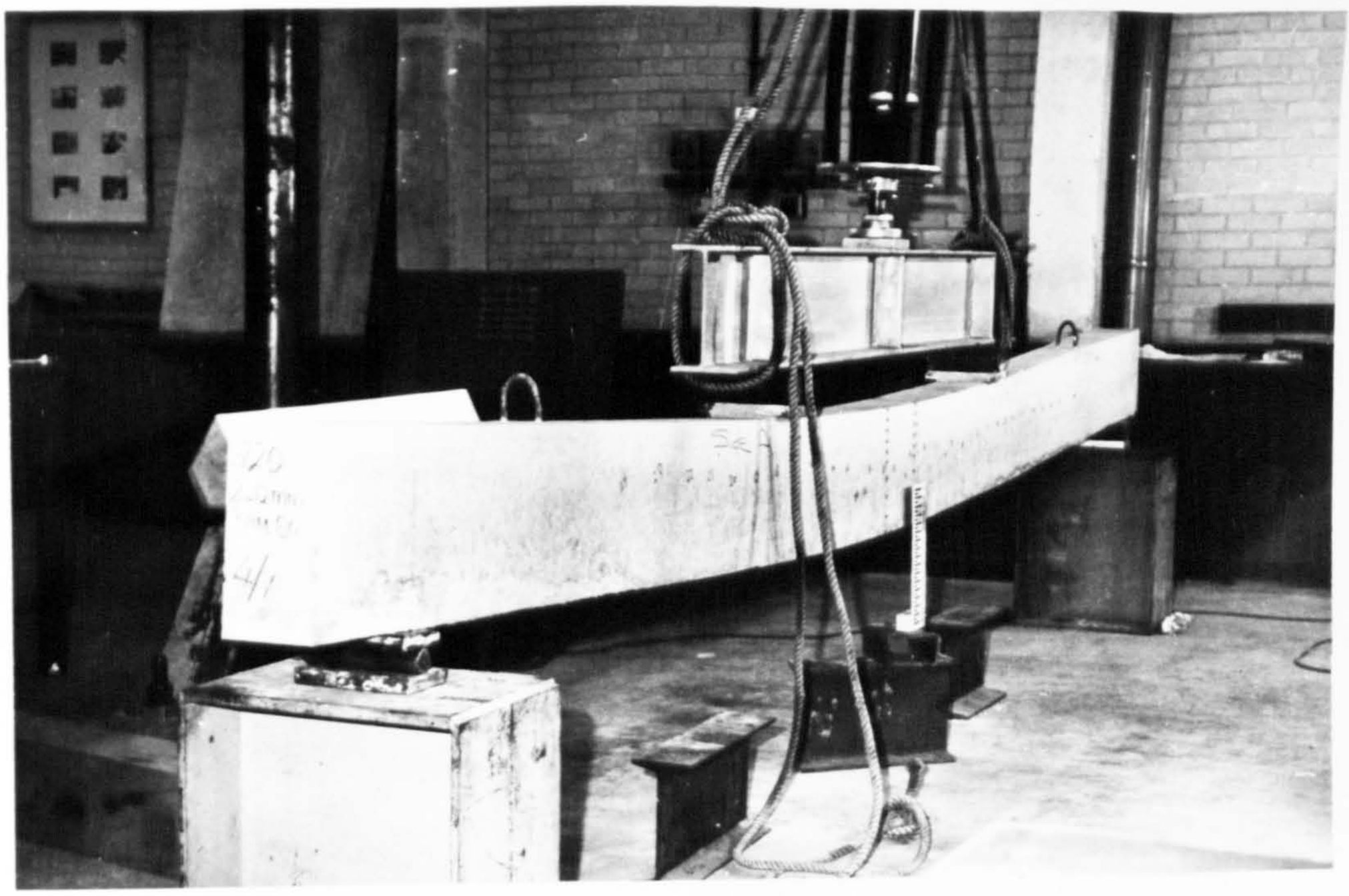

(a) Ordinary reinforced beam (ST10-O)

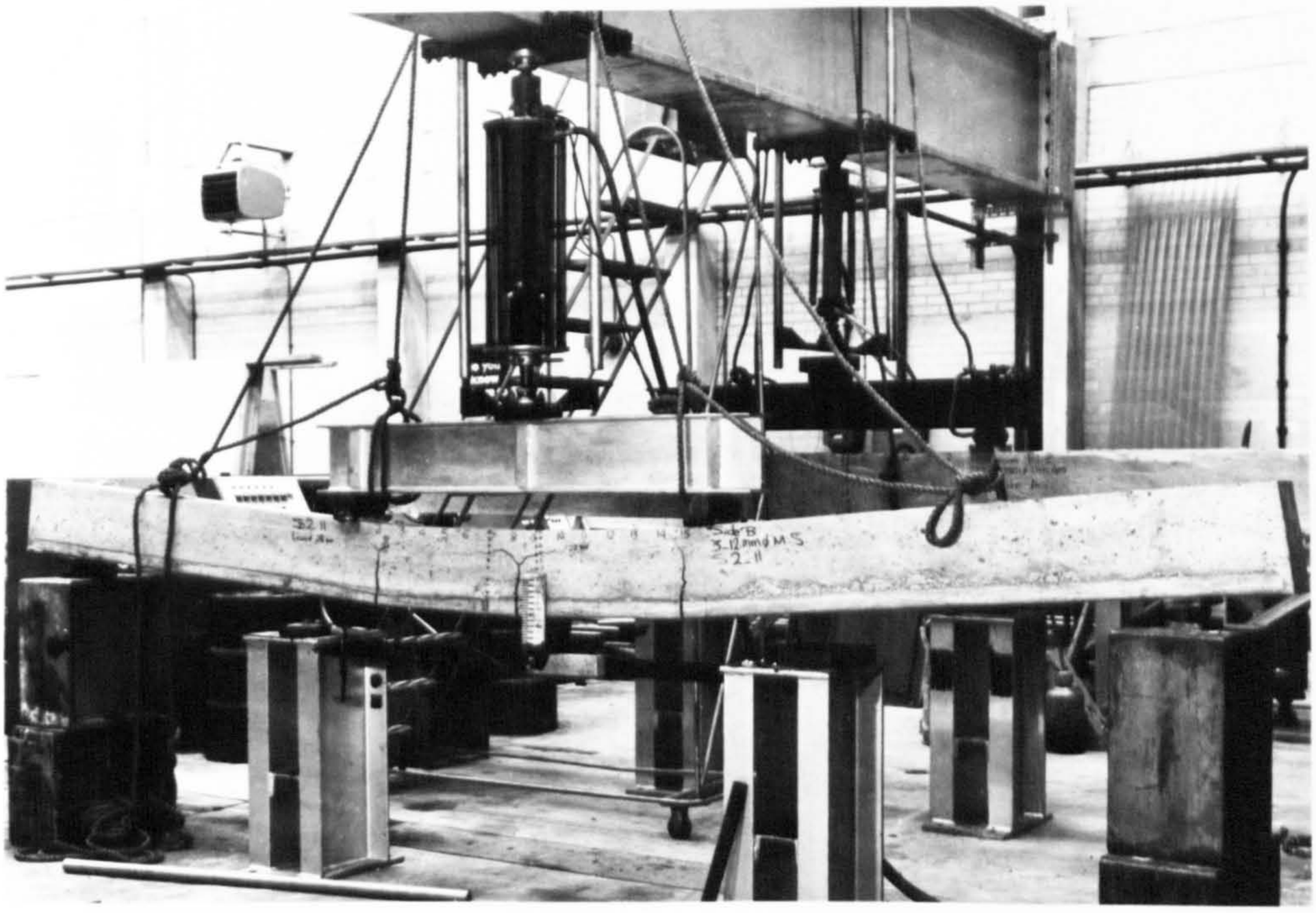

(b) Composite beam (ST11-C)

PLATE 2 CONDITIONS OF BEAMS JUST BEFORE FAILURE

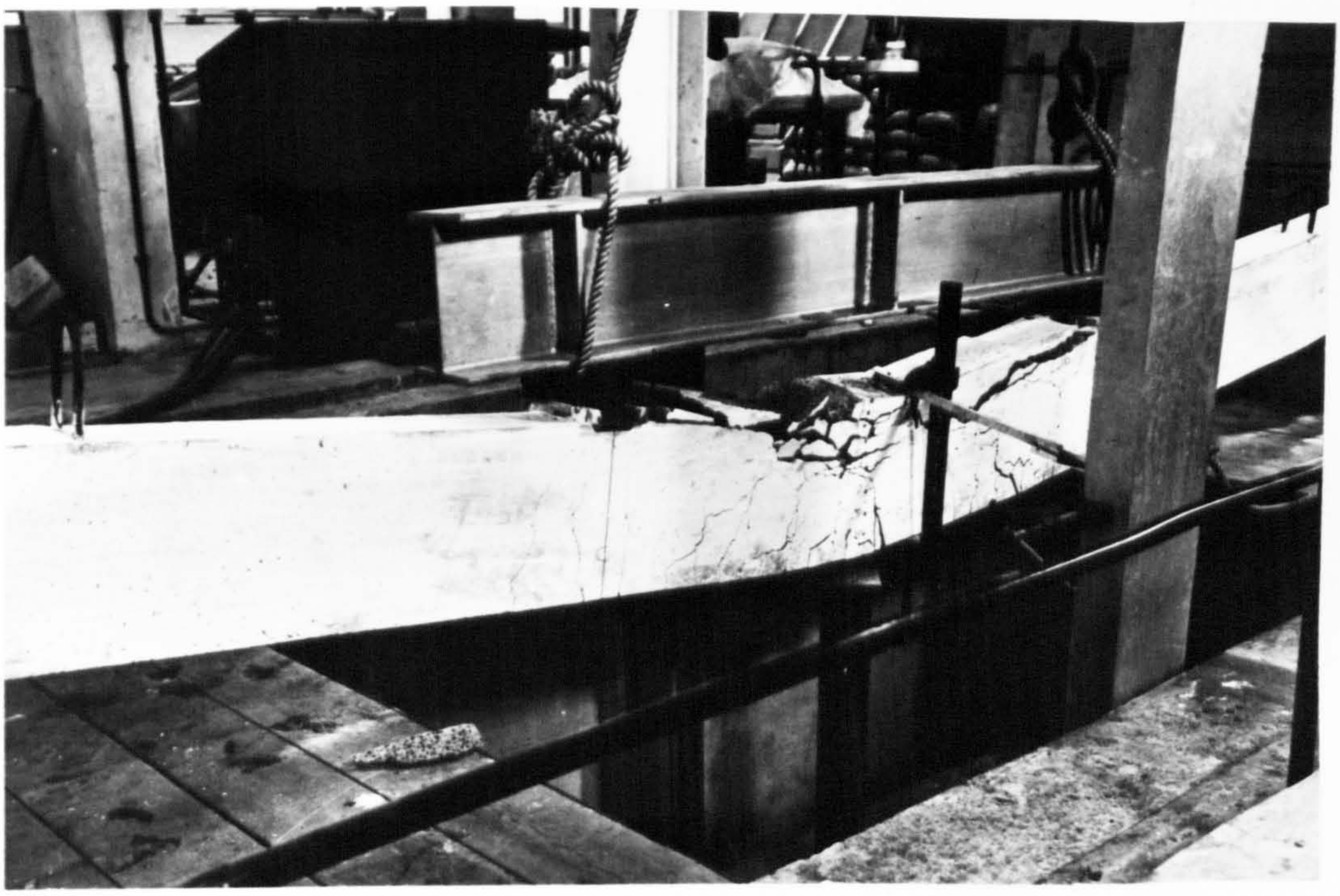

(a) Ordinary reinforced beam (ST3-O)

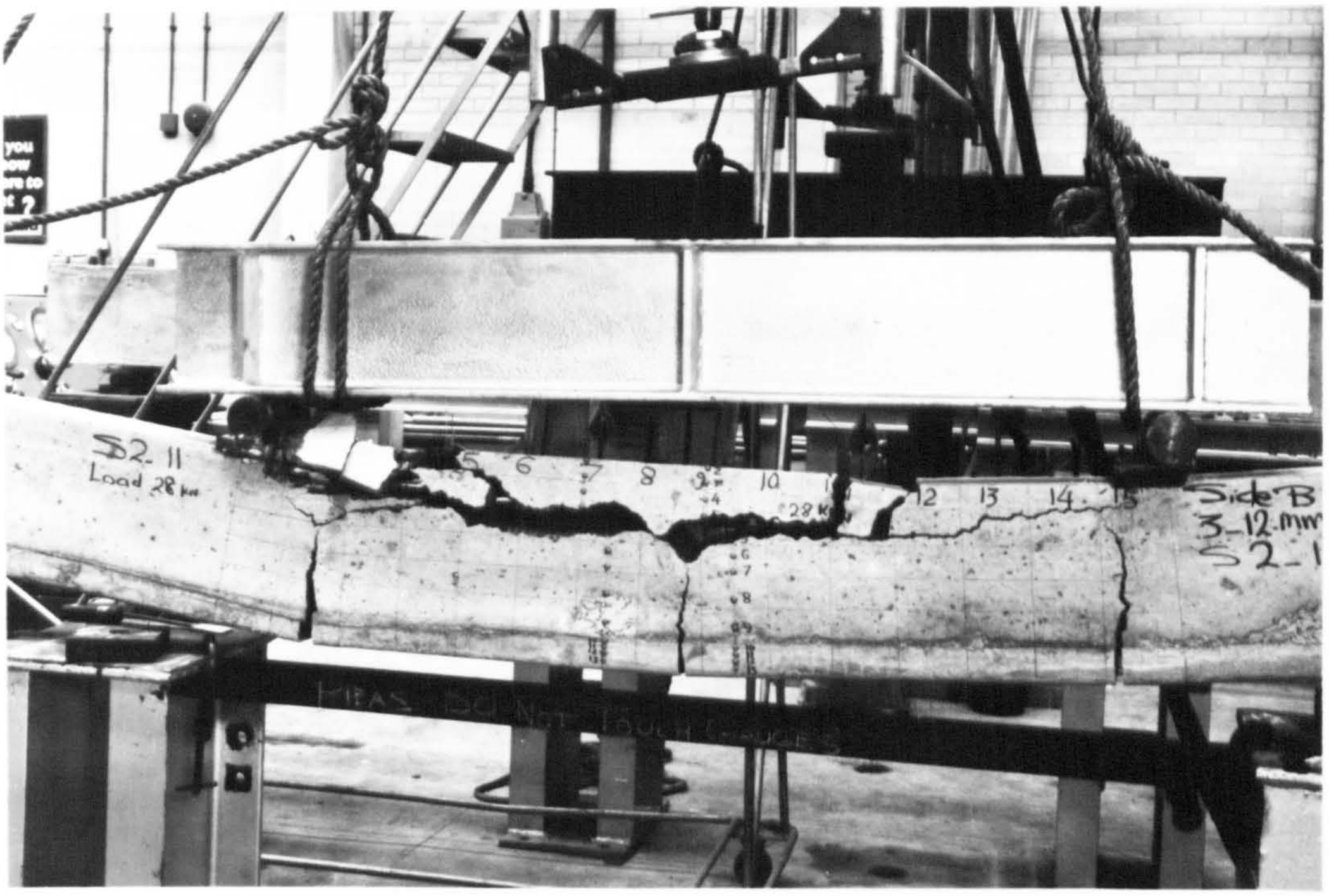

(b) Composite beam (STII-C)

PLATE 3 CONDITIONS OF BEAMS AFTER FAILURE

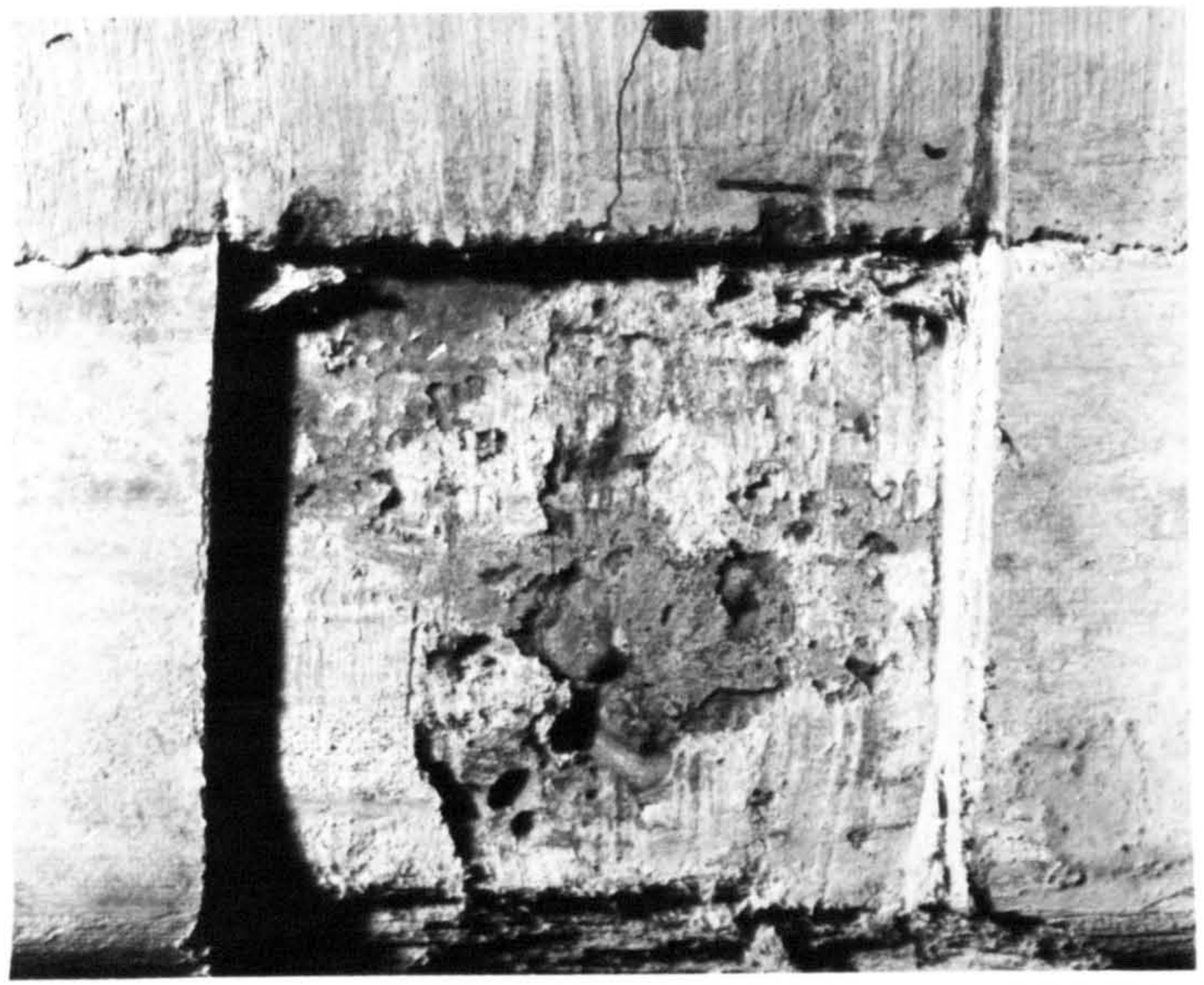

(a)

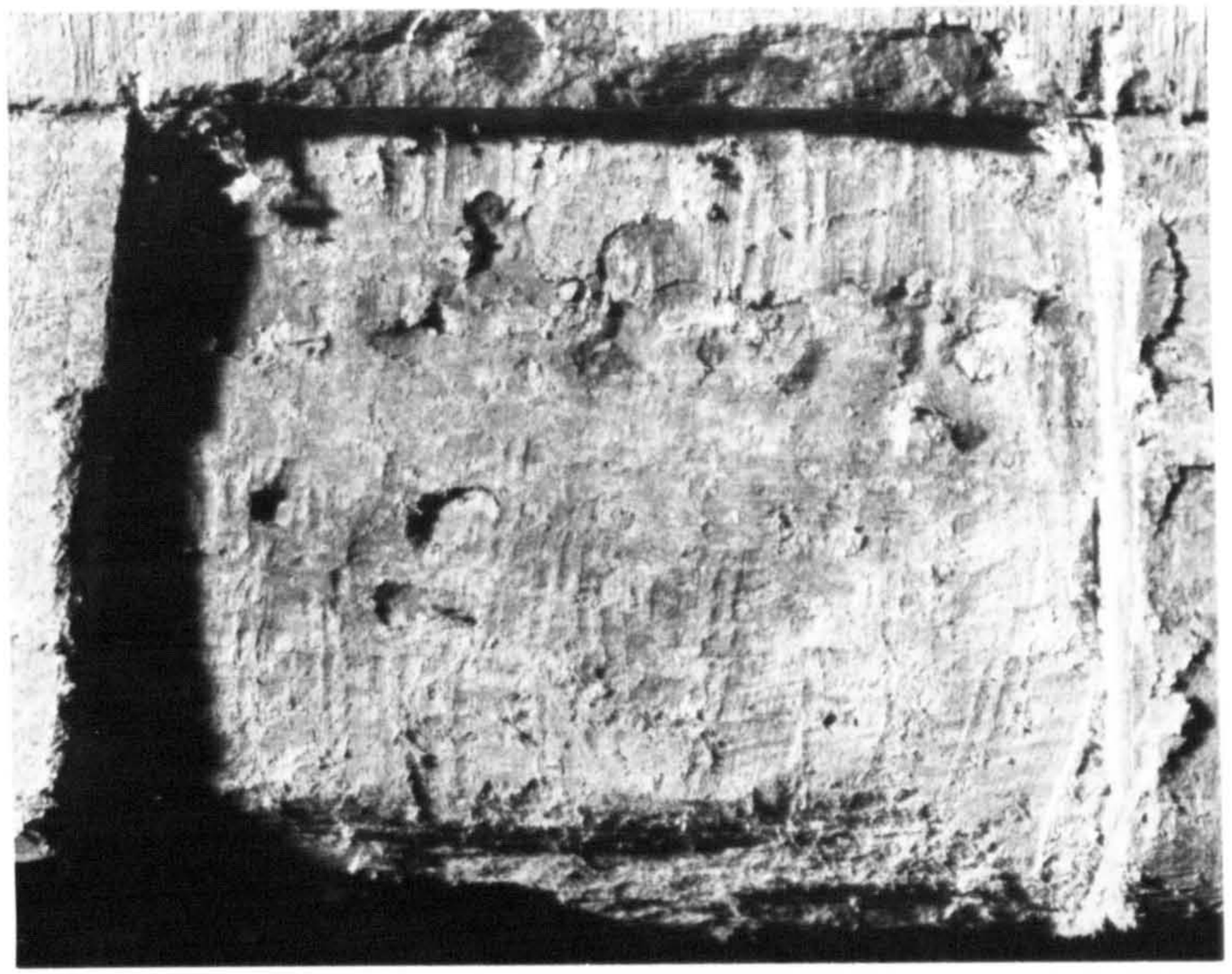

(a)

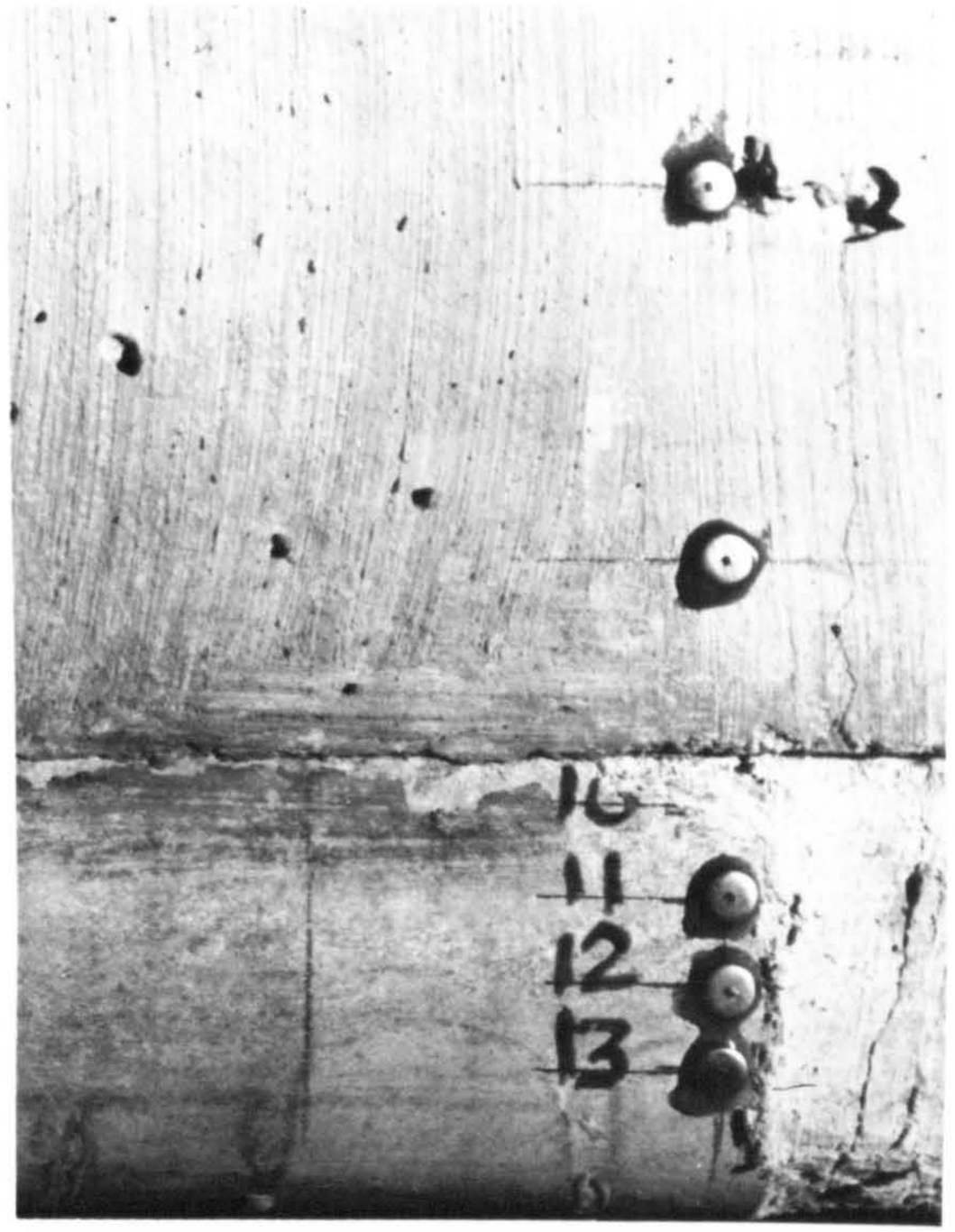

(b)

(a) No visible cracks in the confined concrete (channel did not crack)

(b) Visible cracks in the confined concrete (channel cracked)

PLATE 4 OBSERVATIONS OF CRACKS IN THE CONFINED CONCRETE (ST3-C)

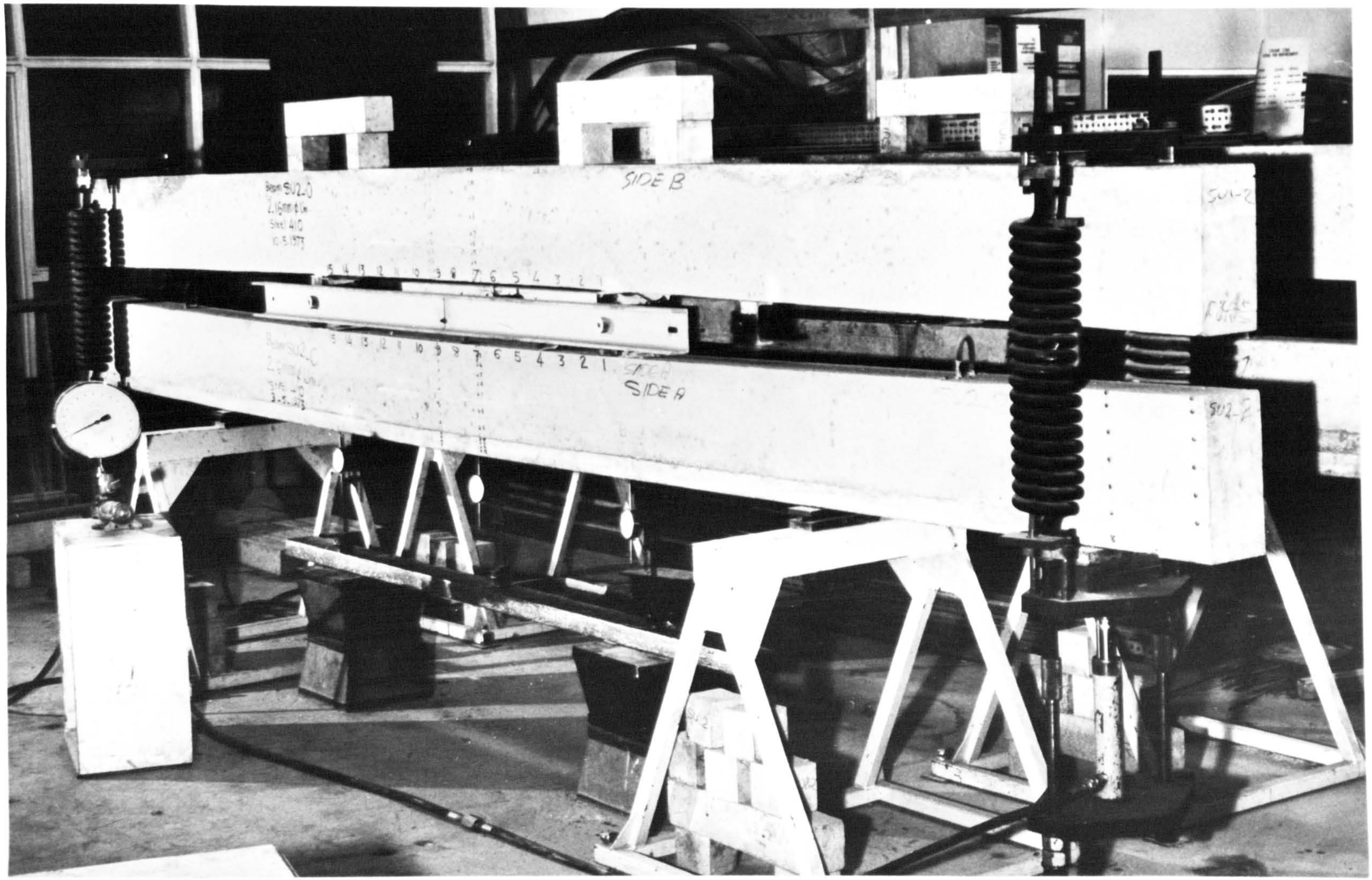

PLATE 5 ARRANGEMENT FOR SUSTAINED LOADING TEST

APPENDIX (A)

Derivation of stress-strain relationship of lightweight concrete

The equation of a parabolic curve Fig. 6a for $0 \leq e_c \leq e_j$ is

$$\sigma_c = ae_c^2 + be_c + c$$

Where a, b, and c are constants

$$\text{At} \quad \sigma_c = 0, \quad e_c = 0 \quad \text{and} \quad c = 0$$

$$\text{At} \quad e_c = e_j, \quad \frac{d\sigma_c}{de_c} = 0$$

Therefore

$$\left(\frac{d\sigma_c}{de_c}\right)_{e_c = e_j} = 0 = 2ae_j + b$$

$$\text{At } e_c = 0 \quad \frac{d\sigma_c}{de_c} = E_c$$

Therefore

$$\left(\frac{d\sigma_c}{de_c}\right)_{c_c = 0} = E_c = b$$

From the above equations

$$b = E_c$$

$$a = -\frac{E_c}{2e_j}$$

Therefore :

$$\sigma_c = E_c e_c - \frac{E_c}{2e_j} e_c^2 = E_c \left(e_c - \frac{e^2_c}{2e_j}\right)$$

By substituting in this equation $\sigma_c = \sigma_o$ and $e_c = e_j$

$$E_c = \frac{2\sigma_o}{e_j}$$

The equation of σ_c can be written as

$$\sigma_C = \frac{2\sigma_o}{e_j} \left(e_c - \frac{e^2_c}{2e_j}\right)$$

The value of e_j therefore can be obtained from the equation

$$e_j = \frac{2\,\sigma_o}{E_c}$$

As per CP110

$$\sigma_o = \frac{0.67\, f_{cu}}{\gamma_m}$$

$$E_c = 5500\sqrt{\frac{f_{cu}}{\gamma_m}}\left(\frac{Dc}{2300}\right)^2$$

Substituting the values of σ_o and E_c as given in CP110.

$$e_j = \frac{2 \times 0.67\, f_{cu}}{\gamma_m \times 5500\sqrt{\frac{f_{cu}}{\gamma_m}}\left(\frac{D_c}{2300}\right)^2} = \frac{1}{4100\left(\frac{D_c}{2300}\right)^2}\sqrt{\frac{f_{cu}}{\gamma_m}}$$

$$= \frac{1.29 \times 10^3}{D_c^2}\sqrt{\frac{f_{cu}}{\gamma_m}} = \frac{1}{2510}\sqrt{\frac{f_{cu}}{\gamma_m}} = \frac{\sqrt{f_{cu}}}{3075} \qquad \text{(for } D_c = 1800 \text{ Kg/m}^3 \text{ and } \gamma_m = 1.5\text{)}.$$

for $f_{cu} = 50\ N/mm^2$

$$e_j = 0.0023$$

Without incorporating the partial safety factor see Fig.6a.

$$e_j = \frac{2 \times 0.67\, f_{cu}}{5500\sqrt{f_{cu}}\left(\frac{D_c}{2300}\right)^2} = \frac{\sqrt{f_{cu}}}{4100\left(\frac{D_c}{2300}\right)^2}$$

$$= \frac{1.29 \times 10^3\sqrt{f_{cu}}}{D_c^2} = \frac{\sqrt{f_{cu}}}{2510} \qquad \text{(for } D_c = 1800 \text{ Kg/m}^3\text{)}$$

For $f_{cu} = 50\ N/mm^2$

$$e_j = 0.00282$$

APPENDIX (B)

Derivation of β and α Factors of the Ultimate Load Conditions

Assume Dc (density of concrete) = 1800 Kg/m^3

(a) Incorporating the materials partial safety factors γ_m (1.5 for concrete and 1.15 for steel).

Refering to Fig. 6a The strain and stress distribution of the ultimate condition across the depth of the beam would be as follows:

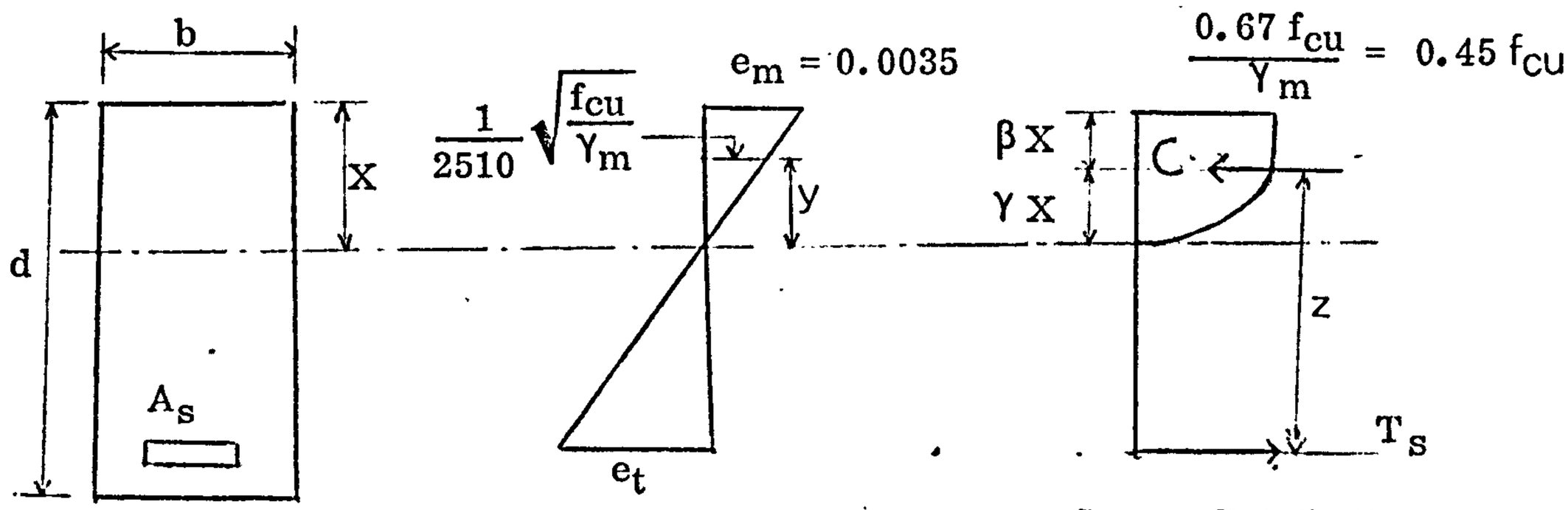

Cross Section | Strain distribution at ultimate condition | Stress distribution at ultimate condition

From strain distribution $y = X\sqrt{f_{cu}}\ /10.76$

Total compressive force $C = 0.45\ f_{cu}.b.X - \frac{1}{3} \times 0.45\ b.X.f_{cu}.\sqrt{f_{cu}}\ /10.76$

$= (0.45 - \frac{0.45\sqrt{f_{cu}}}{3}\ /10.76)\ b.X.f_{cu}.$

$= \alpha.b.X,f_{cu}$

Taking moments of area of the stress block about the neutral axis:

$$\alpha X.\ f_{cu}\ \gamma X = (0.45.\ X.\frac{X}{2}\ f_{cu} - \frac{0.45}{3}\ y.\frac{y}{4}\ f_{cu}).$$

Substituting by y and take X out

$$\alpha\ \gamma = \frac{0.45}{2} - \frac{0.45}{12}\ \frac{f_{cu}}{(10.76)^2}$$

$$\gamma = \frac{694 - f_{cu}}{3087\ \alpha}$$

For the ultimate moment based on steel;

to obtain the neutral axis depth, equate the internal forces

$$C = T_s$$

$$a\ b.X.\ f_{cu} = \frac{f_y}{\gamma_m} \quad A_s$$

$$X = \frac{f_y\ A_s}{\gamma_m a b.f_{cu}}$$

$$\beta = 1 - \gamma$$

$$z\ (\text{lever arm}) = d_1 - \beta X = d_1 - \frac{\beta f_y\ A_s}{a\gamma_m\ b.f_{cu}} = d_1\ (1 - \frac{\beta f_y\ p}{a\gamma_m f_{cu}})$$

The ultimate resistance moment based on steel;

Therefore $M_u = \frac{f_y}{\gamma_m}\ A_s\ d_1\ (1 - \frac{\beta f_y\ p}{a\gamma_m f_{cu}})$

For $f_{cu} = 50\ N/mm^2$ in the equation of the total compressive force

$$a = 0.351$$

Hence:

$$\gamma = 0.594$$

$$\beta = 1 - \gamma = 1 - 0.594 = 0.406$$

Substituting the values of β and γ and ($\gamma m = 1.15$) in the equation of the ultimate resistance moment based on steel:

$$M_u = \frac{f_y}{1.15}\ A_s\ d_1\ (1 - \frac{f_y\ p}{f_{cu}})$$

The ultimate resistance moment based on the concrete would be equal to:

(assume $X = \frac{d_1}{2}$)

$$M_u = a\ b\ \frac{d_1}{2}\ f_{cu}\ (d_1 - \beta\frac{d_1)}{2}$$

$$= 0.351 \times \frac{1}{2}\ d_1^{\,2}\ f_{cu}\ (1 - \frac{0.406)}{2}$$

$$= 0.14\ f_{cu}\ bd_1^{\,2}$$

(b) <u>Without incorporating the material partial safety factors:</u>

The stress-strain relationship of the concrete is shown in Fig. 6a

With the same method of analysis for $f_{cu} = 50\ N/mm^2$

$$\alpha = 0.49$$

$$\gamma = 0.61$$

$$\beta = 0.39$$

Therefore, the ultimate resistance moment based on steel is:

$$M_u = f_y \; A_s \; d_1 \; (1 - \frac{0.793 \, f_y \, p}{f_{cu}})$$

the ultimate resistance moment based on the concrete would be equal to:

(assume $X = \frac{d_1}{2}$)

$$M_u = 0.197 \; f_{cu} \, b \, d_1^{\,2}$$

APPENDIX (C)

Working and Ultimate Moments of Test Beams

Beam ST 3-0 and ST 3-C

Based on nominal strength

$b \times d = 150mm \times 300mm$

$f_y = 550\ N/mm^2$

$f_{cu} = 50\ N/mm^2$

$A_s = 402.286\ mm^2$

$d_1 = 257mm$

$p = 1.044\%$

$L = 4.5m$

$D_c = 1800\ Kg/m^3$

Limit State of Ultimate Strength

Incorporating the partial safety factors of the materials the ultimate design moment of the section is:-

$$M_u = \frac{f_y}{\gamma_m} A_s d_1 \left(1 - \frac{\beta f_y p}{a \gamma_m f_{cu}}\right).$$

For $f_{cu} = 50\ N/mm^2$

$a = 0.351$

$\beta = 0.406$

$$M_u = \frac{550}{1.15} \times 402.286 \times 257 \left(1 - \frac{550 \times 1.044}{50}\right) \times 10^{-6}$$

$= 43.77\ KN.m$

The moment due to the dead weight of the simply supported beam is $\frac{wl^2}{8}$

$$= 1800 \times 0.15 \times 0.3 \times \frac{(4.5)^2}{8} \times \frac{10}{1000} \simeq 2.05\ KN.m \quad (say\ 2KN.m)$$

The partial safety factor (γ_1) due to dead load = 1.4, therefore, the ultimate design moment due to dead load moment = 2 x 1.4 = 2.8 KN.m

The applied ultimate design moment for the beam (live load) is 43.77 - 2.8 = 40.97 KN.m.

The partial safety factor (γ_l) for live load is 1.6, therefore, the applied working design moment of the beam (M_{dw}) is $\frac{40.97}{1.6} = 25.61$ KN.m

The working load (W) is

$$\frac{W}{2} \times 1.5 = 25.61$$

$$W = 34.15 \text{ KN.}$$

Shear resistance

Reference should be made to 3.3.6.1 in CP110, equation 8.

$$v = \frac{V}{bd_1}$$

The ultimate resistance moment of the beam is 43.77 KN.m (appendix C), therefore, with a simply supported beam of 4.5m span loaded at 1/3 the span length,

$$V = \frac{43.77}{0.75} = 58.36 \text{ KN (Ultimate load)}$$

$$v = \frac{58360}{150 \times 257} = 1.514 \text{ N/mm}^2$$

The value of $v_c = 0.6$ N/mm^2 for p = 1% and concrete grade of 40 or more (3.12.4 in CP110)

$v > v_c$ therefore shear reinforcement are needed. Mild steel stirrups of 6mm diameters are to be used.

$$\frac{A_{sv}}{S_v} \geq \frac{(v - v_c)b}{.87 f_{yv}} \qquad \text{(3.3.6.1 CP110.)}$$

$$\frac{56.6}{S_v} = \frac{150 (1.514 - 0.6)}{0.87 \times 275}$$

$S_v = 98.77$mm

The spacing provided was 100mm.

Bond stress

Reference should be made to paragraph (3.11.6 in CP110)

Local bond

(3.11.6.1 in CP110)

$$f_{bs} = \frac{V}{\Sigma u_s d_1}$$

$V = 58.36$ KN

$u_s = 2 \times 16 \times \frac{22}{7} = 100.57$mm

$d_1 = 257$

$$f_{bs} = \frac{58360}{100.57 \times 257} = 2.258 \text{ N/mm}^2$$

The ultimate local bond stress allowed in CP110 for grade 50 lightweight concrete for deformed bars is $0.8 \times 3.4 = 2.72 \text{ N/mm}^2$. (3.11.6.1 and 3.12.11 in CP110)

Anchorage bond

(3.11.6.2 in CP110)

The force in the bar $= \frac{f_y}{\gamma_m} A_s$

$$= \frac{550}{1.15} \times 201.143 = 96.2$$

Anchorage length = 1.5m

effective perimeter of bars $= 16 \times \frac{22}{7} = 50.28$mm

Anchorage bond stress $= \frac{96.2 \times 10^3}{1500 \times 50.28} = 1.276 \text{ N/mm}^2$

The ultimate anchorage bond stress for grade 50 N/mm^2 lightweight concrete for deformed bar in tension is 2.6 N/mm^2

$1.275 < 2.6$ O.K. (3.12.6.2 and 3.12.11 in CP110)

APPENDIX (D)

Derivation of Equations for the Neutral Axis Depth

D1_ Neutral axis depth for uncracked composite section (X_{uc})

Uncracked stage for $0 \leq M/M_u \leq C_o$

Take moments of area about the top edge of the section considering an uncracked transformed section:

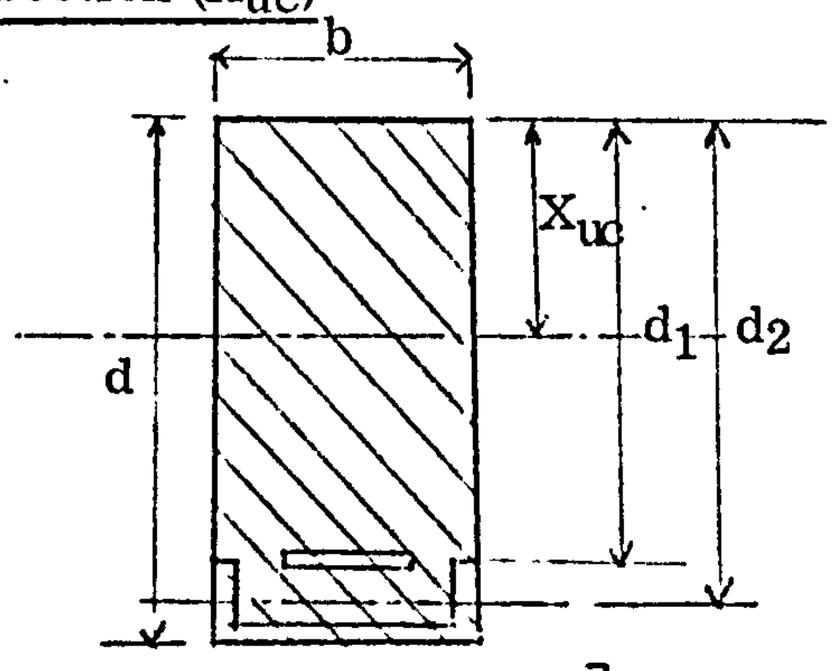

$$bd(d/2) + (m-1)A_s d_1 + (m_1 - 1)A_{ch}\, d_2 = \left[bd + (m-1)A_s + (m_1 - 1)A_{ch}\right] X_{uc}$$

From this equation and by substituting $p = A_s/bd_1$, $p_1 = A_{ch}/bd_2$, $\lambda = d/d_1$

and $\eta = d_2/d_1$

$$n = \frac{X_{uc}}{d_1} = \frac{0.5\ \lambda^2 + (m-1)p + (m_1 - 1)p_1\ \eta^2}{\lambda + (m-1)p + (m_1 - 1)p_1\,\eta}$$

D2_ Neutral axis depth for cracked composite section (X_{cc})

Cracked stage for $C_1 \leq M/M_u \leq C_2$

Take moments of area about the neutral axis level considering a cracked transformed section.

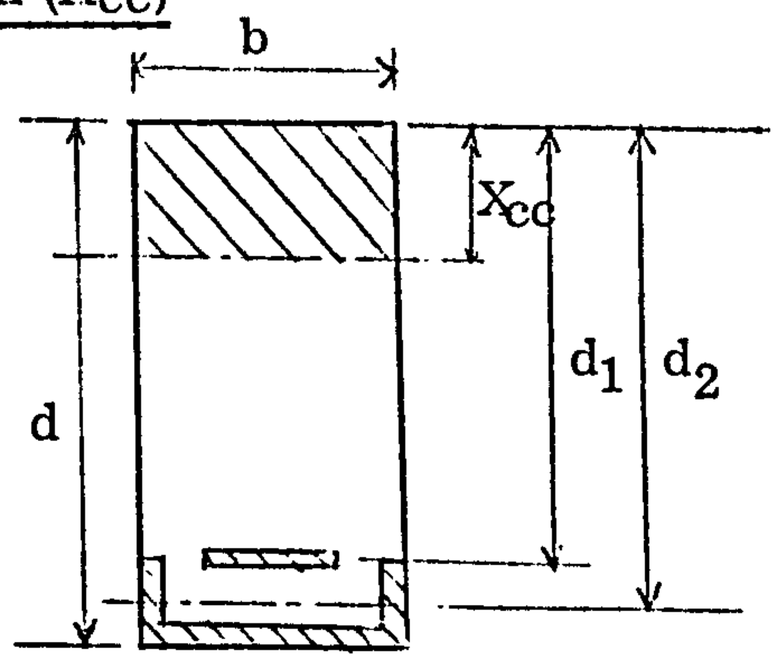

$$b\,X_{cc}\,(X_{cc}/2) = m\,A_s\,(d_1 - X_{cc}) + m_1\,A_{ch}\,(d_2 - X_{cc})$$

For this equation and by substituting $p = A_s/bd_1$, $p_1 = A_{ch}/bd_2$, $\eta = d_2/d_1$

$$n = \frac{X_{cc}}{d_1} = (mp + m_1\,p_1\,\eta\ )\left(\sqrt{1 + \frac{2\,(mp + m_1\,p_1\eta^2)}{(mp + m_1\,p_1\eta)^2}} - 1\right)$$

D3 Neutral axis depth at the transition stage

Transition stage For $C_o \leq M/M_u \leq C_1$ (Composite beams)

Reference can be made to Fig. 10

The equation of the assumed parabolic curve is

$$X = aR^2 + bR + C \qquad (1)$$

Where: $R = M/M_u$ and a, b and c are constants

The boundry conditions are:

$$X = X_{uc} \quad \text{at} \quad R = C_o \qquad (a)$$

$$X = X_{cc} \quad \text{at} \quad R = C_1 \qquad (b)$$

$$dx/dR = 0 \quad \text{at} \quad R = C_1 \qquad (c)$$

Substituting boundry condition (a) in equation 1

$$X_{uc} = a\,C_o^{\,2} + b\,C_o + C \qquad (2)$$

Substituting boundry condition (b)

$$X_{cc} = a\,C_1^{\,2} + b\,C_1 + C \qquad (3)$$

$$C = X_{cc} - a\,C_1^{\,2} - b\,C_1 \qquad (4)$$

Differentiate equation (1) and substitute boundry condition (c)

$$dx/dR = 2aR + b \qquad (5)$$

$$0 = 2aC_1 + b \qquad (6)$$

$$b = -2aC_1 \qquad (7)$$

Substitute equation (7) and equation (4) in equation (2)

$$X_{uc} = a\,C_o^{\,2} - 2aC_1C_o + X_{cc} - a\,C_1^{\,2} + 2aC_1^{\,2} \qquad (8)$$

$$a = \frac{X_{uc} - X_{cc}}{C_o^{\,2} - 2C_1C_o + C_1^{\,2}} \qquad (9)$$

$$b = -2\,\frac{X_{uc} - X_{cc}}{C_o^{\,2} - 2C_1C_o + C_1^{\,2}}\,C_1 \qquad (10)$$

From equation (1):

$$X = aR^2 + bR + X_{cc} - aC_1^{\,2} - bC_1 \qquad (11)$$

$$X = \frac{X_{uc} - X_{cc}}{C_o^{\,2} - 2C_1\,C_o + C_1^{\,2}} \left[R^2 - 2C_1R + C_1^{\,2} \right] + X_{cc}$$

APPENDIX (E)

Derivation of the coefficients β and α to determine the centroid and area of the compressive stress distribution diagram in concrete. Reference can be made to Fig.12

(a) Determination of β

(i) When $e_c \leq e_j$

The equation of the parabola is :

$$\sigma_c = \frac{2\sigma_o}{e_j}\left(e_c - \frac{e_c^2}{2e_j}\right)$$ See appendix (A)

The centroid of the area from the y-axis which can also represent the neutral axis depth in flexural member, at any value of e_c can be obtained from the following:

$$e_o \int_o^{e_c} \sigma_c \, de_c = \int_o^{e_c} \sigma_c \, e_c \, de_c \, .$$ (e_o is the distance for the centroid of the area from the y-axis).

$$e_o \int_o^{e_c} 2\frac{\sigma_o}{e_j}\left(e_c - \frac{e_c^2}{2e_j}\right) de_c = \int 2\frac{\sigma_o}{e_j}\left(e_c - \frac{e_c^2}{2e_j}\right) e_c \, de_c \, .$$

$$e_o\left[\frac{e_c^2}{2} - \frac{e_c^3}{6e_j}\right] = \frac{e_c^3}{3} - \frac{e_c^4}{8e_j}$$

From this equation:

$$e_o = \frac{8e_c\, e_j - 3e_c^2}{12\, e_j - 4e_c}$$

By substituting $e_o = \gamma\, e_c$

$$\gamma = \frac{8e_j - 3e_c}{12\, e_j - 4e_c}$$

The value of β to calculate the distance of the centroid relative to the value e_j is equal to $1 - \gamma$

Therefore $\beta = 1 - \frac{8e_j - 3e_c}{12e_j - 4e_c} = \frac{4e_j - e_c}{12e_j - 4e_c}$

(ii) When $e_j \leq e_c \leq e_{max}$

Taking moments of area about the vertical line at e_c which also represent strain at the extreme element of the compression zone of a flexural member.

$$\left[\sigma_o (e_c - e_j) + \tfrac{2}{3} \sigma_o e_j\right] \beta e_c = \sigma_o (e_c - e_j)^2 / 2 + \tfrac{2}{3} \sigma_o e_j \left(\tfrac{3}{8} e_j + e_c - e_j\right)$$

From this equation the value of the coefficient β at any value of e_c is equal to

$$\beta = \frac{6e_c^2 - 4e_c e_j + e_j^2}{12e_c^2 - 4e_c e_j}$$

(b) Determination of a

(i) When $e_c \leq e_j$

The area at any value of e_c is assumed to be equal to $a \sigma_c e_c$

Considering the equation of the parabola given in appendix (A)

$$a \sigma_c e_c = \frac{2 \sigma_o}{e_j} \int \left(e_c - \frac{e_c^2}{2e_j}\right) de_c$$

Substituting the value of σ_c and integrate

$$a \frac{2 \sigma_o}{e_j} \left(e_c - \frac{e_c^2}{2e_j}\right) e_c = \frac{2 \sigma_o}{e_j} \left[\frac{e_c^2}{2} - \frac{e_c^3}{6e_j}\right]$$

From this equation:

$$a = \frac{3e_j - e_c}{6e_j - 3e_c}$$

(ii) When $e_j \leq e_c \leq e_{max}$

The area at any value of e_c is assumed to be equal to $a \sigma_o e_c$

Therefore

$$a \sigma_o e_c = \tfrac{2}{3} \sigma_o e_j + \sigma_o (e_c - e_j)$$

From this equation:

$$a = \frac{3e_c - e_j}{3e_c}$$

APPENDIX (F)

THEORIES FOR THE CALCULATION OF DEFLECTION

F1- General

In order to calculate the deflection of a flexural member, the distribution of the curvature along the span of the beam should be known. The differential equation of flexural is given in the following expression:-

$$\frac{1}{r_b} = \frac{d^2a}{ds^2} \qquad (A1)$$

where a : Vertical deflection

s : Distance measured along the beam

r_b : Radius of curvature

For beams in which the moment curvature relationship is linear, the equation can be integrated to obtain the following expression :-

$$a = k\,\phi l^2 \qquad (A2)$$

To calculate the curvature of a beam, it is important to classify whether the section is in a cracked or uncracked condition. The curvature of an uncracked member can be calculated using the conventional method based on a homogeneous concrete section as discussed in 5.3.1. For a cracked section, it is important to consider the contribution of the concrete in the tensile zone in calculating the curvature of the member. This, however, has been thought of in the past and the contribution of the concrete in tension was considered in different ways.

In the following, the various methods proposed are discussed.

F2- Assessment of the curvature for a cracked reinforced concrete member

In the past, the analysis of a cracked member was carried out assuming a completly cracked section where the concrete in the tensile zone being ignored. The curvature was obtained from the following equation:-

$$\phi = \frac{M}{E_c I_c} \qquad (A3)$$

or

$$\phi = \frac{e_s}{d_1 - X_c} \qquad (A4)$$

e_s = Strain in the steel reinforcement calculated without considering the contribution of the concrete in tension.

It was realised, however, that this approach considerably over estimated the amount of deflection. This was mainly due to the contribution of the concrete in tension was not considered.

The contribution of the cracked concrete in the tensile zone of flexural members was taken into consideration in the subsequent methods proposed by various investigators in different approaches.

YU and Winter (84) proposed a method where the curvature of the beam under working load can be calculated based on an average second moment of area (I_{ave}) of the beam. The contribution of the concrete between the cracks in the tensile zone is considered in calculating the average second moment of area as follows:

$$I_{ave} = \frac{I_c}{1 - M/M_{dw}} \qquad (A5)$$

In which

$$M = 0.1 \ (f_c')^{\frac{2}{3}} \ bd \ (d - X_c)$$

Consequently the curvature of the beam is calculated from

$$= \frac{M_{dw}}{E_c I_{ave}} \qquad (A6)$$

f_c' = Cylinder compressive strength of concrete.

The derivation of the equation of M' followed an elastic theory approach. A triangular stress distribution of the concrete in the tensile zone was assumed by the stress being equal to the modulus of rupture at the soffit of the beam and zero at the level of the neutral axis. The factor 0.1, however, was obtained empirically based on normal concrete beams data.

In the CEB (79) recommendations, a method was suggested to calculate the curvature by considering a bi-linear relationship for the load-deflection response, i.e. taking into account the initial uncracked behaviour. For a moment (M) greater than the cracking moment of concrete (M_{cr}), the curvature can be obtained from the following expression:-

$$\phi = \frac{M_{cr}}{E_c I_o} + \frac{M - M_{cr}}{0.75 \ E_s A_s \ d_1^2 \ (1 - 2q) \ (1 - 2/3q)} \qquad (A7)$$

For $q < 0.25$ only

In which

$$q = \frac{A_s}{bd_1} \quad \frac{f_y}{f'_c}$$

The derivation of the equatien followed an elastic theory approach.

Branson (83) presented an empirical expression of an average effective second moment of area (I_{eff}) over the entire length of a simply supported uniformly loaded beam. The expression is given in the following form:-

$$I_{eff} = \left(\frac{M_{cr}}{M}\right)^3 \quad I_o \quad + \left[1 - \left(\frac{M_{cr}}{M}\right)^3\right] \quad I_{cr} \qquad (A8)$$

The equation would only apply when M is greater than or equal to M_{cr}, otherwise $I_{eff} = I_o$. It was suggested that the second moment of area (I_o) based on an uncracked transformed section might be more accurately used instead of the gorss section especially when high percentages of steel were employed. The method does allow for the contribution of the concrete along the span length of the beam.

Beeby (85) derived an expression for the curvature taking into consideration a bi-linear relationship for the load deflection response and the variation in the modulus of elasticity of concrete at the uncracked and cracked conditions. Tests on normal weight concrete beams showed that a modified modulus of elasticity (E'_c) equal to $0.57\ E_c$ should be used. This however was simplified and the expression for the curvature was given in the form

$$\phi = \frac{M_c}{E_c\ I_o} \quad + \quad \frac{M - M_c}{0.85\ E_c\ I_{cr}} \qquad (A9)$$

In CP110 it is suggested that the curvature at mid span of a cracked flexural member can be estimated following the elastic theory approach, using the modulus of elasticity for the materials as recommended by the code. A triangular stress distribution for the concrete in tension is assumed, having a value of 1 N/mm^2 at the level of the tension reinforcement and zero at the level of the neutral axis. This would allow the average stresses in concrete and steel to be calculated. The curvature consequently can be calculated from the following :-

$$\phi = \frac{f_{ca}}{XE_c} = \frac{f_{sa}}{(d_1 - X)\,E_s} \qquad \text{(A10)}$$

Where: f_{ca} and f_{sa} are the average stresses in concrete and steel as calculated.

The method requires a trial and error approach to determin the neutral axis depth under the working moment while the tension forces balance the compressive forces in the section.

APPENDIX (G)

Sustained-Load System

(i) Calculation of the distance between the centre line of the beams and the supporting trestle to produce similar moment at mid span of the beams.

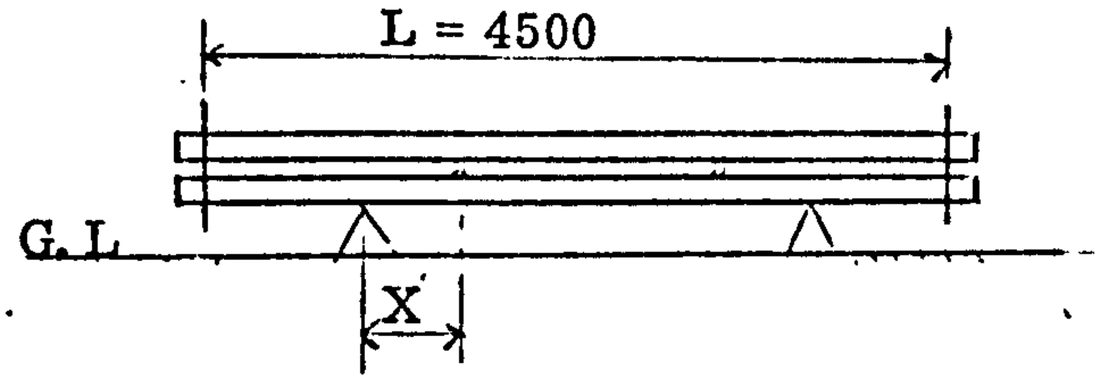

Arrangement

F : Force due to weight of the spring assembly
= 1.6 KN.

w : Weight of the beam per unit length.

$wL = 1800 \times 0.15 \times 0.3 \times 10. \times 4.5 \times 10^{-3} = 3.6$ KN.

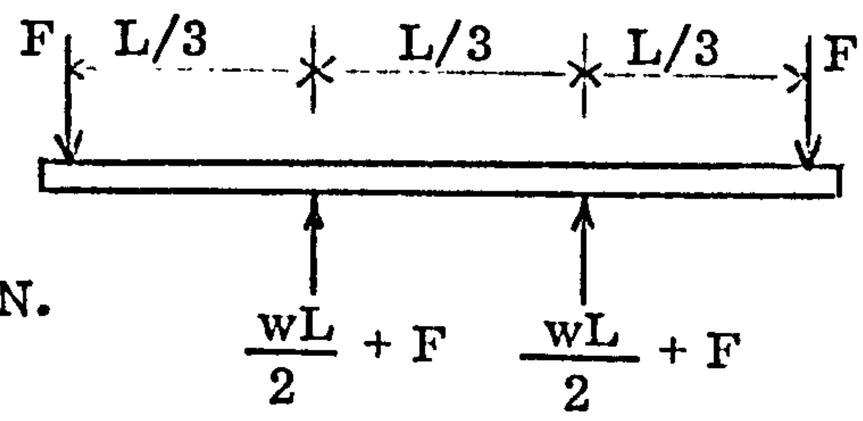

Upper beam

Upper beam

The bending moment M at mid span.

$$M = \frac{FL}{2} + \frac{wL^2}{8} - \left(\frac{wL}{2} + F\right)\frac{L}{6}$$

$$= \frac{FL}{3} + \frac{wL^2}{24}$$

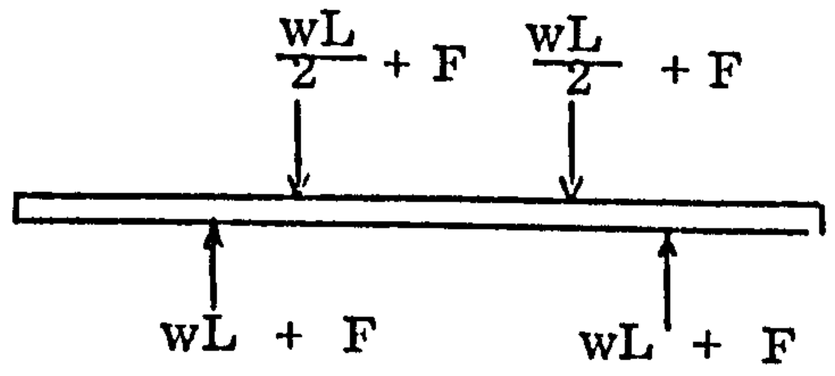

Lower beam

Lower beam

The bending moment at mid span should be equal to that obtained for the upper beam. Assume the distance between the centre line of the beams and the trestle is X. The value of X can be obtained from the following equation:

$$-\frac{wL^2}{8} - \left(\frac{wL}{2} + F\right)\frac{L}{6} + (wL + F)X = \frac{FL}{3} + \frac{wL^2}{24}$$

From this equation:

$$X = \frac{L}{4}\left(\frac{2F + wL}{F + wL}\right)$$

Considering F = 1.6 KN and wL = 3.6 KN.

$$X = \frac{4.5}{4}\left(\frac{2 \times 1.6 + 3.6}{1.6 + 3.6}\right) = 1.47m$$

The bending moment due to dead weights at mid span of the beams is:

$$M = \frac{1.6 \times 4.5}{3} + \frac{3.6 \times 4.5}{24} = 3.077 \text{ KN.m}$$

The ultimate design moment due to dead load is $3.077 \times 1.4 = 4.3$ KN.m

(ii) Deflection calculation:

(Macauley's Method)

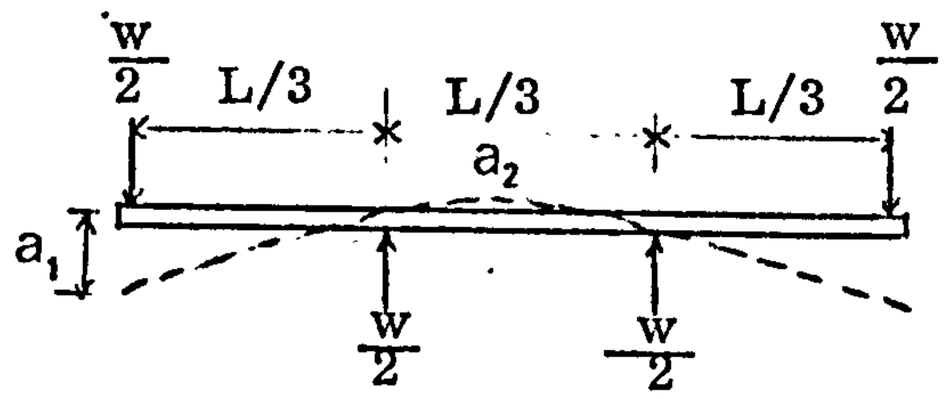

Upper beam

The differential equation to calculate the deflection is:

$$EI \frac{d^2a}{dx^2} = M$$

$$EI \frac{d^2a}{dx^2} = \frac{w}{2} x - \left[\frac{w}{2}\left(X - \frac{L}{3}\right)\right]$$

EI : flexural rigidity

X : distance along the beam

a : deflection

w : total applied load

By integrating the above equation:

$$EI \frac{da}{dx} = \frac{WX^2}{4} - \left[\frac{W}{4}\left(X - \frac{L}{3}\right)^2\right] + C_1$$

At $X = \frac{L}{2}$, $\frac{da}{dx} = 0$, therefore $C_1 = -\frac{WL^2}{18}$

$$EI \frac{da}{dx} = \frac{WX^2}{4} - \left[\frac{W}{4}\left(X - \frac{L}{3}\right)^2\right] - \frac{WL^2}{18}$$

Integrating again gives

$$EI\, a = \frac{WX^3}{12} - \left[\frac{W}{12}\left(X - \frac{L}{3}\right)^3\right] - \frac{WL^2}{18} X + C_2$$

At $X = \frac{L}{3}$, $a = 0$, therefore $C_2 = \frac{5WL^3}{324}$

Hence

$$EI\ a = \frac{WX^3}{12} - \left[\frac{W}{12}(X - \frac{L}{3})^3\right] - \frac{WL^2}{18}X - \frac{5WL^3}{324}$$

The deflection a_1 at $X = 0$ is:

$$EI\ a_1 = \frac{4WL^3}{324} \qquad \text{Since } M = \frac{WL}{6}$$

therefore $a_1 = \frac{5}{54}\frac{M}{EI}L^2$

The deflection a_2 at $X = \frac{L}{2}$ is:

$$a_2 = \frac{1}{72}\frac{M}{EI}L^2$$

The total deflection ($a_1 + a_2$) is equal to 7.7 times the central deflection a_2 measured relative to the supports. This is shown in the following:

$$\frac{a_2 + a_1}{a_2} = \frac{\frac{1}{72} + \frac{5}{54}}{\frac{1}{72}} = \frac{23}{216} \times 72 = 7.7$$

Lower beam

Similar approach can be employed for the lower beam.

The boundry conditions are

At $X = L/2$ $\quad \frac{da}{dx} = 0$

At $X = L/3$ $\quad a = 0$

Hence, the values of the coefficients to calculate the deflections are the same as those for the upper beams.

APPENDIX (H)

Partially Cracked Composite Section

H1_Neutral Axis Depth X_p

In the calculation of the neutral axis depth for a partially cracked concrete section, the elastic theory approach is used.

An assumption is made by considering an uncracked concrete area, which is equivalent to the confined concrete by the presence of the f.r.c. channel, below the neutral axis level. This is discussed in 5.3.4.

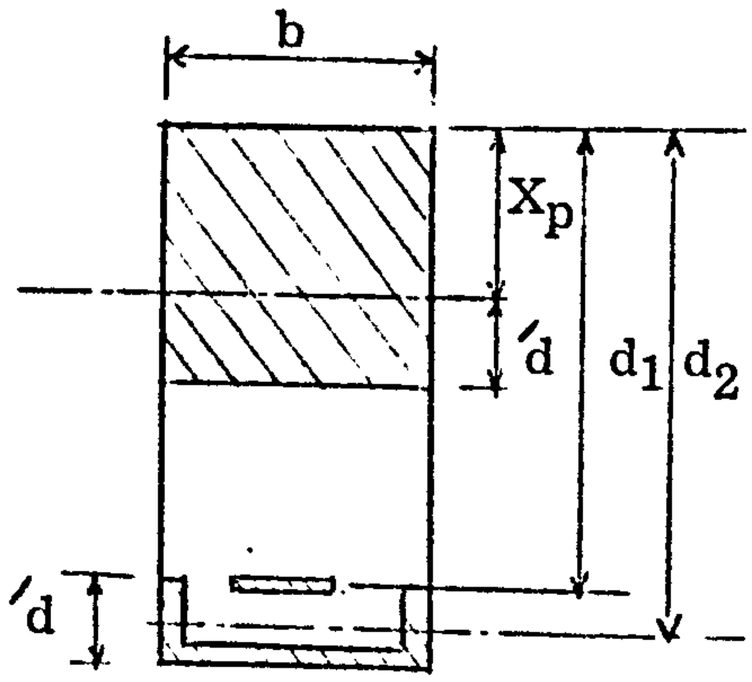

Cross Section

Taking moments of area about the neutral axis level:

$$bX_p \frac{X_p}{2} = m A_s (d_1 - X_p) + m_1 A_{ch} (d_2 - X_p) + b\acute{d}\,\acute{d}/2$$

For this equation and by substituting

$$p = \frac{A_s}{bd_1}, \quad p_1 = \frac{A_{ch}}{bd_2}, \quad \eta = d_2/d_1, \quad \acute{\eta} = \acute{d}/d_1$$

$$n = \frac{X_p}{d_1} \pm (mp + m_1 p_1 \eta) \left[\sqrt{1 + \frac{2(mp + m_1 p_1 \eta^2) + \acute{\eta}^2}{(mp + m_1 p_1 \eta)^2}} - 1 \right]$$

H2_Second Moment of Area (I_p)

The second moment of area for a partially cracked composite section can be obtained from the following:

$$I_p = \frac{b(X_p)^3}{3} + m A_s (d_1 - X_p)^2 + m_1 A_{ch} (d_2 - X_p)^2 + \frac{b\acute{d}^3}{3}$$